

# ScholarWorks@GSU

## Insights into Sulfonated Phthalocyanines; Insights into Anionic Tetraaryl Porphyrins; Irradiation of Cationic Metalloporphyrins Bound to DNA

Authors	Gill, Anila Fiaz
Citation	Gill, Anila Fiaz. (2006). "Insights into Sulfonated Phthalocyanines; Insights into Anionic Tetraaryl Porphyrins; Irradiation of Cationic Metalloporphyrins Bound to DNA". Georgia State University. <a href="https://doi.org/1059250">https://doi.org/1059250</a>
DOI	<a href="https://doi.org/10.57709/1059250">https://doi.org/10.57709/1059250</a>
Rights	I hereby certify that, if appropriate, I have obtained and attached hereto a written permission statement from the owner(s) of each third party copyrighted matter to be included in my thesis, dissertation, or project report, allowing distribution as specified below. I certify that the version I submitted is the same as that approved by my advisory committee. I hereby grant to Georgia State University or its agents the non-exclusive license to archive and make accessible, under the conditions specified below, my thesis, dissertation, or project report in whole or in part in all forms of media, now or hereafter known. I retain all other ownership rights to the copyright of the thesis, dissertation or project report. I also retain the right to use in future works (such as articles or books) all or part of this thesis, dissertation, or project report.
Download date	2026-06-13 21:52:41
Link to Item	<a href="https://hdl.handle.net/20.500.14694/2821">https://hdl.handle.net/20.500.14694/2821</a>

**Insights into Sulfonated Phthalocyanines; Insights into Anionic Tetraaryl  
Porphyrins; Irradiation of Cationic Metalloporphyrins Bound to DNA**

**by**

**Anila Fiaz Gill**

**Under the Direction of Dr. Dabney White Dixon**

**ABSTRACT**

Sulfonated porphyrins and phthalocyanines have been under consideration as microbicides, compounds which, when used in a topical formulation, can prevent transmission of the human immunodeficiency virus. Our studies have been directed toward the characterization of members of these classes. For the sulfonated phthalocyanines, matrix-assisted laser desorption/ionization (MALDI) mass spectrometry was helpful in determining the extent of sulfonation. We present the first report of spectroscopic characterization of a pentasulfonated phthalocyanine. Capillary electrophoresis data were sensitive to the concentration of the compounds (Chapter 1).

Mass spectrometry was also very useful for establishing the extent of sulfonation in series of sulfonated porphyrins. Capillary electrophoresis was very useful in separating mixtures of these species. A study on sulfonation of a series of tetra(difluorophenyl)porphyrins showed that species with red-shifted Soret peaks were being formed. Data were consistent with an intramolecular sulfone bridge from the phenyl substituent to the porphyrin core. Sulfonation of the tetranaphthylporphyrins ring readily gave more than one sulfonic acid group per naphthyl side chain (Chapter 2).

In cancer chemotherapy of solid tumors, it is desired to kill the tumor cells with minimal damage to the surrounding tissue. Brachytherapy seeds have been a considerable help in this regard for some tumors. In further developing approaches to selective tumor damage, we have evaluated a technique, Auger Electron Therapy (AET) in which one introduces a compound that is expected to bind to DNA, absorb the radiation, and then catalyze clustered DNA damage via release of a series of Auger electrons. We chose a series of metals (silver, indium, molybdenum, palladium, platinum, ruthenium, silver and zirconium) with appropriate energy levels to absorb an x-ray photon from the brachytherapy seed and used the tetracationic porphyrin 5,10,15,20-tetrakis(1-methylpyridinium-4-yl) porphyrin (TMPyP4) as a scaffold. The amount of clustered DNA damage was quantitated by a plasmid assay. Experiments evaluated the effect of buffer, concentration of glycerol, irradiation time, and concentration of the porphyrin. No metal studied gave significant double stranded (localized) DNA damage. Significant single stranded DNA damage was observed, however, in the order zirconium >> ruthenium > palladium > platinum > silver ~ indium (Chapter 3).

INDEX WORDS: Sulfonated Phthalocyanines, Anionic Porphyrins, Cationic Porphyrins, Auger Electron Therapy (AET), Capillary Electrophoresis, Mass Spectrometry.

**Insights into Sulfonated Phthalocyanines; Insights into Anionic Tetraaryl  
Porphyrins; Irradiation of Cationic Metalloporphyrins Bound to DNA**

by

**Anila Fiaz Gill**

**A Dissertation Submitted in Partial Fulfillment of the Requirements for the Degree  
of**

**Doctor of Philosophy**

**in the College of Arts and Sciences**

**Georgia State University**

**2006**

Copyright by  
Anila Fiaz Gill  
2006

**Insights into Sulfonated Phthalocyanines; Insights into Anionic Tetraaryl  
Porphyrins; Irradiation of Cationic Metalloporphyrins Bound to DNA**

**by**

**Anila Fiaz Gill**

Major Professor: Dr. Dabney W. Dixon  
Committee Members: Dr. Kathy B. Grant  
Dr. Markus W. Germann

Electronic Version Approved by:  
Office of Graduate Studies  
College of Arts and Sciences  
Georgia State University  
December 2006

## ACKNOWLEDGEMENTS

I am grateful to God for giving me the strength and perseverance for completing the research.

My sincerest gratitude to Dr. Dabney White Dixon, my Ph.D. advisor, for her continued guidance and support during the whole process of completing the Ph.D. program.

Special thanks to my family, my father, Mr. Munawar Fiaz Gill, my mother, Mrs. Gulzar Munawar Gill and my brother Mr. Obaid Fiaz Gill. They have been a constant source of support through their kindness and prayers.

I am very thankful to Rev. Dr. and Mrs. F. B. Davies, my “adopted parents”, for their love, care and support.

I would also like to thank the community of Georgia State University, especially, the members of the Department of Chemistry and of Dr. Dixon’s research group for their support.

## TABLE OF CONTENTS

Acknowledgment.....	iii
List of Tables.....	vi
List of Figures.....	vii

### **Chapter 1: Insights into Anionic Phthalocyanines.**

Section I. Introduction to phthalocyanines.....	1
Section II. Review: Capillary electrophoresis separation of sulfonated phthalocyanines.....	4
Section III. Experiments:	
i. Materials and methods.....	9
ii. Results and discussion.....	10
Section IV. Published work: Characterization of Sulfonated Phthalocyanines by Mass Spectrometry and Capillary Electrophoresis.....	18
Figures.....	40
References.....	63

### **Chapter 2: Insights into Anionic Tetraaryl Porphyrins.**

Section I. Introduction to porphyrins.....	69
Section II. Review: Capillary electrophoresis separation of porphyrins.....	73
Section III. Review: Cyclodextrins and TPPS4.....	91
Section IV. Experiments:	

i. Materials and methods.....	97
ii. Results and discussion.....	98
Section V. Published work: Sulfonated Naphthyl Porphyrins as Agents against HIV-1.....	122
Tables .....	143
Figures.....	148
References.....	175
 <b>Chapter 3: Irradiation of Cationic Metalloporphyrins Bound to DNA.</b>	
Section I. Introduction.....	186
Section II. Experiments:	
i. Materials and methods .....	189
ii. Results and discussion .....	193
Tables .....	206
Figures .....	209
References .....	217

## LIST OF TABLES

### Chapter 2:

Table 2.1. Biological data for the difluoro derivatives of TPPS4. Data from the laboratory of Dr. Compans. ....	143
Table. 2.2. Summary of the capillary electrophoresis and mass spectrometry data of difluoro derivatives of TPPS4. The asterisks indicate the placement of sulfonic acid groups, as directed by the fluoro groups. ....	144
Table 2.3. Summary of the capillary electrophoresis data for the bromo derivatives of TPPS4.....	145
Table 2.4. Summary of the negative ion MALDI data for the bromo derivatives of TPPS4. ....	147
Table 2.5. EC <sub>50</sub> and CC <sub>50</sub> for selected sulfonated metalloporphyrins. Data from the laboratory of Dr. Compans .....	148

### Chapter 3:

Table 3.1. The inner shell energies (keV) of the metals chosen for irradiation. All have L or K edge energies suitable for irradiation by clinically used brachytherapy seeds. ....	206
Table 3.2. Relationship between XlogP and capillary electrophoresis migration times. ....	207
Table 3.3. Summary of the results of plasmid (pUC19) DNA cleavage when irradiated in the presence of the metalloderivatives of TMPyP4. ....	208

## LIST OF FIGURES

### Chapter 1:

Figure 1.1. Structure of phthalocyanine.....	40
Figure 1.2. Weber-Busch method for the synthesis of sulfonated phthalocyanines.....	41
Figure. 1.3. Possible isomers when the starting material, phthalic acid, has the substituent, sulfonic acid, at the 4- or the equivalent 5-position.....	42
Figure 1.4. Examples of the possible isomers when the starting material, phthalic acid, has the substituent, sulfonic acid, at more than one position, i.e., 3- and 4- position.....	43
Figure 1.5. Capillary electropherograms of CuPcS(3444).....	44
Figure 1.6. Capillary electropherograms of CuPcS(4444).....	45
Figure 1.7. Capillary electropherograms of ZnPcS4.....	46
Figure 1.8. Capillary electropherograms of NiPcS4.....	47
Figure 1.9. UV-vis spectra of NiPcS4.....	48
Figure 1.10. Capillary electropherograms of PcS4-S and PcS4-WB. The separation buffer is 10 mM KH <sub>2</sub> PO <sub>4</sub> buffer, pH 9.0.....	49
Figure 1.11. Capillary electropherograms of PcS4-S and PcS4-WB. The separation buffer is 50 mM Na <sub>2</sub> HPO <sub>4</sub> buffer, pH 2.5.....	50
Figure 1.12. UV-vis spectra of PcS4-S. ....	51
Figure 1.13. Capillary electrophoresis separation of TPPS2a (4 min), TPPS3 (5 min), and TPPS4 (6.4 min), pH 9.0 ( $\approx$ 10 $\mu$ M porphyrin, 10 mM phosphate buffer, 30 kV).....	52
Figure 1.14. Negative ion MALDI spectrum (CHCA) of T2NapS. Panel A shows the region corresponding to the monomer. Peaks for the tetrasulfonic ( $\blacklozenge$ ) and the pentasulfonic acid ( $\blacktriangle$ ) as well as their sodium salts are seen. Panel B shows the region corresponding to the dimer. Peaks for the homodimers of the tetrasulfonic ( $\blacklozenge$ ) and pentasulfonic acid ( $\blacktriangle$ ) as well as the heterodimer of the tetrasulfonic/pentasulfonic acid ( $\blacksquare$ ) and their sodium salts are seen. Data interpreted by Brian R. Sook.....	53
Figure 1.15. Negative ion MALDI spectrum of PcS4. Panel A: PcS4-WB (THAP/EDTA). The parent ion is seen (834), as are the mono-, di-, tri-, and	

- tetrasodium salts at intervals of +22 and a peak consistent with loss of  $\text{SO}_3$  (754).
- Panel B:  $\text{PcS}_4\text{-S}$  (CHCA). The parent ion is seen (834), as are the mono- and disodium salts. The peaks at 911 - 914 and 933 - 936 are appropriate for the pentasulfonic acid and its monosodium salt, respectively. Data interpreted by Brian R. Sook .....54
- Figure 1.16. Negative ion mode MALDI spectrum of  $\text{CoPcS}_4$  (CHCA). The parent ion is seen (891), as are the dimer (1782) and peaks consistent with loss of  $\text{SO}_2$  (827) and  $\text{SO}_3$  (811). Data interpreted by Brian R. Sook .....55
- Figure 1.17. Capillary electrophoresis separation of  $\text{ZnPcS}_3$ . Panel A: pH 9.0 (10 mM phosphate buffer, 30 kV). Panel B: pH 2.5 (50 mM phosphate, -20 kV).....56
- Figure 1.18. Negative ion MALDI spectrum (CHCA/EDTA) of  $\text{ZnPcS}_4\text{-WB}$ . The parent is seen (896) as is the loss of  $\text{SO}_3$  (816). Data interpreted by Brian R. Sook .....57
- Figure 1.19. Negative ion MALDI spectrum (CHCA) of  $\text{ZnPcS}_4\text{-I}$ . The region corresponding to the monomer is shown. The mono- and disodium salts, as well as losses of  $\text{SO}_2$  and  $\text{SO}_3$  from the parent ion, are seen. Peaks at 976 and 998 Da are consistent with the pentasulfonic acid and its monosodium salt, respectively. Data interpreted by Brian R. Sook .....58
- Figure 1.20. Negative ion MALDI spectrum (CHCA/EDTA) of  $\text{ZnPcS}_4\text{-I}$ . The region corresponding to the dimer is shown. Peaks for the homodimers of the tetrasulfonic ( $\blacklozenge$ ) and pentasulfonic acid ( $\blacktriangle$ ) as well as the heterodimer of the tetrasulfonic/pentasulfonic acid ( $\blacksquare$ ) and their sodium salts are seen. Data interpreted by Brian R. Sook .....59
- Figure 1.21. Capillary electrophoresis of sulfonated copper phthalocyanines at pH 9.0 (10 mM phosphate, 30 kV). Panel A:  $\text{CuPcS}(3444)$  ( $\sim 2.5 \times 10^{-5}$  M). Panel B:  $\text{CuPcS}(4444)$  ( $\sim 2.5 \times 10^{-4}$  M).....60
- Figure 1.22. UV-vis spectroscopy of sulfonated copper phthalocyanines. Panel A:  $\text{CuPcS}(3444)$ , in DMSO. Panel B:  $\text{CuPcS}(4444)$  in DMSO. Panel C:  $\text{CuPcS}(3444)$  in pH 9.0 buffer. Panel D:  $\text{CuPcS}(4444)$  in pH 9.0 buffer.....61
- Figure 1.23. Positive ion mode MALDI of  $\text{CuPcS}(3444)$  (CHCA/EDTA). The monomer and its sodium salts are seen (895), as are the dimer salts (peaks are centered at 1902; this is the 5 sodium salt) and trimer salts (peaks centered at 2866; this is the octasodium salt). Data interpreted by Brian R. Sook .....62

## Chapter 2:

Figure 2.1. (a) Structure of porphin (left), tetraphenylporphyrin (TPyP4) (center), and tetrasulfonated tetraphenylporphyrin (TPPS4) (right). (b) Structure of naphthyl porphyrin (TNapPS) (left) and anthracyl porphyrin (TAnthPS) (right). .....148

Figure 2.2. UV-vis spectra of TPPS4. In the order of decreasing concentration, the dilution factors are 301, 1001 and 3001 of the stock solution ( $\sim 10^{-3}$  M by weight). ....149

Figure 2.3. UV-vis spectra of CuTPPS4 in water. In the order of decreasing concentration, the dilution factors are 26, 39, 51, 101 and 752 of the stock solution ( $\sim 10^{-4}$  M by weight). .....150

Figure 2.4. UV-vis spectra of TPPS3 (a) H<sub>2</sub>O: In the order of decreasing concentration, the dilution factors are 17, 25, 33, 50, 100, 200 and 1000 of the stock solution ( $10^{-4}$  M by weight). (b) pH 2.5 buffer: In the order of decreasing concentration, the dilution factors are 17, 20, 25, 33, 50, 100, 200 and 500 of the stock solution ( $10^{-4}$  M by weight). .....151

Figure 2.5. Capillary electrophoresis separation of metalloderivatives of TPPS4. Separation conditions: 10 mM KH<sub>2</sub>PO<sub>4</sub> buffer, pH 9.0, 30 kV, 412 nm. ....152

Figure 2.6. Capillary electropherograms of TNapPS. ....153

Figure 2.7. UV-vis spectra of TNapPS. In the order of decreasing concentration, the dilution factors were 101, 151, 216, 301 and 752 of the stock solution ( $\sim 10^{-3}$  M). ....153

Figure 2.8. Capillary electropherograms of TAnthPS. ....154

Figure 2.9. UV-vis spectra of TAnthPS in pH 2.5 buffer. In the order of decreasing concentration, the dilution factors were 101, 151, 216, 301 and 752 of the stock solution ( $\sim 10^{-3}$  M). .....154

Figure 2.10. Structures of the difluoro derivatives of TPPS4. ....155

Figure 2.11. UV-vis spectra of the Cu chelates of difluoro derivatives of TPPS4 in various solvents. H<sub>2</sub>O: \_\_\_ \_\_\_ \_\_\_; 1 mM EDTA: .....; buffer pH 7.1: -----; buffer pH 9.0: \_\_\_\_\_ .....156

Figure 2.12. (a) UV-vis spectra of TPP(2,5-F2)S,Cu (DD713) in various solvents to check for aggregation. (b) UV-vis spectra of various dilutions of TPP(2,5-F2)S,Cu (DD713) in water to check for aggregation. ....157

Figure 2.13. Formation of cyclic structures in tetraphenylporphyrins. (a) the proposed cyclic sulfone ring, (b) cyclic ketone and amine rings in tetrapyrroles reported in literature. ....158

Figure 2.14. (a) Loss of water could result in the formation of sulfone ring, shown here in the case of TPPS(2,5-F)S,Cu (DD713). The *ortho* and *para* positions indicate where the sulfonic acid group(s) will be placed, directed by the fluoro groups. (b) The asterisks indicate the placement of sulfonic acid groups, as directed by the fluoro groups. ....159

Figure 2.15. Capillary electrophoresis separation of fluoro derivatives of TPPS4. Separation conditions: 10 mM KH<sub>2</sub>PO<sub>4</sub> buffer + 1 mM  $\beta$ CD, pH 9.0, 30 kV. ....160

Figure 2.16. (a) Negative ion MALDI mass spectrum of TPP(3,5-F<sub>2</sub>)S,Cu (DD746). Peaks corresponding to mono-( $\nabla$ , 899), di-( $\Delta$ , 979), tri-( $\blacktriangledown$ , 1059) and tetrasulfonic acid ( $\blacktriangledown$ , 1139) and their sodium adducts are seen. The peak at 1040 ( $\diamond$ ) is due to loss of 18 Da from trisulfonic acid. The peak at 1120 ( $\diamond$ ) is due to loss of water from tetrasulfonic acid. (b) Negative ion MALDI mass spectrum of TPP(2,3-F<sub>2</sub>)S,Cu (DD755). Peaks corresponding to tri-( $\blacktriangledown$ , 1059), tetra-( $\blacktriangledown$ , 1139) and pentasulfonic acid ( $\blacktriangle$ , 1219) and their sodium adducts are seen. The peak at 1120 ( $\diamond$ ) is due to loss of 18 Da from tetrasulfonic acid. The peak at 1201 ( $\diamond$ ) is due to loss of water from pentasulfonic acid. ....161

Figure 2.17. (a) Negative ion MALDI mass spectrum of TPP(2,5-F<sub>2</sub>)S,Cu (DD713). Peaks corresponding to di-( $\Delta$ , 979), tri-( $\blacktriangledown$ , 1059) and tetrasulfonic acid ( $\blacktriangledown$ , 1139) and their sodium adducts are seen. The peak at 960 ( $\diamond$ ) is due to loss of water from disulfonic acid. The peak at 1040 ( $\diamond$ ) is due to loss of 18 Da from trisulfonic acid. The peak at 1120 ( $\diamond$ ) is due to loss of water from tetrasulfonic acid. (b) Negative ion MALDI mass spectrum of TPP(2,4-F<sub>2</sub>)S,Cu (DD720). Peaks corresponding to mono-( $\nabla$ , 899), di-( $\Delta$ , 979), tri-( $\blacktriangledown$ , 1059) and tetrasulfonic acid ( $\blacktriangledown$ , 1139) and their sodium adducts are seen. The peaks at 960 ( $\diamond$ ) is due to loss of water from disulfonic acid. The peak at 1040 ( $\diamond$ ) is due to loss of water from trisulfonic acid. The peak at 1120 ( $\diamond$ ) is due to loss of water from tetrasulfonic acid. The peak at 1201 ( $\diamond$ ) is due to loss of 18 Da from pentasulfonic acid. ....162

Figure 2.18. (a) Negative ion MALDI mass spectrum of TPP(2,4-F<sub>2</sub>)S,Cu (DD 720). Peaks corresponding to mono-( $\nabla$ , 899), di-( $\Delta$ , 979), tri-( $\blacktriangledown$ , 1059) and tetrasulfonic acid ( $\blacktriangledown$ , 1139) are seen. The peaks at 1017 and 1039 ( $\odot$ ) are due to loss of SO<sub>2</sub> from sodium adducts of trisulfonic acid. The peaks at 1097, 1119 and 1141 ( $\bullet$ ) are due to loss of SO<sub>2</sub> from sodium adducts of tetrasulfonic acid. The peaks at 1177, 1199 and 1221( $\odot$ ) are due to loss of SO<sub>2</sub> from sodium adducts of pentasulfonic acid. (b) Negative ion MALDI mass spectrum of TPP(2,3-F<sub>2</sub>)S,Cu (DD 755). Peaks corresponding to tri-( $\blacktriangledown$ , 1059), tetra-( $\blacktriangledown$ , 1139) and pentasulfonic acid ( $\blacktriangle$ , 1219) are seen. The peaks at 1075, 1097, 1119 and 1141 ( $\bullet$ ) are due to loss of SO<sub>2</sub> from tetrasulfonic acid and its sodium adducts. The

- peaks at 1155, 1177, 1199 and 1221( $\odot$ ) are due to loss of  $\text{SO}_2$  from pentasulfonic acid and its sodium adducts. ....163
- Figure 2.19. Structures of bromo derivatives of TPPS4. ....164
- Figure 2.20. Capillary electropherograms of bromo derivatives of TPPS4. Separation conditions: 10 mM  $\text{KH}_2\text{PO}_4$ , pH 9.0 buffer with 1 mM  $\beta\text{CD}$ . ....165
- Figure 2.21. UV-vis spectra of bromo derivatives of TPPS4 in water. ....166
- Figure 2.22. Structures of sulfonated 1-naphthyl (T1NapS, left) and 2-naphthyl T2NapS, right) porphyrins. Tetrasulfonated porphyrins with one sulfonic acid on each side chain are shown. M is Cu, Fe or 2H. ....167
- Figure 2.23. CE separation of T2Nap5S,Cu in pH 9.0, 10 mM  $\text{KH}_2\text{PO}_4$  buffer. A: with 1 mM  $\beta$ -cyclodextrin; B: with 1 mM  $\gamma$ -cyclodextrin. ....168
- Figure 2.24. CE of T2NapS made by sulfonation for 5 h (A, T2Nap5S) and 20 h (B, T2Nap20S) (pH 9.0, 10 mM  $\text{KH}_2\text{PO}_4$  buffer, 1 mM  $\gamma$ -cyclodextrin). ....169
- Figure 2.25. CE of T2NapS,Cu (pH 9.0, 10 mM  $\text{KH}_2\text{PO}_4$  buffer, 1 mM  $\gamma$ -cyclodextrin). Sulfonation for 5 h (- . - . -), 10 h (- - - -) and 20 h (\_\_\_\_\_). ....170
- Figure 2.26. Negative ion MALDI mass spectrum of T2Nap5S,Cu. Peaks corresponding to the tetrasulfonic acid ( $\blacktriangledown$ , 1195) and pentasulfonic acid ( $\blacktriangle$ , 1275) are seen. The peaks at 1257 and 1337 are attributed to the sulfones (loss of water) from pentasulfonic acid ( $\blacktriangle$ ) and hexasulfonic acid ( $\blacksquare$ ), respectively. ....171
- Figure 2.27. Negative ion MALDI mass spectrum of T2Nap20S,Cu showed peaks appropriate for the pentasulfonic acid ( $\blacktriangle$ ); the hexa- ( $\blacksquare$ ) and heptasulfonic acids ( $\blacklozenge$ ) and their M -  $\text{H}_2\text{O}$  peaks; and the M -  $\text{H}_2\text{O}$  peak corresponding to the octasulfonic acid ( $\bullet$ ). Sodium salts of some of the sulfonic acid species are also seen. ....172
- Figure 2.28. Negative ion ESI MS/MS of the pentasulfonic acid peak ( $\blacktriangle$ ) at 1274 of T2Nap5S,Cu. The peak at 1210 is attributed to loss of  $\text{SO}_2$  ( $\diamond$ ). Successive losses of  $n\text{SO}_3$  ( $\square$ ) and  $[\text{SO}_2 + (n-1)\text{SO}_3]$  ( $\circ$ ) can be seen ( $n = 2 - 4$ ). Peaks are also seen for losses of two  $\text{SO}_2$  and either one or two  $\text{SO}_3$ . ....173
- Figure 2.29. Activity of sulfonated naphthyl porphyrins against HIV-1 IIIB. Compounds at a concentration of 50  $\mu\text{g}/\text{ml}$  were incubated with HIV-1 IIIB in the dark for 1 h; the compound/virus mixture was diluted 10-fold and used to inoculate MAGI-CCR5 cells. HIV infectivity was measured after three days by removal of the media, fixation and staining with X-gal. The activity against HIV was measured by dividing the number of infected,  $\beta$ -gal expressing cells in wells infected with compound-treated virus by the

number in wells infected with untreated virus. Data are plotted as the mean of one or two experiments, each with three or four replications. Error bars represent standard deviations. The naphthyl porphyrins were sulfonated for 5 and 10 hours (T1Nap) and 5, 10 and 20 hours (T2Nap). .....174

### Chapter 3:

Figure 3.1. Thermal melting profiles of 10 mer duplex DNA (5'- GCGAATTCGC-3') alone (46.9 °C) and after complexation with the alkyl derivatives of InTRPyP4 (59.0 ± 1 °C). .....209

Figure 3.2. Capillary electrophoresis separation of the indium derivatives of InTPyP4. Separation conditions are discussed in the experimental section.....210

Figure 3.3. UV-vis spectra of (a) Zr and (b) Mo derivatives of TMPyP4. The porphyrin solutions are in water (\_\_\_) and in pH 3.2 (\_\_\_) and 8.1 (----) buffers. ....211

Figure 3.4. Enhancement of pUC19 cleavage was observed due to longer irradiation times. Experimental conditions: 20 μM pUC19 in 10 mM phosphate buffer (pH 7.0) + 2 mM glycerol; Rh target tube, 50 kV, 20 mA, 40 Gy/min. ....212

Figure 3.5. Increasing porphyrin concentration enhanced pUC19 cleavage. “Dimming” of the bands was also observed. Experimental conditions: 10 μM pUC19 in 10 mM phosphate buffer (pH 7.0) + 2 mM glycerol; 4 s irradiation; Rh target tube, 50 kV, 20 mA, 40 Gy/min. ....213

Figure 3.6. An increased fraction of OC was observed by the addition of 3,3'-diamino-*N*-methylpropylamine to a mixture of plasmid (pUC19) DNA and InTBzPyP4 that was incubated for 30 days. This indicated the formation of abasic sites on the DNA due to the prolonged incubation with the porphyrin, even in a frozen solution (-20 °C). Experimental conditions: 10 μM pUC19 and 1 μM InTBzPyP4 in 10 mM phosphate buffer (pH 7.0) + 2 mM glycerol. ....214

Figure 3.7. Extents of SC, OC and L forms of pUC19 as a function of irradiation time, no porphyrin added. Reactions were run in 10 mM phosphate buffer at pH 7.0 with 2 mM glycerol. Lines are global fits of the data to the Freifelder-Trumbo equations using Mathematica. (a) no porphyrin, (b) 1 μM Ru(CO)TMPyP4. ....215

Figure 3.8. The extent of single strand cutting (ssb) and double strand cutting (dsb) and the nss/nds ratio as a function of the metal chelated in the porphyrin. Unless otherwise noted, all porphyrins are TMPyP4. Experimental conditions and data analysis are described in the text. ....216

## Chapter 1

### Insights into Anionic Phthalocyanines

In collaborative studies, we observed that a number of sulfonated phthalocyanines had excellent antiviral activity against the human immunodeficiency virus (Vzorov et al., 2003), pox virus (Chen-Collins et al., 2003) and herpes simplex virus (Dixon, Gill, Maraili, Hodge and Sears, unpublished data). Because these compounds had low toxicity, they were, for a time, under consideration as new vaginal microbicides, compounds which are used topically to protect against viral infection. In the end, a compound that was not a phthalocyanine was chosen for clinical trials. However, we performed a number of studies to look in detail at the structures and spectra of possible metallophthalocyanine therapeutic candidates. The majority of this work has been published (Dixon et al., 2004), and is given as Section IV of this chapter. Below are a brief overview of phthalocyanines (Section I), a review of capillary electrophoresis of sulfonated phthalocyanines (Section II) and experiments that were not published (Section III).

#### Section I.

##### Introduction to phthalocyanines.

##### i. Structure.

A phthalocyanine is a planar, 18-electron heterocyclic aromatic system (**Figure 1.1**). It has four isoindole units linked by aza nitrogen atoms (Leznoff & Lever, 1989).

Many water-soluble derivatives can be synthesized by adding groups to the isoindole units, e.g., amino, carboxylic and sulfonic acid groups (Barbosa et al., 1997). Similarly, many metalloderivatives of phthalocyanines can be synthesized; more than 60 metals have been reported as inserted in the phthalocyanine ring (Leznoff & Lever, 1989).

## **ii. Spectral properties.**

Phthalocyanines absorb in the 670 - 680 nm region, known as the Q-band, the result of a  $\pi - \pi^*$  ring transition (Leznoff & Lever, 1989; Leznoff & Lever, 1993). Phthalocyanines have high extinction coefficients, in the range of  $10^5 \text{ M}^{-1}\text{cm}^{-1}$ , and appear blue in color. A weaker absorption, due to vibronic coupling, is observed at 610 - 620 nm. Another low intensity band, due to electronic transitions, the B or Soret band, appears at 350 nm.

Phthalocyanines are known to aggregate in both aqueous and organic solvents. For aggregated phthalocyanines, there is a strong peak at  $\sim 620 - 630 \text{ nm}$  (Barbosa et al., 1997). This is face-to-face aggregation, which is the result of extensive interaction between the  $\pi$ -systems of adjacent rings (Zelina et al., 1999). The nature of metal in the ring affects the aggregation properties of the phthalocyanine (Barbosa et al., 1997). Aggregation is also affected by the solvent, pH, ionic strength and temperature of the solutions, as well as the concentration of the phthalocyanine.

## **iii. Applications.**

Phthalocyanines are used as catalysts, pigments, electrodes, and even as drugs, e.g., as sensitizers in photodynamic therapy (PDT) (Leznoff & Lever, 1989). The importance of phthalocyanines and their derivatives lies in their variety, structural

flexibility, stability and resistivity to chemical and photochemical degradation. Some phthalocyanines are known to be nontoxic; the LD<sub>50</sub> of certain phthalocyanines is >10 g/kg body weight (Leznoff & Lever, 1989). Our interest has been in the use of sulfonated phthalocyanines as antiviral agents.

#### **iv. Synthesis of phthalocyanines and derivatives.**

There are two main methods for the synthesis of sulfonated phthalocyanines (Leznoff & Lever, 1989). The first method involves the sulfonation of the phthalocyanine ring. Sulfonation has historically been thought to lead to a mixture of mono-, di-, tri-, and tetrasulfonated products. The second method involves the condensation of the sulfonated precursors in the presence of urea, the selected metal salt and a catalyst. This is called the Weber-Busch method, after an early report in which sodium salt of 4-sulfophthalic acid was used to synthesize tetrasodium (2,9,16,23-tetrasulfophthalocyaninato) cobalt(II) in the presence of urea, nitrobenzene, cobalt chloride salt and ammonium molybdate as a catalyst at 170 - 190 °C (Weber & Busch, 1965) (**Figure 1.2**). The condensation method using the 4-sulfonic acid as starting material leads to isomeric mixtures, though all the molecules are presumably tetrasulfonated (Leznoff & Lever, 1989). Sulfonated metallophthalocyanines are synthesized either by inserting metal into the free base tetrasulfonated phthalocyanine or by the sulfonation of the appropriate metalloderivative.

#### **v. Mixtures/isomers of phthalocyanines.**

Depending on the position of the substituent groups on the outer isoindole rings, phthalocyanines can have various isomers. Even if one starts with the precursor, sulfonated phthalic acid, with the sulfonic acid uniquely at the 4-position of the ring,

phthalocyanine isomers are formed because the sulfonic acid can be found at either the 4- or 5-position on each of the four isoindole rings of the phthalocyanine, giving a total of four isomers (**Figure 1.3**). If, however, the sulfonated phthalic acid is a mixture of compounds with sulfonic acid at the 3-position and 4-position on the ring, there can be multiple isomers (**Figure 1.4**).

## **Section II.**

### **Review.**

**Capillary electrophoresis separation of sulfonated phthalocyanines.** Capillary electrophoresis (CE) has been used for the analysis of phthalocyanines and its derivatives in a variety of contexts.

#### **i. CE for monitoring the progress of reactions.**

Barbosa et al. monitored the various purification steps involved in synthesis of sulfonated Co(II) phthalocyanine [Co(II)PcS] by CE (Barbosa et al., 1997). Co(II)PcS was synthesized by the Weber-Busch condensation method.

CE analysis was performed under reversed polarity at constant voltage, with spectroscopic detection at 260 nm and 630 nm for crude and purified products, respectively. The difference in the spectra of crude and purified product was observed at 260 nm. A 20 mM citrate buffer (pH 2.5) was used for the analysis of crude and purified products. Cetyltrimethylammonium bromide (CTAB) was used to enhance the separation.

Conneely et al. utilized CE to follow the biodegradation of copper phthalocyanine dyes and the appearance of new organic entities (Conneely et al., 2002). *Phanerochaete*

*chryso sporium* (white-rot fungi) PC 671 was used for the degradation. The copper phthalocyanine dyes studied were Remazol Turquoise Blue G133, Everzol Turquoise Blue and Heligon Blue S4.

As copper is strongly bound to the phthalocyanine structure, free copper ions would be indicative of the degradation of the phthalocyanine ring. The dyes were metabolized to give free copper ions, and presumably also non-copper and copper-containing metabolites. By the fifth day CE electropherograms did not have the parent dye peak, but only a large free copper ion peak, which reached maximum height by the seventh day, presumably indicating full degradation of the dyes.

The background electrolyte contained 0.025 M CTAB and 0.0385 M sodium tetraborate (Borax). Separations were carried out under reverse polarity, with the detector set at 254 and 666 nm. The presence of CTAB resulted in longer migration times for the dyes; Remazol TB, 25.79 min, Everzol TB, 25.65 min and Heligon TB, 24.53 min. Conneely et al. suggested that longer migration times in the presence of CTAB indicated that the dyes interacted electrostatically at the surface of the positively charged micelles of CTAB, while the rest of the dyes' essentially hydrophobic structure was embedded in the hydrocarbon center of the micelles. Generally shorter migration times observed for the metabolites suggested less interaction with the charged surface of the micelles and/or less affinity for the hydrophobic center of the micelles.

**ii. CE for analyzing the counter ions.**

Barbosa et al. analyzed the presence of counter ions during the purification steps of the synthesis of Co(II)PcS by CE (Barbosa et al., 1997). The anionic (chloride, sulfate, carbonate and 4-sulphothalate, prepared at 100 mg/L concentration) and cationic (ammonium, potassium, barium, calcium, sodium, manganese and cobalt(II), as chloride salts, prepared at 100 mM concentration) standards were used to compare the inorganic anions and cations of the purified fractions. Indirect detection was done at 254 nm and 214 nm. For anion analysis, 5 mM chromate buffer (pH 9.0) containing 0.1 mM CTAB was used. For the cation analysis, 5 mM imidazole (pH 5.0) containing 5 mM hydroxyisobutyric acid (HIBA) was used.

**iii. CE for analyzing the components of phthalocyanines.**

Schofield and Asaf used capillary electrophoresis for the analysis of various components of zinc, copper and cobalt derivatives of sulfonated phthalocyanines (Schofield & Asaf, 1997). They synthesized tetrasulfonated phthalocyanines by a modification of the Weber-Busch method.

The CE separation of the various components of each sulfonated phthalocyanine was based on the difference in the degree of sulfonation, i.e., on the basis of its net charge. The migration times were similar for the zinc, copper and cobalt derivatives of tetrasulfonated phthalocyanines.

Schofield and Asaf also compared the separation of two samples of chloroaluminum sulfonated phthalocyanine, synthesized by two different methods (Schofield & Asaf, 1997). The first sample was obtained by converting the sulfonyl

chloride groups of chloroaluminum phthalocyanine to sulfonic acid groups. The second sample was prepared as chloroaluminum phthalocyanine. It was then chlorosulfonated and finally hydrolyzed to give the chloroaluminum sulfonated phthalocyanine.

Separations were performed under high pH conditions (9.0, 10 mM  $\text{KH}_2\text{PO}_4$ ). Both the samples gave the same number of peaks, with similar migration times, but had different intensities/proportions of the peaks. Enhancement of CE separation by using ammonium acetate buffer with acetonitrile was not observed.

Tapley reported the separation of more than 12 colored components of Procion Turquoise H-A, a reactive phthalocyanine-based chlorotriazinyl dye (Tapley, 1995). It is a commercial copper phthalocyanine derivative with two different functional groups, and occurs as a mixture of related compounds. Various buffer compositions were investigated. Tapley used 6 mM  $\text{KH}_2\text{PO}_4$  buffer with 10 mM sodium borate, 10 mM sodium dodecylsulfate (SDS) and acetonitrile-water (1:9) for best separation. The electropherograms for the dye solution were the same at pH 7 and pH 11. At 20 mM SDS, the peaks were not baseline-separated, appearing between 13 and 26 min. A ratio of 1:9 of acetonitrile-water at pH 9.0 generally improved the resolution of the various components of the sample. The hydrolysis of the dye was studied by heating a pH 11 dye solution to 80 °C for 1 h; the electropherograms obtained were different from the initial electropherograms due to the loss or addition of peaks as a result of hydrolysis.

Peng et al. reported the separation of nine photosensitizer isomers of tetrasulfonated phthalocyanine by CE (Peng et al., 2005b). The isomers have different positions of sulfonate groups on the aromatic rings and occur to different extents in the

mixture. Peng et al. studied the effect on the separation of isomers by the use of various buffers, organic solvents, and additives. The best separation was achieved with a high concentration borate buffer (120 mM) at high pH (9.2) with SDS (10 mM) and at a high % of acetonitrile (50%). Separation was not enhanced by the presence of Brij 35 and cholate.

Pokric et al. reported the separation of Tinolux BBS, a sulfonated mixture of aluminum phthalocyanines,  $AlPcS_n$  (Pokric et al., 1999). They were interested in real-time processing of snapshot data from a CE instrument. Separation was performed using a 20 mM 3-cyclohexylamino-1-propanesulfonic acid buffer (CAPS), pH 10.5. The peaks for mono-, di-, tri-, and tetra-sulfonated species were separated within 50 s.

Dixon et al. have reported the separation of sulfonated phthalocyanines (Dixon et al., 2004). The details are discussed in Section IV of this chapter.

#### **iv. Detection of phthalocyanines.**

The overall spectral features of metallophthalocyanines are similar irrespective of the metal in the macrocycle (Barbosa et al., 1997). The dimer absorbs at 630 nm (Q band) and the monomer absorbs at 680 nm.

UV-vis detectors and fast scanning detectors have been regularly employed for the detection of peaks (Tapley, 1995; Barbosa et al., 1997; Schofield & Asaf, 1997; Conneely et al., 2002). Laser-induced fluorescence detection (LIF) has also been used. Separation of nine photosensitizer isomers of phthalocyanine tetrasulfonate by CE was reported using a UV detector set at 214 nm, as well as a LIF detector with excitation at 442/488 nm and emission at 690 nm (Peng et al., 2005a). The separation of  $AlPcS_n$  was

monitored by a charge coupled device LIF system to achieve high sensitivity (Pokric et al., 1999).

### **Section III.**

#### **Experiments.**

##### **i. Material and methods.**

Copper phthalocyanine-3,4',4'',4'''-tetrasulfonic acid tetrasodium salt [CuPcS(3444)] was from Aldrich (St. Louis, MO). Copper phthalocyanine-4,4',4'',4'''-tetrasulfonic acid [CuPcS(4444)] was obtained from Fluka (St. Louis, MO). Sulfonated zinc phthalocyanine, (ZnPcS4) and sulfonated nickel phthalocyanine (NiPcS4) were from Frontier Scientific (Logan, UT). Sulfonated phthalocyanine was available made via the Weber-Busch synthesis method (PcS4-WB) and via sulfonation of phthalocyanine (PcS4-S) (Midcentury Chemicals, Chicago, IL).

A stock solution of each compound was prepared in deionized water. The stock solutions were diluted 10- and 100-fold for capillary electrophoresis (CE) separations. The CE separations were conducted under two pH conditions, pH 9.0 (10 mM KH<sub>2</sub>PO<sub>4</sub> buffer) and pH 2.5 (50 mM Na<sub>2</sub>HPO<sub>4</sub> buffer). The details of the CE experiments are discussed in Section IV of this chapter.

The concentration of each stock solution was determined via UV-vis spectroscopy. The extinction coefficients ( $\epsilon$ ) used for determining the concentrations were:  $9.98 \times 10^4 \text{ M}^{-1}\text{cm}^{-1}$  in 50% ethanol-water mixture for PcS at 697 nm (Reynolds & Kolstad, 1976),  $1.47 \times 10^5 \text{ M}^{-1}\text{cm}^{-1}$  at 677 nm in DMSO for CuPcS(3444) (Zelina &

Rusling, 1995),  $1.77 \times 10^5 \text{ M}^{-1}\text{cm}^{-1}$  at 673 nm in 20% THF-water mixture for ZnPcS4 (Rajendiran & Santhanalakshmi, 2002), and  $1.03 \times 10^5 \text{ M}^{-1}\text{cm}^{-1}$  at 658 nm in 50% ethanol-water mixture for NiPcS4 (Amaral & Politi, 1997). From the stock solution in water, dilutions were made in the specified solvents and in water. From the absorbances in solvents, concentrations were calculated in water.

## **ii. Results and discussion.**

CE electropherograms were recorded over a concentration range of  $10^{-3}$  -  $10^{-5}$  M to observe any differences in CE peak pattern due to aggregation of the phthalocyanine at higher concentrations. Herein, is discussed the CE data at the highest and lowest concentrations of the phthalocyanines, unless stated otherwise. The migration time increased with an increase in the buffer concentration and decreased with an increase in the pH of the buffer (data not shown). The data was collected at  $\sim 350$  nm, the B-band or Soret region. The peaks intensities are weaker in this region compared to those in the Q-band region ( $\sim 670$  -  $680$  nm). The aggregated phthalocyanines absorb in the 620 - 630 nm region. In the presence of aggregates, the intensities of the peaks in the B-band region ( $\sim 350$  nm) are comparable to the intensities of the peaks in the aggregate region (620 - 630 nm) (Zelina & Rusling, 1995). The 260 nm region can be monitored for the presence of impurities (Barbosa et al., 1997). For most of the phthalocyanines a significant number of peaks were observed in this region.

The UV-vis spectra of the compounds were recorded under the same conditions as used for the CE separations, i.e., at the same concentration of the phthalocyanine, and in the same buffers. The UV-vis spectra indicated that the compounds were in the aggregated form under the CE separation conditions. Various solvents (reported in literature) were used to study the monomeric forms.

#### **a. Analysis of CuPcS4(3444) and CuPcS4(4444).**

These two commercially available compounds were tested for HIV activity (in the laboratory of Dr. Compans). The name CuPcS(3444) indicates that three of the four sulfonic acids are at the 4-position of the phenyl rings and one is at the 3-position. The name CuPcS(4444) indicates that all four sulfonic acids are at the 4-position of the phenyl rings. The “3444” isomer was much more active than the “4444” isomer. Because the “3444” compound also had very low toxicity, it was, for a time, considered as a possible therapeutic candidate. In view of the possible therapeutic use of one of these compounds, it was important to have a detailed understanding of the structural differences. Given the names, these two structures should have differed only in the position of a sulfonic acid group on one of the phthalocyanine rings.

##### **1. CuPcS4(3444).**

Under pH 9.0 (10 mM KH<sub>2</sub>PO<sub>4</sub> buffer) separation conditions, a  $3.58 \times 10^{-3}$  M solution of CuPcS(3444) gave four major peaks appearing between 11 and 14 min (**Figure 1.5a**). A  $4.25 \times 10^{-5}$  M solution showed a single sharp peak at  $\sim 13$  min and a

few small and broad peaks (**Figure 1.5b**). The electropherogram at 260 nm showed many peaks between 2.5 and 5 min (data not shown).

Under pH 2.5 (50 mM Na<sub>2</sub>HPO<sub>4</sub> buffer) separation conditions, a  $3.58 \times 10^{-3}$  M solution of CuPcS(3444) showed a broad unresolved peak at 6 min and a very short peak at ~ 7 min (**Figure 1.5c**). A  $4.25 \times 10^{-5}$  M solution showed a single sharp peak at ~ 6 min, in a broad plateau region from 5 to 9 min (**Figure 1.5d**).

The four CE peaks at the high concentration of  $3.58 \times 10^{-3}$  M CuPcS(3444), under pH 9.0 (10 mM KH<sub>2</sub>PO<sub>4</sub> buffer) separation conditions, could be due to aggregation, isomers, and/or due to the presence of other components in the compound. Because the electropherograms change significantly as the concentration of the compound changes under high pH separation conditions, the  $3.58 \times 10^{-3}$  M solution of CuPcS(3444) might be aggregated under high pH conditions.

In DMSO, the UV-vis spectra of both the solutions,  $3.58 \times 10^{-3}$  M and  $4.25 \times 10^{-5}$  M, of CuPcS(3444) had a monomer/dimer peak ratio of 6, indicating that either there is no or only slight aggregation in the presence of DMSO (data shown in Section IV of this chapter). UV-vis spectra were taken over the concentration range of  $4.7 \times 10^{-7}$  -  $1.45 \times 10^{-5}$  M, to see the change in spectra with concentration (data not shown). In DMSO, Beer's law was followed over the entire concentration range studied.

## 2. CuPcS4(4444).

A stock solution of CuPcS(4444) was prepared in deionized water to give a theoretical concentration of  $\sim 2.5 \times 10^{-3}$  M. Under pH 9.0 (10 mM  $\text{KH}_2\text{PO}_4$  buffer) separation conditions, the stock solution gave a single peak centered at  $\sim 8$  min (**Figure 1.6a**). A 2-fold diluted solution of CuPcS(4444) (theoretical concentration of  $\sim 1.3 \times 10^{-3}$  M) gave a peak at  $\sim 7$  min (**Figure 1.6b**). The 10-fold diluted solution was too dilute to give an appreciable signal (data not shown). The profiles at 260 nm showed peaks between 2.5 and 5 min, indicating presence of impurities (data not shown).

Under pH 2.5 (50 mM  $\text{Na}_2\text{HPO}_4$  buffer) separation conditions, the stock solution ( $\sim 2.5 \times 10^{-3}$  M) gave a sharp and tall peak and a very short shoulder peak at  $\sim 7$  min (**Figure 1.6c**). The 4-fold diluted solution (theoretical concentration of  $\sim 6.3 \times 10^{-4}$  M) also gave a sharp peak at  $\sim 7$  min (**Figure 1.6d**). The 10-fold diluted solution was too dilute to give an appreciable signal (data not shown). The profiles at 260 nm showed additional peaks between 5 and 10 min (data not shown).

The UV-vis spectra of a micromolar solution of CuPcS(4444) in DMSO showed a significant amount of a dimer band over the region of 550 - 650 nm (data shown in Section IV of this chapter). The monomer/dimer peak ratio increased as the concentration of the compound was lowered, indicating less aggregation at lower concentrations.

Comparing the capillary electropherograms of CuPcS(3444) and CuPcS(4444), it can be observed that they were very different, with the former having significantly longer

migration time, consistent with a higher net negative charge. Later work on the mass spectrometry of these systems showed that the putative tetrasulfonated CuPcS(4444) had, in fact, significantly fewer than four sulfonic acid groups on each phthalocyanine macrocycle (data shown and discussed in Section IV of this chapter).

#### **b. Analysis of ZnPcS4.**

Under pH 9.0 (10 mM  $\text{KH}_2\text{PO}_4$  buffer) separation conditions, a solution of  $1.05 \times 10^{-4}$  M ZnPcS4 gave a broad, short peak centered at  $\sim 8$  min and two short peaks between 11 and 13 min (**Figure 1.7a**). A solution of  $9.01 \times 10^{-5}$  M ZnPcS4 was too dilute to give an appreciable signal (data not shown). The electropherograms at 260 nm showed many additional peaks between 2.5 and 5 min (data not shown).

Under pH 2.5 (50 mM  $\text{Na}_2\text{HPO}_4$  buffer) separation conditions, a  $4.26 \times 10^{-4}$  M ZnPcS4 solution gave unresolved peaks between 5 and 9 min (**Figure 1.7b**). A  $9.01 \times 10^{-5}$  M solution gave a short and broad peak at 6.5 min (data not shown). The profiles at 260 nm showed a few additional peaks appropriate for impurities (data not shown).

The capillary electropherograms of ZnPcS4 showed that the resolution was somewhat better at pH 9.0 than at pH 2.5, that is, the bands appeared over 8 min at pH 9.0 but only over  $\sim 3$  min at pH 2.5. The breadth of the peaks indicated that the compound was aggregated under the CE conditions used.

To study the monomeric form of ZnPcS4, spectra were taken in 20% THF/ $\text{H}_2\text{O}$ , as reported in literature (Rajendiran & Santhanalakshmi, 2002) (data not shown). The

UV-vis spectra of ZnPcS4 in 20% THF/H<sub>2</sub>O showed a sharp monomeric band at ~ 675 nm, with a hint of a shoulder at ~ 610 nm for both the above mentioned concentrations,  $1.05 \times 10^{-4}$  M and  $9.01 \times 10^{-5}$  M. UV-vis spectra were taken over the concentration range of  $9.8 \times 10^{-7}$  -  $1.45 \times 10^{-5}$  M to see the change in spectra with concentration (data not shown). Beer's law was followed only in the concentration range of  $10^{-7}$  -  $10^{-6}$  M of the total concentration range studied.

### c. Analysis of NiPcS4.

Under pH 9.0 (10 mM KH<sub>2</sub>PO<sub>4</sub> buffer) separation conditions, a  $2.82 \times 10^{-3}$  M solution of NiPcS4 showed a very broad peak between 7 and 12 min, centered at ~ 10 min (**Figure 1.8a**). A  $7.05 \times 10^{-4}$  M solution of NiPcS4 (4-fold dilution of the first solution) showed a broad peak between 7 and 11 min (data not shown). The electropherogram at 260 nm showed very few additional peaks (data not shown).

Under pH 2.5 (50 mM Na<sub>2</sub>HPO<sub>4</sub> buffer) separation conditions, a solution of  $2.82 \times 10^{-3}$  M NiPcS4 gave a sharp tall peak between 5 and 8 min, centered at ~ 7 min (**Figure 1.8b**). A solution of  $3.08 \times 10^{-5}$  M also gave a single broad peak between 4 and 8.0 min, centered at ~ 7 min (data not shown). The profiles at 260 nm showed very few peaks (data not shown). The single band observed in the CE electropherograms, under both the separation conditions, might indicate that NiPcS4 was aggregated.

The UV-vis spectra of NiPcS4 are shown in **Figure 1.9**. The spectra in water and in pH 9.0 buffer were almost identical, with a peak at 654 nm, the monomer peak

(Amaral & Politi, 1997) and a shoulder peak at 620 nm, the dimer peak (Zelina & Rusling, 1995) (**Figure 1.9a and 1.9c**). The ratio of the monomer (654 nm) and dimer (620 nm) peaks was 1.22 and 1.33, in water and in the pH 9.0 buffer, respectively. In pH 2.5 buffer, the main peak was seen at 620 nm and a shoulder peak at 650 nm (**Figure 1.9d**). The ratio of the absorbances at 650 and 620 nm was 0.85. At low pH (2.5) and high salt concentration (50 mM Na<sub>2</sub>HPO<sub>4</sub>) more aggregation was seen, as the peaks appearing in the region 620 to 640 nm are due to aggregates. In a 50% ethanol/H<sub>2</sub>O mixture a peak was seen at ~ 663 nm and a shoulder peak at 597 nm, indicating that the compound was largely monomeric in this solvent (**Figure 1.9b**). UV-vis spectra were taken over the concentration range of  $3.7 \times 10^{-7}$  -  $1.2 \times 10^{-5}$  M to see the change in spectra with concentration for NiPcS4 solutions in 50% ethanol/H<sub>2</sub>O (data not shown). Beer's law was followed over the total concentration range studied.

**d. Analysis of PcS [synthesized via sulfonation method (PcS4-S) and via condensation method or the Weber-Busch (PcS4-WB) method]**

Under pH 9.0 (10 mM KH<sub>2</sub>PO<sub>4</sub> buffer) separation conditions, a solution of  $1.46 \times 10^{-2}$  M PcS4-S, made via the sulfonation method, showed a small broad peak at ~ 9 min and a larger broad peak at ~ 12 min (**Figure 1.10a**). A solution of  $1.73 \times 10^{-3}$  M showed sharper peaks at approximately the same migration time (**Figure 1.10b**).

Under pH 2.5 (50 mM Na<sub>2</sub>HPO<sub>4</sub> buffer) separation conditions, a  $1.46 \times 10^{-2}$  M solution of PcS4-S gave a single, relatively sharp peak at ~ 7 min, with a hint of a shoulder (**Figure 1.11a**). A  $1.73 \times 10^{-3}$  M solution showed a single sharp peak at 6 min

(data not shown). The profiles at 260 nm showed no additional peaks appropriate for impurities (data not shown).

PcS4-WB, made via WB method, had similar electropherograms to that of PcS4-S. Under pH 9.0 (10 mM  $\text{KH}_2\text{PO}_4$  buffer) separation conditions, a solution of  $3.78 \times 10^{-3}$  M of PcS4-WB showed a single broad peak at  $\sim 10$  min (**Figure 1.10c**). A solution of  $1.58 \times 10^{-3}$  M PcS4-WB showed a narrower peak at  $\sim 11$  min (**Figure 1.10d**). The profiles at 260 nm showed no additional peaks (data not shown). A  $1.51 \times 10^{-4}$  M solution was too dilute to give an appreciable signal (data not shown).

Under pH 2.5 (50 mM  $\text{Na}_2\text{HPO}_4$  buffer) separation conditions, a solution of  $3.78 \times 10^{-3}$  M PcS4-WB gave a tall peak at  $\sim 7$  min (**Figure 1.11b**). A  $1.58 \times 10^{-3}$  M solution showed a sharp peak at approximately the same time (data not shown). The profiles at 260 nm showed no additional peaks (data not shown).

UV-vis spectra of PcS4-S and PcS4-WB were essentially the same in all the four solvents mentioned below. The UV-vis spectra of PcS4-S are shown in **Figure 1.12** (data not shown for PcS4-WB). The spectra in water and in pH 9.0 and pH 2.5 buffers showed a broad band centered at  $\sim 625$  nm. In a 50% ethanol/ $\text{H}_2\text{O}$  mixture, two bands were seen at 694 and 659 nm. These bands are due to the monomeric species (Reynolds & Kolstad, 1976). The absence of the sharp band at 694 nm in water or in the two buffers, pH 9.0 and pH 2.5, indicated that PcS4-S was mainly aggregated.

UV-vis spectra of PcS4-S and PcS4-WB were taken at concentrations which would give the optical absorbances similar to those observed in CE separations. The UV-vis spectra indicated that PcS4-S and PcS4-WB were aggregated under the CE separation conditions, at pH 9.0, as well as at pH 2.5.

#### **Section IV.**

Characterization of sulfonated phthalocyanines by mass spectrometry and capillary electrophoresis

Journal of Porphyrins and Phthalocyanines, 2004, vol. 8, pp. 1300 - 1310.

Dabney W. Dixon, Anila F. Gill and Brian R. Sook

Department of Chemistry, Georgia State University, Atlanta, GA 30303.

#### **Abstract**

We report the characterization of sulfonated phthalocyanines using capillary electrophoresis and mass spectrometry. Derivatives investigated included the copper, cobalt, zinc and metal-free sulfonated phthalocyanines. In general, sulfonated phthalocyanines were found as aggregates in capillary electrophoresis separations, even at low concentration. Separations were much better at pH 9.0 than at pH 2.5. The addition of  $\beta$ -cyclodextrin did not alter the electropherograms significantly. The electropherograms of commercially available copper phthalocyanine-3,4',4'',4'''-tetrasulfonic acid and 4,4',4'',4'''-tetrasulfonic acid were very different, consistent with the latter compound having a structure that is not fully sulfonated. Matrix-assisted laser

desorption/ionization (MALDI) and electrospray ionization (ESI) were used to characterize the sulfonated phthalocyanines. In general, MALDI gave better results than ESI. Mass spectral evidence was obtained for a pentasulfonated species of both the metal-free phthalocyanine and zinc phthalocyanine when these species were made by sulfonation of the metal-free phthalocyanine (followed by zinc insertion in the latter case). Sulfonated tetraphenylporphyrin derivatives were used as standards for mass spectrometry and to estimate the effect of net charge on the capillary electrophoresis migration time for sulfonated tetrapyrroles. Clean separation of the sulfonated tetraphenylporphyrin derivatives [5,10,15,20-tetrakis(4-sulfonatophenyl)porphyrin (TPPS4); 5,10,15-tris(4-sulfonatophenyl)-20-phenylporphyrin (TPPS3); and 5,10-bis(4-sulfonatophenyl)-15,20-diphenylporphyrin (TPPS2a)] was observed by capillary electrophoresis.

### **Introduction.**

Sulfonated phthalocyanines (PcS) are under increasing consideration as therapeutic agents. Phthalocyanines have been used clinically as photodynamic agents in chemotherapy (Wainwright, 1996; Phillips, 1997; Sobolev et al., 2000; Allen et al., 2001; Tedesco et al., 2003). The most widely studied phthalocyanines for photodynamic therapy are the aluminum sulfonated phthalocyanines (AlPcSn) (Stranadko et al., 1999; Allen et al., 2001). The sulfonated zinc phthalocyanines have also been the focus of significant study (Brasseur et al., 1988; Fingar et al., 1993; Margaron et al., 1996; Howe & Zhang, 1997; Howe & Zhang, 1998; Halkiotis et al., 1999; Tabata et al., 2000).

Photodynamic treatment with phthalocyanines has been investigated for decontamination of red blood cell concentrates for transfusion (Ben-Hur et al., 1997; Wainwright, 2002).

Other recent studies have found that sulfonated phthalocyanines have biological activity that is not dependent on the photosensitization characteristics of the phthalocyanine. For example, the tetrasulfonated phthalocyanine without a central metal (PcS<sub>4</sub>) has been shown to inhibit transmissible spongiform encephalopathies (Priola et al., 2000). We have shown that sulfonated phthalocyanines have significant activity against vaccinia (Chen-Collins et al., 2003).

Studies in our laboratories also have shown that some commercially available sulfonated phthalocyanines have significant activity against the human immunodeficiency virus (HIV-1) (Vzorov et al., 2003). For the sulfonated zinc phthalocyanines, little difference in activity was observed as a function of the level of sulfonation of the material. For the sulfonated copper phthalocyanines, copper phthalocyanine-3,4',4'',4'''-tetrasulfonic acid tetrasodium salt [CuPcS(3444), the 1,9,16,23 isomer] was more active than copper phthalocyanine-4,4',4'',4'''-tetrasulfonic acid tetrasodium salt [CuPcS(4444), the 2,9,16,23 isomer] (Vzorov et al., 2003). These two structures ostensibly differ only in the position of a sulfonate on one of the phthalocyanine rings. Because there was no clear correlation between activity and the ostensible extent and position of sulfonation, we have characterized the molecular structure of these phthalocyanines in more detail. Specifically, we have studied copper, cobalt, zinc and metal-free sulfonated phthalocyanines using capillary electrophoresis (CE) and both matrix-assisted laser desorption/ionization (MALDI) and electrospray

ionization (ESI) mass spectrometry. Some compounds were made using the Weber-Busch template synthesis (WB) (Weber & Busch, 1965), which is expected to give a phthalocyanine with four sulfonic acid groups. Others were made via sulfonation of the parent phthalocyanine; these may be mixtures of products with various extents of sulfonation. Sulfonated tetraphenylporphyrin (TPPS<sub>n</sub>) derivatives were used for comparison of capillary electrophoresis migration times and mass spectral fragmentation patterns.

## **Experimental.**

### **Phthalocyanines and Porphyrins.**

Sulfonated phthalocyanine was available via the Weber-Busch synthesis (PcS<sub>4</sub>-WB) (Weber & Busch, 1965) and via sulfonation of phthalocyanine (PcS<sub>4</sub>-S) (Midcentury Chemicals, Chicago, IL). Co(II)PcS<sub>4</sub>, made via the Weber-Busch synthesis, was a gift from Dr. Jerry Bommer (Frontier Scientific, Logan, UT). Copper phthalocyanine-3,4',4'',4'''-tetrasulfonic acid tetrasodium salt [CuPcS(3444)] was obtained from Aldrich (St. Louis, MO). Copper phthalocyanine-4,4',4'',4'''-tetrasulfonic acid [CuPcS(4444)] was obtained from Fluka (St. Louis, MO). Sulfonated zinc phthalocyanines, synthesized either via the Weber-Busch procedure (ZnPcS<sub>4</sub>-WB) or via zinc insertion into sulfonated phthalocyanine (ZnPcS<sub>4</sub>-I), were also gifts from Dr. Bommer. Sulfonated zinc phthalocyanine was also available in a less sulfonated form from Midcentury (ZnPcS<sub>3</sub>). The sulfonated tetraphenylporphyrins (TPPS<sub>n</sub>) used were

TPPS2a (Frontier Scientific), TPPS3 (Midcentury) and TPPS4 (Aldrich). Ethylenediaminetetraacetic acid (EDTA, Aldrich) was added to some samples.

### **Capillary Electrophoresis.**

Capillary electrophoresis was performed on a Beckman P/ACE 5500 series with Beckman Gold chromatography software and a Beckman diode array detector. A fused silica capillary column (Beckman, 375  $\mu\text{m}$  o.d., 75  $\mu\text{m}$  i.d., 57 cm overall, 50 cm to detector) was built in an eCAP capillary cartridge (Beckman, 100 x 800  $\mu\text{m}$  aperture). Phosphate buffers were prepared by dissolving  $\text{NaH}_2\text{PO}_4$ ,  $\text{Na}_2\text{HPO}_4$  or  $\text{KH}_2\text{PO}_4$  in deionized water and adjusting the solution to the desired pH with phosphoric acid, NaOH or KOH. All running solutions were filtered through a 0.2  $\mu\text{m}$  membrane filter (FP-200, Gelman Science Inc., Ann Arbor, MI) before use.

New capillary columns were rinsed with 1.0 M sodium hydroxide for 1 h, then with deionized water for 20 min, then with running buffer for 30 min. The capillary column was regenerated between runs with 0.1 M sodium hydroxide for 5 min, then with deionized water for 5 - 15 min, then with the running buffer for 10 min. A sample solution was prepared by dissolving a small amount of the porphyrin or phthalocyanine (1 - 2 mg) in deionized water (0.5 mL). Further dilutions were done in water.

Separations were performed with normal polarity from the inlet vial (anode) to the outlet vial (cathode) for high pH and reverse polarity for low pH separations. Pressure injections of 6 s were used. Voltages were chosen in the range of 20 - 30 kV. The column temperature was approximately 24 °C.

### **Mass Spectrometry.**

Electrospray ionization experiments were performed using a Finnegan MAT (San Jose, CA) LCQ quadrupole ion trap mass spectrometer in positive mode, and the mass range scanned was 200 - 2000 Da. Samples were prepared by taking approximately 3 mg of sample and dissolving in 200  $\mu$ L MeOH. The solution was then diluted 10-fold with 0.5% acetic acid and 50:50 H<sub>2</sub>O:MeOH. The spray voltage was 4.5 kV and the flow rate was 3  $\mu$ L/minute. For MS<sup>n</sup>, the collision energy was 60%. Negative ion mode electrospray analysis of porphyrins was also performed on a Micromass Quattro LC triple quadrupole instrument (Beverly, MA) with Ar as the collision gas and a collision voltage of 60 V.

MALDI experiments were performed using an ABI Voyager DE-Pro (Applied Biosystems, Warrington, UK) MALDI reflectron time-of-flight spectrometer. The mass range scanned was 200 - 4000 Da in positive and negative modes. Some samples were run with 2,4,6-trihydroxyacetophenone (THAP) and EDTA as the matrix. The THAP matrix was prepared as a 10 mg/ml solution in 50:50 mixture of 0.14 M EDTA in H<sub>2</sub>O and acetonitrile. The sample was dissolved in MeOH (0.5 mg/ml). The sample solution was mixed with the matrix solution in a 1:20 ratio and the resulting solution spotted on the MALDI target plate. Some samples were run with  $\alpha$ -cyano-4-hydroxycinnamic acid (CHCA) as the matrix. CHCA was prepared at 10 mg/ml in a 50:50 mixture of MeOH and acetonitrile. The sample was dissolved in MeOH (0.5 mg/ml) and mixed with CHCA. The sample solution was mixed with the matrix solution in a 1:20 ratio and

spotted on the MALDI target plate. Throughout the text, peaks are rounded to the nearest unit.

### **Sulfonation of 5,10,15,20-tetra(2-naphthyl)porphyrin.**

The porphyrin was synthesized following the literature (Rocha Gonsalves et al., 1991). Sulfonation was performed following the procedure of Sutter et al. (Sutter et al., 1993). 5,10,15,20-Tetra(2-naphthyl)porphyrin (200 mg, 0.24 mmol) was added to 5 ml of concentrated sulfuric acid (Aldrich). The reaction mixture was heated at 100 °C for 20 h. Ice was added to the green mixture. The acid was neutralized carefully by the addition of 50% NaOH solution and ice until the color turned red (*caution, very exothermic, keep the flask on ice and add the NaOH very slowly*). The pH of the solution was adjusted to 7. The liquid was evaporated under vacuum. The resulting solid was pulverized and the sulfonated porphyrin was extracted into methanol with a Soxhlet apparatus for approximately 24 h. Evaporation of the solvent gave solid material that was purified by a Sephadex LH-20 (Pharmacia) column (6 g of Sephadex for 100 mg of porphyrin) using methanol as the eluent. The column was prepared by putting the Sephadex in methanol and was used immediately. The purple-colored band (continuous, streaking) was collected and evaporated to obtain the desired product (T2NapS).

## Results.

### Sulfonated Tetraphenylporphyrins.

Initial background studies were performed with sulfonated tetraphenylporphyrins. Partial sulfonation of TPP gives a mixture of sulfonated derivatives (all sulfonic acids in the 4-position): the monosulfonated (TPPS1), disulfonated (*adjacent*, TPPS2a and *opposite*, TPPS2o), trisulfonated (TPPS3) and tetrasulfonated (TPPS4) derivatives. These compounds, which can be cleanly separated by column chromatography on silica C-18 (Sutter et al., 1993; Rubires et al., 1999) or pyridine-chloroform-water on silica gel (Winkelman et al., 1967; Fleischer et al., 1971; Zhang et al., 2003), are commercially available. Because these compounds can be isolated as individual pure species, they can be used as standards to assess the fragmentation patterns of sulfonated tetrapyrroles.

The negative ion mode MALDI spectrum of TPPS4 ( $M^-$ , CHCA) showed the molecular ion at 934 Da, with the mono-, di-, tri-, and tetrasodium salts at intervals of +22 Da. No peaks corresponding to loss of  $SO_2$  (870) or  $SO_3$  (854) were observed. The negative ion MALDI spectrum of TPPS3 (CHCA) also gave a clean molecular ion, again with no loss of  $SO_2$  or  $SO_3$ .

The positive ion mode ESI spectrum of TPPS4 showed the molecular ion at 935 ( $M+H^+$ ) Da, with the mono-, di-, tri-, and tetrasodium salts at intervals of +22 Da. There was no peak at 855 Da, indicating that TPPS4 did not lose  $SO_3$ . MS/MS analysis of the 935 Da peak showed loss of  $SO_2$  (871),  $SO_3$  (855) and  $PhSO_3$  (778).  $MS^3$  analysis of the 855 fragment showed loss of  $SO_2$  (791),  $SO_3$  (775) and a peak at 711 which might be attributed to loss of both  $SO_2$  and  $SO_3$ . In the negative ion mode ESI spectra, TPPS4,

TPPS3, TPPS2a and TPPS2o all showed only very small peaks for the molecular ions; by far the most prominent peaks were for the doubly charged ions. The spectra of TPPS2o and TPPS2a were identical. MS/MS of the 386  $[(M-2H^+)^{-2}]$  peaks of TPPS2a and TPPS2o were also identical, with the largest peaks for loss of  $SO_3$  and  $SO_3 + SO_2$ .

The TPPSn isomers were also used as standards for capillary electrophoresis separation. TPPS2a, TPPS3 and TPPS4 separated by capillary electrophoresis at pH 9.0 with migration times of 4.0, 5.0, and 6.4 min, respectively, both individually and in a mixture of all three (**Figure 1.13**).

As an example of a more complicated system, the sulfonation product of 5,10,15,20-tetra(2-naphthyl)porphyrin T2NapS was studied. Sulfonation with concentrated sulfuric acid at 100 °C for 20 h gave a number of products, as shown by a series of peaks in the CE. The negative ion MALDI (CHCA) showed the tetrasulfonic acid (1134) and its mono-, di-, and trisodium salts as well as the pentasulfonic acid (1214) and its mono-, di-, tri-, and tetrasodium salts (**Figure 1.14A**).

A dimer of the tetrasulfonic acid with three sodium ions was seen starting at 2334, with salts bearing 4, 5, 6, and 7 sodium ions at increments of +22 (**Figure 1.14B**). Smaller peaks attributable to the dimer of the pentasulfonic acid with five sodium ions centered at around 2539 with salts bearing 6, 7, 8, and 9 sodium ions were also seen. Finally, a heterodimer of the tetrasulfonic/pentasulfonic acid with four sodium ions was seen centered at 2437, with salts bearing 5, 6, 7 and 8 sodium ions at increments of +22.

### **Sulfonated Phthalocyanine.**

PcS4-WB (synthesized via the Weber-Busch process) and PcS4-S (synthesized via sulfonation of phthalocyanine) each appeared as one peak by capillary electrophoresis, eluting at 11 min (pH 9). Because sulfonated phthalocyanines aggregate easily, aggregation was assessed by taking the UV/vis spectra at optical absorbances very similar to those in the CE experiments. PcS4-WB and PcS4-S in water, pH 2.5 buffer and pH 9.0 buffer all showed a broad band between 550 and 750 nm with a  $\lambda_{\text{max}}$  at about 640 nm and a shoulder at about 655 nm. The peak at shorter wavelengths has been ascribed to an aggregated form (Reynolds & Kolstad, 1976), indicating that these species are largely aggregated under CE conditions.

The negative ion MALDI mass spectrum (THAP) of PcS4-WB showed the molecular ion at 834 ( $M^-$ ) Da as well as the mono-, di-, tri-, and tetrasodium salts (**Figure 1.15A**). A peak at 754 was seen, corresponding to loss of sulfonate. Throughout this work we assume that phthalocyanines synthesized via the Weber-Busch procedure are the tetrasulfonates, though trisulfonates present in the product would give the same mass spectrum as loss of  $\text{SO}_3$  in the mass spectrometer itself. No peak at 770, corresponding to loss of  $\text{SO}_2$ , was observed. Spectra with CHCA, CHCA/EDTA and THAP/EDTA were generally similar. No peaks attributable to dimers or trimers were seen (CHCA/EDTA or THAP/EDTA).

The negative ion MALDI mass spectrum (CHCA) of PcS4-S showed the molecular ion at 834 Da as well as the mono-, di-, and trisodium salts (**Figure 1.15B**). Of interest were peaks at 911 - 914 Da, appropriate for the pentasulfonated

phthalocyanine (M of 914). Peaks at 933 - 936 Da appropriate for the monosodium salt of the pentasulfonated species were also seen. The peak at 779 is most likely a matrix artifact, as it was generally observed in compounds tested under these conditions. In positive ion mode, the most prominent peaks in the spectrum were that of the pentasulfonic acid and its four sodium salts.

### **Sulfonated Cobalt Phthalocyanine.**

CoPcS4-WB (synthesized via the Weber-Busch process) was studied using negative ion mode MALDI mass spectrometry (CHCA, **Figure 1.16**). The molecular ion (891,  $M^-$ ) and its mono- and disodium (935) salts were seen. Small peaks were observed for loss of  $SO_2$  and loss of  $SO_3$  (827 and 811 Da, respectively). The dimer was also observed at 1782 Da [ $(2M)^-$ ]. The spectrum in THAP/EDTA was very similar to that in CHCA, with an additional small peak attributed to the trimer.

### **Sulfonated Zinc Phthalocyanine.**

Three forms of sulfonated zinc phthalocyanine were studied, that made via Weber-Busch synthesis (ZnPcS4-WB) and two samples made via sulfonation of phthalocyanine. One of the latter was a mixture with an average of less than four sulfonates per molecule (ZnPcS3) and the other was a mixture with an average of about four sulfonates per molecule, made by sulfonation of the metal-free phthalocyanine, followed by insertion of zinc (ZnPcS4-I). The CE of ZnPcS3 ( $2.5 \times 10^{-3}$  M) at pH 9.0 showed a series of sharp peaks from 7 to 14 min (**Figure 1.17**). This separation was

substantially better than that at pH 2.5. The addition of  $\beta$ -cyclodextrin made very little difference in the electropherogram. The electropherograms of ZnPcS4-I and ZnPcS4-WB were very different from those of ZnPcS3. At an injection concentration of approximately  $2.5 \times 10^{-4}$  M, the electropherograms of ZnPcS4-I and ZnPcS4-WB were dominated by a single broad peak which appeared at about 10 min. The substantial difference between the electropherograms of ZnPcS3, and ZnPcS4-I and ZnPcS4-WB might be due to differential aggregation of the samples. Previous studies have shown that the presence of many isomers in a ZnPcSn mixture reduces the tendency to aggregate; ZnPcSn mixtures averaging 3-4 sulfonates are generally less aggregated than ZnPcS4 (Brasseur et al., 1987; Martin et al., 1991; Rajendiran & Santhanalakshmi, 2002; Kuznetsova et al., 2003). Aggregation was assessed by taking the UV/vis spectra at optical absorbances very similar to those in the CE experiments. ZnPcS4-I and ZnPcS4-WB in pH 9.0 buffer both showed a broad band between 550 and 750 nm with a  $\lambda_{\text{max}}$  at about 630 nm and a shoulder at about 675 nm. The peak at shorter wavelengths has been ascribed to an aggregated form (Brasseur et al., 1987; Martin et al., 1991; Spikes et al., 1995; Rajendiran & Santhanalakshmi, 2002), indicating that these compounds were largely aggregated under CE conditions. The UV/vis spectra of ZnPcS3 in water, in buffers at pH 9.0 and 2.5, and in DMSO were all essentially the same, with a major band at approximately 675 nm; this has been previously identified as the spectrum of the monomeric form of ZnPcS3 (Brasseur et al., 1987; Martin et al., 1991; Rajendiran & Santhanalakshmi, 2002). Thus, it appears that ZnPcS3 is not aggregated under CE conditions.

In the negative ion mode MALDI (CHCA/EDTA), ZnPcS4-WB showed the molecular ion (896 Da,  $M^-$ ), as well as the mono- and disodium salts (**Figure 1.18**). An intense peak ascribed to loss of  $SO_3$  was also seen (816 Da). The spectrum in CHCA without EDTA was not as clear. The spectrum in the THAP/EDTA matrix was similar to that in CHCA/EDTA, except that no loss of  $SO_3$  was seen.

ZnPcS4-I (negative ion mode, CHCA) showed the molecular ion, as well as the mono- and disodium salts (**Figure 1.19**). Small peaks attributable to loss of  $SO_2$  and  $SO_3$  were seen (832 and 816 Da). A series of peaks between 972 and 979 were appropriate for a pentasulfonated species ( $M$  at 976 Da). The monosodium salt was also seen. A dimer of the tetrasulfonic acid was seen at approximately 1792, with the mono-, di-, and trisodium salts (**Figure 1.20**). Small peaks attributable to the dimer of the pentasulfonic acid at around 1952 with the mono- and disodium salts were also seen. Finally, a heterodimer of the tetrasulfonic/pentasulfonic acid was seen at approximately 1872, with the mono-, di-, and trisodium salts. A few very small peaks attributable to dianionic dimers were seen, e.g., 929 [(tetrasulfonic acid dimer + 3 Na) $^{-2}$ ] and 776 [(tetrasulfonic acid dimer - 3  $SO_3$ ) $^{-2}$ ]. These peaks are differentiable from those due to monomeric phthalocyanine species because they have added or lost an uneven number of at least one molecular group from the dimer (e.g., addition of 3 Na or loss of 3  $SO_3$  giving the appearance of the addition of 1.5 Na or loss of 1.5  $SO_3$ , respectively). With THAP/EDTA as the matrix, ZnPcS4-I showed peaks at 896 and 918, appropriate for the molecular ion and the corresponding monosodium salt, respectively. A peak for loss of  $SO_2$  from the tetrasulfonic acid was seen. As for the spectra with CHCA as a matrix, a

peak appropriate for the pentasulfonic acid was observed. Running the sample with added  $\text{Na}_2\text{SO}_4$  in the matrix (CHCA, negative ion mode) did not change the relative intensity of the peaks, consistent with the assignment of the peak attributed to the pentasulfonic acid as the molecular species, rather than a salt of the tetrasulfonated phthalocyanine and sulfate.

### **Sulfonated Copper Phthalocyanine.**

CuPcS(3444) and CuPcS(4444) were compared using both CE and mass spectrometry. Capillary electrophoresis of CuPcS(3444) showed a major peak eluting at 9.5 min (**Figure 1.21A**). The UV/vis spectra of CuPcS(3444) in water and in buffer (**Figure 1.22**) at pH 9.0 were essentially the same with bands at 660 nm attributed to the monomer and 625 nm attributed to the aggregated form (Zelina et al., 1999). CuPcS(3444) in DMSO was quite different than that in aqueous solution, with a major band at approximately 675 nm (**Figure 1.22A**); Rusling has proposed that the compound is entirely monomeric in DMSO (Zelina et al., 1999). Capillary electrophoresis of CuPcS(4444) showed a single, comparatively broad peak, centered at 5.3 min (**Figure 1.21B**). The UV/vis spectra of CuPcS(4444) in water and in buffer at pH 9.0 were essentially the same, showing broad bands centered at 605 and 695 nm. In DMSO, the bands remained very broad, with a short, sharp peak at 672 nm, presumably attributable to monomeric phthalocyanine (**Figure 1.22B**). The UV/vis spectra are consistent with significant aggregation of CuPcS(4444), even in DMSO.

CuPcS(3444) was studied using positive and negative ion modes with both MALDI and ESI mass spectrometry. In the positive ion MALDI (CHCA/EDTA), the parent ion and the mono-, di-, tri-, and tetrasodium species were seen (**Figure 1.23**). No peaks corresponding to loss of SO<sub>2</sub> or SO<sub>3</sub> were seen. Clear peaks for the dimers and 3 to 7 sodium ions were seen. Peaks were also seen for the trimers with 5 to 10 sodium ions; no peaks corresponding to the tetramer and its sodium salts were observed. Negative ion mode MALDI mass spectrometry (CHCA/EDTA) also showed the parent ion, and the mono-, di-, and trisodium salts, but no loss of SO<sub>2</sub> or SO<sub>3</sub>. Clear peaks for the dimers and 1 to 7 sodium ions were seen. No peaks for the trimers were seen with negative ion mode MALDI. Neither positive nor negative ESI showed the molecular ion.

Mass spectra of CuPcS(4444) were taken using positive and negative ion MALDI and positive and negative ion ESI. In no case was a peak for the molecular ion observed. The positive ion MALDI (CHCA) gave peaks which could be attributed to the parent CuPc (575 Da, no sulfonic acids) and CuPc with one sulfonic acid (655 Da); a small peak which might be attributable to CuPc with two sulfonic acids was also seen (735 Da). There was no evidence for trisulfonated or tetrasulfonated species. Negative ion MALDI (CHCA) did not give a good spectrum. Negative ion MALDI with CHCA/EDTA again gave a peak that could be attributed to the parent CuPc (no sulfonic acids) but no clear peaks for any monomeric sulfonated species with a single negative charge. Significant peaks were also observed for an extensive series of dimers with a net negative charge of -1 and varying net numbers of sulfonic acid groups and sodium ions. The negative ion

ESI showed peaks which could be attributed to CuPc, the parent with one sulfonic acid, and to the doubly charged tetrasulfonic acid species.

## **Discussion.**

### **Capillary Electrophoresis.**

Previous separations of sulfonated phthalocyanines as a function of pH have used both low (pH 2.5) (Barbosa et al., 1997) and high (pH 9 – 10.5) (Tapley, 1995; Schofield & Asaf, 1997; Pokric et al., 1999) pH buffers. The studies herein indicate that the phthalocyanine components are separated substantially more readily at high pH than at low pH. The addition of  $\beta$ -cyclodextrin (Andrighetto et al., 2000) did not alter the electropherograms significantly. Schofield and Asaf have previously observed that the addition of acetonitrile or 10 mM ammonium acetate to a 10 mM  $\text{KH}_2\text{PO}_4$  (pH 9.0) buffer also had little effect on the separation of  $\text{ZnPcS}_n$  (Schofield & Asaf, 1997).

Sulfonated phthalocyanines are prone to aggregation, even at low concentrations. This can give electropherograms that depend on the concentration of the phthalocyanine. It can also give electropherograms that show very little separation of a mixture of compounds because the individual species in the mixture are aggregated under the capillary electrophoresis conditions. The propensity of the compounds to stack under CE conditions was investigated by taking the UV/vis spectrum of the phthalocyanines with the same buffer and same net absorbance as that found in the capillary electrophoresis experiments. The optical bands indicated substantial dimer or aggregate for most of the phthalocyanines. For example, optical spectroscopy indicated that both PcS4-WB and

PcS4-S were found in the dimer/aggregated state. Both also had very similar capillary electrophoresis migration times, with a single broad peak, presumably due to the aggregated mixture. A very similar situation was observed for ZnPcS4-I and ZnPcS4-WB. Again, optical spectroscopy indicated that both of these phthalocyanines were found in the dimer/aggregated state and both also had very similar capillary electrophoresis migration times, with a single broad peak. In contrast, the UV/vis spectra of ZnPcS3 indicated that this compound was found as the monomer under CE conditions. The ZnPcS3 sample has a substantial number of components, which reduces aggregation compared to the more symmetrical ZnPcS4, even though ZnPcS3 has a smaller average net charge. It has been observed previously that ZnPcS<sub>n</sub> mixtures averaging 3-4 sulfonates are generally less aggregated than ZnPcS4 (Brasseur et al., 1987; Martin et al., 1991; Rajendiran & Santhanalakshmi, 2002; Kuznetsova et al., 2003). van Lier and co-workers have noted that an isomeric mixture of sulfonated phthalocyanines obtained by sulfonation of zinc phthalocyanine was ten times more active in photosensitization of V-79 Chinese hamster cells than the homogeneous derivative prepared via the Weber-Busch synthesis (Brasseur et al., 1988), presumably because the former preparation was more monomeric.

The difference in the electropherograms of CuPcS(3444) and CuPcS(4444) was significant. The major peak for CuPcS(3444) appeared at 9.5 min. CuPcS(4444) showed no peak at this migration time; all the material appeared as a broad peak coming earlier at 5.3 min. The earlier migration time indicates that the average net charge on the phthalocyanine ring is less than -4. In a capillary electrophoresis study of AlPcS<sub>n</sub>, Pokrić

et al. observed approximately 50 seconds separation between each of the mono-, di-, tri-, and tetrasulfonated species (20 mM 3-cyclohexylamino-1-propanesulfonic acid, pH 10.5 buffer) (Pokric et al., 1999). In our study of sulfonated tetraphenylporphyrins, we observed approximately two minutes separation between TPPS2a, TPPS3 and TPPS4. These three derivatives are monomeric at optical concentrations (absorbance < 0.1) at pH values  $\geq 7$  (Corsini & Herrmann, 1986; Rubires et al., 1999; Zhang et al., 2003). Both Pokrić's data and our data indicate that sulfonated tetrapyrroles can separate cleanly as a function of net charge in a homologous series. However, our data on the copper and zinc sulfonated phthalocyanines indicate that the phthalocyanines do not separate cleanly if they are aggregated.

The difference in the structure of CuPcS(3444) and CuPcS(4444) was also indicated by their spectra in DMSO. CuPcS(3444) appeared monomeric, with a peak at 675 nm, as reported previously by Rusling and co-workers (Zelina et al., 1999). CuPcS(4444), in contrast, showed only a small peak attributable to the monomer in DMSO (672 nm), with the majority of the material giving a broad peak from 500 to 750 nm (**Figure 1.22B**).

### **Mass Spectrometry.**

Mass spectrometry has been used to characterize sulfonated phthalocyanines. A number of studies have only reported the parent ion, including those of AlPcS2 via positive mode secondary ion MS (Beeby et al., 1992); ZnPcS4 via negative ion ESI (Beeby et al., 2001); trisulfonated phthalocyanines and their zinc chelates via ESI and

MALDI (Kudrevich et al., 1997); and the alkylammonium salts of various metallo PcS using ESI (Sanchez et al., 2001). In their characterization of AlPcS<sub>2</sub> using negative ion FAB mass spectrometry, Ambroz observed the parent ion and reported extensive fragmentation (Ambroz et al., 1991). Bressan and co-workers used positive ion ESI to characterize Ru(II) tetrasulfophthalocyanine made via template-catalyzed condensation (Bressan et al., 2000). They observed the parent tetrasulfonic acid as well as the parent with one, two, three, and four sodium ions. A peak attributed to five sodium ions was also observed. Smyth and co-workers have investigated the mass spectrometry of CuPcS(3444) (Conneely et al., 2001). The ESI spectrum showed the parent ion as a major peak at 896 and MS<sup>n</sup> consecutive losses of 64 (SO<sub>2</sub>), 80 (SO<sub>3</sub>), 80 (SO<sub>3</sub>) and 80 (SO<sub>3</sub>) Da. Electron autodetachment from NiPcS and ZnPcS has been studied by FT-ICR (Arnold et al., 2003).

Herein, we used positive and negative ion mode ESI and MALDI to characterize the sulfonated phthalocyanines. In general, negative ion MALDI conditions gave the best spectra. In all cases, sodium salt peaks were seen. Peaks were often seen for loss of SO<sub>3</sub>, and sometimes for loss of SO<sub>2</sub> as well. Both CHCA and THAP matrices usually gave good spectra, although often one was better than the other for a given compound. EDTA served to chelate any dications that might induce aggregation. In a number of cases, the addition of EDTA gave clearer sodium salt patterns, which helped in interpretation of the data.

Sulfonated phthalocyanine made via the Weber-Busch procedure (PcS<sub>4</sub>-WB) and via sulfonation of phthalocyanine (PcS<sub>4</sub>-S) showed somewhat different mass spectra.

The former was largely the tetrasulfonic acid. The parent peak was at 834 Da, indicating that this was the radical ion; Smyth and co-workers have observed radical ions in the mass spectra of sulfonated copper phthalocyanines (Conneely et al., 2001). In contrast to PcS4-WB, PcS4-S showed peaks appropriate for a pentasulfonic acid, indicating that one of the peripheral rings on the structure had sulfonated more than once. Although a previous study has noted mixtures of a sulfonated copper phthalocyanine that seem to have high levels of sulfonation (Oppenheimer, 1981), this is, to our knowledge, the first report of mass spectral evidence for a pentasulfonic acid in a mixture of sulfonated phthalocyanines. Sulfonation of aromatic rings can give species with more than one sulfonic acid on a given ring (Cerfontain et al., 1994b). Porphyrins with more than one sulfonic acid per peripheral ring, made via sulfonation of the parent porphyrin, have been reported (Hoffmann et al., 1990; Sutter et al., 1993; Rocha Gonsalves et al., 1996). It has been reported that the Weber-Busch synthesis can give phthalocyanines with more than a total of four sulfonic acids if some of the starting sulfonated phthalic acid derivative carries two sulfonic acid groups (Sanderson, 2000).

ZnPcS4-WB gave peaks appropriate for the tetrasulfonic acid, as expected because this molecule was made via template synthesis. ZnPcS4-I also showed peaks for the tetrasulfonic acid, as well as its dimer. A peak corresponding to loss of 80 Da could either be loss of SO<sub>3</sub> from the tetrasulfonic acid, or trisulfonic acid in the mixture. Of particular interest was a peak that was appropriate for the pentasulfonic acid. This appeared both as a monomer and as a dimer. A series of peaks appropriate for the mixed tetrasulfonic/pentasulfonic acid heterodimer was also seen.

Mass spectrometry was used to compare CuPcS(3444) and CuPcS(4444). CuPcS(3444) gave a spectrum readily attributed to the copper tetrasulfonated phthalocyanine. No loss of SO<sub>2</sub> or SO<sub>3</sub> was observed in either the positive or negative ion MALDI. Smyth and co-workers previously observed peaks attributable to the loss of both SO<sub>2</sub> and SO<sub>3</sub> from CuPcS(3444) (Conneely et al., 2001). Our mass spectrometry conditions appear to result in less fragmentation than those of Smyth and co-workers.

CuPcS(4444) showed a very different mass spectrum than CuPcS(3444). A very large number of peaks were observed, consistent with dimers bearing various numbers of sulfonic acids, and the sodium salts corresponding to these species. Thus, the CE, UV/vis spectroscopy and mass spectrometry are all consistent with the conclusion that CuPcS(4444) is a mixture of phthalocyanines, dominated by species with fewer than four sulfonic acids per ring. This mixture is observed in the dimer/aggregated form by UV/vis, mass spectrometry and CE.

The negative ion MALDI mass spectrum of the sulfonated naphthyl porphyrin showed peaks appropriate for the tetra- and pentasulfonic acids, as well as their homodimers and the tetrasulfonic/pentasulfonic acid heterodimer. Small peaks for the trimers were also observed. Formation of the pentasulfonic acid reflects the ease with which more than one sulfonic acid can be added to the naphthyl system. Work of Cerfontain and colleagues has shown that the model compound 2,2'-binaphthalene sulfonates initially at the 8-position, followed by sulfonation at the 8' position, and then at the 6- or 4-positions. Six equivalents of SO<sub>3</sub> (in CH<sub>2</sub>Cl<sub>2</sub> at 22 °C, 40 min) gave only 9% of the species with one sulfonic acid on each ring, 34% of species with a total of three

sulfonic acids (two on one ring) and 57% of species with a total of four sulfonic acids (two on both rings) (Cerfontain et al., 1994a). Thus, addition of more than one sulfonic acid to a naphthyl ring is facile.

### **Conclusions.**

Capillary electrophoresis separation of sulfonated phthalocyanines is substantially better at high than at low pH. In general, the compounds are aggregated under CE conditions, making analysis of mixtures of compounds difficult. Using mass spectrometry, evidence was found for a pentasulfonic acid for molecules synthesized by sulfonation of phthalocyanine itself (PcS4-S and ZnPcS4-I). Spectra of dimers of the sulfonated phthalocyanines were useful in characterizing the mixtures. Overall, both ESI and MALDI are effective for mass spectral characterization of sulfonated phthalocyanines, with negative mode MALDI usually giving the best data.

### **Acknowledgments.**

This study was supported by NIH grant AI45883. We thank Drs. David Bostwick and Siming Wang for help with the mass spectrometry, Drs. Peter Hambright and Jerry Bommer for samples and useful conversations, Dr. Lingamallu Giribabu for assistance with the synthesis and Atia Alam and Sarah Shealy for technical assistance.

The manuscript was compiled by Dr. D. W. Dixon. Brian R. Sook interpreted the mass spectra. Anila F. Gill recorded the UV-vis spectra and capillary electrophoresis data.

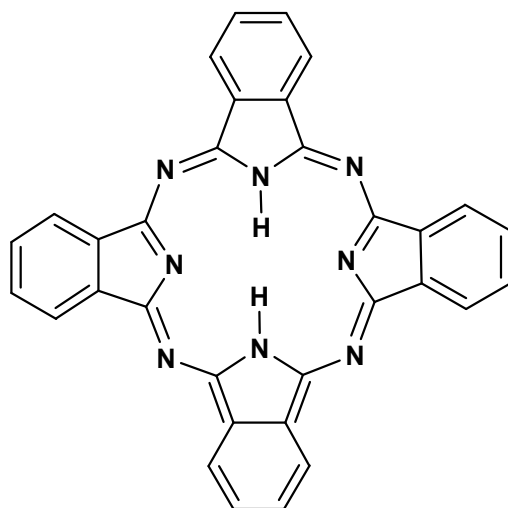


Figure 1.1. Structure of phthalocyanine.

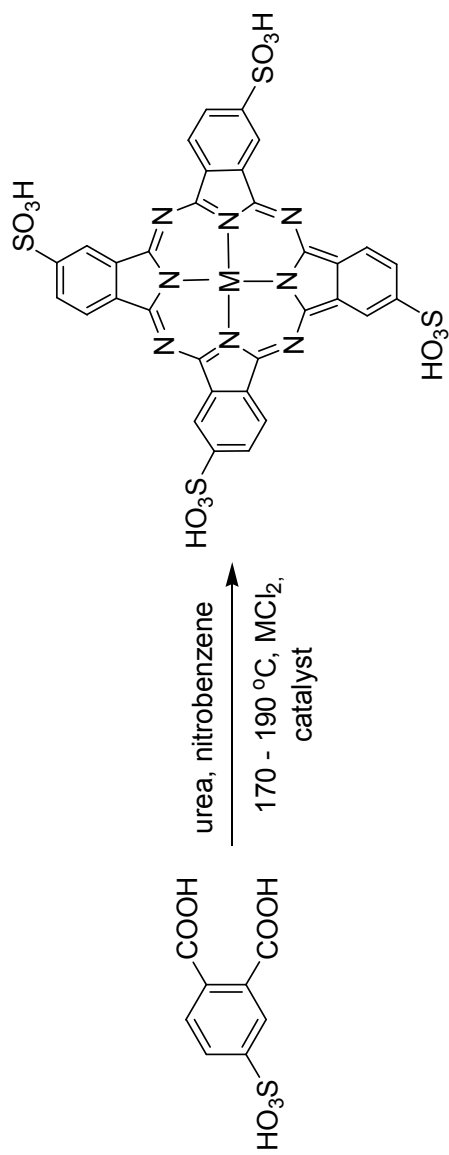
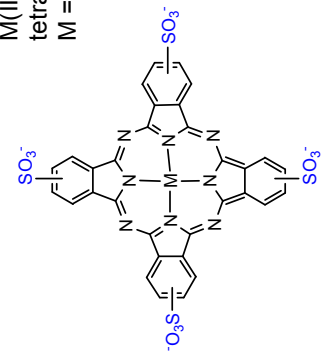


Figure 1.2. Weber and Busch method for the synthesis of sulfonated phthalocyanines.

M(II) Phthalocyanine  
tetrasulfonicacid (4444)  
M = Metal



4-Sulfophthalic acid

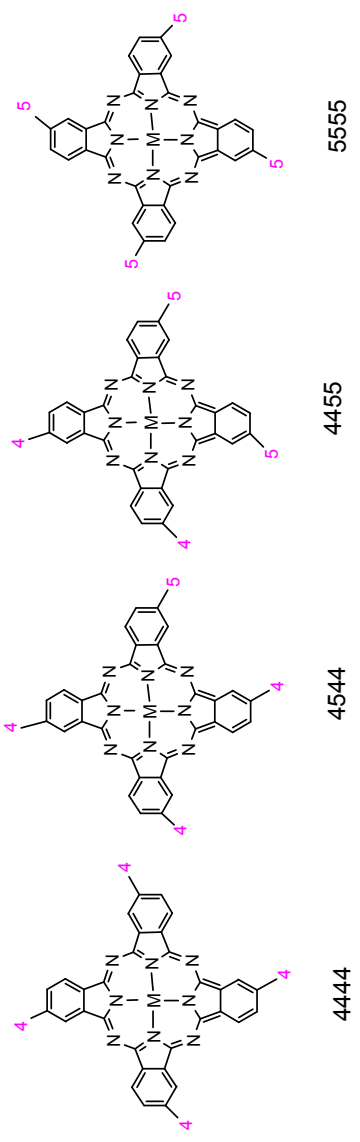
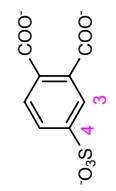


Figure. 1.3. Possible isomers when the starting material, phthalic acid, has the substituent, sulfonic acid, at the 4- or the equivalent 5-position.

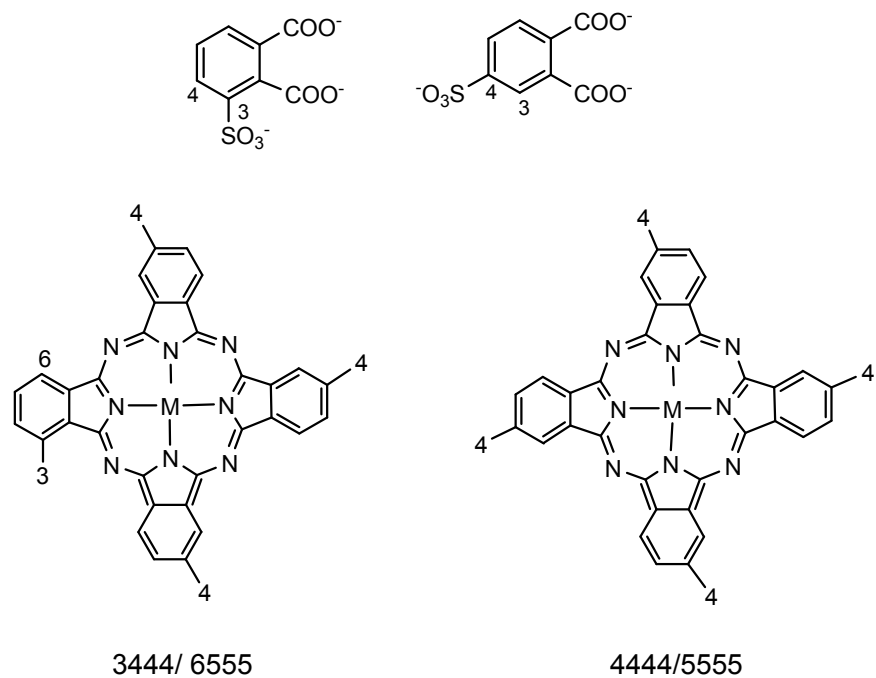


Figure. 1.4. Examples of some of the possible isomers when the starting material, phthalic acid, has the substituent, sulfonic acid, at the 3- and 4- position.

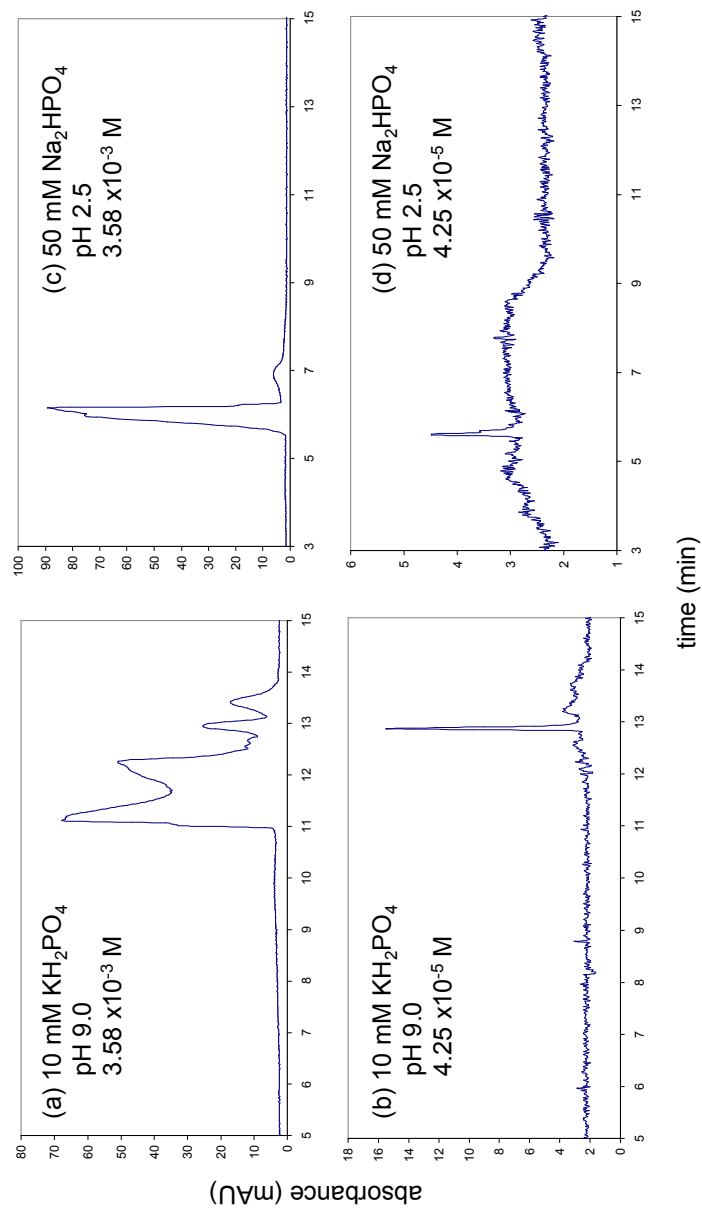


Figure 1.5. Capillary electropherograms of CuPeS(3444).

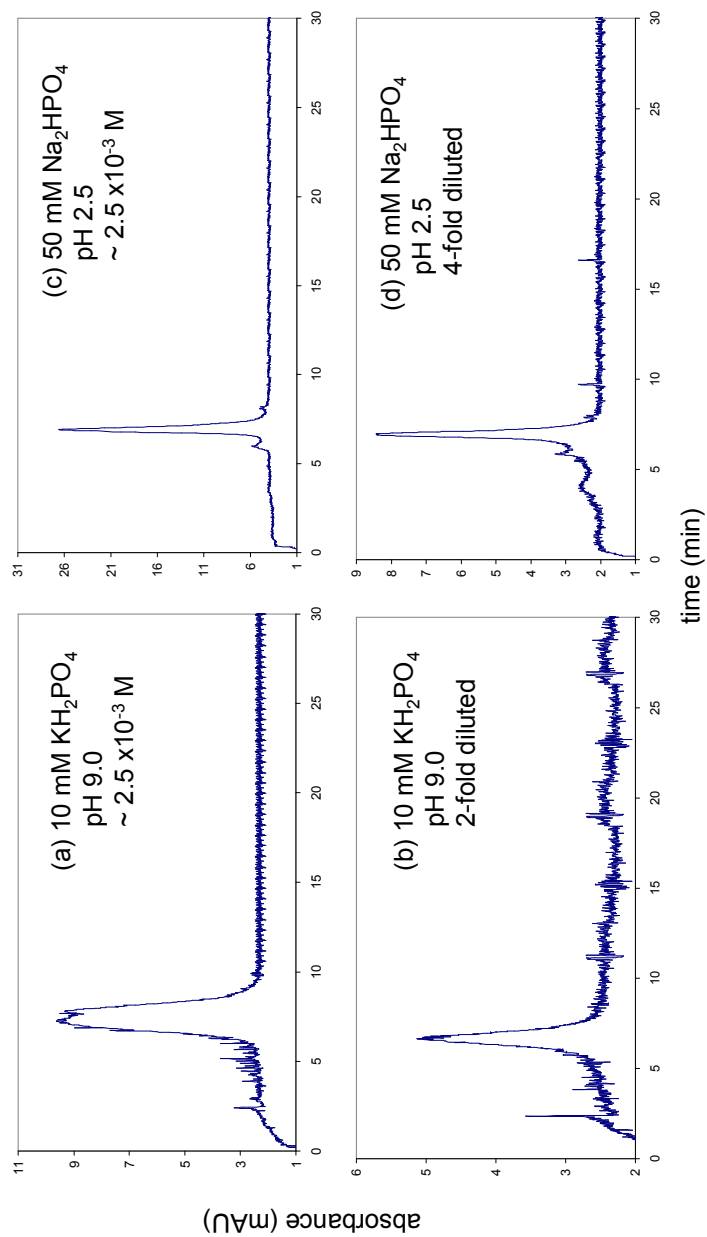


Figure 1.6. Capillary electropherograms of CuPcS(4444).

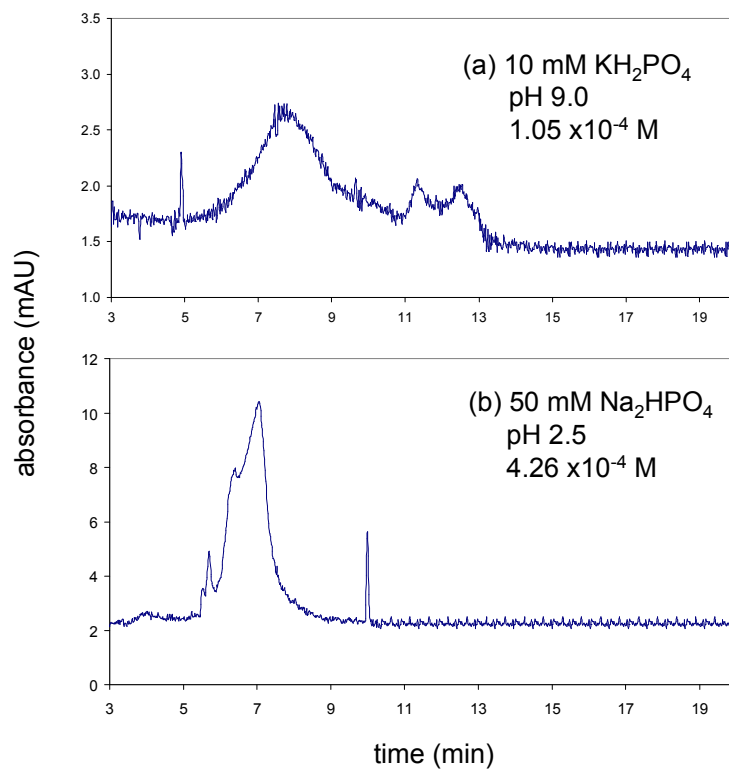


Figure 1.7. Capillary electropherograms of ZnPcS4.

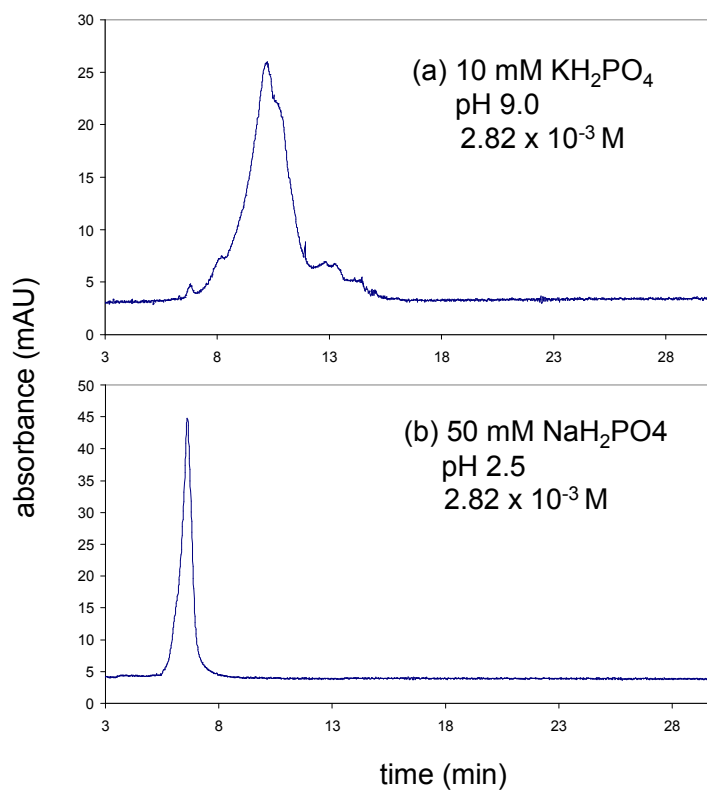


Figure 1.8. Capillary electropherograms of NiPcS4.

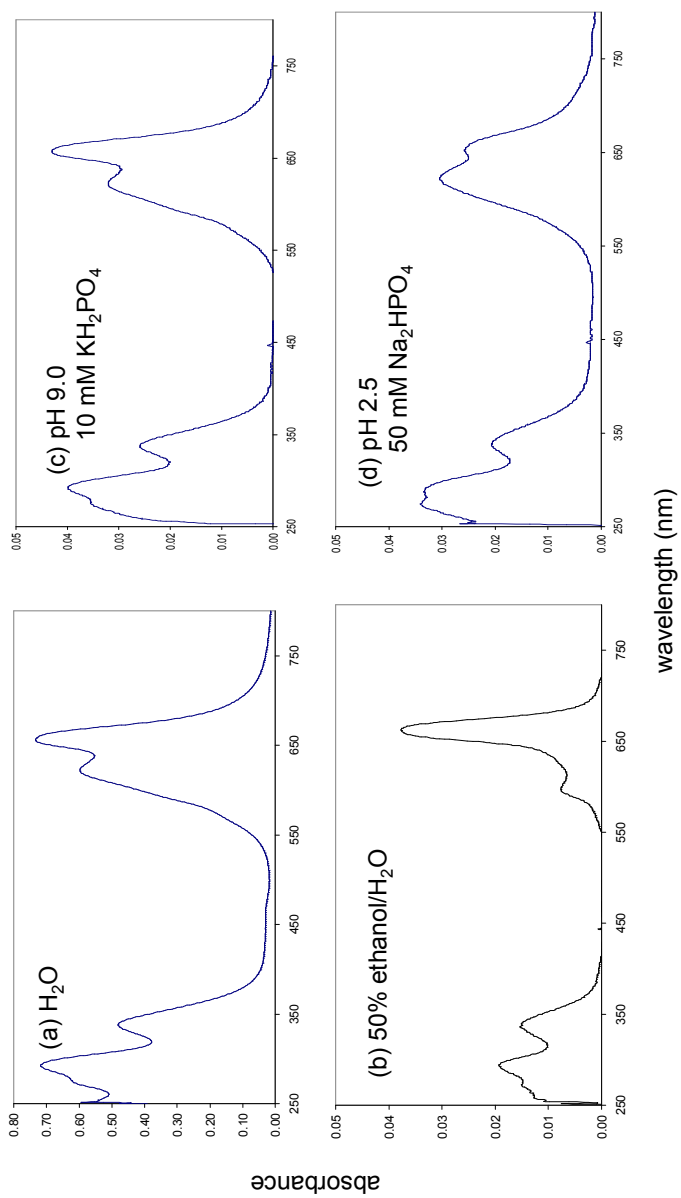


Figure 1.9. UV-vis spectra of NiPcS4.

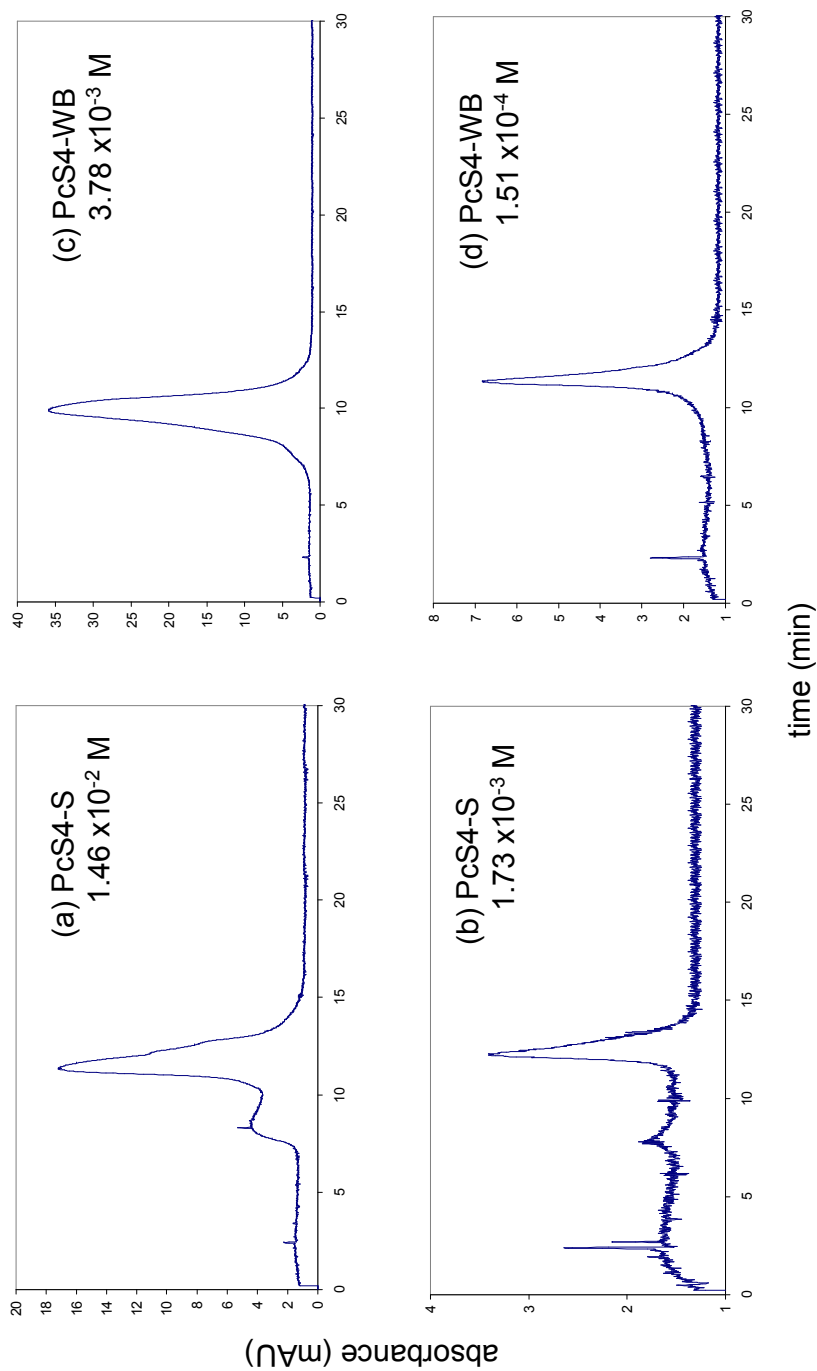


Figure 1.10. Capillary electropherograms of PcS4(S) and PcS4-WB. The separation buffer is 10 mM  $\text{KH}_2\text{PO}_4$ , pH 9.0

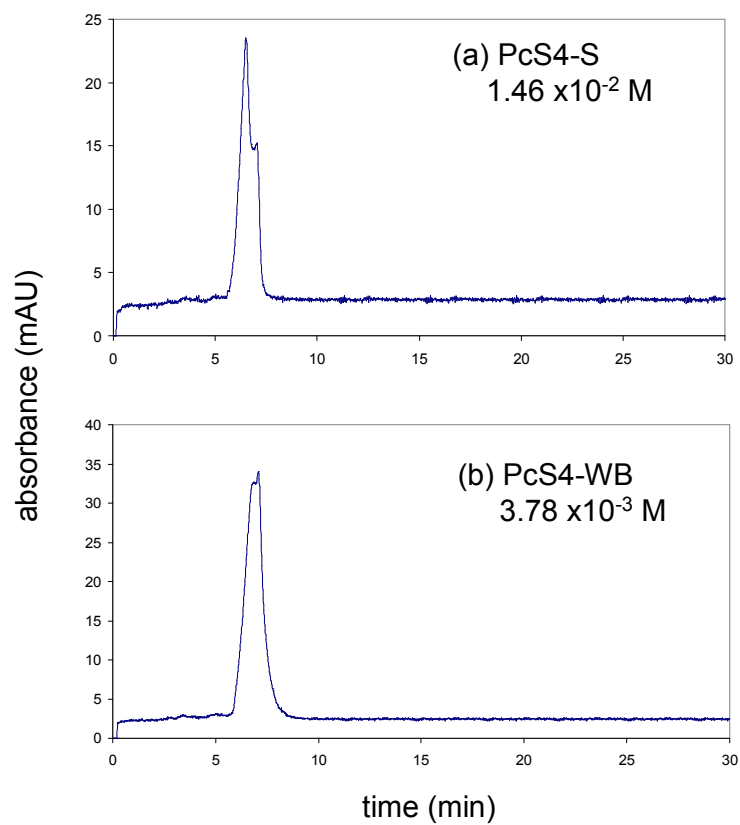


Figure 1.11. Capillary electropherograms of PcS4-S and PcS4-WB. The separation buffer is 50 mM  $\text{Na}_2\text{HPO}_4$  buffer, pH 2.5.

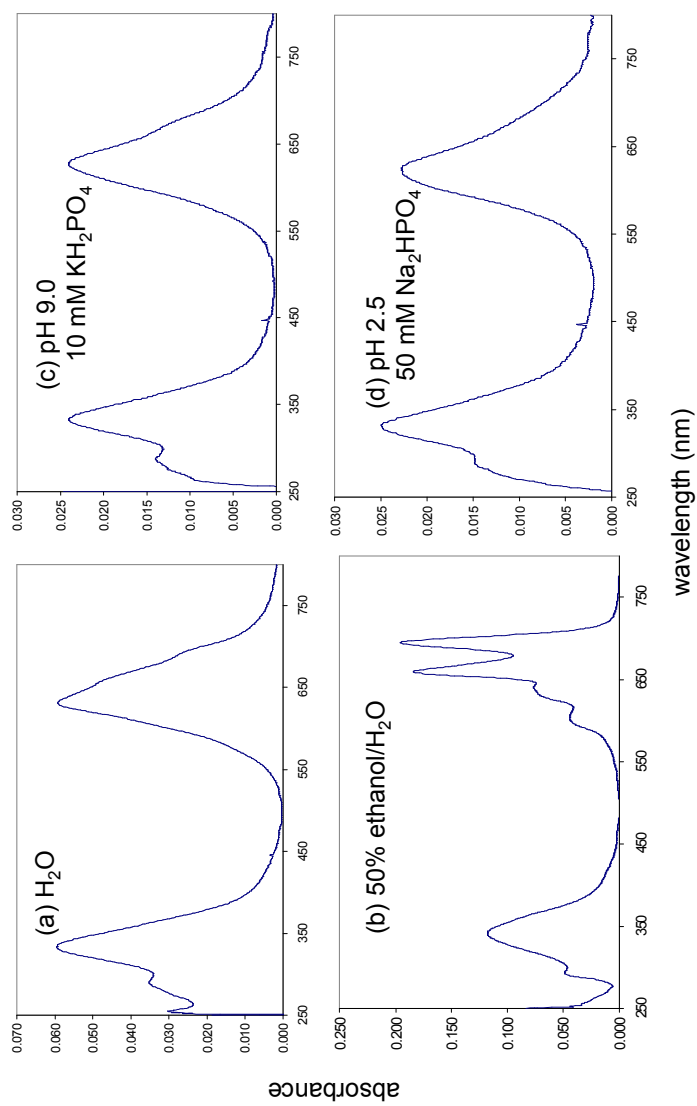


Figure 1.12. UV-vis spectra of PcS4-S.

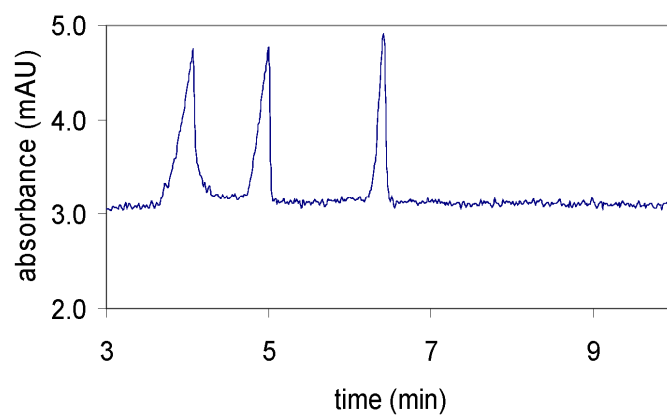


Figure 1.13. Capillary electrophoresis separation of TPPS2a (4 min), TPPS3 (5 min), and TPPS4 (6.4 min), pH 9.0 ( $\approx 10 \mu\text{M}$  porphyrin, 10 mM phosphate buffer, 30 kV).

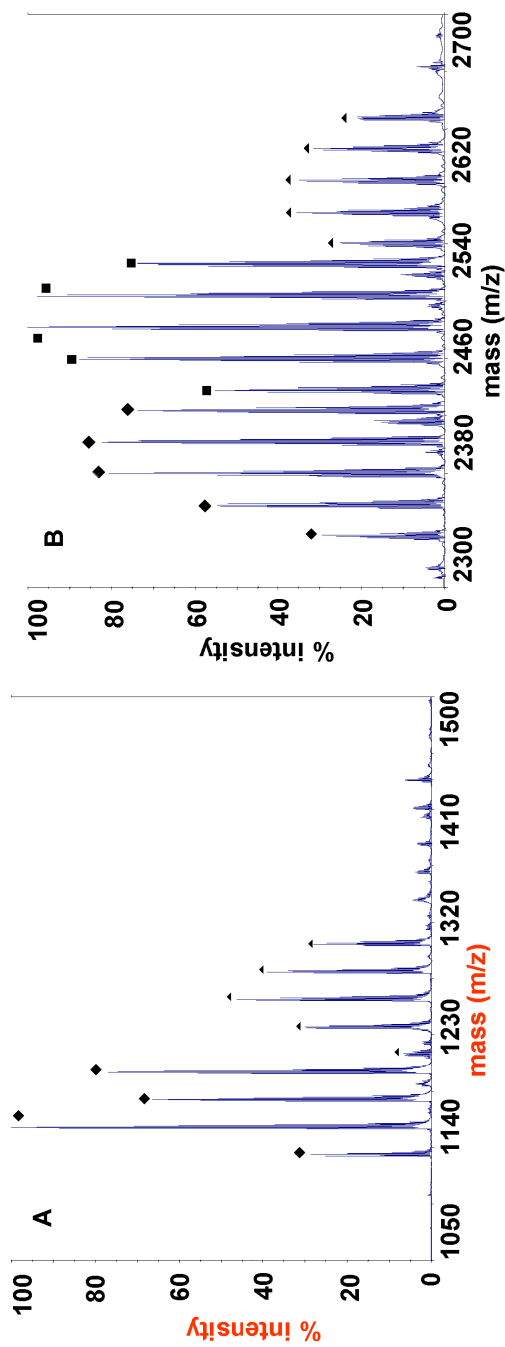


Figure 1.14. Negative ion MALDI spectrum (CHCA) of T2NapS. Panel A shows the region corresponding to the monomer. Peaks for the tetrasulfonic (♦) and the pentasulfonic acid (▲) as well as their sodium salts are seen. Panel B shows the region corresponding to the dimer. Peaks for the homodimers of the tetrasulfonic (♦) and pentasulfonic acid (▲) as well as the heterodimer of the tetrasulfonic/pentasulfonic acid (■) and their sodium salts are seen. Data interpreted by Brian R. Sook.

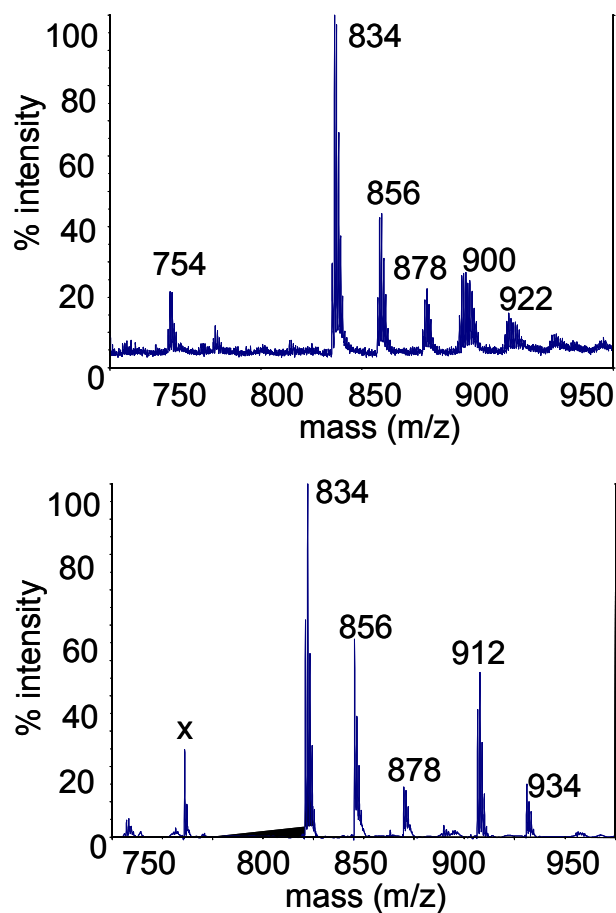


Figure 1.15. Negative ion MALDI spectrum of PcS4. Panel A: PcS4-WB (THAP/EDTA). The parent ion is seen (834), as are the mono-, di-, tri-, and tetrasodium salts at intervals of +22 and a peak consistent with loss of SO<sub>3</sub> (754). Panel B: PcS4-S (CHCA). The parent ion is seen (834), as are the mono- and disodium salts. The peaks at 911 - 914 and 933 - 936 are appropriate for the pentasulfonic acid and its monosodium salt, respectively. Data interpreted by Brian R. Sook.

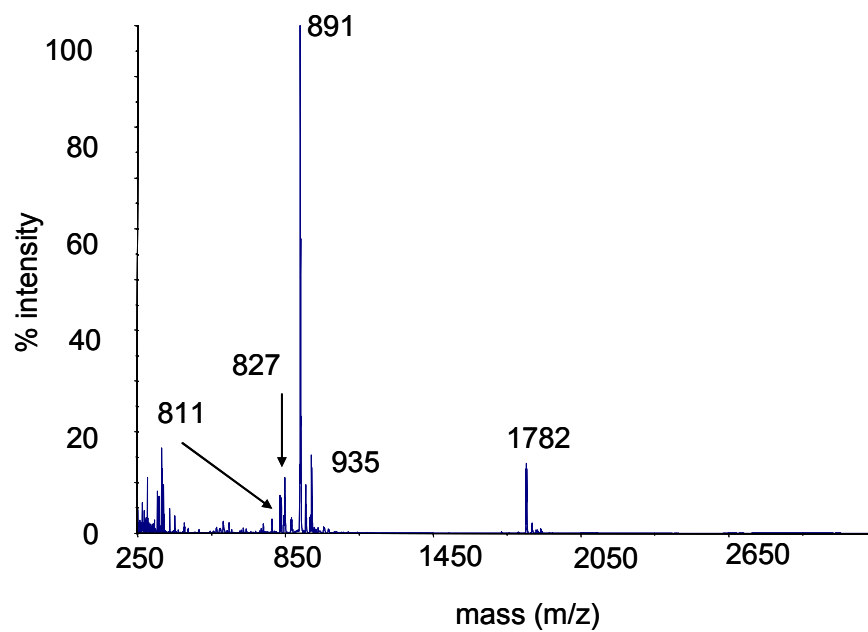


Figure 1.16. Negative ion mode MALDI spectrum of CoPcS<sub>4</sub> (CHCA). The parent ion is seen (891), as are the dimer (1782) and peaks consistent with loss of SO<sub>2</sub> (827) and SO<sub>3</sub> (811). Data interpreted by Brian R. Sook.

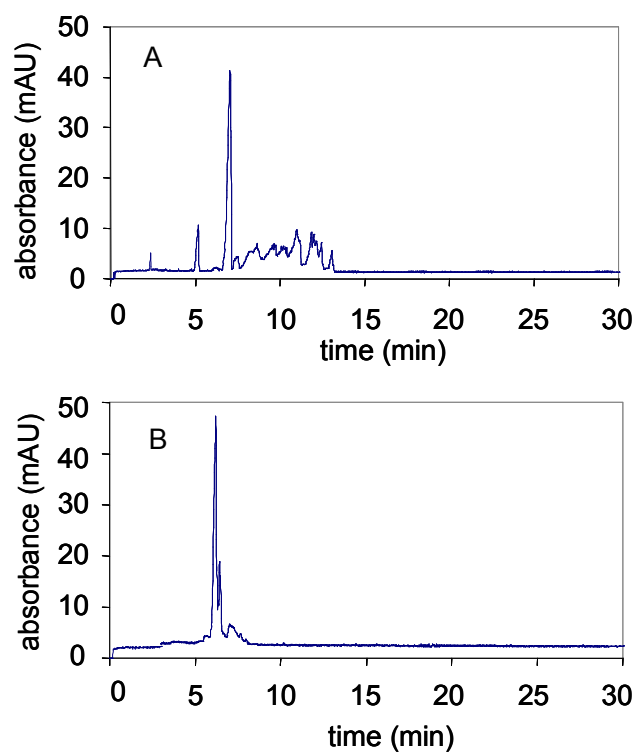


Figure 1.17. Capillary electrophoresis separation of ZnPcS3.  
Panel A: pH 9.0 (10 mM phosphate buffer, 30 kV). Panel B: pH 2.5  
(50 mM phosphate, -20 kV).

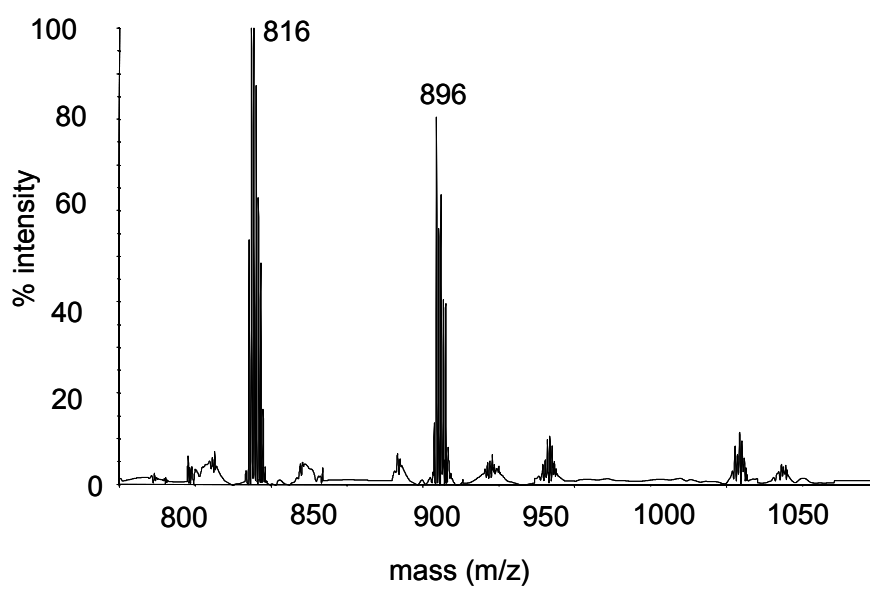


Figure 1.18. Negative ion MALDI spectrum (CHCA/EDTA) of ZnPcS<sub>4</sub>-WB. The parent is seen (896) as is the loss of SO<sub>3</sub> (816). Data interpreted by Brian R. Sook.

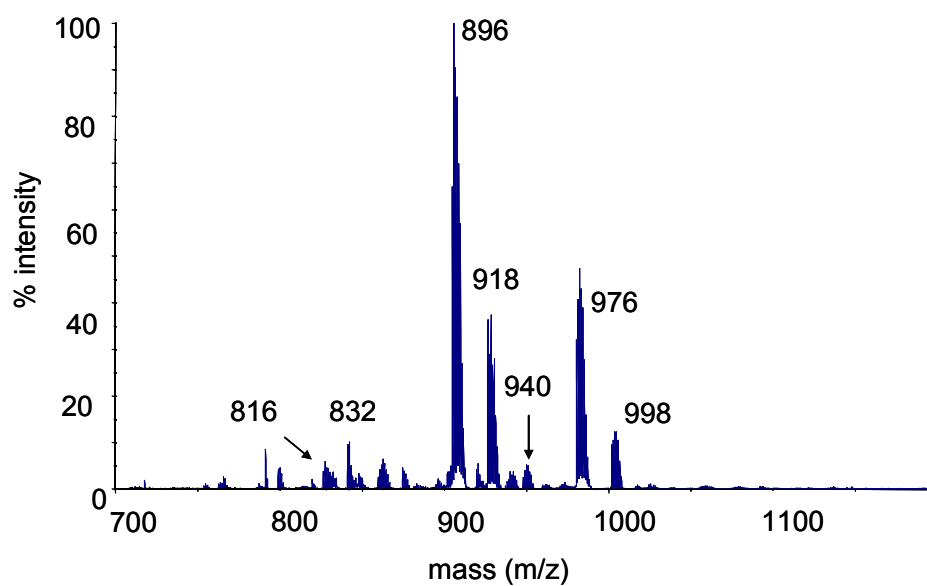


Figure 1.19. Negative ion MALDI spectrum (CHCA) of ZnPcS<sub>4</sub>-I. The region corresponding to the monomer is shown. The mono- and disodium salts, as well as losses of SO<sub>2</sub> and SO<sub>3</sub> from the parent ion, are seen. Peaks at 976 and 998 Da are consistent with the pentasulfonic acid and its monosodium salt, respectively. Data interpreted by Brian R. Sook.

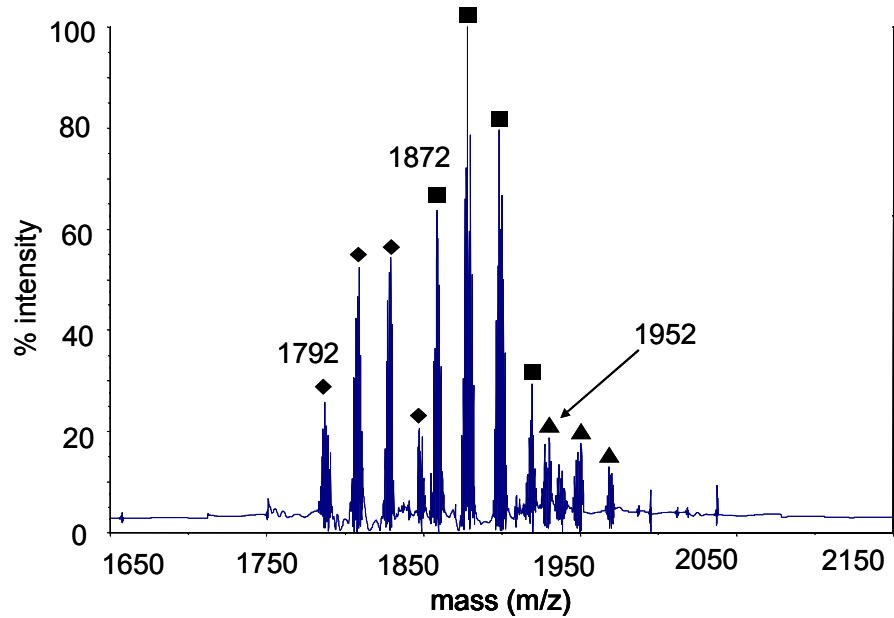


Figure 1.20. Negative ion MALDI spectrum (CHCA/EDTA) of ZnPcS4-I. The region corresponding to the dimer is shown. Peaks for the homodimers of the tetrasulfonic (◆) and pentasulfonic acid (▲) as well as the heterodimer of the tetrasulfonic/pentasulfonic acid (■) and their sodium salts are seen. Data interpreted by Brian R. Sook.

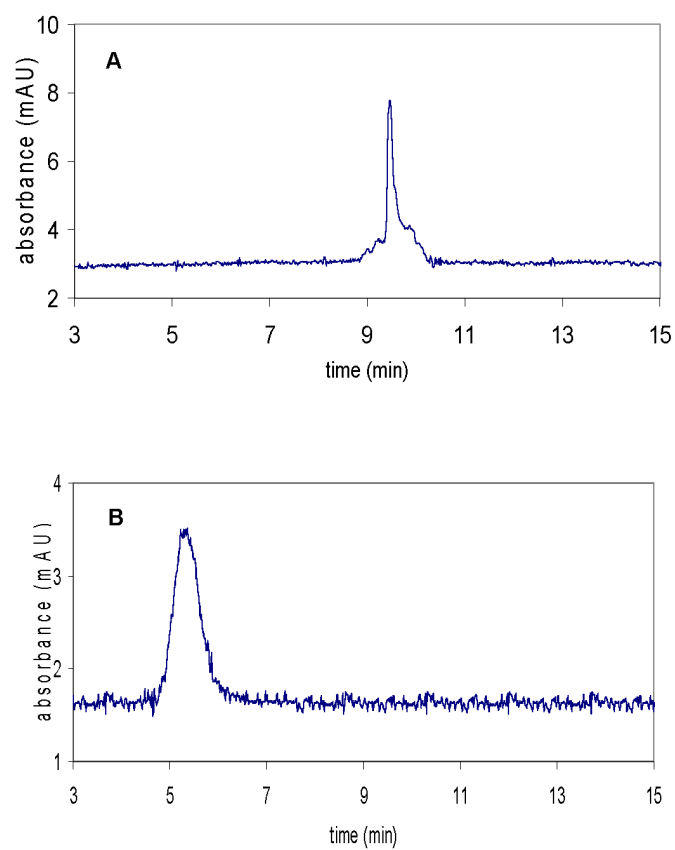


Figure 1.21. Capillary electrophoresis of sulfonated copper phthalocyanines at pH 9.0 (10 mM phosphate, 30 kV). Panel A: CuPcS(3444) ( $\sim 2.5 \times 10^{-5}$  M). Panel B: CuPcS(4444) ( $\sim 2.5 \times 10^{-4}$  M).

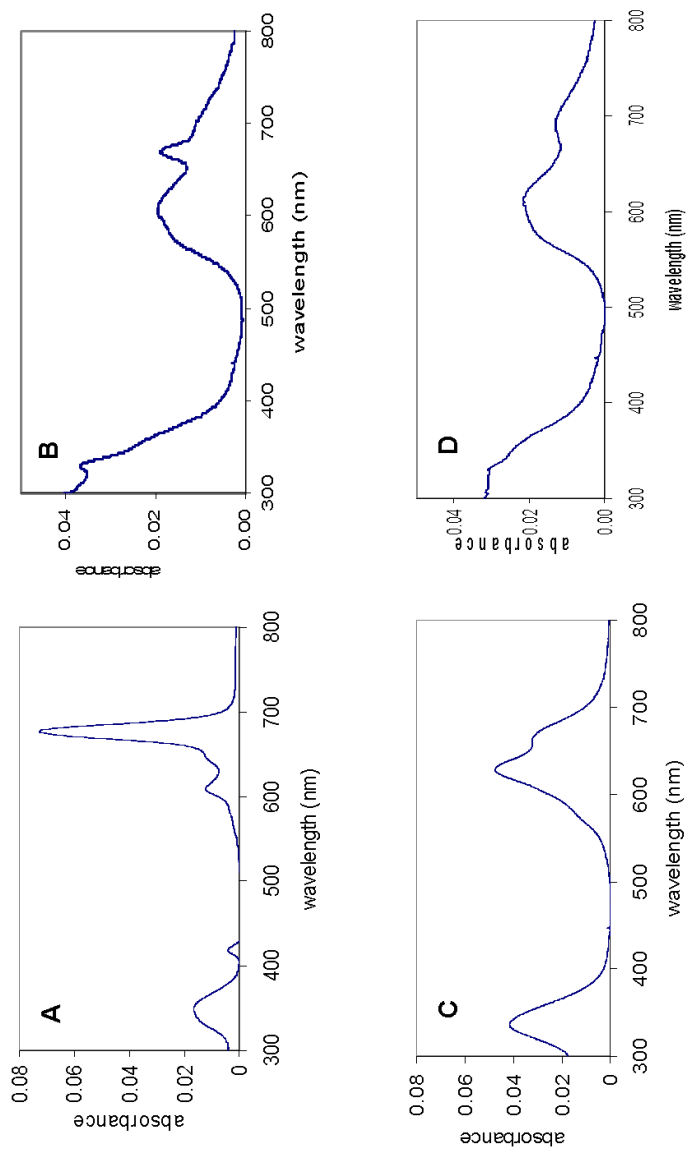


Figure 1.22. UV/vis spectroscopy of sulfonated copper phthalocyanines. Panel A: CuPcS(3444), in DMSO. Panel B: CuPcS(4444) in DMSO. Panel C: CuPcS(3444) in pH 9.0 buffer. Panel D: CuPcS(4444) in pH 9.0 buffer.

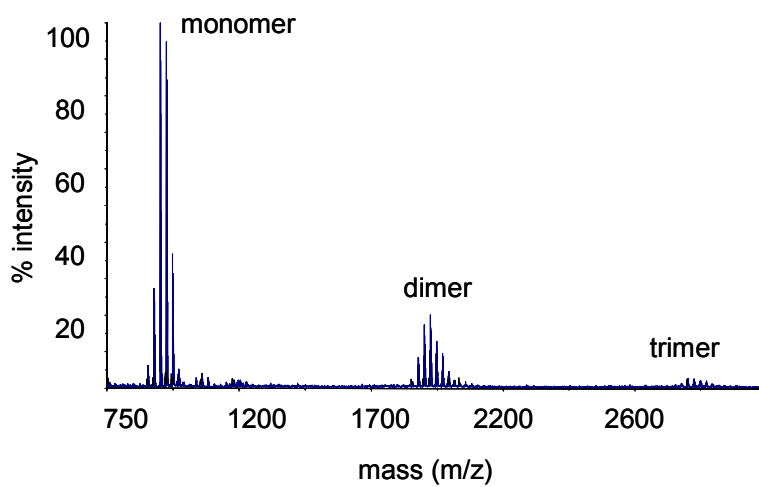


Figure 1.23. Positive ion mode MALDI of CuPcS(3444) (CHCA/EDTA). The monomer and its sodium salts are seen (895), as are the dimer salts (peaks are centered at 1902; this is the 5 sodium salt) and trimer salts (peaks centered at 2866; this is the 8 sodium salt). Data interpreted by Brian R. Sook.

## References

- Allen, C. M., Sharman, W. M., and van Lier, J. E. (2001). Current status of phthalocyanines in the photodynamic therapy of cancer. *J. Porph. Phthalo.* **5**, 161-169.
- Amaral, C. L. C. and Politi, M. J. (1997). Effect of urea on the dimerization equilibrium of nickel tetrasulfonated phthalocyanine in bulk and in the hydrophilic compartment of AOT reversed micelles. *Langmuir* **13**, 4219-4222.
- Ambroz, M., Beeby, A., MacRobert, A. J., Simpson, M. S., Svensen, R. K., and Phillips, D. (1991). Preparative, analytical and fluorescence spectroscopic studies of sulphonated aluminium phthalocyanine photosensitizers. *J. Photochem. Photobiol. B* **9**, 87-95.
- Andrighetto, P., Carofiglio, T., Fornasier, R., and Tonellato, U. (2000). Capillary electrophoresis behavior of water-soluble anionic porphyrins in the presence of  $\beta$ -cyclodextrin and its O-methylated derivatives. *Electrophoresis* **21**, 619-626.
- Arnold, K., Balaban, T. S., Blom, M. N., Ehrler, O. T., Gilb, S., Hampe, O., van Lier, J. E., Weber, J. M., and Kappes, M. M. (2003). Electron autodetachment from isolated nickel and copper phthalocyanine-tetrasulfonate tetraanions: Isomer specific rates. *J. Phys. Chem. A* **107**, 794-803.
- Barbosa, C. A. S., Constantino, V. R. L., and Tavares, M. F. M. (1997). Use of capillary electrophoresis in the characterization of sulfonated metallophthalocyanines: A comparative evaluation of purification procedures following synthesis by the condensation method. *J. Capillary Electrophor.* **4**, 157-166.
- Beeby, A., Bishop, S. M., Khoo, B. J., MacRobert, A. J., and Phillips, D. (1992). Chemical and spectroscopic characterization of disulphonated aluminum phthalocyanine. In "Photodynamic Therapy and Biomedical Lasers: Proceedings of the International Conference on Photodynamic Therapy and Medical Laser Applications" (P. Spinelli, M. Dal Fante, and R. Marchesini, Eds.), pp. 845-850. Elsevier Science, Amsterdam.
- Beeby, A., FitzGerald, S., and Stanley, C. F. (2001). Protonation of tetrasulfonated zinc phthalocyanine in aqueous acetonitrile solution. *Photochem. Photobiol.* **74**, 566-569.
- Ben-Hur, E., Barshtein, G., Chen, S., and Yedgar, S. (1997). Photodynamic treatment of red blood cell concentrates for virus inactivation enhances red blood cell aggregation: Protection with antioxidants. *Photochem. Photobiol.* **66**, 509-512.
- Brasseur, N., Ali, H., Langlois, R., and van Lier, J. E. (1988). Biological activities of phthalocyanines-IX. Photosensitization of V-79 chinese hamster cells and EMT-6 mouse mammary tumor by selectively sulfonated zinc phthalocyanines. *Photochem. Photobiol.* **47**, 705-711.

- Brasseur, N., Ali, H., Langlois, R., Wagner, J. R., Rousseau, J., and van Lier, J. E. (1987). Biological activities of phthalocyanines--V. Photodynamic therapy of EMT-6 mammary tumors in mice with sulfonated phthalocyanines. *Photochem. Photobiol.* **45**, 581-586.
- Bressan, M., Celli, N., d'Alessandro, N., Liberatore, L., Morvillo, A., and Tonucci, L. (2000). Ruthenium sulfophthalocyanine catalyst for the oxidation of chlorinated olefins with hydrogen peroxide. *J. Organometal. Chem.* **594**, 416-420.
- Cerfontain, H., Zou, Y. S., and Bakker, B. H. (1994a). On the positional reactivity order in the sulfonation of phenyl-substituted and naphthyl-substituted naphthalenes with SO<sub>3</sub>. *Rec. Trav. Chim. Pays-Bas* **113**, 517-523.
- Cerfontain, H., Zou, Y. S., and Bakker, B. H. (1994b). The positional reactivity order in the sulfur-trioxide sulfonation of benzene and naphthalene derivatives containing an electron-withdrawing substituent. *Rec. Trav. Chim. Pays-Bas* **113**, 403-410.
- Chen-Collins, A. R. M., Dixon, D. W., Vzorov, A. N., Marzilli, L. G., and Compans, R. W. (2003). Prevention of poxvirus infection by tetrapyrroles. *BMC Infect. Dis.* **3**, 9.
- Conneely, A., McClean, S., Smyth, W. F., and McMullan, G. (2001). Study of the mass spectrometric behaviour of phthalocyanine and azo dyes using electrospray ionisation and matrix-assisted laser desorption/ionisation. *Rapid Commun. Mass Spectrom.* **15**, 2076-2084.
- Conneely, A., Smyth, W. F., and McMullan, G. (2002). Study of the white-rot fungal degradation of selected phthalocyanine dyes by capillary electrophoresis and liquid chromatography. *Anal. Chim. Acta* **451**, 259-270.
- Corsini, A. and Herrmann, O. (1986). Aggregation of *meso*-tetra(*p*-sulphonatophenyl)porphine and its Cu(II) and Zn(II) complexes in aqueous solution. *Talanta* **33**, 335-339.
- Dixon, D. W., Gill, A. F., and Sook, B. R. (2004). Characterization of sulfonated phthalocyanines by mass spectrometry and capillary electrophoresis. *J. Porph. Phthal.* **8**, 1300-1310.
- Fingar, V. H., Wieman, J. T., Karavolos, P. S., Weber Doak, K., Ouellet, R., and van Lier, J. E. (1993). The effects of photodynamic therapy using differently substituted zinc phthalocyanines on vessel constriction, vessel leakage and tumor response. *Photochem. Photobiol.* **58**, 251-258.
- Fleischer, E. B., Palmer, J. M., Srivastava, T. S., and Chatterjee, A. (1971). Thermodynamic and kinetic properties of an iron-porphyrin system. *J. Am. Chem. Soc.* **93**, 3162-3167.

Halkiotis, K., Yova, D., and Pantelias, G. (1999). In vitro evaluation of the genotoxic and clastogenic potential of photodynamic therapy. *Mutagenesis* **14**, 193-198.

Hoffmann, P., Labat, G., Robert, A., and Meunier, B. (1990). Highly selective bromination of tetramesitylporphyrin: An easy access to robust metalloporphyrins, M-Br<sub>8</sub>TMP and M-Br<sub>8</sub>TMPS. Examples of application in catalytic oxygenation and oxidation reactions. *Tetrahedron Lett.* **31**, 1991-1994.

Howe, L. and Zhang, J. Z. (1997). Ultrafast studies of excited-state dynamics of phthalocyanine and zinc phthalocyanine tetrasulfonate in solution. *J. Phys. Chem. A* **101**, 3207-3213.

Howe, L. and Zhang, J. Z. (1998). The effect of biological substrates on the ultrafast excited-state dynamics of zinc phthalocyanine tetrasulfonate in solution. *Photochem. Photobiol.* **67**, 90-96.

Kudrevich, S. V., Brasseur, N., La Madeleine, C., Gilbert, S., and van Lier, J. E. (1997). Syntheses and photodynamic activities of novel trisulfonated zinc phthalocyanine derivatives. *J. Med. Chem.* **40**, 3897-3904.

Kuznetsova, N. A., Gretsova, N. S., Derkacheva, V. M., Kaliya, O. L., and Luk'yanets, E. A. (2003). Sulfonated phthalocyanines: Aggregation and singlet oxygen quantum yield in aqueous solutions. *J. Porph. Phthalo.* **7**, 147-154.

Leznoff, C. C. and Lever, A. B. P. (1989). "Phthalocyanines: Properties and Applications - Vol I." New York, NY.

Leznoff, C. C. and Lever, A. B. P. (1993). "Phthalocyanines: Properties and Applications - Vol III." VCH, New York.

Margaron, P., Grégoire, M. J., Šcasnár, V., Ali, H., and van Lier, J. E. (1996). Structure-photodynamic activity relationships of a series of 4-substituted zinc phthalocyanines. *Photochem. Photobiol.* **63**, 217-223.

Martin, P. C., Gouterman, M., Pepich, B. V., Renzoni, G. E., and Schindele, D. C. (1991). Effects of ligands, solvent, and variable sulfonation of dimer formation on aluminum and zinc phthalocyaninesulfonates. *Inorg. Chem.* **30**, 3305-3309.

Oppenheimer, L. E. (1981). Ion-pair chromatography of sulfonated copper phthalocyanine. *J. Chrom. Sci.* **19**, 266-269.

Peng, X., Sternberg, E., and Dolphin, D. (2005a). Separation of porphyrin-based photosensitizer isomers by laser-induced fluorescence capillary electrophoresis. *Electrophoresis* **26**, 3861-3868.

- Peng, X., Sternberg, E., and Dolphin, D. (2005b). Separation of porphyrin-based photosensitizer isomers by laser-induced fluorescence capillary electrophoresis. *Electrophoresis* **26**, 3861-3868.
- Phillips, D. (1997). Chemical mechanisms in photodynamic therapy with phthalocyanines. *Prog. React. Kinet.* **22**, 175-300.
- Pokric, B., Allinson, N. M., Bergström, E. T., and Goodall, D. M. (1999). Dynamic analysis of capillary electrophoresis data using real-time neural networks. *J. Chromatogr. A* **833**, 231-244.
- Priola, S. A., Raines, A., and Caughey, W. S. (2000). Porphyrin and phthalocyanine antiscrapie compounds. *Science* **287**, 1503-1506.
- Rajendiran, N. and Santhanalakshmi, J. (2002). Interaction of sulfur dioxide with zinc(II) tetrasulfophthalocyanine in aqueous medium: steady state fluorescence quenching studies. *Polyhedron* **21**, 951-957.
- Reynolds, W. L. and Kolstad, J. J. (1976). Aggregation of 4,4',4'',4'''-tetrasulfophthalocyanine in electrolyte solutions. *J. Inorg. Nucl. Chem.* **38**, 1835-1838.
- Rocha Gonsalves, A. M. D., Johnstone, R. A. W., Pereira, M. M., de SantAna, A. M. P., Serra, A. C., Sobral, A. J. F. N., and Stocks, P. A. (1996). New procedures for the synthesis and analysis of 5,10,15,20- tetrakis(sulphophenyl)porphyrins and derivatives through chlorosulphonation. *Heterocycles* **43**, 829-838.
- Rocha Gonsalves, A. M. D., Varejao, J. M. T. B., and Pereira, M. M. (1991). Some new aspects related to the synthesis of *meso*-substituted porphyrins. *J. Heterocycl. Chem.* **28**, 635-640.
- Rubires, R., Crusats, J., El-Hachemi, Z., Jaramillo, T., Lopez, M., Valls, E., Farrera, J. A., and Ribó, J. M. (1999). Self-assembly in water of the sodium salts of *meso*-sulfonatophenyl substituted porphyrins. *New J. Chem.* **23**, 189-198.
- Sanchez, M., Fache, E., Bonnet, D., and Meunier, B. (2001). Synthesis of organo-soluble metallophthalocyanines bearing electron-withdrawing substituents. *J. Porph. Phthalo.* **5**, 867-872.
- Sanderson, W. A. (2000). Di- & octa-sulpho-phthalocyanine & naphthalocyanine dye derivatives for use in tissue demarcation, imaging & diagnosis of tumour cells & diseased lymph nodes. *UK Patent Application GB 2,343,187A*.
- Schofield, J. and Asaf, M. (1997). Analysis of sulfonated phthalocyanine dyes by capillary electrophoresis. *J. Chromatogr. A* **770**, 345-348.

- Sobolev, A. S., Jans, D. A., and Rosenkranz, A. A. (2000). Targeted intracellular delivery of photosensitizers. *Prog. Biophys. Mol. Biol.* **73**, 51-90.
- Spikes, J. D., van Lier, J. E., and Bommer, J. C. (1995). A comparison of the photoproperties of zinc phthalocyanine and zinc naphthalocyanine tetrasulfonates - model sensitizers for the photodynamic therapy of tumors. *J. Photochem. Photobiol. A* **91**, 193-198.
- Stranadko, E. F., Meshkov, V. M., Koraboyev, U. M., and Riabov, M. V. (1999). Clinical photodynamic therapy using Russian photosensitizers Photoheme and Photosense: six-year experience. *Proc. SPIE* **4059**, 25-31.
- Sutter, T. P. G., Rahimi, R., Hambright, P., Bommer, J. C., Kumar, M., and Neta, P. (1993). Steric and inductive effect on the basicity of porphyrins and on the site of protonation of porphyrin dianions. *J. Chem. Soc. Faraday Trans.* **89**, 495-502.
- Tabata, K., Fukushima, K., Oda, K., and Okura, I. (2000). Selective aggregation of zinc phthalocyanines in the skin. *J. Porph. Phthalo.* **4**, 278-284.
- Tapley, K. N. (1995). Capillary electrophoretic analysis of the reactions of bifunctional reactive dyes under various conditions including a study of the analysis of the traditionally difficult to analyze phthalocyanine dyes. *J. Chromatogr. A* **706**, 555-562.
- Tedesco, A. C., Rotta, J. C. G., and Lunardi, C. N. (2003). Synthesis, photophysical and photochemical aspects of phthalocyanines for photodynamic therapy. *Curr. Org. Chem.* **7**, 187-196.
- Vzorov, A. N., Marzilli, L. G., Compans, R. W., and Dixon, D. W. (2003). Prevention of HIV-1 infection by phthalocyanines. *Antiviral Res.* **59**, 99-109.
- Wainwright, M. (1996). Non-porphyrin photosensitizers in biomedicine. *Chem. Soc. Rev.* **25**, 351-359.
- Wainwright, M. (2002). The emerging chemistry of blood product disinfection. *Chem. Soc. Rev.* **31**, 128-136.
- Weber, J. H. and Busch, D. H. (1965). Complexes derived from strong field ligands. XIX. Magnetic properties of transition metal derivatives of 4,4',4'',4'''-tetrasulfophthalocyanine. *Inorg. Chem.* **4**, 469-471.
- Winkelman, J., Slater, G., and Grossman, J. (1967). The concentration in tumor and other tissues of parenterally administered tritium and <sup>14</sup>C-labeled tetraphenylporphinesulfonate. *Cancer Res.* **27**, 2060-2064.

Zelina, J. P., Njue, C. K., Rusling, J. F., Kamau, G. N., Masila, M., and Kibugu, J. (1999). Influence of surfactant-based microheterogeneous fluids on aggregation of copper phthalocyanine tetrasulfonate. *J. Porph. Phthalo.* **3**, 188-195.

Zelina, J. P. and Rusling, J. F. (1995). Molecular orientation in self-assembled films of copper phthalocyanine tetrasulfonate and a cationic surfactant. *Micr. Mat.* **5**, 203-210.

Zhang, Y. H., Chen, D. M., He, T., and Liu, F. C. (2003). Raman and infrared spectral study of *meso*-sulfonatophenyl substituted porphyrins (TPPS<sub>n</sub>, n = 1, 2A, 2O, 3, 4). *Spectrochim. Acta A Mol. Biomol. Spectrosc.* **59**, 87-101.

## Chapter 2

### Insights into Anionic Tetraaryl Porphyrins

In collaborative studies, we observed that a number of sulfonated porphyrins also had excellent antiviral activity against the human immunodeficiency virus (Vzorov et al., 2002) and pox virus (Chen-Collins et al., 2003). These compounds had varying levels of toxicity and viral inhibition activities. Finally a copper chelate of 5,10,15,20-tetra(2-naphthyl)porphyrin (T2NapS,Cu) was proposed for clinical trials. We performed a number of studies to look in detail at the structures and spectra of possible metalloporphyrin therapeutic candidates. The majority of this work has been published (Dixon et al., 2005) and is given as Section V of this chapter. Below is a brief overview of porphyrins (Section I), a review of capillary electrophoresis of porphyrins (Section II), a review of the study of cyclodextrins with porphyrins (Section III) and experiments that were not published (Section IV).

#### Section I.

##### Introduction to porphyrins.

##### i. Structure.

Porphyrins are naturally occurring aromatic macrocyclic compounds derived from *porphin* (**Figure 2.1a**), a tetradentate ligand with four pyrrole rings linked via methine bridges. Substitution of some or all of the hydrogens on the pyrrole rings and/or at the methine bridge of the *porphin* results in porphyrins (**Figure 2.1a and 2.1b**) (Falk, 1964).

The pyrrole rings are designated by Arabic numbers. The methine bridges, also called the *meso* positions, are designated by the Greek letters,  $\alpha$ ,  $\beta$ ,  $\gamma$ , and  $\delta$ . Porphyrins are planar structures, however; there can be deviations from planarity due to factors such as peripheral substitutions, metal incorporation and axial ligation of the central metal.

### **ii. Spectral properties.**

The optical absorption and emission are determined by the  $\pi$ -electrons of the ring of the porphyrin. The absorption and emission change slightly due to the presence of the metal in the ring. The UV-vis absorption spectrum shows intense absorption at  $\sim 400$  nm, the Soret band. It has a high extinction coefficient in the range of  $2 - 4 \times 10^5 \text{ M}^{-1}\text{cm}^{-1}$ , followed by several weaker absorption bands (Q-bands) at higher wavelengths (450 - 700 nm) (Lindsey et al., 1987). The free-base or metal-free form has a four band,  $D_{2h}$ -type spectrum. The acid dication or the protonated dicationic form, with a proton attached to each central nitrogen, has a two band  $D_{4h}$ -type spectrum.

The metalloporphyrins have an intense Soret band between 380 nm and 420 nm, depending on the metal. Two visible bands are seen between 500 and 600 nm, with the extinction coefficient in the narrow range of  $1.2 - 2 \times 10^4 \text{ M}^{-1}\text{cm}^{-1}$  (Falk, 1964). To the blue of the Soret are weaker bands M and N, at  $\sim 215$  and  $\sim 325$  nm and between the two is another weaker band, the L band.

### **iii. Stability.**

Certain porphyrins are stable even in the presence of concentrated acids, such as sulfuric acid under certain conditions (Buchler, 1975). However, degradation of the tetrapyrrole to monopyrroles has been reported with chromic acid, potassium

permanganate and hydriodic acid. The two pyrrolic nitrogen atoms, bearing lone pairs of electrons, can be protonated easily with acids such as trifluoroacetic acid (Falk, 1964). Strong bases such as alkoxides can remove the protons ( $pK_a \sim 16$ ) from the inner nitrogen atoms of a porphyrin to form a dianion. The porphyrin complexes with transition metal ions are very stable, e.g., the stability constant for the zinc derivative of tetraphenylporphyrin (ZnTPP),  $\log K_s$ , is 29 (Falk, 1964).

#### **iv. Synthetic porphyrins.**

The general method of synthesis of porphyrins is simple. It involves the condensation of the appropriate aldehyde with pyrrole. The earliest method was reported by Rothmund in 1939 involving the condensation of more than 25 aliphatic, aromatic and heterocyclic aldehydes with pyrrole to form porphyrins (Rothmund, 1939). The earliest methods involved harsh conditions during the synthesis, e.g., using sealed tube under anaerobic conditions, in pyridine solution, at 220 °C, under nitrogen for 48 h. The yields were very low, only 5%, and there were contaminants such as chlorin. More modern synthetic methods do not require harsh conditions and give higher yields. Adler et al. condensed equimolar amounts of benzaldehyde and pyrrole for 30 min by refluxing in propionic acid at 141 °C, in open air (Adler et al., 1967). The yield was 20%. This method still had several disadvantages. It required harsh conditions, needed benzaldehydes (which can not be used with sensitive functional groups), produced tar and gave poor reproducibility. To overcome such problems another method was reported by Lindsey (Lindsey et al., 1987). The condensation reaction was carried out at room

temperature under nitrogen in methylene chloride, in the presence of a water scavenger, as well as an acid catalyst, followed by the addition of an oxidant. The yield was 50%.

Any porphyrin derivative in which at least one of the central nitrogen atoms of a porphyrin forms a bond to a metal atom is called a metalloporphyrin. Metalloporphyrins found in nature have metals such as Mg (chlorophylls), Mn (blood), Fe (hemes), Co (vitamin B<sub>12</sub>), V (mineral oils), Zn (yeast mutants), etc (Dolphin, 1978). Many synthetic metalloporphyrins have been synthesized; almost all metals and some semimetals can be inserted into the *porphin* core. Synthetic metalloporphyrins are made via the reaction of a free base/parent or free acid form with a metal salt. When coordination occurs, two protons are removed from the pyrrole nitrogen atoms, leaving a charge of -2 on the porphyrin ring.

#### **v. Anti-HIV activities of porphyrins and their metalloderivatives.**

Synthetic porphyrins showed antiviral activity against HIV infection in assays that measured inhibition of viral replication. Sulfonated derivatives of tetraphenylporphyrin (TPPS) have been shown to be active, as have other selected tetraaryl porphyrins (Dixon et al., 1990; Dixon et al., 1992; Neurath et al., 1992; Neurath et al., 1992; Debnath et al., 1994; Neurath et al., 1994a; Neurath et al., 1995; Song et al., 1997; Vzorov et al., 2002). In general, activity against HIV was in the micromolar range in such antiviral assays. Recently it was found that porphyrins can inhibit the initial infection process by inactivating the infectivity of cell-free virus (Vzorov et al., 2002).

## **Section II.**

### **Review.**

#### **Capillary electrophoresis separation of porphyrins.**

##### **i. Natural porphyrins.**

A number of groups have analyzed natural porphyrins via capillary electrophoresis (CE). Various modes of CE have been used to study natural porphyrins, e.g., micellar electrokinetic chromatography (MEKC), microemulsion electrokinetic chromatography (MEEKC), and nonaqueous CE, described in more detail below. Much of the interest in separations of natural porphyrins comes from efforts to characterize blood levels of the porphyrins involved in porphyrias. Porphyrias are genetic diseases caused by enzyme deficiencies in heme production (Alla & Bonkovsky, 2005). CE is used in clinical laboratory methods for diagnosis of porphyrias (Zaider & Bickers, 1998).

##### **Optimization of capillary electrophoresis for the separation of natural porphyrins.**

There has been extensive effort to enhance separations via CE. The separations can be enhanced by the use of organic solvents, alone or in combination with surfactants. This review reports the optimization studies specifically directed towards the investigation of the effects of three parameters on separation enhancement: organic solvents, surfactants and detectors.

##### **a. Use of organic solvents.**

Organic solvents can be used as pure nonaqueous solvents, aqueous/organic mixtures, or as a combination of an organic solvent with other organic modifier(s). They

can be used in the sample matrix and/or in separation buffer. The separation of natural porphyrins is hindered due to their limited solubility in solvents.

Optimization of organic solvents in CE separations is a very common method to enhance the signal and to improve the resolution of separation. Robert and Spinks reported the enhancement of separation of metallated petroporphyrins found in crude oils, by the studying the effect of solvents and the surfactant sodium dodecyl sulfate (SDS) (Robert & Spinks, 1997). The metalloderivatives separated were Ni(II) and V(IV)O, with various porphyrin ring types, e.g., etioporphyrin and octaethylporphyrin. Robert and Spinks studied the effect of various concentrations of SDS (20 - 100 mM) with borate buffer at high pH and observed no resolution enhancement (Robert & Spinks, 1997). The porphyrins co-migrated with the micelles. It was reported that porphyrin solubility in buffer increased with increasing SDS concentration, evidenced by the increasing peak areas. The effect of acetone in borate buffer at high pH was studied by varying the acetone concentration from 0 - 30%. At 30% acetone, all the four porphyrins were resolved in less than 31 min. The effect of other solvents was also reported, including methyl ethyl ketone, acetonitrile (ACN) and methanol. A 30% v/v solvent with 70% buffer containing 40 mM SDS was reported to give best separation. Acetone was reported to be the best organic modifier. ACN and methanol did not improve the separation.

The enhancement of separation of six porphyrin methyl esters was reported in both aqueous and nonaqueous media, by the use of various organic solvents (Li et al., 2005). Li et al. compared four techniques, micellar electrokinetic chromatography, MEKC (aqueous and nonaqueous), microemulsion electrokinetic chromatography,

MEEKC (nonaqueous) and CE (nonaqueous). Using aqueous MEKC, they reported separations at various concentrations of ACN (0 - 50% v/v) in CAPS buffer at high pH with 60 mM SDS. They recommended the use of 20 - 35 % of ACN. At 20 and 30% ACN all components were separated, but not to the baseline. Although the resolution was enhanced, the peak areas were not fully reproducible. They separated the six porphyrins with  $\text{KH}_2\text{PO}_4$  buffer in *N*-methyl-formamide, using various concentrations of SDS (100, 120 and 140 mM). The best separation observed was over the longest migration time, using the highest concentration of SDS. MEEKC separations were performed with a borate buffer (pH 9.0) containing SDS microemulsion. The best separation (almost to baseline) was achieved with 30% 2-propanol in a system with 0.8% w/w *n*-heptane, 2.25% w/w SDS, 1.0% w/w Brij 35, 6.6% w/w 1-butanol, and 30% v/v 2-propanol. They also performed separations using the above mentioned conditions, but without heptane and 1-butanol in the system, with 10% or 20% 2-propanol, giving peaks which were comparatively less resolved. Nonaqueous CZE separations in strongly acidic conditions (10 mM perchloric acid) with ACN and methanol gave the best separation of all the techniques tested. With a 50:50 mixture of methanol and ACN, all six peaks were baseline resolved in as little as 3 min.

So et al. (So et al., 2001) reported the separation of the two coproporphyrin isomers, I and III (negatively charged), using various additives in the general buffer, 20 mM CAPS at high pH. They studied the effect of three surfactants on separation: sodium cholate (SC), sodium taurodeoxycholate (STDC) and SDS, in the presence of three organic solvents, ACN, methanol or DMF. The separation in the presence of DMF and

methanol in the buffer was partially and/or baseline resolved. However, longer migration times were required, and/or larger baseline noise levels were observed. In comparing the surfactants, the best separation was observed with 60 mM SC with 20% ACN. This separation condition was further studied with various amounts of ACN, with and without NaCl. It was reported that the best separation of the two isomers was achieved with 1% NaCl and 20% ACN. Stacking (with NaCl) concentrates the analyte in the column. So et al. reported that NaCl with ACN increased the ionic strength in the sample and facilitated the removal of any proteins in the system, which can get adsorbed on the capillary walls. Sharper and taller peaks were observed with the addition of ACN, e.g., with 50% ACN and 1% NaCl w/v.

#### **b. Use of surfactants.**

Surfactants have been regularly used in CE to control the selectivity of the separation, reduce aggregation of the analyte and increase the efficiency of the separation. Wu et al. reported the use of a mixture of anionic surfactant for the separation of various natural porphyrins (Wu et al., 1994). The natural porphyrins studied were both hydrophobic and hydrophilic: porphyrin carboxylic acids, hematoporphyrin derivatives, four types of isomers of coproporphyrin and other clinically important porphyrins. They used a laser-induced fluorescence (LIF) detector (discussed in more detail below). They studied the enhancement in separation due to surfactants, SDS and Triton QS-15, in combination with bile salts [taurodeoxycholic acid (TDC) and deoxycholic acid (DCA)], in borate buffer. Along with this, the effect of the presence of ACN, at both neutral and high pH, was also analyzed. Bile salts have been reported to be good biological

surfactants due rigid helical micellar aggregates (Pico & Houssier, 1989). It was reported that separation of the six porphyrins with Triton and TDC alone was not successful. However, the combination of the two at pH 7.4 with 15% ACN improved the separation. Only four out of seven peaks were observed when SDS alone was used. However, with a combination of Triton and TDC with 10% ACN, all seven peaks were observed at physiological pH. They reported good separation of the isomers of coproporphyrin with a combination of Triton and DCA with 15% ACN at high pH (9.0). They also separated hematoporphyrin derivatives under various conditions.

Kiyohara et al. separated six porphyrins [free base, copper and zinc complexes of hematoporphyrin (HP) and protoporphyrin (PP)] using MEKC (Kiyohara et al., 1993). They used varying concentrations of SDS, DMF and CAPS (3-cyclohexylamino) buffer at pH 11. Kiyohara et al. observed that when CAPS alone was used, the three HP compounds [ $H_2HP$ , Cu(HP), Zn(HP)] moved towards the negative electrode, indicating that the electrophoretic mobility for these negatively charged HP species were smaller than that of the electroosmotic flow of the solution. SDS (25 mM) was added to the buffer to increase the solubility of each porphyrin, but a decrease in the reproducibility of the migration velocities was observed. DMF was added up to 10% (v/v), which did not improve the reproducibility but did improve the solubility. Both SDS and DMF enhanced reproducibility and solubility. The effect of the concentration of SDS on the migration behavior was also studied, and it was found that the capacity factor (the ratio of the amount of a solute in the micelle phase to that in the bulk aqueous phase) did not always increase with increasing concentration of SDS.

Separation of six urinary porphyrins were compared by regular CE and MEKC using 20 mM CAPS at pH 11 by absorbance and fluorescence detection (Weinberger et al., 1990). The limit of detection (100 pmol/ml range) was reported with an optimized fluorescence system. The separation without the presence of surfactant in the running buffer was performed in the presence of 10% methanol with baseline separation within 12 min. In the case of MEKC, various concentrations of SDS were studied, with and without 15% methanol. They also analyzed the effect of temperature and voltage on separation. Increasing the concentration of SDS from 100 mM to 150 mM at 45 °C (no methanol) only increased the migration time slightly but did not enhance the separation. Weinberger et al. reported that electrostatic repulsion of the negative nature of both the analytes and surfactants, under those separation conditions, was the reason for the longer migration time. Methanol was used to solubilize the analyte and to increase the sharpness of the peaks. Higher temperature (55 °C) and voltage (30 kV) were used to reduce the migration time.

Bowser et al. reported using Brij 35 in a nonaqueous, methanol-based 20 mM CAPS (pH 10.5) buffer for disaggregation, as well as for controlling the selectively of separation of hematoporphyrin, hydroxyethylvinyl-deuteroporphyrin, protoporphyrin, as well as Photofrin (Bowser et al., 1996). Various concentrations of the surfactant were used (5 - 35 mM). The polyether chain of Brij 35 does not form micelles in the presence of methanol. However, it can complex with the analyte through hydrogen bonding resulting in separation. They reported partial separation of 60 peaks for Photofrin within 30 min using 5 mM Brij 35. In case of Photofrin, various separations conditions had to be

used because any one set of conditions was not applicable due to the complexity of this analyte. Bowser et al. reported that because hematoporphyrin, hydroxyethylvinyl-deuteroporphyrin, and protoporphyrin have similar sizes and charges, the separation was mainly due to the difference in the extent of complexation of Brij 35 and the analytes, especially at lower Brij 35 concentrations. At higher Brij 35 concentrations there were more monomeric species of the analyte. Hence more complexation was seen with Brij 35 as the peaks converged. Bowser et al. reported that the separation at high Brij 35 concentration was governed by the difference in the charge to size ratio of the monomer-additive complex instead of the extent of complexation. Bowser et al. reported the separation of the porphyrin acid monomers, mesoporphyrin, corpoporphyrin, pentacarboxylporphyrin, hexacarboxylporphyrin, heptacarboxylporphyrin and uroporphyrin, ascribing the separation to pure electrostatic ion-dipole interaction with Brij 35 (Bowser et al., 1996).

### **c. Detection/signal enhancement.**

UV detection is often utilized with CE separations because it is simple to use, rugged, and inexpensive. UV detectors have important advantages, i.e., fluorescent analytes are not required and sources are available that cover the whole UV and visible range (Chiang & Li, 1997). Other detection methods have also been employed, due to their higher sensitivity and lower detection limit, e.g., LIF.

Since porphyrins without a central metal are intrinsically fluorescent, no further modification is required for LIF detection. Wu et al. reported a detection limit in the 1 -

10 nM range for the natural porphyrins. The separation by the use of surfactants and organic modifier has been discussed earlier in this section.

In a review on the use of chemiluminescence (CL) for detection of biomolecules by CE, Garcia-Campana et al. reported that Tsukagoshi's group developed a new CE apparatus with on-line CL detection using the luminol-H<sub>2</sub>O<sub>2</sub> system for analyzing hematin as an iron (III) porphyrin complex (Garcia-Campana et al., 2003). The CL reagent solution (luminol + H<sub>2</sub>O<sub>2</sub>) was left for more than 24 h before use, as a fresh solution resulted in noise and nonreproducibility. It was reported that almost constant CL intensity was observed after the solution was allowed to stand for about 12 h.

ICP-MS detection has been reported to offer absolute detection limits that are slightly lower than those obtained with UV-vis spectrophotometer (Ackley et al., 2000). Other advantages, including high sensitivity, are element specificity and scans for multiple mass to charge ratios. Ackley et al. compared the separation of vitamin B<sub>12</sub>, CoPP, MnPP, and ZnPP using standard on-column UV detection and ICP-MS.

## **ii. CE analysis of charged synthetic porphyrins.**

### **a. Separation of anionic aromatic porphyrins.**

Simple mixtures of sulfonated aromatic porphyrins can be separated by CE as a function of charge. Most studies have shown enhanced separation with organic modifiers and surfactants, as discussed in the sections below.

Kalny et al. reported the separation of Pd(II)TPPS and TPPS (Kalny et al., 2001). Their efforts were directed towards demonstrating the analytical method for the determination of traces of Pd (0.8 µg /L) by CE, with no interference from Pt, using

citrate buffer at low pH (3.5). They reported the quantitative analysis method of the metal concentration using a linear calibration curve. They compared their studies to an earlier study using spectrophotometric determination of Pd(II) in the form of Pd(II)TPPS. The metalloporphyrins which did not interfere with the Pd were complexes of Mn, Co, Ni, Cu and Zn. These were analyzed via CE under the same separation conditions. Pd(II)TPPS eluted at 8.12 min while the free base eluted at 11 min.

### **1. Addition of surfactants and organic modifiers to enhance separation.**

There are several studies based on micellar electrokinetic capillary chromatography (MECC), where surfactants have been used to enhance CE separations. Lim et al. used SDS in sodium borate buffer for the separation of Temoporfin, 5,10,15,20-tetra(*m*-hydroxyphenyl)chlorin (*m*-THPC) and its conjugate with poly(ethylene)glycol (PEG), temoporfin–poly(ethylene glycol) conjugates (*m*-THPC–PEG) (Lim et al., 2000). Lim et al. reported good separation and quantitative measurement of both *m*-THPC and *m*-THPC-PEG conjugates in less than 10 min. However, the detection was not sensitive enough to measure levels in plasma, due to the limited clinical sample volume.

Zhang et al. used MECC to separate MnTPPS4 and CoTPPS4. They used 10 mM sodium borate buffer, pH 9.6 (Zhang et al., 1998). Zhang et al. demonstrated the separation with 10, 20 and 50 mM of SDS. They reported that separation was best with 20 mM SDS. The buffer contained 1 mM luminol, since the efforts were directed towards improving the apparatus for on-line chemiluminescence (CL) detection with CE.

Porphyrins are used as catalysts for the CL reaction between luminol and  $\text{H}_2\text{O}_2$ ; the detection details are discussed below.

Peng et al. reported that the combined use of various surfactants (e.g., SDS) and organic solvents (e.g., ACN), while varying their concentrations, resulted in good separation and acceptable time profiles (Peng et al., 2002). They separated synthetic, unsymmetrical photosensitizer isomers (a variety of optical and region isomers of porphyrins, and chlorins with different physicochemical properties): benzoporphyrin derivative monoacid, benzoporphyrin ethyl monoacid, 2-[1-hexyloxyethyl]-2-devinylpyropheophorbide-a, diethyleneglycol diester benzoporphyrin derivative and tin ethyl etiopurpurin. However, only the separation of the first two compounds will be reviewed here as they were anionic under the separation conditions. Individual separation of the two compounds and their two enantiomers was performed using a 40 mM borate buffer, pH 9.2 with 30% ACN and 10 mM SDS. The presence of ACN and SDS helped to remove the aggregation problem.

Peng et al. have shown that the simultaneous CE separation of the two compounds, each into its two enantiomers, could be enhanced at a lower voltage of 10 kV with 120 mM borate, 28% ACN, and 15 mM SDS (Peng et al., 2002). This recipe also reduced the current during the separation significantly. Effect on separations due to SDS concentration, ACN amount, buffer types, or buffer ionic strength was also studied. It was reported that separation efficiency improved by the presence of ACN and DMF in the running buffer; however, the presence of methanol or propanol did not improve the separations.

In an other study, Peng et al. again reported the use of surfactants and organic modifiers for the analysis and separation of two synthetic, unsymmetrical photosensitizer isomers, derivatives of benzoporphyrin (BPD) (Peng et al., 2005). The separations were performed at various pH values, with various buffers. The first compound was benzoporphyrin derivative monoacid, BPDMA. The second compound was the principal metabolite, benzoporphyrin derivative diacid, which has two enantiomers. Peng et al. reported that BPD enantiomers are very easily hydrolyzed at high pH (CAPS buffer, pH > 11). They did not recommend the use of high concentrations of ammonium acetate buffer, because it caused formation of bubbles inside the capillary. In citric acid buffer, the BPD enantiomers were protonated at the propionic side chain. The effective charge was the same for BPDDA and BPDMA, and the electrophoretic mobility difference between the two enantiomers was very small. However, at pH > 3.5 BPDDA and BPDMA were deprotonated. The preferred buffer was borate due to its high buffering capacity and its ability to be used at high concentrations. BPDMA and BPDDA enantiomers were poorly separated at pH 8.1. They could be separated to some extent at pH 8.6 and were completely separated at pH 9.2 with less than 1% decomposition in 1 h. By increasing the pH to 9.6, the BPD enantiomers were further distinguished but a decrease in signal was reported. At this high pH, the fluorescence was adversely affected and the migration time was longer.

Peng et al. have also discussed the separation enhancement by the use of chiral selectors, HP- $\beta$ -CD, DM- $\beta$ -CD,  $\beta$ -CD and  $\gamma$ -CD and bile salts (Peng et al., 2005). They

reported bile salts, especially sodium cholate (20 - 25 mM) to give the best separation of all the chiral selectors used. None of the other additives improved chiral separation.

Peng et al. have also discussed the effect of organic solvents in enhancing the separation in the case of BPD derivatives. The organic solvents alter the polarity and viscosity of the buffer, by acting as solvents for the analytes which are poorly soluble in aqueous solution. The organic solvents increase solvation of solutes and modify the affinities of hydrophobic solutes. ACN, DMF, methanol, DMSO, *n*-propanol and isopropanol were studied. Separations of the enantiomeric forms were reported by varying the percentage of ACN. It was reported that 10 - 15% ACN was ideal.

Andrighetto et al. reported the effect on CE separation due to the presence of cyclodextrins (CDs) and organic modifiers (Andrighetto et al., 2000). They studied water-soluble anionic porphyrins, such as TCPP [*meso*-tetrakis(4-carboxyphenyl)porphyrin], TSPP [*meso*-tetrakis(4-sulfonatophenyl) porphyrin] and its zinc and copper complexes (Andrighetto et al., 2000). The aggregation of the porphyrins in aqueous solutions was prevented by using cyclodextrins (CDs) and organic modifiers.  $\beta$ -CD and its *O*-methylated derivatives, DM- $\beta$ CD [heptakis-(2,6-di-*O*-methyl)- $\beta$ -cyclodextrin] and TM- $\beta$ CD [heptakis-(2,3,6-tri-*O*-methyl)- $\beta$ -cyclodextrin] were used to separate CuTPPS and TPPS. Andrighetto *et al.* used a high concentration phosphate buffer. The separations were performed at low pH, < 3 to minimize the electroosmotic flow (EOF) and the analysis times. The addition of 1 mM  $\beta$ CD to the buffer resulted in sharper peaks and longer migration times. In the presence of 1 mM DM- $\beta$ CD the peaks were not separated and the migration times increased. In the presence of TM- $\beta$ CD, a

stronger complexation was observed, where the two porphyrins comigrate to give a single peak. Andrighetto *et al.* concluded that the binding of cyclodextrins to the porphyrins increased in the order of  $\beta\text{CD} < \text{DM-}\beta\text{CD} < \text{TM-}\beta\text{CD}$ , which is opposite to the order for separation of the porphyrins.

Andrighetto *et al.* also used the organic modifier, 20% DMSO, to separate TSPP, CuTPPS and ZnTPPS with 0.75 mM  $\beta\text{CD}$ . At this concentration of  $\beta\text{CD}$ , CuTPPS and ZnTPPS peaks could not be resolved but the peak for TPPS was observed. Changing the  $\beta\text{CD}$  concentration did not help to separate the two porphyrins. The addition of DMSO to the buffer reduced the binding affinity between the porphyrin and  $\beta\text{CD}$ , allowing for better separation. The reason reported for this observation was the formation of inclusion compounds between  $\beta\text{CD}$  and the organic solvents, due to the hydrophobic effect. This gives these complexes more stability in aqueous solutions than in organic solvents or in mixed water-organic solvent mixtures (Zhang *et al.*, 1998). In the presence of 20% DMSO in the buffer, only two peaks were observed. However, the presence of 0.75 mM  $\beta\text{CD}$  resulted in baseline separation of the three porphyrins and even some minor porphyrin impurities.

Dixon *et al.* showed that simple mixtures of sulfonated naphthyl porphyrins can be separated as a function of charge by capillary electrophoresis at high pH (Dixon *et al.*, 2004). This work has been reported in its entirety as Section V of this chapter. Separation was enhanced by the use of cyclodextrins. The sulfonated naphthyl porphyrins studied were mixtures of numerous compounds, in which the porphyrin had been sulfonated to variable extents or had various positional isomers. The compounds analyzed were

sulfonated 5,10,15,20-tetra(1-naphthyl)porphyrin (T1NapS) and sulfonated 5,10,15,20-tetra(2-naphthyl)porphyrin (T2NapS) and their Cu or Fe derivatives.

The electropherograms of the T1NapS and T2NapS species were in general similar. The comparison of the separation of T2Nap5S,Cu in the presence of  $\beta$ CD and  $\gamma$ CD showed that  $\beta$ CD gave a series of poorly resolved peaks from approximately 4 - 6 min;  $\gamma$ CD showed three prominent peaks from 3.5 - 4.5 min. The electropherogram of T1Nap5S,Cu in the presence of CD was very similar to that of T2Nap5S,Cu. However, unlike the 2-naphthyl T2Nap5S,Cu, the 1-naphthyl T1Nap5S,Cu showed three distinct peaks even in the absence of cyclodextrin. This could be the result of reduction in self-stacking of the 1-naphthyl porphyrin; its atropisomers have hindered rotation around the 1-naphthyl-porphine bond. As for the 2-naphthyl isomers T2NapS,  $\beta$ CD seemed to show more components, but without baseline separation. The extent of sulfonation was greater for T1Nap10S (10 h sulfonation) than for T1Nap5S (5 h sulfonation), as indicated by an additional peak at 7 min for T1Nap10S. The addition of a metal to the central core affected the detailed pattern of the peaks and the net migration times. CE separation of T2NapS,Fe species did not give good separation even with cyclodextrins, presumably due to the axial ligation of the iron (various axial ligands in exchange as well as the equilibrium between the monomer and  $\mu$ -oxo dimer).

## **2. Detection methods/signal enhancement.**

Zhang et al. reported the enhancement of CE signal by the use of on-line chemiluminescence (CL) detection (Zhang et al., 1998). For chemiluminescence reactions involving various analyte separations, luminol in NaOH was added to H<sub>2</sub>O<sub>2</sub>.

The metalloporphyrins were used as catalysts for this reaction. Zhang et al. reported the separation and detection of MnTPPS4 and CoTPPS4. The separation conditions for CoTPPS4 were: 0.01 M phosphate buffer electrophoretic buffer with 0.001 M luminol at pH 4.5, adjusted with 0.001 M nitric acid. For the separation of MnTPPS4 the separation conditions were: 0.01 M borate buffer with 0.001 M luminol at pH 9.6.

**b. Cationic Porphyrins.** Dixon et al. reported the separation of symmetrical and unsymmetrical, synthetic cationic porphyrins at low pH (2 - 5) based on the difference in charge and/or mass of the analytes (Dixon et al., 1998). The porphyrins were synthesized by alkylation of the parent tetrapyridylporphyrin (TPyP) to give various pyridinium porphyrins, including the tetramethylated (TMPyP4), tetrabutylated (TBPpyP4), and tetraoctylated (TOPpyP4) derivatives. The methylation of TPyP resulted in a mixture of the mono-, *cis*-di-, *trans*-di-, tri and tetramethylated porphyrins (TMPyP4). The other porphyrins had side chain of aminopropyl and ethylcarboxylic acid. Porphyrins with pyridinium group at the 2-position, on the phenyl ring (TMPyP2) were also studied.

The effect of pH on separation was showed by the separation of a mixture of TMPyP4, TBuPyP4 and TOcPyP4 at pH 3.0, 3.7 and 4.4. The best separation was seen at the lowest pH. The migration time was dependent on the length of the side chain on the pyridyl group, TOcPyP4 having the longest migration time.

Tetraphenylporphyrins with a single substituent at the 2-position, in which each ring has identical substituents, have four isomers, termed atropisomers:  $\alpha\alpha\alpha\alpha$ ,  $\alpha\alpha\alpha\beta$ ,  $\alpha\alpha\beta\beta$  and  $\alpha\beta\alpha\beta$ . Separation of the fully methylated tetra-2-pyridyl porphyrin was done at high concentration of the phosphate buffer at three different pH values (2.0, 3.0 and

4.0). The different atropisomers had different mobilities, presumably resulting from different shapes and dipole moments.

Capillary electrophoresis separations were also reported for the synthetic mixture of authentic samples of the monomethylated, *cis*-dimethylated, trimethylated and tetramethylated TMPyP4. Good separation was achieved with a 75 mM phosphate buffer at pH 2.0, 3.0, 4.0 and 5.0. The separation was sensitive to pH and ionic strength of the buffer, as well as to the applied voltage. At pH 2, only three peaks were observed. When the pH was higher than 5, no baseline separation was observed. The best resolution of this mixture was observed at pH 3 - 4, where the unalkylated pyridyl rings are presumably protonated. The ionic strength of buffer was also important for this separation. With a lower concentration buffer, 50 mM, only a single peak was observed. At a buffer concentration of 100 mM, only a diffuse and broad peak was observed. When the voltage was higher than 10 kV, the separation time was shorter but the resolution was poorer. At voltages lower than 10 kV, peak broadening occurred. At pH values where the pyridyl nitrogens were not protonated (pH.5), good separations were not achieved, presumably because the cationic porphyrins interacted with the partial negative charges of the silica on the capillary walls. Also, the four components were not separated completely at low pH (pH 2).

Dixon et al. also showed the separation of TPyP derivatives bearing additional charges. Optimal separation of the propionate TPyP derivatives by capillary electrophoresis was achieved at 13 kV with a 50 mM phosphate buffer at pH 2.5. Voltages higher or lower than 13 kV gave different resolutions, but did not affect the

separation significantly. Relatively low pH values ( $< 3$ ) were needed to achieve this separation. No separation was observed at pH 5, where these propionate TPyP derivatives were presumably zwitterions with a net charge of zero, and hence had no electrophoretic mobility.

Dixon et al. reported that cobalt<sup>III</sup>, copper<sup>II</sup>, iron<sup>III</sup>, manganese<sup>III</sup>, palladium<sup>II</sup>, tin<sup>IV</sup>, vanadyl (VO) and zinc<sup>II</sup> derivatives of TMPyP4 complexes can be separated. Separation conditions involved high concentration phosphate buffer at low pH (2.1).

**iii. Complexation between a synthetic, aromatic and anionic porphyrins (organic anion) organic cation and an organic anion in aqueous solutions.** It has been shown that the complexation of a organic anionic group and an organic cation can be enhanced by the addition oligosaccharides, e.g., TPPS4 with Methylene Blue in the presence of CDs (Hamai & Satou, 2001). Hamai et al. studied the complexation between TPPS4 and the organic cationic groups octyltrimethylammonium bromide (OTMA) and hexyltrimethylammonium bromide (HTMA) in the presence of  $\gamma$ CD (Hamai et al., 2006). In the case of both OTMA and HTMA micelles were not formed due to using low concentrations of both. They have used spectrometric methods and CE in this study.

Hamai et al. reported the absorption spectra of the complex of TSPP (1  $\mu$ M) with OTMA (variable concentrations) in  $\gamma$ CD (5 mM) solution at pH 7.3. They proposed the formation of a ternary inclusion complex of 1:1:1 CD:TPPS4:OTMA, via ICD (induced circular dichroism). The addition of OTMA did not dissociate the TPPS4-CD complex. Hamai et al. reported the fluorescence spectra of TPPS4 in the presence of  $\gamma$ CD at pH 7.3, with varying concentrations of OTMA. The formation of the  $\gamma$ CD-TSPP-OTMA ternary

inclusion complex was shown via fluorescence; the 1:2 TPPS4-OTMA complex might be formed at high OTMA concentration. Equilibrium constant was not evaluated using fluorescence for the formation of the  $\gamma$ CD-TSPP-OTMA in the presence of 5 mM CD and variable OTMA concentrations. Equilibrium constant was not evaluated due to the less than 10% variation in fluorescence intensity change. However, equilibrium constant was reported via CE studies. The equilibrium constants for TPPS4.OTMA ( $K_1$ ) and TPPS4.2OTMA ( $K_2$ ) complexes were evaluated via fluorescence studies. The same analytical analysis was performed with HTMA and similar trends were seen; formation of the 1:1 and 1:2 TPPS4-HTMA complex. The  $K_1$  for HTMA was greater than that for OTMA and the  $K_2$  for HTMA was smaller than that for OTMA. It was reported that this was probably due to hydrophobic and hence cooperative interactions between the two OTMA compared to the interactions TPPS4 and OTMA. The formation of the 1:2 TPPS4-OTMA-HTMA complex was cooperatively preferred. Hamai et al. proposed that since the cooperative interactions of OTMA seemed to be much stronger than those of HTMA, it lead to the greater  $K_2$  value for OTMA.

The CE studies were performed using the same buffers which were also used for spectroscopic studies (6.7 mM phosphate buffer, pH 7.3). Electropherograms were reported for 10  $\mu$ M TPPS4 with variable CD concentration. Hamai et al. reported that as the CD concentration increased, the migration time of TPPS4 shortened, indicating the formation of  $\gamma$ CD-TPPS4 inclusion complex. The incorporation of TSPP into the  $\gamma$ CD cavity increased the apparent molecular volume of TPPS4. The apparently increased volume of a TPPS4 molecule increased the electrophoretic mobility of TPPS4, because

TPPS4 is negatively charged. The complex formed was 1:1  $\gamma$ CD-TPPS4. The equilibrium constant for the formation was determined via electrophoretic mobility of TPPS4.

Electropherograms were also reported where the concentration of TPPS4 was 10  $\mu$ M, CD was 5 mM and the concentration of OTMA was variable. The migration time of the EOF marker indicated the adsorption of OTMA on the walls of the capillary. The electrophoretic mobility of TPPS4 increased with increased OTMA concentration, indicating complexation. It was reported that the equilibrium constant for the formation of 1:1 TPPS4.OTMA ( $K_1$ ) was twice that of the equilibrium constant measured via fluorescence. It was reported that 1:2 TPPS4.OTMA could not be formed due to low OTMA concentrations.

### **Section III.**

#### **Review.**

#### **Cyclodextrins and TPPS4.**

A considerable amount of work has been reported concerning the complexation of cyclodextrins (CDs) and the tetrasulfonated 5,10,15,20-tetraphenylporphyrin (TPPS4). In our study, capillary electrophoresis (CE) was used to analyze analytes, including TPPS4. Cyclodextrins were added to the running buffer in the CE experiments to enhance the signal, obtain sharper peaks, prevent aggregation of sample, and if possible, reduce the migration time of the analytes. The experimental details are discussed in Section IV and V of this chapter. This section reviews the work of various research groups on cyclodextrins and TPPS4 and the effects of this complexation.

Cyclodextrins are cyclic oligosaccharides, named according to the number of D-glucopyranose units:  $\alpha$ CD has 6,  $\beta$ CD has 7, and  $\gamma$ CD has 8 units (Gubitz & Schmid, 1997). They are cone-shaped with a hollow cavity. They are soluble in water due to the presence of the primary and secondary hydroxy groups, positioned at the narrow and the wide rim of the cyclodextrin cavity, respectively. However, the core is very hydrophobic, enabling a wide variety of organic compounds to form inclusion complexes with cyclodextrins in aqueous solution.

Along with the native  $\alpha$ -,  $\beta$ - and  $\gamma$ CD, their various modified cyclodextrins have also been studied. Cyclodextrins modified by spacers are not reviewed herein. Studies of both uncharged and charged cyclodextrins (cationic and anionic) have been reported. TPPS4 has been studied with the *O*-methylated derivatives, DM- $\beta$ CD and TM- $\beta$ CD (Andrighetto et al., 2000), the 2-hydroxypropyl derivatives (Hamai & Koshiyama, 1999; Mosinger et al., 2000); the ionic cyclodextrins, sulfobutylether- $\beta$ CD (SBE- $\beta$ CD) and carboxymethyl- $\beta$ CD (CM- $\beta$ CD), have also been used (Wang et al., 2001a; Wang et al., 2002). Complexation between TPPS4 and different cyclodextrins has been studied via fluorescence spectroscopy, polarography, TLC and NMR (Wang et al., 2002). For ionic cyclodextrins the charge interaction plays an important role in the inclusion procedure (Wang et al., 2002).

#### **i. Aggregation of TPPS4.**

Before detailing the interaction of TPPS4 with cyclodextrins, it is useful to review the aggregation of TPPS4, for example, in aqueous solutions. Aggregation has been reported in neutral conditions at 40  $\mu$ M and basic conditions at 20  $\mu$ M concentration of

the porphyrin (Ribó et al., 1995). TPPS4 aggregation in acidic aqueous solutions at 1 mM concentration has also been studied (Rubires et al., 1999). Aggregation has been proposed to be due to the hydrophobic phenyl groups leading to lateral aggregation (Rubires et al., 1999; El Hachemi et al., 2001). Under neutral conditions, staggered  $\pi$ - $\pi$  stacking is due to the hydrophobic interaction between porphyrin macrocycles, where TPPS4 aggregates into stacks of no particular geometry (Ribó et al., 1995). When TPPS4 is diprotonated (acidic conditions) aggregation results through the electrostatic interactions between the positively charged porphyrin ring and the sulfonate groups (edge-to-edge or J-aggregates). These J-aggregates give different arrays depending on the meso-substitution pattern (Rubires et al., 1999). H-aggregates (face-to-face) are reported for porphyrin species with less than four sulfonic acid groups or phenyl rings. It was proposed that it was easy to convert from homoassociates of TPPS4 to heteroassociates of cyclodextrin-TPPS4. This was facilitated by the free rotation of the sulfonatophenyl group inside the cyclodextrin cavity (Ribó et al., 1995).

#### **ii. The effect of cyclodextrins on the aggregation of TPPS4.**

Using techniques such as NMR (Ribó et al., 1995; El Hachemi et al., 2001) and adsorption and fluorescence spectroscopy (Wang et al., 2001b) it has been reported that cyclodextrins help in disintegrating the easily formed aggregates in case of concentrated aqueous solutions of TPPS4.

El-Hachemi et al. studied a series of sulfonatophenyl *meso*-substituted porphyrins with varying degree of sulfonation (TPPS<sub>n</sub>), including TPPS4, with native cyclodextrin (El Hachemi et al., 2001). They used NMR, where the concentration of the porphyrin was

high, resulting in partially aggregated TPPS4. The effect of the extent of homoassociation on the ratio of sulfonatophenyl to phenyl substituents was studied. The less sulfonated porphyrins aggregated more, utilizing their hydrophobic phenyl groups. Cyclodextrins did not have significant effect on porphyrin disaggregation, as seen by small or no changes in the NMR spectra of the porphyrin aggregates. El-Hachemi et al. also reported the competition between porphyrin homoassociation and porphyrin-cyclodextrin heteroassociation. El-Hachemi et al. proposed that the complexation between the porphyrin and the cyclodextrin can hinder the formation of staggered stacks of porphyrin homoassociates ( $\pi$ - $\pi$  stacking) but has less effect on aggregation due to the homoassociation through the hydrophobic region of the phenyl substituents (lateral aggregation).

El-Hachemi et al. reported that at least partial, and under certain experimental conditions complete, disaggregation of TPPS4 occurred with  $\beta$ - and  $\gamma$ CD; studies were performed at 500 MHz over a temperature range of 7 - 67 °C. Disaggregation occurred at higher temperature and also with the addition of cyclodextrins. This was detected through a significant change of the chemical shifts of the porphyrin signals and also through an increase in signal resolution. For TPPS4 disaggregation was possible at high cyclodextrin concentration at room temperature. For the less sulfonated porphyrins, both high temperatures and high cyclodextrin concentrations were necessary to obtain  $^1\text{H}$  NMR spectra of good resolution.

### **iii. Complexation through the meso-phenyl group.**

Ribó *et al.* reported that TPPS4 in neutral media forms inclusion assemblies, through its *meso*-phenyl groups, with  $\beta$ CD and  $\gamma$ CD, but not with  $\alpha$ CD (Ribó *et al.*, 1995). This was suggested by the presence of an NOE signal observed between the internal protons of cyclodextrins and the *ortho* and *meta* protons of TPPS4 for  $\beta$ CD and  $\gamma$ CD, but not with  $\alpha$ CD. Ribó *et al.* proposed that the phenyl ring of the porphyrin penetrates to a similar extent for both of the larger cyclodextrins. In the case of diprotonated TPPS4, inclusion complexes were formed only with  $\beta$ CD. This is because the inclusion complex formed between diprotonated TPPS4 and  $\beta$ CD could place the phenyl groups of the porphyrin nearly orthogonal to the porphyrin ring. However, with  $\gamma$ CD, inclusion complexes are not formed. This is because the phenyl groups of the porphyrin are planar to the porphyrin ring in the inclusion complex. This might cause steric hindrance between the cyclodextrin CH<sub>2</sub>OH groups and the phenyl rings.

### **iv. Complexation of TPPS4 takes place through the primary and secondary face for $\gamma$ CD and $\beta$ CD, respectively.**

Primary and secondary hydroxy groups are positioned at the narrow and wide rim of the cyclodextrin cavity, respectively. The ends are referred as primary and secondary face of the cyclodextrin, respectively (Ribó *et al.*, 1995).

Studies of native,  $\beta$ - and  $\gamma$ CD have been able to show how these cyclodextrins interact with the porphyrin. NMR studies indicated that  $\beta$ - and  $\gamma$ CD complex with TPPS4 through the secondary and primary face, respectively. This was indicated by the significant chemical shifts for the hydrogens placed in the primary face in the case of

$\gamma$ CD and for hydrogens placed in the internal secondary face in the case  $\beta$ CD (Ribó et al., 1995; Hamai & Koshiyama, 1999; El Hachemi et al., 2001). UV-vis absorption and fluorescence studies were used to propose the complexation geometries through the binding constant calculations (Mosinger et al., 2000). Mosinger et al. used the modified cyclodextrin, HP- $\beta$ CD, and reported that complexation involves the primary face of the modified cyclodextrin with a binding constant,  $K_b$ , of about  $10^2$  times the  $K_b$  for native  $\beta$ CD.

**v. Different cyclodextrins complex with TPPS4 with different stoichiometries.**

The equilibrium constant for the 1:1 complexation between TPPS4 and  $\beta$ -CD have been reported (Venema et al., 1998; Mosinger et al., 2000). Ribó et al. studied the complex formation in aqueous solution using NMR and electronic absorption spectroscopy (Ribó et al., 1995). A 2:1 complexation ratio with  $\beta$ - and  $\gamma$ CD, but not with  $\alpha$ CD was reported. Wang et al., in an earlier (Wang et al., 2001c) and also in a more recent work (Wang et al., 2002), with native as well as modified cyclodextrins, e.g.,  $\gamma$ CD,  $\beta$ CD, HP- $\beta$ CD, SBE- $\beta$ CD and CM- $\beta$ CD, reported 1:1, as well as 1:2 complexations with the cyclodextrins. Hamai and Koshiyama studied the complexation of TPPS4 with  $\alpha$ CD,  $\beta$ CD, TM- $\beta$ CD and  $\gamma$ CD by absorption, fluorescence and induced circular dichroism spectra in basic solutions (pH 10.1) (Hamai & Koshiyama, 1999). They proposed that  $\alpha$ CD and  $\beta$ CD most likely form 1:1 and 2:1 host-guest complexes with TPPS4, while TM- $\beta$ CD and  $\gamma$ CD form 2:1 and 1:1 complexes with TPPS4, respectively. Mosinger et al. proposed a 1:1 complexation between TPPS4 and HP-CDs in aqueous neutral solutions (Mosinger et al., 2000).

## Section IV.

### Experiments.

#### i. Materials and methods.

The porphyrins purchased from Frontier Scientific (Logan, Utah) were: TPP, *meso*-tetraphenylporphine; TPPS<sub>4</sub>, *meso*-tetraphenylporphyrin tetrasulfonate; Co(II)TPPS<sub>4</sub>, the cobalt chelate of *meso*-tetraphenylporphyrin tetrasulfonate and Cu(II)TPPS<sub>4</sub>, the copper chelate of *meso*-tetraphenylporphyrin tetrasulfonate. The porphyrins obtained from Midcentury Chemicals (Chicago, IL) were TPPS<sub>3</sub>, *meso*-tetraphenylporphyrin trisulfonated (Midcentury Chemicals, Chicago, IL); Mn(III)TPPS<sub>4</sub>, the manganese chelate of *meso*-tetraphenylporphyrin tetrasulfonate; Ag(II)TPPS<sub>4</sub>, the silver chelate of *meso*-tetraphenylporphyrin tetrasulfonate; TNapPS, sulfonated 5,10,15,20-tetra-naphthalenophenylporphyrin; TAnthPS, sulfonated 5,10,15,20-tetra-anthracenophenylporphyrin; TPP(8Br)S,Cu, the copper chelate of sulfonated beta-Br<sub>8</sub>-tetraphenylporphyrin; TPP(16F)S,Cu the copper chelate of sulfonated tetra(2,3,5,6-tetrafluoro)phenylporphyrin; TPP(2,3-F<sub>2</sub>)S,Cu, the copper chelate of sulfonated tetra(2-3-difluoro)phenylporphyrin; TPP(2,4-F<sub>2</sub>)S,Cu, the copper chelate of sulfonated tetra(2-4-difluoro)phenylporphyrin; TPP(2,5-F<sub>2</sub>)S,Cu, the copper chelate of sulfonated tetra(2-5-difluoro)phenylporphyrin; and TPP(3,5-F<sub>2</sub>)S,Cu, the copper chelate of sulfonated tetra(3-5-difluoro)phenylporphyrin.

The letter 'S' in the designation indicates that the parent porphyrin was sulfonated. A compound abbreviation followed by a metal refers to the metal chelate of that compound; e.g., TPPS<sub>4</sub>,Cu is the copper chelate of TPPS<sub>4</sub>.

## **ii. Results and discussion.**

### **Capillary electrophoresis analysis of porphyrins.**

Porphyrin stock solutions of  $\sim 2 \times 10^{-3}$  M were prepared by weight. The stock solution was diluted to 10- and 100-fold. The data at higher concentrations was not very helpful due to porphyrin aggregation in solutions. Separations were performed at two pH conditions; with a low pH buffer, 50 mM phosphate (pH 2.5; reverse polarity) and with a high pH buffer, 10 mM phosphate (pH 9.0; normal polarity).

The UV-vis spectra were recorded under the same conditions as used for CE separations (pH 2.5 and 9.0), as well as in other solvents. The dilutions for UV-vis studies were made from the same stock solution which was used for CE separations.

#### **a. Capillary electrophoresis analysis of porphyrins with phenyl groups with sulfonic acid groups only as substituents:**

##### **1.1. Capillary electrophoresis separation of TPPS<sub>4</sub>.**

A single peak was seen at 5.9 min under pH 9.0 separation conditions ( $\lambda_{\text{max}}$  413.5 nm) and 13.9 min under pH 2.5 separation conditions ( $\lambda_{\text{max}}$  433 nm) (data not shown). The migration times varied with concentration of the porphyrin solution, especially for separations at pH 9.0. The electropherograms at higher concentrations showed multiple, asymmetric peaks with longer migration times perhaps due to porphyrin stacking. The shift of the  $\lambda_{\text{max}}$  from 412 nm under pH 9.0 separation conditions to  $\sim 433$  nm under pH

2.5 separation conditions is due to the protonation of the inner nitrogens of the porphyrin at low pH (Jimenez et al., 1991).

## 1.2. UV-vis spectra of TPPS4.

The UV-vis spectra of TPPS4 in deionized water showed the characteristic porphyrin peaks for the three dilutions of the stock solution ( $\sim 2 \times 10^{-3}$  M by weight; the dilution factors of 301, 1001 and 3001, in the concentration range of  $\sim 3 \times 10^{-6}$  -  $3 \times 10^{-7}$  M by weight) (**Figure 2.2a**). The major peak (Soret) was observed at 413.5 nm and the smaller peaks (Q-band) at 515, 553, 579 and 633 nm. An almost identical pattern of peaks was seen in a 10 mM  $\text{KH}_2\text{PO}_4$  buffer (pH 9.0) (**Figure 2.2b**). In a 50 mM  $\text{Na}_2\text{HPO}_4$  buffer (pH 2.5) at the lower concentrations of TPPS4 ( $\sim 10^{-5}$  and  $10^{-6}$  M by weight), a major peak at  $\sim 434$  nm and two minor peaks at  $\sim 644$  and 592 nm were seen (**Figure 2.2c**). However, a solution of dilution factor 301 ( $\sim 10^{-4}$  M by weight), in the low pH buffer, showed two additional peaks at  $\sim 490$  nm and  $\sim 705$  nm, along with the rest of the peaks appearing at lower concentrations. These two additional peaks have been ascribed to the formation of J aggregates of the diacid ( $\text{H}_4\text{TPPS}_4^{-2}$ ) (Ohno et al., 1993). This occurs at high TPPS4 concentrations, where Beer's law is no longer followed. The appearance of the 490 nm peak for TPPS4 has also been attributed to aggregate formation upon protonation of the porphine monomers (Akins et al., 1996b).

### 2.1. Capillary electrophoresis separation of CuTPPS4.

Under pH 9.0 separation conditions, a sharp peak with slight fronting at 7.0 min ( $\lambda_{\max}$  410 nm, with a second band at 537 nm) was observed (data not shown). Under pH 2.5 separation conditions, only a single sharp peak at 6.2 min with tailing and a  $\lambda_{\max}$  of 411 nm was observed (data not shown). The  $\lambda_{\max}$  shifted slightly from 405 nm to 411 nm as the concentration of the porphyrin solution decreased (over a concentration range of  $\sim 10^{-4}$  -  $10^{-6}$  M by weight) under pH 2.5 separation conditions. The reason is unknown for the small shift observed in the  $\lambda_{\max}$  with concentration in the CE experiment but not in the UV-vis experiment.

### 2.2. UV-vis spectra of CuTPPS4.

The UV-vis spectra of CuTPPS4 in deionized water (**Figure 2.3**) and in 10 mM  $\text{KH}_2\text{PO}_4$  buffer (pH 9.0) (data not shown) showed the characteristic porphyrin peak at 412 nm and a second peak at 540 nm for all five dilutions of the stock solution ( $\sim 10^{-4}$  M by weight; the dilution factors of 26, 39, 51, 101 and 752 in the concentration range of  $\sim 4 \times 10^{-6}$  -  $1 \times 10^{-7}$  M by weight). The Q-band region consisted of a single peak, as expected for a metalloporphyrin (Herrmann et al., 1978). The spectra of dilutions of TPPS4 in 50 mM  $\text{Na}_2\text{HPO}_4$  buffer (pH 2.5) were almost identical to those in the 10 mM  $\text{KH}_2\text{PO}_4$  buffer (pH 9.0) (data not shown). The reason for similar spectra at both the high and low pH conditions is due to the fact that CuTPPS4 does not undergo core protonation and remains tetraanionic in moderately acidic solutions (Herrmann et al., 1978).

### 3.1. Capillary electrophoresis separation of TPPS3.

Under pH 9.0 separation conditions an unresolved peak, with slight fronting, was observed at 4.7 min (412 nm) (data not shown). The fronting effect was observed at the both high and low concentrations of the porphyrin. Under pH 2.5 separation conditions the peak height was much lower than that in the case of pH 9.0 for equivalent concentrations (data not shown). An unresolved, sharp peak at 14.4 min with a short peak at 14.8 min was observed (433 nm). The shift of  $\lambda_{\max}$  from 412 nm under pH 9.0 separation conditions to 433 nm under pH 2.5 separation conditions was observed due to protonation of inner nitrogens at low pH.

### 3.2. UV-vis spectra of TPPS3.

The UV-vis spectra of TPPS3 in deionized water ( $\sim 10^{-4}$  M by weight; the dilution factors of 17, 25, 33, 50, 100, 200 and 1000 in the concentration range of  $\sim 1 \times 10^{-5}$  -  $3 \times 10^{-7}$  M by weight) (**Figure 2.4a**). The Soret peak shifted slightly from  $\sim 418$  to  $\sim 415$  nm as the sample concentration was increased, indicating possible aggregation. The Q-bands were seen at  $\sim 515$ , 555, 584 and 634 nm. Pasternack et al. reported the spectral data for TPPS3 in an 80 - 90% ethylene glycol-water mixture at pH 7.5. The Soret peak was reported at 418 nm, while the Q-band at 514, 550, 587 and 642 nm (Pasternack, 1973). Rubires et al. reported the UV-vis spectral data of TPPS3 in water for  $5 \times 10^{-6}$  M and  $2 \times 10^{-4}$  M aqueous solutions (Rubires et al., 1999). In both cases the  $\lambda_{\max}$  was  $\sim 412$  nm and the Q-bands were  $\sim 515$ , 553, 580 and 636 nm. In a more recent study, after ours and others earlier research, Zhang et al. reported the UV-vis spectra of TPPS3 under three

different conditions (Zhang et al., 2003a). In neutral solution the Soret band was reported at 413 nm and four weak Q bands at 516, 553, 580, and 634 nm.

The Q-bands of TPPS3 and TPPS4 spectra are slightly different in a pH 9.0 buffer (data not shown). For TPPS4 the peak heights decreased in going from 515 nm to 633 nm (the first to the fourth peak of the Q-band) whereas for TPPS3 the first two peaks of the Q-band at 515 and 555 nm are essentially of the same height and the third peak at  $\sim 584$  nm is quite broad. This was observed at all concentrations studied.

The UV-vis spectra of TPPS3 in 50 mM Na<sub>2</sub>HPO<sub>4</sub> buffer (pH 2.5) ( $\sim 10^{-4}$  M by weight; the dilution factors of 17, 20, 25, 33, 50, 100, 200 and 500 in the concentration range of  $\sim 1 \times 10^{-5}$  -  $5 \times 10^{-7}$  M by weight) are shown in **Figure 2.4b**. It is known that TPPS3 shows extensive aggregation and low solubility in water (Kalyanasundaram & Neumann-Spallart, 1982). Our UV-vis data is consistent with all the previous and more recent studies. In mildly acidic solution (pH 4 - 5), the Soret was red-shifted to 434 nm and the Q-bands were at 595 and 647 nm due to the formation of N-protonated diacid (H<sub>4</sub>TPPS3<sup>2+</sup>, reported earlier). When the pH of the solution decreased below 2, new bands of the aggregated porphyrin diacid (H<sub>4</sub>TPPS3<sup>2+</sup>) appeared at 489 and 708 nm with higher intensity than the Soret at 434 and the Q-band at 647 nm.

A broad and split Soret peak was observed with  $\lambda_{\text{max}}$  of 421 and 433 nm (**Figure 2.4b**). As the concentration of the porphyrin was increased, the peak height at 421 nm increased at the expense of the 433 nm peak. Four peaks were seen in the Q-band region,  $\sim 556, 594, 645$  and  $700 - 707$  nm. The peak at  $\sim 700 - 707$  nm is known to be due to the

formation of J-aggregates in the case of TPPS4 (Akins et al., 1996a). As in the case of TPPS4, a peak  $\sim 490$  nm was seen even at very low concentrations of the sample. Rubires et al. reported the UV-vis data for the three different concentrations of TPPS3,  $2 \times 10^{-6}$ ,  $2 \times 10^{-5}$  and  $2 \times 10^{-4}$  M solutions in 0.1 M HCl (Rubires et al., 1999). The Soret peak was shifted to  $\sim 440$  nm for the two higher concentrations. The prominent peak was not the Soret peak but the peak at 490 nm. The aggregation was more pronounced in the work of Rubires et al., due to the presence of 0.1 M HCl, compared to 50 mM  $\text{Na}_2\text{HPO}_4$  buffer (pH 2.5) as used in this study. The band at  $\sim 700$  nm was almost the same height as the Soret band.

#### **4. Capillary electrophoresis separation of a mixture of metalloderivative of TPPS4.**

A solution mixture containing Mn(III), Co(II), Cu(II) and Ag(II) derivatives of TPPS4 was prepared ( $\sim 10^{-5}$  M each by weight). Peaks were seen at 4.29 min (Mn, 400 nm), 5.33 min (Co, 425 nm), 6.38 min (Cu, 412 nm) and 7.7 0 min (Ag, 420 nm) (**Figure 2.5**). The peaks were assigned according to their migration time from their individual separations. The clear separation indicated that CE was a useful technique for the separation of metalloTPPS4 mixtures.

#### **b. Capillary electrophoresis analysis of commercial samples of porphyrins with aryl groups with sulfonic acid groups as substituents (naphthyl and anthracyl groups):**

### 1.1. Capillary electrophoresis separation of TNapPS.

A commercially available sample had four peaks at 5.7, 7.6, 10.6 and 16.1 min under pH 9.0 separation conditions (**Figure 2.6a**). Under pH 2.5 separation conditions, four peaks at 6.0, 8.3, 10.7 and 16.6 min were observed (**Figure 2.6b**). The shift of  $\lambda_{\text{max}}$  from 420 nm under pH 9.0 separation conditions to 444 nm under pH 2.5 separation conditions could be due to the protonation of the inner nitrogens at low pH (Herrmann et al., 1978). The peaks were much taller under pH 9.0 separation conditions for equivalent concentrations.

The multiple peaks under both high and low pH separation conditions could be due to the presence of species that were sulfonated to different extents. The observation that the peak pattern does not change with dilution indicates that TNapPS is less prone to self-stacking than TPPS4, probably because the naphthyl rings are larger than the phenyl rings. Hanyz and Wrobel reported that the substitution of the porphyrins with larger naphthyl groups probably leads to the delocalization of the  $\pi$  electrons in the porphyrin ring due to the various structures and symmetry of the porphyrin (Hanyz & Wrobel, 2002).

### 1.2. UV-vis spectra of the TNapPS.

The UV-vis spectra of TNapPS in deionized water were taken for five dilutions of the stock solution ( $\sim 1 \times 10^{-3}$  M; the dilution factors of 101, 151, 216, 301 and 752, in the concentration range of  $\sim 1 \times 10^{-5}$  -  $1 \times 10^{-6}$  M by weight) (**Figure 2.7a**). The major peak

(Soret) at 419 nm and the smaller peaks (Q-band) at ~ 516, 553, 579 and 633 nm were observed. The heights of the 553 and 580 nm peaks were different from those of TPPS4. In the case of TPPS4, the 553 nm peak was taller than the 580 nm peak but the reverse was seen in the case of TNapPS, where 553 nm was more of a plateau-shaped region. In both the cases the 516 nm peak was the tallest peak of the Q-band. Absorbance was also observed in the 250 - 350 nm region, with a slight indication of a peak at ~ 278 nm. An almost identical pattern of peaks was seen in the pH 9.0 buffer (data not shown).

In the pH 2.5 buffer a major, a relatively broad peak at ~ 444 nm and two minor peaks at ~ 636 and 683 nm (Q-band) were observed (versus the four peaks in water or in a pH 9.0 buffer (**Figure 2.7b**)).

### **2.1. Capillary electrophoresis separation of TAnthPS.**

A commercially available sample had multiple peaks with shoulder peaks, at 8.8, 10.2 and 10.5 min (435 nm) under pH 9.0 separation conditions. Under pH 2.5 separation conditions the sample had only a small single peak at ~ 6.3 min (434 nm) (**Figure 2.8a**). The peak heights were about twice higher under pH 2.5 separation conditions (**Figure 2.8b**). TAnthPS does not stack under the CE conditions at both pH, shown by the same peak pattern at both high and low concentrations of the sample (data not shown).

### **2.2. UV-vis spectra of the TAnthPS.**

The UV-vis spectra of TAnthPS in deionized water (data not shown), and in buffers at pH 2.5 (**Figure 2.9**) and pH 9.0 (data not shown) are almost identical. Five

dilutions of the stock solution ( $\sim 1 \times 10^{-3}$  M; the dilution factors of 101, 151, 216, 301 and 752, in the concentration range of  $\sim 1 \times 10^{-5}$  -  $1 \times 10^{-6}$  M by weight) were used. The Soret peak was observed at  $\sim 434$  nm, usually observed at  $\sim 415$  nm at neutral and high pH for most porphyrins. The Q-band region had two peaks, at  $\sim 560$  nm, and very low absorbance at  $\sim 517$  nm.

**c. Sulfonated tetraphenylporphyrin with two fluoro-groups on the phenyl rings:**

**TPP(2,6-F2)S (free base, DD194), TPP(2,3-F2)S,Cu (DD755), TPP(2,4-F2)S,Cu (DD720), TPP(2,5-F2)S,Cu (DD713) and TPP(3,5-F2)S,Cu (DD746).**

The sulfonated derivatives of five difluoro tetraphenylporphyrins were studied: derivatives with 2,3-, 2,4-, 2,5-, 2,6- and 3,5-difluoro substituent patterns (**Figure 2.10**). The 2,6-derivative is the free-base. These derivatives differed only in the position of the two fluorine substituents on the peripheral phenyl rings. Biological tests (done in Dr. Compan's laboratory) indicated that these porphyrins inhibited the HIV-1 virus to different extents (**Table 2.1**). The goal of this study was to determine if there was a correlation between the structure of the porphyrins and their biological activities.

**i. UV-vis spectroscopy.**

**1. The 445 - 450 nm spectral band.**

The aqueous solutions of these porphyrins did not have the same color. TPP(2,3-F2)S,Cu (DD755), TPP(2,5-F2)S,Cu (DD713) and TPP(3,5-F2)S,Cu (DD746) gave green aqueous solutions while TPP(2,6-F2)S (free base, DD194) and TPP(2,4-F2)S,Cu (DD720) gave red aqueous solutions.

The UV-vis spectrum of the free base TPP(2,6-F2)S (DD194) was red-shifted slightly from a  $\lambda_{\text{max}}$  (Soret) at 412 nm in a pH 9.0 buffer to a  $\lambda_{\text{max}}$  of 417 nm in a pH 2.5 buffer (data not shown). This red-shift in acidic medium could be due to the partial protonation of the inner nitrogens at low pH (Herrmann et al., 1978). For TPPS4, the Soret at 412 nm is shifted to even longer wavelengths, to  $\sim 430$  nm upon protonation of the inner nitrogens at pH 2.5 (Ribo et al., 1994). Protonation of the inner nitrogens of TPP(2,6-F2)S derivatives might be reduced, in comparison to TPPS4, either because the fluoro groups remove electron density from the porphyrin or because the *ortho* fluoro groups prevent the bending of the porphyrin which is a consequence of protonation.

**Figure 2.11** shows the UV-vis spectra of the copper chelates of the difluoro porphyrins in four different solvents: water, 1 mM EDTA, and phosphate buffers at pH 7.1 and 9.0. The UV-vis spectrum of TPP(2,4-F2)S (DD720), a red aqueous solution, had a  $\lambda_{\text{max}}$  at 410 nm in all four solvents. The UV-vis of the two difluoro compounds, TPP(2,3-F2)S,Cu (DD755) and TPP(2,5-F2)S,Cu (DD713), had a 445 - 450 nm spectral band, in addition to the Soret at  $\sim 410$  nm, in all four solvents; the aqueous solutions of these compounds were green. The 455 nm peak was taller than the 410 nm peak in case of TPP(2,5-F2)S,Cu (DD713) in all the four solvents. TPP(3,5-F2)S,Cu (DD746) did not have a 410 peak, but only a broad, short band at 450 nm with a slight shoulder at  $\sim 475$  nm in all the four solvents; the aqueous solutions of this compound was green.

## **2. Possible origins of the 445 - 450 nm band.**

There are at least four possible origins of the 445 - 450 nm band. First, the 445 - 450 nm band might be due to the presence of a different metalloporphyrin as an impurity,

along with the copper derivatives. For example, W<sup>V</sup>OTPPS4 (451 nm) (Fleischer et al., 1979) and PbTFPS (463 nm) (Langley & Hambright, 1985) are substantially red-shifted in comparison to the other metalloderivatives of TPPS4, including copper (412 nm) (Kadish et al., 1989). However, it seems unlikely that such large and varying amounts of another metal would have been introduced inadvertently in the synthesis, because the compounds were all made by Dr. Peter Hambright (Howard University) within a few weeks of one another. In our laboratory, precautions were taken so that porphyrin did not pick up metals from the surroundings. Glassware was washed with EDTA, and reagents (e.g., methanol) were refluxed with EDTA. Reagents with no or minimum traces of metals were used (e.g., sulfuric acid). EDTA was added to the solutions to sequester any free metal in the sample.

A second possible reason for the observation of long wavelength band is the protonation of the inner core nitrogens of the porphyrin at low pH, shifting the Soret to longer wavelengths (Herrmann et al., 1978). In this study, however, the porphyrins studied were copper chelates and the inner core was prevented from being protonated due to complexation of the inner nitrogens with copper. It is unlikely that the copper was lost because copper porphyrins are in stability class II, and only lose copper when treated with 100% H<sub>2</sub>SO<sub>4</sub> at 25 °C for 2 h (Buchler, 1975). The spectra were independent of pH, also consistent with protonation not being the correct explanation for the red-shift of the Soret band.

Self-stacking of sulfonated porphyrins can lead to significantly red-shifted Soret band. Akins et al. reported that the appearance of the 490 nm peak for TPPS4 could be

due to aggregate formation upon protonation of the porphine monomers (Akins et al., 1996b). However, the cause for the appearance of the 445 - 450 nm band was not aggregation of the compounds under study, because no changes in the UV-vis spectra of the compounds were observed even with the addition of DMSO or methanol to the porphyrin solution (regularly used to break aggregates of porphyrins) (**Figure 2.12a**). Also, no changes in the UV-vis spectra were observed upon varying the concentration of the compounds (**Figure 2.12b**). The ratios of the Soret peak and the 445 - 450 nm peak were the same for all the different concentrations.

A long wavelength band could also be due to additional conjugation within the porphyrin that develops as a result of sulfonation. This would be most likely due to the formation of the intramolecular sulfone, formed by loss of water between a sulfonic acid, at the *ortho* position of one of the phenyl rings, and a neighboring pyrrole position. There is precedence for this in the formation of the related cyclic ketones, first reported by Richeter et al. (**Figure 2.13**) (Richeter et al., 2003). The addition of unsaturated rings fused to the porphyrin system results in bathochromic shifts of all bands. Metal-free 5,10,15,20-tetraphenylporphyrin (H<sub>2</sub>TPP) has a  $\lambda_{\text{max}}$  of 418 nm. The addition of one intramolecular ketone to the structure results in a shift of the Soret from 418 nm to 466 nm in dichloromethane. In further work, Richeter and co-workers made all six isomeric porphyrin diketones and observed that the shift in Soret bands up to 560 nm in dichloromethane (Richeter et al., 2001; Richeter et al., 2004). Richeter also made the derivatives in which an amine link replaced the ketone (Richeter et al., 2004). These also showed a red-shifted Soret.

The hypothesis that the red-shifted bands arise from intramolecular sulfone formation is strengthened by correlating the extent of the formation of the 445 - 450 nm band to the substituent patterns of the difluoro porphyrins. Fluoro groups are predominantly *para* directing (99.1%) and *ortho* directing (0.9%) in sulfonation (March, 1992). Thus, the rings are sulfonated at either *para* or *ortho* position to the two fluoro groups on the phenyl rings. This results in the placement of sulfonic acid groups in the *ortho* position on the phenyl ring (and thus in the close proximity to the pyrrole ring of the porphyrin core), in case of TPP(2,3-F<sub>2</sub>)S,Cu (DD755), TPP(2,5-F<sub>2</sub>)S,Cu (DD713) and TPP(3,5-F<sub>2</sub>)S,Cu (DD746). If these sulfonates near the pyrrole were to lose a water molecule from the sulfonic acid group and the adjacent pyrrole ring, a cyclized sulfone would result (**Figure 2.14a**). The text below looks at the compounds in turn to estimate to what extent they might form the sulfone, and compare this with the experimental observations.

TPP(2,6-F<sub>2</sub>)S (free base, DD194) cannot sulfonate in the positions *ortho* to the porphyrin, closer to the pyrrole ring, because both of these positions are blocked by fluorines themselves (**Figure 2.14b**). In line with a cyclic sulfone hypothesis, no 450 nm band was observed. TPP(2,4-F<sub>2</sub>)S (DD720) should not have sulfonated in the position *ortho* to the porphyrin, closer to the pyrrole ring, because this is *meta* to both fluorines (**Figure 2.14b**). Again, in line with a cyclic sulfone hypothesis, no 450 nm band was observed. TPP(3,5-F<sub>2</sub>)S,Cu (DD746) has two positions *ortho* to the porphyrin, each of which is *para* to a fluorine. These *ortho* positions are therefore the most likely to be sulfonated. This compound showed the Soret as a 450 nm band, consistent with the

extensive formation of the sulfone. TPP(2,5-F<sub>2</sub>)S,Cu (DD713) has one open position *ortho* to the porphyrin; this 6-position is *ortho* to one fluorine and *meta* to another (**Figure 2.14b**). The 3- and 4-positions on the phenyl ring are each *ortho* to one fluorine and *meta* to another. Thus, all three positions on the ring might be expected to sulfonate. Sulfonic acid groups at the 3- and 4-positions can not ring-close to give the sulfone, whereas a sulfonic acid group at the 6-position can ring-close to give the sulfone. Consistent with this, significant bands at both 410 and 450 nm were seen. TPP(2,3-F<sub>2</sub>)S,Cu (DD755) is expected to sulfonate at the 5- and 6-positions. The latter can ring-close; the former cannot. Both 410 and 450 nm bands were observed (**Figure 2.14b**). Overall, there is a high correlation between the likelihood that a porphyrin will sulfonate adjacent to the porphine ring, and the observation of intensity at 450 nm in the optical spectrum. This is in line with the proposed formation of an intramolecular sulfone.

These experiments may explain our previous observations on efforts to “over-sulfonate” porphyrins, i.e., to add more than one sulfonic acid group per phenyl ring in tetraphenylporphyrins. When TPP was treated with fuming sulfuric acid (15% oleum) for long periods of time, it was observed that the porphyrin was sulfonated beyond four sulfonic acid groups (shown by TLC, data not shown here). The resulting species had only a 450 nm absorption band (and no Soret peak at ~ 410 - 420 nm). Thus, oversulfonation may ultimately result in sulfone formation. This could be due to the presence of more sulfonic acid on at least one phenyl ring of the porphyrin, improving the chances of sulfonic acid group being in close proximity of a pyrrole ring, to form the sulfone.

## ii. CE separation.

Further analysis was done via CE to gain insight into the components of the difluoro derivatives and the 445 - 450 nm band. The CE data is summarized in **Table 2.2**. Simple mixtures of negatively charged sulfonated porphyrins can be separated as a function of charge by capillary electrophoresis. We have separated the negatively charged TPPS2a, TPPS3 and TPPS4 by capillary electrophoresis at pH 9.0 (Dixon et al., 2004). The three compounds had migration times of 4.0, 5.0, and 6.4 min, respectively, i.e., the least charged species had the shortest migration time under the separation conditions. The sulfonated difluoro derivatives had multiple peaks, indicating the presence of porphyrin species with varying extents of sulfonation.

**Figure 2.15** shows the CE separations of the difluoro derivatives. Separations of these compounds at low pH (2.5) were not well resolved (data not shown). **Table 2.2** gives this data as well as that in phosphate buffer, pH 9.0, without  $\beta$ CD.

**TPP(2,6-F2)S (DD194), free base**, had four unresolved peaks between 7.3 and 7.6 min ( $\lambda_{\text{max}}$  412 - 416 nm) (data not shown).

**TPP(2,3-F2)S,Cu (DD755), TPP(2,4-F2)S,Cu (DD720), TPP(2,5-F2)S,Cu (DD713) and TPP(3,5-F2)S,Cu (DD746)** all showed multiple peaks when separations were performed with a 10 mM phosphate buffer (9.0) containing 1 mM  $\beta$ CD. At least two peaks for each compound, at both high (data not shown) and low concentrations of the compounds (up to 100-fold difference between the high and low concentrations of the compounds) (**Figure 2.15**). Addition of  $\beta$ CD to the running buffer decreased the migration time (**Table 2.2**). The effect of  $\beta$ CD on the enhancement of separation was not

the same for all the four compounds. In the case of TPP(2,4-F2)S,Cu (DD720), two sharp peaks at 5.0 and 6.1 min with  $\lambda_{\max}$  of 409 and 414 nm, respectively, were observed (**Figure 2.15**). No change in the electropherograms was observed due to the addition of 1 mM  $\beta$ CD to the running buffer. The negative ion MALDI data (below) indicated that this compound was a mixture with significant amounts of at least three compounds, the di-, tri- and tetrasulfonated species. However, under the CE separation conditions used, only two major CE peaks were observed.

In the case of TPP(2,5-F2)S,Cu (DD713), separation without  $\beta$ CD resulted in several sharp unresolved peaks between 6.0 and 9.0 min, with only one peak at 6.5 min with both 414 and 450 nm bands (data not shown). The rest of the peaks had a  $\lambda_{\max}$  of  $\sim$  420 nm. With 1 mM  $\beta$ CD in the running buffer, three distinct peaks were observed, at 4.3, 5.1 and 6.3 min (**Figure 2.15**). Only the peak at 4.3 min had both the 416 nm and 449 nm UV-vis bands. The other two peaks had a  $\lambda_{\max}$  of  $\sim$  420 nm. Close inspection of the first peak, at 4.3 min showed that the ratio of the 414 nm and 450 nm bands changed as one moved through the peak. Thus, it is likely that this peak in the CE was a result of two different compounds co-eluting under one apparent peak.

For TPP(2,3-F2)S,Cu (DD755), the three major peaks were observed without  $\beta$ CD at 5.2, 6.4 and 7.7 min (data not shown). There were also shorter peaks at  $\sim$  4.5 and 12.0 min. The peaks at 5.2 and 7.7 min had  $\lambda_{\max}$  values of 409 and 419 nm, respectively. The peaks at 6.4 min had  $\lambda_{\max}$  values of 414 and 443 nm. With the addition of 1 mM  $\beta$ CD to the running buffer, the three major peaks were still observed at 5.1, 6.2 and 7.4

min, although more short peaks also appeared. The peaks at 5.1 and 7.4 min had  $\lambda_{\max}$  values of 409 and 420 nm, respectively. The peaks at 6.2 min had  $\lambda_{\max}$  values of 414 and 444 nm.

TPP(3,5-F2)S,Cu (DD746) gave unresolved peaks without  $\beta$ CD between 5.0 and 10.0 min (data not shown). All the peaks had  $\lambda_{\max}$  values of  $\sim$  440 nm. The addition of  $\beta$ CD did not resolve the peaks significantly; four unresolved peaks between 4.0 and 10.0 min were observed (**Figure 2.15**). All the CE peaks had  $\lambda_{\max}$  of about  $\sim$  440 nm. If 440 nm bands were due to cyclic sulfones, then more than one component of this compound had this moiety.

### iii. Mass spectrometry.

The negative ion MALDI technique was used to gain information about the substitutions of these compounds. While one can sometimes see dimers in the mass spectrometry of sulfonated tetrapyrroles (Dixon et al., 2004), only in the case of TPP(3,5-F2)S,Cu (DD746) were trace amounts of homo- and heterodimers observed in this work. **Table 2.2** summarizes the MS and CE data of difluoro derivatives of CuTPPS4.

#### 1. Number of sulfonic acid groups.

The negative ion MALDI data for almost all the difluoro derivatives showed peaks appropriate for the tri- and tetrasulfonated species and their sodium adducts (**Figure 2.16 and 2.17**). Traces of the monosulfonate (896 Da) and its monosodium adduct were seen for TPP(2,4-F2)S,Cu (DD720). Peaks appropriate for the disulfonated species and its monosodium adduct were seen for TPP(2,4-F2)S,Cu (DD720) and

TPP(2,5-F<sub>2</sub>)S,Cu (DD713). Traces of the pentasulfonate (1219 Da) and its mono- and disodium adducts were seen for TPP(2,3-F<sub>2</sub>)S,Cu (DD755). Consistent with this observation, the CE electropherogram showed peaks appearing at migration times longer than for other porphyrins, indicating species with higher negative charge, and hence a greater extent of sulfonation.

The spectrum for TPP(3,5-F<sub>2</sub>)S,Cu (DD746) had very few peaks compared to the other compounds. It was interesting to observe that the parent sulfonated species (molecular ion peaks of the sulfonated species) were missing. Some peaks seemed to be consistent with their sodium adducts.

## **2. Loss of 18 Da.**

All four copper chelates showed peaks consistent with the loss of 18 Da from the sulfonated species (**Figure 2.16 and 2.17**). However, in most cases the loss of 18 Da was not observed from the sodium adducts of these sulfonated species. This may indicate that the loss occurred more readily from the fully protonated species rather than from their sodium adducts. This 18 Da loss is very likely the loss of water from a sulfonic acid and a pyrrole ring, which are in close proximity, as discussed earlier in this section.

TPP(2,5-F<sub>2</sub>)S,Cu (DD713) showed a peak at 1040 Da consistent with the loss of water from the parent trisulfonated species (1058 Da) (**Figure 2.17a**). The 960 Da peak was appropriate for the loss of water from the parent disulfonated species (978 Da). A significant peak appropriate for the loss of water from the tetrasulfonated porphyrin (1138 Da) was not observed at 1120 Da. This peak might have overlapped with the sodium adduct of the trisulfonated species, i.e., the peak at 1124 Da was more appropriate

for the sodium adduct of trisulfonated species than for the water loss from the tetrasulfonate species. The loss of water could happen for this compound, for at least for one of its sulfonated species, based on observation of the CE data for this compound. The CE data of this compound showed one peak, out of the three major peaks, with the 450 nm band along with the Soret band.

There were many overlapping peaks in the mass spectrum of TPP(2,3-F2)S,Cu (DD755) (**Figure 2.16b**). The 1120 Da peak was appropriate for the loss of water from the parent tetrasulfonated species (1138 Da). A peak appropriate for the loss of water (1200 Da) from the pentasulfonated species (1218) might have overlapped with the peak for the sodium adduct of the tetrasulfonated species. The water loss in case of this compound possibly results in the formation of the sulfone ring, at least in case of one of the sulfonated species. That species could be di-, tri- or tetrasulfonated. CE data indicated that only the one peak out of the three major peaks, at 6.4 min, had the 445 nm band along with the Soret band. The other CE peaks did not have the 445 nm band.

In the case of TPP(2,4-F2)S,Cu (DD 720), the tallest peak was not for the loss of water, but for the trisulfonated species (**Figure 2.17b**). Peaks for the loss of water at 960 Da, 1040 and 1120, respectively, were seen for the di- (978 Da), tri- (1058 Da) and tetrasulfonated (1218 Da) porphyrins. But according to our reasoning for the loss of water and consequential sulfone formation, TPP(2,4-F2)S,Cu (DD720) which does not sulfonate on the *ortho* or *para* positions of the ring cannot lose water to form the sulfone ring. Therefore, the 18 Da loss for this compound could not be the loss of water resulting in sulfone formation. This is supported by the CE data for this compound, where neither

of the two CE peaks had the 445 - 450 nm band. The origins of the -18 Da peaks are not known at this point.

In the case of TPP(3,5-F2)S,Cu (DD746), the parent sulfonated peaks were missing (**Figure 2.16a**). The peaks observed were appropriate for the loss of 18 Da from the tri- and tetrasulfonated species and their sodium adducts. However, the taller peaks seemed to be consistent with the sodium adducts of the trisulfonated species. This is the compound which is most likely to have lost water to form a sulfone. All the CE peaks of this compound had the  $\lambda_{\text{max}}$  of  $\sim 440$  nm. Thus, the UV-vis and mass spectrometry data is consistent and lead to the conclusion that the sulfonation products of this molecule have lost water to form the sulfone.

### 3. Loss of SO<sub>2</sub>.

Loss of SO<sub>2</sub> has been observed previously for the sulfonated tetrapyrroles (Dixon et al., 2004). The sulfonic acid group can lose SO<sub>2</sub> to form phenol (Conneely et al., 2001). Loss of a SO<sub>2</sub> was not significant in the case of TPP(2,5-F2)S,Cu (DD713) and TPP(3,5-F2)S,Cu (DD746). These are the two compounds which had very prominent red-shifted bands, at 445 - 450 nm. Presumably, loss of SO<sub>2</sub> was not significant for the sulfonated parent peaks which lost water to give the sulfone peaks.

On the other hand, loss of SO<sub>2</sub>, and not the loss of water, was significant in the case of TPP(2,4-F2)S,Cu (DD720) and TPP(2,3-F2)S,Cu (DD755) (**Figure 2.18**). TPP(2,4-F2)S,Cu (DD720) did not have the 445 - 450 nm UV-vis band and for TPP(2,3-F2)S,Cu (DD755) the band was not as significant. Peaks appropriate for the loss of one SO<sub>2</sub> were observed from the tetra- and pentasulfonated species. Peaks appropriate for the

loss of one SO<sub>2</sub> were also observed from their mono-, di- and trisodium adducts (**Figure 2.18**).

**Conclusions about the difluoro derivatives from UV-vis spectroscopy, capillary electrophoresis and negative ion MALDI data:**

The UV/vis Soret band at about 450 nm is best explained as due to additional conjugation in the ring. This is most easily explained as an intramolecular sulfone. An intramolecular sulfone can form by condensation of a sulfonic acid, at the *ortho* position of the phenyl ring, with the pyrrole ring. In comparing the various difluoro derivatives, we note that the more likely the porphyrin is to sulfonate in the *ortho* position of the phenyl ring, the more 450 nm band intensity is observed. Thus, the presence and intensity of the 450 band are consistent with the predicted sulfonation pattern of the difluoro porphyrins. All of the sulfonated difluoro derivatives were mixtures, as shown by capillary electrophoresis and mass spectrometry. In general, only a few of the peaks had the optical signature of the intramolecular sulfone in the CE. The MALDI data showed that the porphyrins had various extents of sulfonation, consistent with the observation of a number of peaks in the capillary electropherograms. Significant peaks in the MALDI spectra were attributed to loss of water from the parent species, again consistent with the intramolecular sulfone structure. Although the intramolecular sulfone species has not been reported in the porphyrin literature to our knowledge, extended conjugation via either a carbonyl or amine linkage is known, and results in a red-shifted Soret (Richeter et al., 2001; Richeter et al., 2004).

Regarding the MALDI fragmentation patterns, in general loss of water seemed to come from the sulfonic acid forms, not their sodium adducts, as might be expected. It also appeared that some parent peaks would lose H<sub>2</sub>O and some SO<sub>2</sub>; the mass spectral patterns were not consistent with a single molecular entity losing either H<sub>2</sub>O or SO<sub>2</sub>.

Although it is in general possible to add more than one sulfonic acid to a phenyl ring via sulfonation, “oversulfonated” tetraphenyl porphyrins (e.g., a pentasulfonated derivative) have not been reported in the literature. In our case, TPP treated under forcing sulfonation conditions gave species that absorbed at 450 nm but were not the protonated parent TPP. In view of our work on the difluoro porphyrins, we now believe these species to be the intramolecular sulfones.

**d. Sulfonated tetraphenylporphin with bromo groups on the phenyl rings:**

**TPP(4-Br)S (free base) (DD709), TPP(2-Br)S,Cu (DD774), TPP(3-Br)S,Cu (DD707), and TPP(4-Br)S,Cu (DD710).**

Four bromo derivatives of TPPS<sub>4</sub> and CuTPPS<sub>4</sub> were studied (**Figure 2.19**). These derivatives differed only in the position of the bromo substituent on the peripheral phenyl rings. The compounds showed good inhibitory activity against HIV virus and were not especially toxic (biological tests done at Dr. Compan's laboratory). The goal of this work was to study the structural properties of these compounds.

**i. CE separation.**

**Figure 2.20** shows the CE separation of these compounds in a pH 9.0 buffer with 1 mM  $\beta$ CD. The results are summarized in **Table 2.3**. In the presence of 1 mM  $\beta$ CD, the

electropherograms of the free base TPP(4-Br)S (DD709) and its Cu derivative TPP(4-Br)S,Cu (DD710) had several peaks, not resolved to the baseline. The general pattern of the peaks was the same for the two compounds. However, the Cu derivative of TPP(4-Br)S (DD709), TPP(4-Br)S,Cu (DD710) had more unresolved components. The broad peak at longer migration time appeared at even longer migration time, i.e., ~ 15 min. Multiple peaks and longer migration time indicate greater extent of sulfonation (Dixon et al., 2004). TPP(2-Br)S,Cu (DD774) had several peaks with considerable resolution between 4.5 and 9.5 min in the presence of 1 mM  $\beta$ CD. The major peaks, however, were observed between 5.5 and 6.5 min. TPP(3-Br)S,Cu (DD707) had only two sharp peaks and had the shortest migration time amongst all the four compounds. Overall, 1 mM  $\beta$ CD did help in resolving peak components and improving the shape of the peaks (data without  $\beta$ CD not shown).

## ii. UV-vis spectra.

**Figure 2.21** shows the UV-vis spectra of these compounds in water. The  $\lambda_{\max}$  were in the range of 412 - 419 nm. A Q-band was seen ~ 540 nm. In case of TPP(3-Br)S,Cu (DD707) a hint of a 450 nm band was observed. According to our previous discussion of difluoro derivatives of TPPS<sub>4</sub>, the 450 nm band could be a result of loss of water from a sulfonic group on the phenyl ring and the pyrrole ring to form a sulfone. For the formation of the sulfone ring the sulfonic ring would have to be in close proximity of the pyrrole ring. This is directed by the position of the halogen substituent on the phenyl ring; the 3-bromo substituent, TPP(3-Br)S,Cu (DD707), should have a sulfonic groups adjacent to the pyrrole ring.

Spectra were also taken in various solvents and at various pH values; in water, 1 mM EDTA, and phosphate buffers at pH 7.1 and 9.0 (data not shown). No difference in spectra, except for peak heights, was observed under the different conditions.

### iii. Mass spectrometry.

The data is summarized in **Table 2.4**. The multiple CE peaks for each compound indicated the presence of more than one sulfonic acid group on the phenyl ring. This is also shown by the negative ion MALDI data. Peaks appropriate for the loss of a SO<sub>2</sub> group from the parent sulfonated species were not observed.

The mass spectrometry data indicated that the free base TPP(4-Br)S (DD709) had peaks for the di- (1086 Da), tri- (1166 Da), tetrasulfonated (1246 Da) species and their sodium adducts. TPP(4-Br)S,Cu, (DD710) showed peaks appropriate for the di- (1086 Da), tri- (1166), and tetrasulfonated (1246) species, as well as their sodium adducts.

TPP(3-Br)S,Cu (DD707) data was different from other compounds in that no peak for the tetrasulfonated species was seen. Peaks appropriate for the di- and trisulfonated species and the peaks for the sodium adducts of the trisulfonated species were not very significant. The other peaks in the spectrum, including the tallest peak, could not be assigned. The pattern of the peaks could not be assigned.

In the case of TPP(2-Br)S,Cu (DD774), the prominent peak was for the pentasulfonated species (1326 Da) and its sodium adducts. Trace amounts of the tetrasulfonated species (1246 Da) and its sodium salts were also observed.

**Section V.****Sulfonated Naphthyl Porphyrins as Agents Against HIV-1**

Journal of Inorganic Biochemistry, 2005, vol. 99, pp. 813 – 821.

Dabney W. Dixon,\*<sup>1</sup> Anila F. Gill,<sup>1</sup> Lingamallu Giribabu,<sup>1</sup> Andrei N. Vzorov,<sup>2</sup> Atia B. Alam,<sup>1</sup> and Richard W. Compans<sup>2</sup>

<sup>1</sup>Department of Chemistry, Georgia State University, Atlanta, GA 30303.

<sup>2</sup>Department of Microbiology and Immunology, Emory University, Atlanta, GA 30322.

**Abstract**

Sulfonated 5,10,15,20-tetra(1-naphthyl)porphyrin (T1NapS) and 5,10,15,20-tetra(2-naphthyl)porphyrin (T2NapS) and their copper and iron chelates show activity against the human immunodeficiency virus (HIV-1). The porphyrins were prepared by sulfonation of the parent structures with sulfuric acid. More highly sulfonated structures were prepared by sulfonation for longer times. Matrix-assisted laser desorption/ionization (MALDI) mass spectrometry showed species with as many as eight sulfonates. Some of the mass spectral peaks for the copper chelates were consistent with loss of water, apparently from intermolecular sulfone formation between two adjacent naphthalene rings that took place during copper insertion. The compounds could be separated using capillary electrophoresis; addition of  $\beta$ - or  $\gamma$ -cyclodextrin gave substantially better separation of the components. Activity against HIV was evaluated using an epithelial HeLa-CD4-CCR5 cell line;  $EC_{50}$  values for HIV-1 IIIB and HIV-1 JR-FL ranged from 1 to 15. The compounds exhibit low toxicity for human epithelial cells

and have potential as microbicides which might be used to provide protection against sexual transmission of HIV.

### **Introduction.**

Although many important strides have been made in both pharmaceutical approaches and in changing social practices, the cost of the human immunodeficiency virus (HIV) epidemic in both human and economic terms continues to be staggering. One approach to slowing the spread of HIV is to prevent initial infection by the virus. This is most likely to be effected with microbicides, topical agents which are designed to prevent infection, rather than attempting to minimize its later ravages (Stone, 2002; Turpin, 2002; Harrison et al., 2003; D'Cruz & Uckun, 2004). Microbicides need to be safe, effective, convenient, and affordable as they will be used on a long-term basis.

Porphyrins have been known for some years to show antiviral activity against HIV infection in assays that measured inhibition of virus replication. Studies investigated protoporphyrin (Asanaka et al., 1989), hemin (Leverie et al., 1991; Neurath et al., 1991) and other related natural porphyrins and metalloporphyrins (Dixon et al., 1990; Neurath et al., 1991; Neurath et al., 1992; DeCamp et al., 1992; Debnath et al., 1994; Neurath et al., 1994a; Neurath et al., 1994b; Debnath et al., 1999; Vzorov et al., 2002; Dairou et al., 2004). In general, activity against HIV is in the micromolar range in such antiviral assays. In the synthetic porphyrin class, sulfonated derivatives of tetraphenylporphyrin have also been shown to be active, as have other selected tetraaryl porphyrins (Dixon et al., 1990; Neurath et al., 1992; Dixon et al., 1992; Debnath et al.,

1994; Neurath et al., 1994a; Neurath et al., 1995; Song et al., 1997; Vzorov et al., 2002). Recently, we have found that porphyrins can inhibit the initial infection process by inactivating the infectivity of cell-free virus, and therefore have potential as microbicides (Vzorov et al., 2002). Porphyrins can chelate metals, specifically copper and iron, giving structures that are stable, not photoactive, have chemistry that is independent of pH over the values expected in the female genital tract, and are without redox chemistry that would interfere with pharmacological use. All of these are important in the development of a microbicide. Three classes of porphyrins were studied (Vzorov et al., 2002): I) natural porphyrins, II) metal chelates of tetraphenylporphyrin tetrasulfonate (TPPS4), and III) sulfonated tetraaryl porphyrin derivatives. None of the natural porphyrins studied reduced infection by more than 80% at a concentration of 5  $\mu\text{g/ml}$  in these assays. Some metalloTPPS4 were more active and a number of sulfonated tetraaryl derivatives showed significantly higher activity. Some of the most active compounds were the sulfonated tetranaphthyl porphyrins (T1NapS and T2NapS, **Figure 2.22**). The present study extends our previous work by further defining the chemistry and antiviral activity of naphthyl porphyrins. The characterization of the sulfonated naphthyl porphyrins is of interest not only in conjunction with their antiviral activity, but also their use as photosensitizers (Ion et al., 1998; Ion, 1999) and with respect to the effect of the naphthyl group on the spin state of the central metal atom (Silver & Taies, 1988).

**Experimental.**

**a. Synthesis.** 5,10,15,20-Tetra(1-naphthyl)porphyrin (T1Nap) (Treibs & Haeberle, 1968; Fonda et al., 1993) and 5,10,15,20-tetra(2-naphthyl)porphyrin (T2Nap) (Fonda et al., 1993; Rao & Maiya, 1994) were synthesized according to the general literature procedure (Abraham et al., 1975). A recent synthetic procedure involving heating for 10 days at lower temperatures may give more facile access to larger quantities of the pure parent porphyrins (George & Padmanabhan, 2003). Sulfonation was performed following the literature (Miller et al., 1987; Ion et al., 1998; Sutter et al., 1993). Sulfonation with concentrated sulfuric acid (Miller et al., 1987; Sutter et al., 1993) gave cleaner products than sulfonation with fuming sulfuric acid (Sutter et al., 1993; Ion et al., 1998). As an example, T1Nap (200 mg, 0.24 mmol) was added to 5 ml of concentrated sulfuric acid (Aldrich). The reaction mixture was heated at 100 °C for 5 h. Ice was then added to the green mixture (*when working at larger scale, it is safer to pour the sulfuric acid mixture over ice*). The acid was neutralized carefully by the addition of 50% NaOH solution and ice until the color turned red (*caution: very exothermic, keep the flask in ice and add the NaOH very slowly*). The pH of the solution was adjusted to 7. The liquid was evaporated under vacuum. The resulting solid was pulverized and the sulfonated porphyrin was extracted into methanol with a Soxhlet apparatus for approximately 24 h. Evaporation of the solvent gave solid material which was purified by a Sephadex LH-20 (Pharmacia) column (6 g of Sephadex for 100 mg of porphyrin) using methanol as the eluent. The column was prepared by putting the Sephadex in methanol and was used immediately. The purple-colored band (continuous, streaking) was collected and

evaporated to obtain the desired product. The T2Nap sulfonation products were made analogously. Components could be separated by thin layer chromatography (TLC) (Merck, RP-18 F, 60/40 MeOH/H<sub>2</sub>O).

Copper insertion was performed by the copper oxide method (Herrmann et al., 1978). The porphyrin (30 mg) was added to refluxing water which contained 500 mg of copper oxide. The reaction mixture was refluxed for 12 h. The completion of the reaction was indicated by UV/vis spectroscopy (four Q-bands of free-base porphyrin reduced to two bands of metalloporphyrin). The solvent was filtered to remove excess copper oxide. The solvent was evaporated under vacuum to get solid material. This was passed down a column of ion-exchange resin (5 g; Dowex-50W; H<sup>+</sup> form; 100-200 mesh, washed with water 3 to 4 times prior to loading solid material to remove excess acid), eluting with water. The red colored band was collected and evaporated to dryness under reduced pressure to obtain the desired product. Studies of copper insertion using copper oxide showed that the insertion was often complete by stirring at room temperature for about 6 h (30 mg porphyrin and 500 mg copper oxide).

Iron insertion was achieved by adding the porphyrin (30 mg) to refluxing water, which contained 500 mg of powdered iron (Herrmann et al., 1978). The reaction mixture was refluxed for 6 h. The completion of the reaction was indicated by UV/visible (UV/vis) spectroscopy (four Q-bands of free-base porphyrin reduced to two bands of metalloporphyrin). The solvent was filtered to remove excess iron. The product was worked up as described above for the copper chelate.

As in previous studies of sulfonated naphthyl porphyrins, (Miller et al., 1987; Ion et al., 1998; Ion, 1999), pure materials were not isolated, presumably due to the presence of inorganic salts and water. In this work, purities were estimated by UV/vis. The extinction coefficients of T1Nap and T2Nap in chloroform have been measured as  $4.4 \times 10^5$  and as  $4.5 \times 10^5 \text{ M}^{-1} \text{ cm}^{-1}$ , respectively (425 nm) (George & Padmanabhan, 2003). Previous work had shown that the extinction coefficients of TPP in  $\text{CHCl}_3$  (Dudic et al., 1999) and CuTPPS4 in aqueous solution (Gibbs et al., 1980) were very similar. Therefore, we used the published T1Nap and T2Nap extinction coefficients for our sulfonated copper derivatives. A similar analysis for iron, using the extinction coefficient of FeTPPS4 (Fleischer et al., 1971) indicated that the iron chelate should have an extinction coefficient at the Soret of about  $1.5 \times 10^5 \text{ M}^{-1} \text{ cm}^{-1}$ . Purities, expressed as the percent of the material that was porphyrin (assuming a tetrasulfonate with four sodium counterions), were then estimated as T1Nap,Cu (35%); T2NapS,Cu (36%); T1NapS,Fe (38%); and T2NapS,Fe (59%). For comparison, T1NapS prepared by sulfonation with concentrated sulfuric acid was estimated to be 61% porphyrin (assuming the fully protonated porphyrin dication) by elemental analysis (Miller et al., 1987). Analytical figures were not given for the iron complex (T1NapS,Fe) in that study, because samples contained variable amounts of  $\text{Na}_2\text{SO}_4$  (Miller et al., 1987).

**b. Capillary electrophoresis.** Capillary electrophoresis was performed on a Beckman P/ACE 5500 series with Beckman Gold chromatography software and a Beckman diode array detector. A fused silica capillary column (Agilent, Wilmington, DE, 375  $\mu\text{m}$  o.d., 75  $\mu\text{m}$  i.d., 57 cm overall, 50 cm to detector) was built in an eCAP capillary cartridge

(Beckman, 100 x 800  $\mu\text{m}$  aperture). Phosphate buffers were prepared by dissolving  $\text{KH}_2\text{PO}_4$  in deionized water and adjusting the solution to the desired pH with phosphoric acid or KOH. All running solutions were filtered through a 0.2  $\mu\text{m}$  membrane filter (FP-200, Gelman Science Inc., Ann Arbor, MI) before use.

New capillary columns were rinsed with 1.0 M sodium hydroxide for 1 h, followed by deionized water for 20 min and running buffer for 30 min. The capillary column was regenerated between runs with 0.1 M sodium hydroxide for 5 min, followed by deionized water for 5 - 15 min and running buffer for 10 min. A sample solution was prepared by dissolving a small amount of the porphyrin (1 - 2 mg) in deionized water (0.5 mL). Further dilutions were done with water. Separations were performed with normal polarity from the inlet vial (anode) to the outlet vial (cathode). Pressure injections of 6 s were used. The voltage was 30 kV. The column temperature was 24  $^{\circ}\text{C}$ .

**c. Mass spectrometry (MS).** Matrix-assisted laser desorption/ionization (MALDI) experiments were performed using an ABI Voyager DE-Pro (Applied Biosystems, Warrington, UK) MALDI reflectron time-of-flight spectrometer. The mass range scanned was 200 - 6000 Da in positive and negative modes. The samples were run with  $\alpha$ -cyano-4-hydroxycinnamic acid (CHCA) as the matrix. CHCA was prepared at 10 mg/ml in a 50:50 mixture of MeOH and acetonitrile. The sample was dissolved in MeOH (0.5 mg/ml) and mixed with CHCA. The sample solution was generally mixed with the matrix solution in a 1:20 ratio and spotted on the MALDI target plate. Throughout the text, peaks are rounded to the nearest unit. Data analysis concentrated on

the region around the molecular ion (net charge of -1 for negative ion MALDI). Samples were isolated as the sodium salts; partial exchange of the sodium for protons presumably occurred in the matrix.

A QTOF (quadrupole-time-of-flight) spectrometer (Waters Micromass Q-TOFTM micro, Waters Corporation, Milford, MA) was used to carry out the electrospray (ESI) mass spectrometric experiments. Nitrogen supplied by a nitrogen generator (Model 75-72, Parker Balston, Haverhill, MA) was used as the cone gas at 50 L/h, and as the drying gas heated to 150 °C at a flow-rate of 450 L/h to evaporate solvents in the spray chamber. Argon was used as the collision gas. The voltage settings for the API electrospray interface were capillary, 2700 V; sample cone, 35 V; extraction cone, 0.5 V. The source temperature was at 80 °C and the desolvation temperature was 150 °C. Samples in negative ion mode were in 50% MeOH. All solutions were continuously infused by means of a syringe pump at a typical flow rate of 5  $\mu\text{l min}^{-1}$  into the electrospray probe. MassLynx (version 4.0) software was used for instrument control, data acquisition and processing.

**d. Molecular modeling** was performed using PCModel (version 8.0, Serena Software, Bloomington, IL) and the MMX force field.

**e. Screening of porphyrins for activity against HIV-1.** HIV-1 IIIB (laboratory-adapted CCXCR4 usage virus) and JR-FL (primary CCR5 usage virus) were obtained from the NIH AIDS Research and Reference Reagent Program, and grown as previously described

(Vzorov et al., 2002). The virucidal activity of the sulfonated naphthyl porphyrins was evaluated using MAGI-CCR5 cells (NIH AIDS Research and Reference Reagent Program), which are epithelial HeLa cells with human receptor CD4, coreceptor CCR5, and an integrated LTR- $\beta$ -galactosidase gene (Chackerian et al., 1997). Porphyrin stock solutions were prepared at concentrations of 5 mg/ml, diluted 100-fold in Dulbecco's minimal essential medium (DMEM), and mixed with virus stock. Samples were left in the dark at room temperature for 1 h. For the assays, 25  $\mu$ l of virus/compound mixture was mixed with 225  $\mu$ l of growth medium containing DEAE-dextran (15  $\mu$ g/ml) and 50  $\mu$ l added to wells with confluent monolayers of MAGI-CCR5 cells. At 2 h post infection, an additional 200  $\mu$ l of complete DMEM was added. After three days residual virucidal activity was measured as described previously (Vzorov et al., 2002) by removal of the media, fixation with 1% formaldehyde and 0.2% glutaraldehyde and staining with 5-bromo-4-chloro-3-indolyl- $\beta$ -D-galactopyranoside (X-gal). We observed about 50 - 60 separate blue nuclei per well for the positive control. Scoring of blue nuclei in a 96-well format was greatly enhanced by using a planar lens [Olympus (Japan) 4x] to visualize the entire well. Comparison of the number of blue cells in wells infected with compound-treated virus to the number found in wells infected with untreated virus was used to determine residual viral infectivity (expressed in percent).

**f. Cytotoxicity test.** A 3-(4,5-dimethylthiazol-2-yl)-2,5-diphenyltetrazolium bromide (MTT) assay (Pauwels et al., 1988) was performed using the human endometrial adenocarcinoma cell line HEC-1-B (obtained from the American Type Culture

Collection, Manassas, VA) and the human epithelial MAGI-CCR5 cell line. For the MTT assay, compounds of varying concentrations (1000, 100, 20, 5, and 0.5  $\mu\text{g/ml}$ ) in growth medium were added to 96-well plates with HEC-1-B or MAGI-CCR5 cells. Following a 72 h incubation, cells were washed with Hanks' balanced salt solution to remove colored compounds and 100  $\mu\text{l}$  of growth medium with 10  $\mu\text{l}$  of MTT (10 mg/ml) reagent was added to each well. After 4 - 12 h incubation at 37  $^{\circ}\text{C}$ , 100  $\mu\text{l}$  acidic isopropanol (0.04 M HCl in absolute isopropanol) was added. The absorbance was read in a computer-controlled photometer. The absorbance at 690 nm was automatically subtracted from the absorbance at 540 nm to eliminate the effects of non-specific absorption. Data are reported as the average of quadruplicate assays for each compound.

## Results

**a. Synthesis.** The 1-naphthyl and 2-naphthyl porphyrins were synthesized following a literature procedure (Abraham et al., 1975). A recent synthetic procedure involving heating for 10 days at lower temperatures may give more facile access to larger quantities of the pure parent porphyrins (George & Padmanabhan, 2003). The naphthyl porphyrins were sulfonated with sulfuric acid at 100  $^{\circ}\text{C}$  (Sutter et al., 1993) for 5 and 10 hours (T1Nap) and 5, 10 and 20 hours (T2Nap) to give samples with increasing extents of sulfonation on the naphthalene rings. Cu or Fe were inserted into both the T1Nap and T2Nap ring systems, for a total of fifteen sulfonated naphthyl porphyrins.

**b. Capillary electrophoresis (CE).** Simple mixtures of sulfonated porphyrins can be separated as a function of charge by capillary electrophoresis (Pokric et al., 1999; Andrighetto et al., 2000; Dixon et al., 2004). The sulfonated naphthyl porphyrins are mixtures of numerous compounds, however, making separation more difficult. For example, the T2NapS derivatives were generally one broad peak under standard conditions of pH 9.0, 10 mM  $\text{KH}_2\text{PO}_4$  buffer. The addition of cyclodextrins aided the separation. The electropherograms of T2Nap5S,Cu in the presence of  $\beta$ - and  $\gamma$ -cyclodextrin are shown in **Figure 2.23**.  $\beta$ -Cyclodextrin gave a series of poorly resolved peaks from approximately 4 to 6 min;  $\gamma$ -cyclodextrin showed three prominent peaks from 3.5 to 4.5 min.

Electropherograms of samples prepared by 5, 10 and 20 h of sulfonation were compared. **Figure 2.24** shows the capillary electrophoresis separation of the free base porphyrin sulfonated for 5 and 20 h. In both cases, many peaks were seen. The peaks for T2Nap5S came between 3 and 6 min while those for T2Nap20S came largely between 4 and 7 min. Because more sulfonated species have longer migration times under the conditions of the experiment, this observation indicates that T2Nap20S is more sulfonated than T2Nap5S, as expected.

**Figure 2.25** compares the three sulfonation levels of T2NapS,Cu. T2Nap5S,Cu and T2Nap10S,Cu have very similar electropherograms, with large peaks at approximately 3.5 and 4 min. T2Nap20S,Cu shows some material at these times, but has a considerable amount of material with longer migration times (5 to 7 min), indicating higher levels of sulfonation. Comparing the electropherogram of free base T2Nap20S

(**Figure 2.24B**) with that T2Nap20S,Cu (**Figure 2.25**) shows that the addition of a metal to the central core affects the detailed pattern of the peaks; the net migration times, however, are similar. Capillary electrophoresis of the T2NapS,Fe species did not give good separation even with cyclodextrins, presumably due to the axial ligation of the iron (various axial ligands in exchange as well as the equilibrium between the monomer and  $\mu$ -oxo dimer) (Hambright, 2000). A previous study on the optical spectroscopy of a sulfonated naphthyl porphyrin was interpreted in terms of self-stacking of this species (Silver & Taies, 1988).

The electropherograms of the T1NapS species were in general similar to that of the T2NapS. For example, the electropherogram of T1Nap5S,Cu in the presence of  $\gamma$ -cyclodextrin (not shown) was very similar to that of T2Nap5S,Cu (**Figure 2.23B**). However, unlike the 2-naphthyl T2Nap5S,Cu, the 1-naphthyl T1Nap5S,Cu showed three distinct peaks even in the absence of cyclodextrin. This may be due to less self-stacking of the 1-naphthyl porphyrin resulting from atropisomers due to hindered rotation around the 1-naphthyl-porphine bond. As for the 2-naphthyl isomers,  $\beta$ -cyclodextrin seemed to show more components, but without baseline separation. The extent of sulfonation was greater in T1Nap10S than in T1Nap5S as shown by an additional peak at 7 min in the former product.

### **c. Mass spectrometry.**

**c. 1. Effect of central metal ion.** As reported previously, the negative ion MALDI (CHCA matrix) of T2Nap5S showed a very simple, clear pattern for the tetrasulfonic acid

(1134, M<sup>-</sup>) and its mono-, di- and trisodium salts (Dixon et al., 2004). The pentasulfonic acid (1214, M<sup>-</sup>) and its mono-, di-, tri-, and tetrasodium salts were also seen. Very small peaks consistent with sodium salts of the hexasulfonic acid were seen as well. In the higher mass region, homodimers of the tetrasulfonic acid and pentasulfonic acid, as well as a heterodimer of the tetrasulfonic acid and pentasulfonic acid were seen.

The copper chelate of the molecule gave a very different mass spectral pattern. T2Nap5S,Cu showed a large peak for the tetrasulfonic acid at 1195, but essentially no peaks attributable to the sodium salts of this species (**Figure 2.26**). A smaller peak at 1275 was attributable to the pentasulfonic acid. Peaks attributable to the homo- and heterodimers of the tetra- and pentasulfonic acids were seen. Additional large peaks were observed at 1257 and 1337. These have the mass corresponding to loss of water from pentasulfonic acid and hexasulfonic acid, respectively. The (parent)/(parent - water) ratios were approximately 85, 0.5 and 0.05 for the tetrasulfonic acid, pentasulfonic acid and hexasulfonic acid, respectively. In the Fe series, T2Nap5S,Fe showed a MALDI spectrum very similar to that of the free base, i.e., with the parent ion and its mono-, di- and trisodium salts, but without significant peaks due to loss of water.

The negative ion MALDI of T1Nap5S,Cu showed a clean pattern for the tetrasulfonic acid and its mono-, di- and trisodium salts. The mono- and disodium salts of pentasulfonic acid - H<sub>2</sub>O and small peaks appropriate for the same salts of hexasulfonic acid - H<sub>2</sub>O were also observed. T1Nap5S showed peaks for the tetrasulfonic acid and its sodium salts, as well as those for the dimers and trimers.

**c. 2. Effect of extent of sulfonation.** In the Cu series, the T2Nap5S,Cu showed peaks appropriate for the tetra-, penta- and hexasulfonic acids or their loss of water ( $M - H_2O$ ) peaks. T2Nap10S,Cu was quite similar, consistent with the very similar electropherograms of these mixtures. T2Nap20S,Cu showed peaks appropriate for the penta-, hexa-, hepta- and octasulfonic acids or their loss of water peaks (**Figure 2.27**). For the pentasulfonic acid, only the parent peak ( $M$ ), and not that for loss of water ( $M - H_2O$ ), was observed, while for the octasulfonic acid, only the peak for loss of water ( $M - H_2O$ ), and not the parent ( $M$ ), was observed. The (parent)/(parent -  $H_2O$ ) ratios were approximately 5 and 0.2 for the hexa- and heptasulfonic acid, respectively. Water loss was not observed in the MALDI spectra of either the free base or iron porphyrins.

To establish whether water loss had occurred during copper insertion or was occurring in the gas phase, we looked at the negative ion electrospray ionization (ESI) spectrum of T2Nap5S,Cu. The ESI spectrum itself showed peaks for the tetrasulfonic acid (but not tetrasulfonic acid -  $H_2O$ ), the pentasulfonic acid and pentasulfonic acid -  $H_2O$ , and both the hexa- and heptasulfonic acids -  $H_2O$  (but no significant peaks corresponding to the molecular ion of these species). The MS/MS spectrum of the pentasulfonic acid of T2Nap5S,Cu is shown in **Figure 2.28**. A clear pattern of fragmentation can be seen. The parent compound (1274,  $M^-$ ) loses  $SO_2$  (64) and  $SO_3$  (80) to give peaks at 1210 and 1194, respectively. These species can each lose either  $SO_2$  or  $SO_3$  again to give species assigned as ( $M^- - 2SO_2$ ), ( $M^- - SO_2 - SO_3$ ) and ( $M^- - 2SO_3$ ) at 1146, 1130 and 1114, respectively. The pattern continues down through loss of  $SO_2$  from

the monosulfonic acid. A very similar pattern was seen for the fragmentation of the tetrasulfonic acid of T2Nap5S,Cu. Loss of water in the gas phase was not seen in these experiments, indicating that the M – 18 peaks are probably due to products formed during copper insertion. An experiment in which T2NapS was allowed to stir with copper oxide for 3, 6, and 22 h showed significant water loss for the more highly sulfonated species, but did not show increasing water loss with increasing copper oxide contact time.

**d. Inhibition of viral infection.** To measure the inhibition of HIV-1 by the compounds we used human epithelial HeLa-CD4-CCR5 cells stably transfected with a plasmid containing the HIV-1 LTR fused to the  $\beta$ -galactosidase gene. This indicator cell line allows rapid quantification of infectious HIV-1, including primary isolates (Chackerian et al., 1997). **Figure 2.29** shows that most compounds gave similar levels of inhibition of the virus for HIV-1 IIB. In general, these compounds inactivated 80 – 95% of viral infectivity at a final compound concentration of 5  $\mu$ g/mL. Little effect of the central metal was observed. For T2NapS and T2NapS,Fe, the most highly sulfonated product had the least activity. No dependence of the activity on the degree of sulfonation was observed for T1NapS or its copper or iron chelates, or for T2NapS,Cu. In previous work, we observed that viral inhibition by TNapS was very rapid, being essentially complete within two minutes (Vzorov et al., 2002). We have also shown that, for some of the sulfonated porphyrins, HIV-1 remains inactivated after the removal of the compound (Vzorov et al., 2002).

To determine the effective concentration of some of the porphyrins, virus samples were mixed with the compounds at varying concentrations.  $EC_{50}$  values for HIV-1 IIIB were lower than those for the primary isolate HIV-1 JR-FL (**Table 2.5**).

Cell viabilities were determined using an MTT assay with the human endometrial adenocarcinoma cell line HEC-1-B or MAGI-CCR5 cells. The compounds exhibited low toxicity in both cell lines.  $CC_{50}$  values for MAGI-CCR5 cells ranged from 415 to 1000  $\mu\text{g/ml}$  (**Table 2.5**). Therapeutic indices for HIV-1 IIIB varied from 86 to 925, with T1Nap20S,Cu having the highest index. The compounds had lower therapeutic indices with HIV-1 JR-FL, varying from 32 to 132.

## **Discussion**

**a. Extent of sulfonation.** The extent of sulfonation was expected to increase as the time of sulfonation increased, as was generally observed to be the case. In general, the longer the sulfonation time, the longer the average capillary electrophoresis migration time. For example, the electropherograms of the T2NapS,Cu series were consistent with species with net charges of -4, -5 and -6 from the 5 h sulfonation and species with net charges of -5 and higher from the 20 h sulfonation. The MALDI mass spectra also generally showed higher levels of sulfonation with longer sulfonation times. The data indicate that a significant fraction of the porphyrins have one or more naphthyl rings with more than one sulfonic acid.

Addition of more than one sulfonic acid group per naphthyl ring is expected to be facile. Work of Cerfontain and colleagues has shown that the model compound 1,1'-

binaphthalene sulfonates initially at the 4-position, followed by sulfonation at the 4'-position, and then with almost equal facility at the 6- or 7-position. Six equivalents of SO<sub>3</sub> (in CH<sub>2</sub>Cl<sub>2</sub> at 22 °C, 40 min) gives only about 10% of the species with one sulfonic acid on each ring; all the rest of the material has two sulfonic acids on at least one ring (Cerfontain et al., 1994a). 2,2'-Binaphthalene sulfonates initially at the 8-position, followed by sulfonation at the 8'-position (Cerfontain et al., 1994a). The subsequent sulfonic acids are added at the 6- or 4-positions. Six equivalents of SO<sub>3</sub> (in CH<sub>2</sub>Cl<sub>2</sub> at 22 °C, 40 min) give only 9% of species with only one sulfonic acid on each ring. As for the 1-naphthyl system, addition of more than one sulfonic acid to the naphthyl ring is facile. The positional isomers upon sulfonation with sulfuric acid are expected to be very similar to those obtained with sulfonation with SO<sub>3</sub> in CH<sub>2</sub>Cl<sub>2</sub> (Cerfontain et al., 1982). Neither naphthyl system sulfonates to give sulfonic acids adjacent to one another in either the *ortho* or *peri* positions.

**b. Loss of water.** Significant peaks were seen for loss of water in a number of MALDI mass spectra of the copper chelates for both the T1Nap and T2Nap structures, but not for the free bases, or for the iron chelates. Loss of water for the copper chelates was also observed in the ESI mass spectrum. However, no loss of water was observed in the ESI MS/MS experiment, indicating that water loss was probably not occurring in the gas phase. These data are consistent with water loss occurring during copper insertion (using copper oxide). Rocha Gonsalves and colleagues have noted degradation of sulfonated

porphyrins upon copper insertion when the porphyrin was left in contact with the copper for extended periods (Rocha Gonsalves et al., 1996).

Loss of water could be a result of either sulfone or sulfonic anhydride formation. For the naphthyl porphyrins, molecular modeling shows that sulfones bridging the 7,7'-positions in the 1-naphthyl series or the 4,8' or 8,8'-positions in the 2-naphthyl series can be formed without substantial deformation of the porphyrin central core. It is also possible that an anhydride might be formed from two sulfonic acids. Sulfonic acid anhydrides are quite sensitive to water, however, generally hydrolyzing rapidly in the absence of steric compression (Cerfontain et al., 1997); Christensen has measured a half-life of less than 10 seconds at room temperature (Christensen, 1966). Because the copper insertion was performed in water, it is likely that the products are the sulfones. As outlined above, the extent of loss of water increased with the level of sulfonation in the T2Nap,Cu series. This may indicate that sulfone formation is more facile for the more highly sulfonated species, as might be expected both because there are more sulfonic acid groups in appropriate positions for sulfone formation and because sulfone formation will minimize electrostatic repulsion in more highly sulfonated derivatives.

**c. CE separation.** In the current study, some separation of the components of the 1-naphthyl mixture was achieved without the addition of cyclodextrins. This may reflect the conformations of the 1-naphthyl groups, which extend above and beneath the porphyrin plane, reducing self-stacking. Previous work has shown that self-stacking reduces the CE separation of tetrapyrroles (Dixon et al., 2004). In the 2-naphthyl series,

separation was aided significantly by the addition of cyclodextrins;  $\beta$ - and  $\gamma$ -cyclodextrins gave quite different patterns. The electropherogram of T2NapS (**Figure 2.24**) shows a multiplicity of peaks, indicating molecules with different numbers of sulfonic acids as well as different positions of the sulfonic acids. Cyclodextrins have been shown to be effective in separating the positional isomers of naphthalene sulfonic acids (Alonso et al., 1999; Fischer et al., 2003; Chen & Ding, 2004). Some of the peaks may also be due to atropisomers; separation of atropisomers using a cyclodextrin has been observed previously in a different system (Zerbinati & Trotta, 2003).

**d. Antiviral activity.** Small polyanionic molecules have been shown to inhibit HIV replication by preventing virus attachment (adsorption) to the surface of the host cell (De Clercq, 2002). The viral entry process involves the interaction of gp120 with the primary cellular receptor, CD4 (Dalglish et al., 1984). Such binding results in a conformational change in gp120 (Sattentau & Moore, 1991) which in turn enables gp120 to interact with a co-receptor, generally either CCR5 or CXCR4. Studies have shown that changes in the conformation of the V3 loop of gp120 may lead to the inhibition of virus entry into susceptible cells (Trujillo et al., 2000; Cormier & Dragic, 2002; Dettin et al., 2003). The interaction of polyanionic substances with HIV can be considered specific, as repeated passage in the presence of polyanions can lead to resistance mediated by mutations in the envelope glycoprotein gp120, particularly in the V3 loop (Este et al., 1997; Cabrera et al., 1999).

A number of studies have indicated that negatively charged porphyrins can inhibit HIV via interaction with the V3 loop of gp120 (Debnath et al., 1994; Debnath et al., 1999; Neurath et al., 1995; Neurath et al., 1992; Neurath et al., 1991; Song et al., 1997; Dairou et al., 2004). The sulfonated naphthyl porphyrins presumably also interact with the the V3 loop, which is rich in arginine and lysine residues. In doing so, the polyanions could shield the V3 loop and therefore interfere with binding of the HIV virions to cell surface components (Gallaher et al., 1995). Recent work on sulfonated phthalocyanines has shown no correlation of anti-HIV activity and inhibition of gp120-CD4 binding, however, indicating that the mechanism of inhibition of these compounds may involve inhibition of binding to the co-receptor, or that some other mechanism of blocking of HIV infection is operative (Vzorov et al., 2003). The present results demonstrate that the anti-HIV activity of the sulfonated naphthyl porphyrins is relatively independent of the degree of sulfonation and the nature of the central metal atom, indicating that a range of structures may be effective for viral inhibition.

### **Acknowledgments**

This study was supported by NIH grant AI45883. The authors thank Dahvide Taylor for assistance with the biological assays, Dr. Siming Wang and Ms. Sarah Shealy for the mass spectra and Dr. Peter Hambright for useful discussions.

The manuscript was compiled by Dr. D. W. Dixon. Anila F. Gill recorded the UV-vis spectra and capillary electrophoresis data and interpreted the mass spectrometry data. Dr. Lingamallu Giribabu synthesized the compounds. Dr. Richard W. Compans directed

the biological studies at Emory University and Andrei N Vzorov performed those experiments and provided the data. Atia B. Alam provided both the technical and record-keeping assistance.

Table 2.1. Biological data for the difluoro derivatives of TPPS.  
From the laboratory of Dr. Compans.

Abbreviation	HIV % infected remaining	Min. toxicity	Tox. (trypan blue)% viable cells	Tox. (growing cells)	Tox. (MTT)	Comments
TPP(2,3-F2)S,Cu (DD755)	0	39	88	39	93	active, probably not toxic
TPP(2,4-F2)S,Cu (DD720)	40	38	64	38	89	not very active, probably not toxic
TPP(2,5-F2)S,Cu (DD713)	0	20	20	29	90	active, somewhat toxic
TPP(3,5-F2)S,Cu (DD746)	3	4	12	4	20	active, toxic

Table 2.2. Summary of the capillary electrophoresis and mass spectrometry data for the difluoro derivatives of TPPS4. The asterisks indicate the placement of sulfonic acid groups, as directed by the fluoro groups.

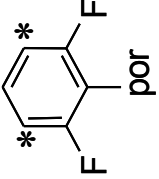
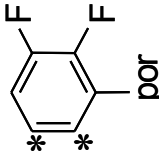
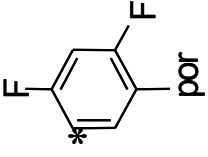
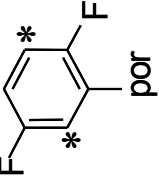
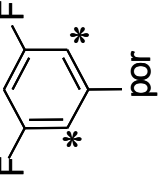
							
	2,6	2,3	2,4	2,5	3,5		
Compounds	10 mM phosphate buffer - migration times	$\lambda_{\max}$ (nm)	buffer + 1 mM $\beta$ CD - migration times	$\lambda_{\max}$ (nm)	MS peaks for sulfonated species	Sulfonated species losing water	Sulfonated species losing $\text{SO}_2$
TPP(2,6-F2)S,Cu (DD194)	4 unresolved peaks, 7.3 - 7.6 min	412 - 416 nm	Not attempted	Not attempted	4S, 5S, 6S	-	4S, 5S, 6S
TPP(2,3-F2)S,Cu (DD755)	5.2 min 6.4 min 7.7 min	409 nm 414 and 443 nm 419 nm	5.1 min 6.2 min 7.4 min	409 nm 414 and 444 nm 420 nm	3S, 4S, 5S (traces)	4S, 5S	4S, 5S
TPP(2,4-F2)S,Cu (DD720)	5.0 min 6.1 min	409 nm 414 nm	4.7 min 6.1 min	410 nm 414 nm	1S (traces), 2S, 3S, 4S	2S, 3S, 4S	4S, 5S
TPP(2,5-F2)S,Cu (DD713)	Several unresolved peaks, 6.0 - 9.0 min	only the peak at 6.5 min had both 414 nm and 450 nm bands; the other peaks ~ 420 nm	4.3 min 5.1 min 6.3 min	416 and 449 nm 421 nm 419 nm	2S, 3S, 4S	3S, 4S	-
TPP(3,5-F2)S,Cu (DD746)	3 unresolved peaks, 5.0 - 10 min	~ 440 nm	4 unresolved peaks, 4.0 - 10 min	~ 440 nm	2S, 3S, 4S (traces)	3S, 4S (traces)	-

Table 2.3. Summary of the CE data for the bromo derivatives of TPPS4.

Compounds	10 mM phosphate buffer (pH 9.0) - migration times	$\lambda_{\text{max}}$ (nm)	buffer + 1 mM $\beta$ CD - migration times	$\lambda_{\text{max}}$ (nm)
TPP(4-Br)S (DD709)	several unresolved peaks, 4 - 6 min	413 - 417 nm	5 - 6 peaks with only slight resolution, 3.5 - 7.5 min	416 - 417 nm
TPP(2-Br)S,Cu (DD774)	A few unresolved peaks and 2 short peaks, 5.5 - 8 min	418 - 423 nm	~ 9 peaks moderately resolved, 4.5 - 9.5 min	419 - 423 nm
TPP(3-Br)S,Cu (DD707)	A broad peak of several unresolved components, 4 - 7 min	415 nm with a slight hint of 450 nm	3 min 3.5 min	415 nm
TPP(4-Br)S,Cu (DD710)	A broad peak of several unresolved components, 4 and 7 min	412 - 414 nm	Several unresolved peaks b/w 5 and 10 min and a broad peak at 16 min	415 - 419 nm

Table 2.4. Summary of the negative ion MALDI data for the bromo derivatives of TPPS4.

<b>TPP(4-Br)S (DD709) (M)</b>	<b>2S</b>	<b>3S</b>	<b>4S</b>	<b>5S</b>
Na adducts	0, 1, 2	0, 1, 2	0, 1, 2, 3	
<b>TPP(2-Br)S,Cu (DD774)</b>				
Na adducts			0, 1, 2, 3	0, 1, 2, 3, 4, 5
<b>TPP(4-Br)S,Cu (DD710)</b>				
Na adducts	0, 1, 2	0, 1, 2, 3	0, 1, 2	

M = molecular ion peak or the parent sulfonated species peak

Table 2.5. EC<sub>50</sub> and CC<sub>50</sub> for selected sulfonated metalloporphyrins. Data from the laboratory of Dr. Compans.

Compound	Inactivation HIV-1 IIB EC <sub>50</sub> (µg/ml)	Inactivation HIV-1 JR-FL EC <sub>50</sub> (µg/ml)	CC <sub>50</sub> (µg/ml) <sup>a</sup>	Therapeutic index (HIV-1 IIB) <sup>b</sup>	Therapeutic index (HIV-1 JR- FL) <sup>b</sup>
T1Nap20S,Cu	1	7	925	925	132
T2Nap20S,Cu	2	12	500	250	42
T1Nap10S,Fe	2	13	415	208	32
T2Nap10S,Fe	10	14	860	86	61

<sup>a</sup>Results obtained by MTT assay using MAGI-CCR5 cells

<sup>b</sup>The therapeutic index value was defined as the CC<sub>50</sub>/EC<sub>50</sub>

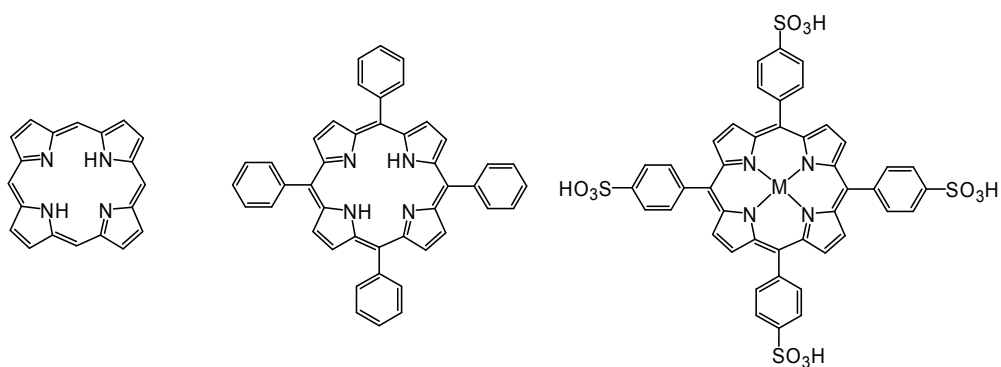


Figure 2.1a. Structure of porphyrin (left), tetraphenylporphyrin (TPyP4) (center), and tetrasulfonated tetraphenylporphyrin (TPPS4) (right).

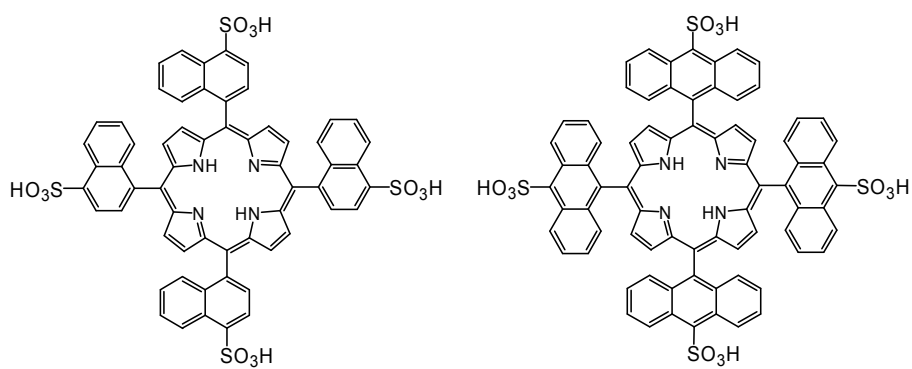


Figure 2.1b. Structure of naphthyl porphyrin (TNapPS) (left) and anthracyl porphyrin (TAnthPS) (right).

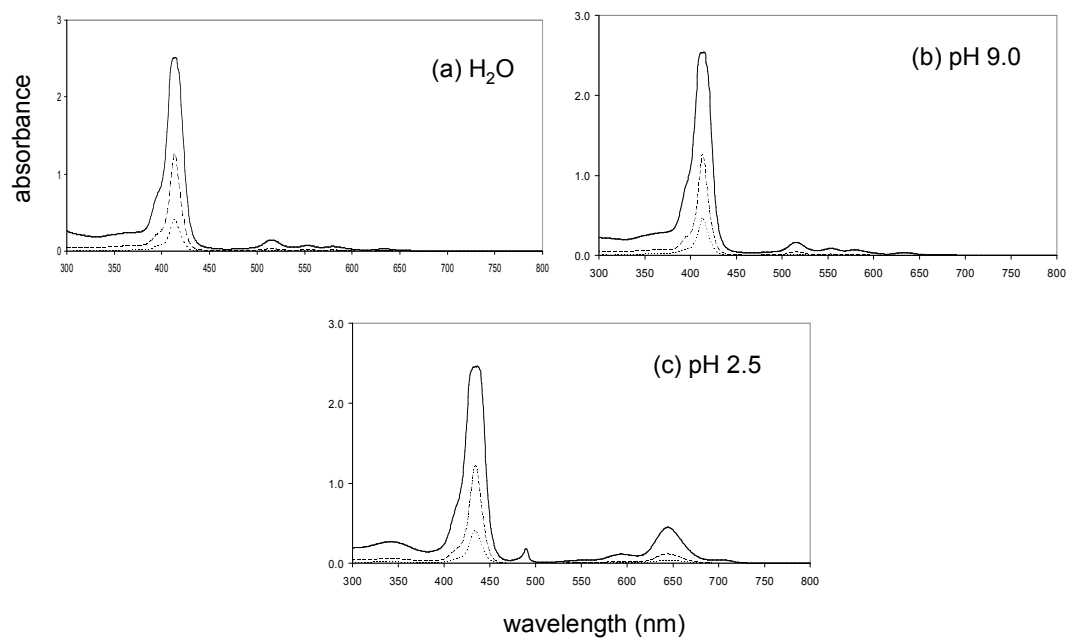


Figure 2.2. UV-vis spectra of TPPS4. In the order of decreasing concentration, the dilution factors are 301, 1001 and 3001 of the stock solution ( $\sim 10^{-3}$  M by weight).

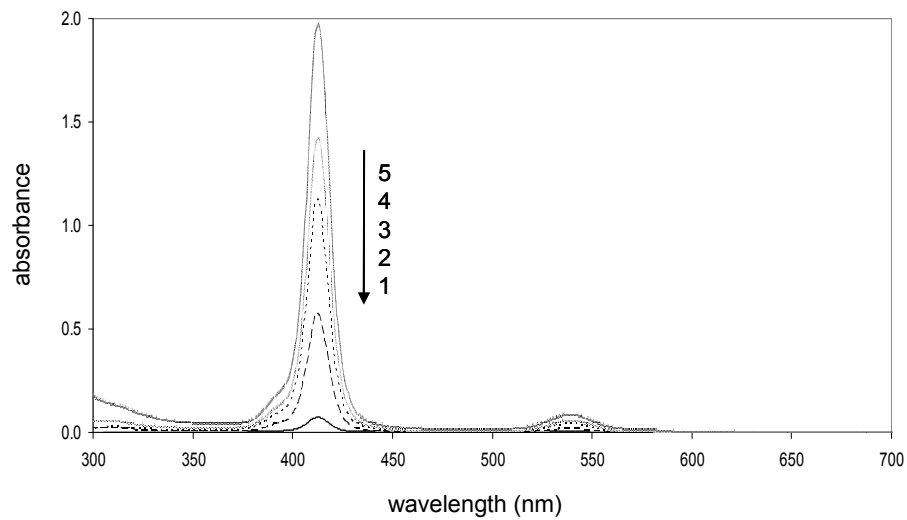


Figure 2.3. UV-vis spectra of CuTPPS4 in water. In the order of decreasing concentration, the dilution factors are 26, 39, 51, 101 and 752 of the stock solution ( $\sim 10^{-4}$  M by weight).

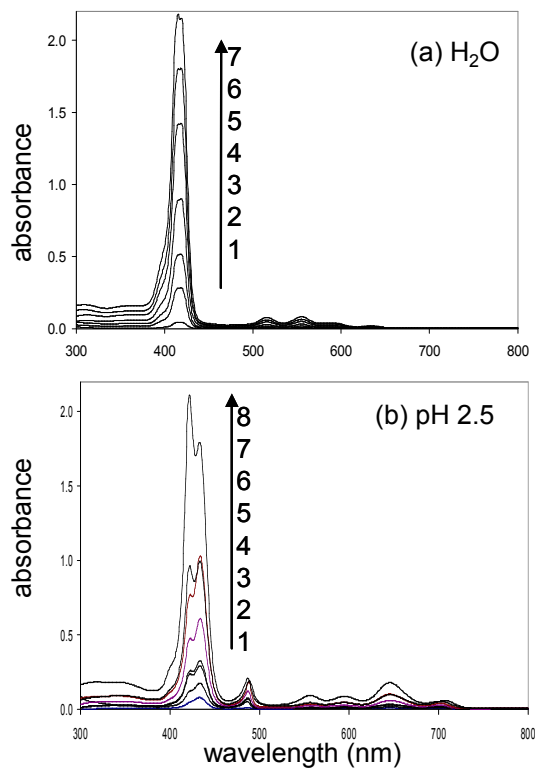


Figure 2.4. UV-vis spectra of TPPS3 in water: (a) In the order of decreasing concentration, the dilution factors are 17, 25, 33, 50, 100, 200 and 1000 of the stock solution ( $10^{-4}$  M by weight). (b) In the order of decreasing concentration, the dilution factors are 17, 20, 25, 33, 50, 100, 200 and 500 of the stock solution ( $10^{-4}$  M by weight).

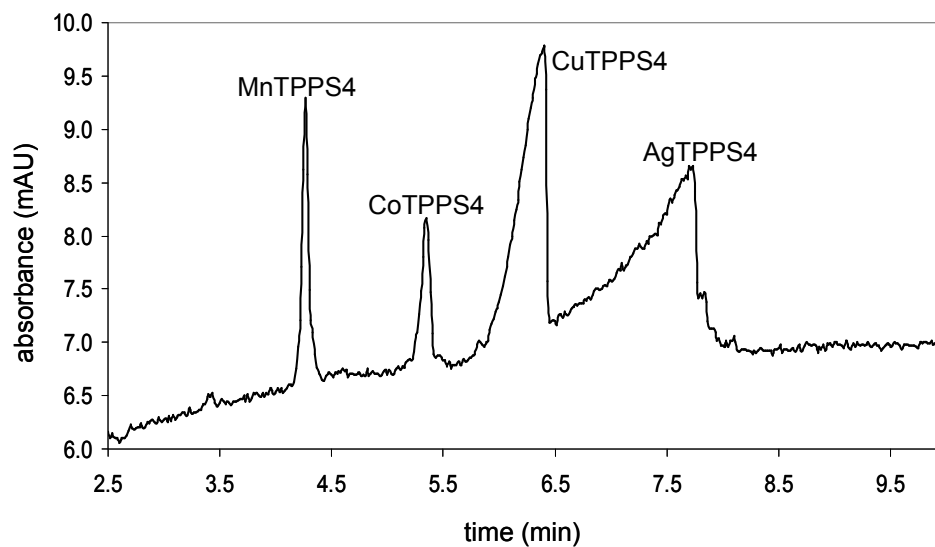


Figure 2.5. Capillary electrophoresis separation of metalloderivatives of TPPS4. Separation conditions: 10 mM  $\text{KH}_2\text{PO}_4$  buffer, pH 9.0, 30 kV, 412 nm.

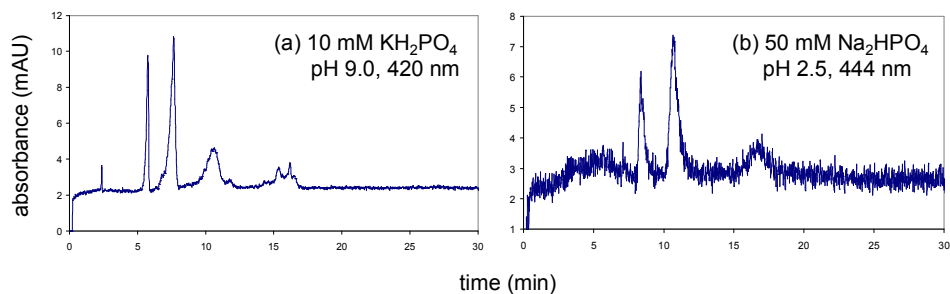


Figure 2.6. Capillary electropherograms of TNapPS.

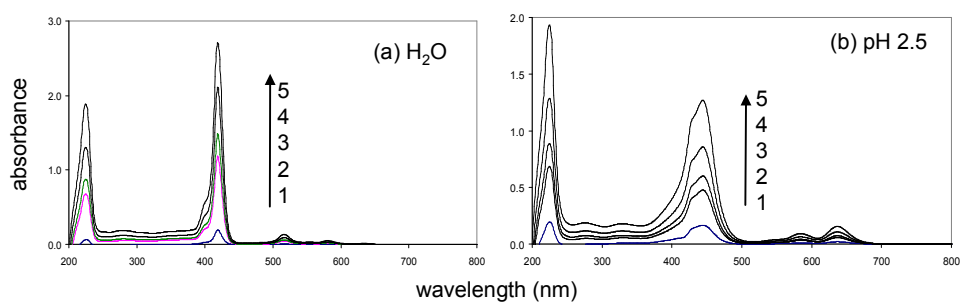


Figure 2.7. UV-vis spectra of TNapPS. In the order of decreasing concentration, the dilution factors were 101, 151, 216, 301 and 752 of the stock solution ( $\sim 10^{-3}$  M).

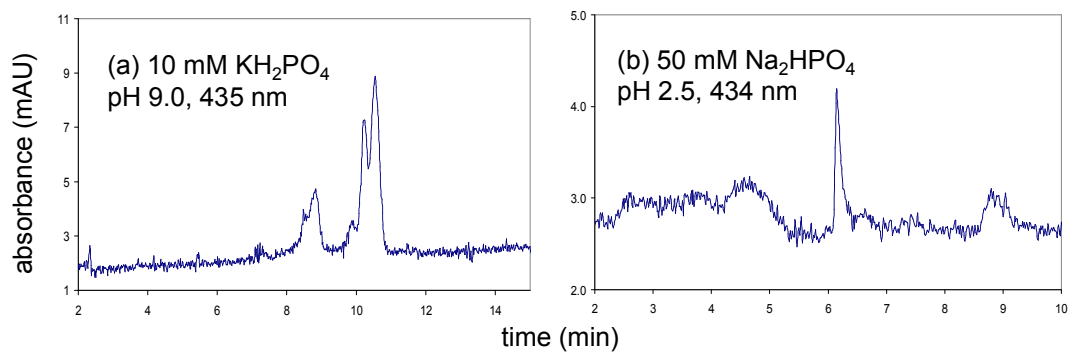


Figure 2.8. Capillary electropherograms of TAnthPS.

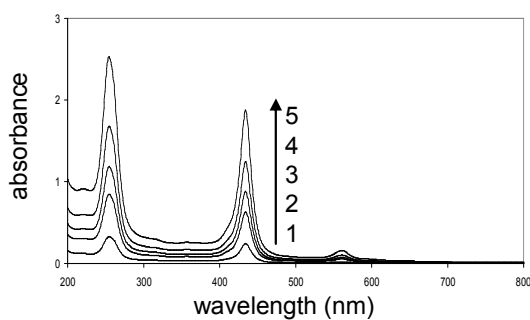


Figure 2.9. UV-vis spectra of TAnthPS in pH 2.5 buffer. In the order of decreasing concentration, the dilution factors were 101, 151, 216, 301 and 752 of the stock solution ( $\sim 10^{-3}$  M).

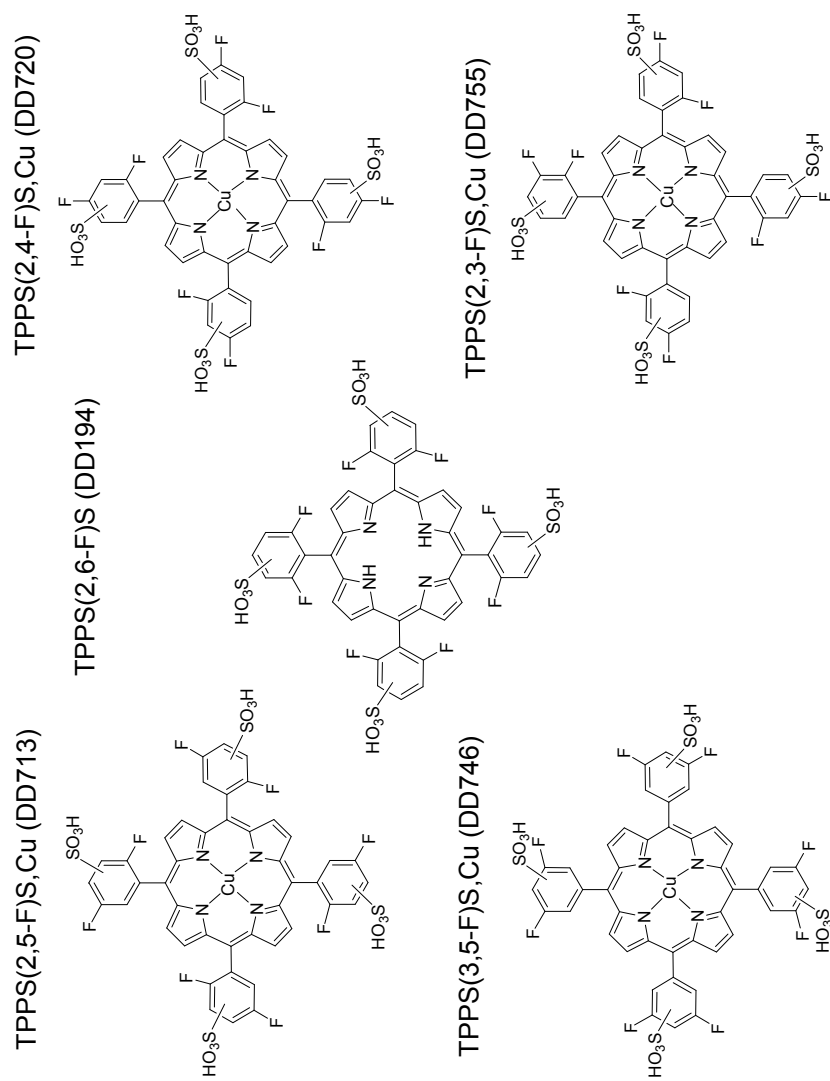


Figure 2.10. Structures of the difluoro derivatives of TPPS4.

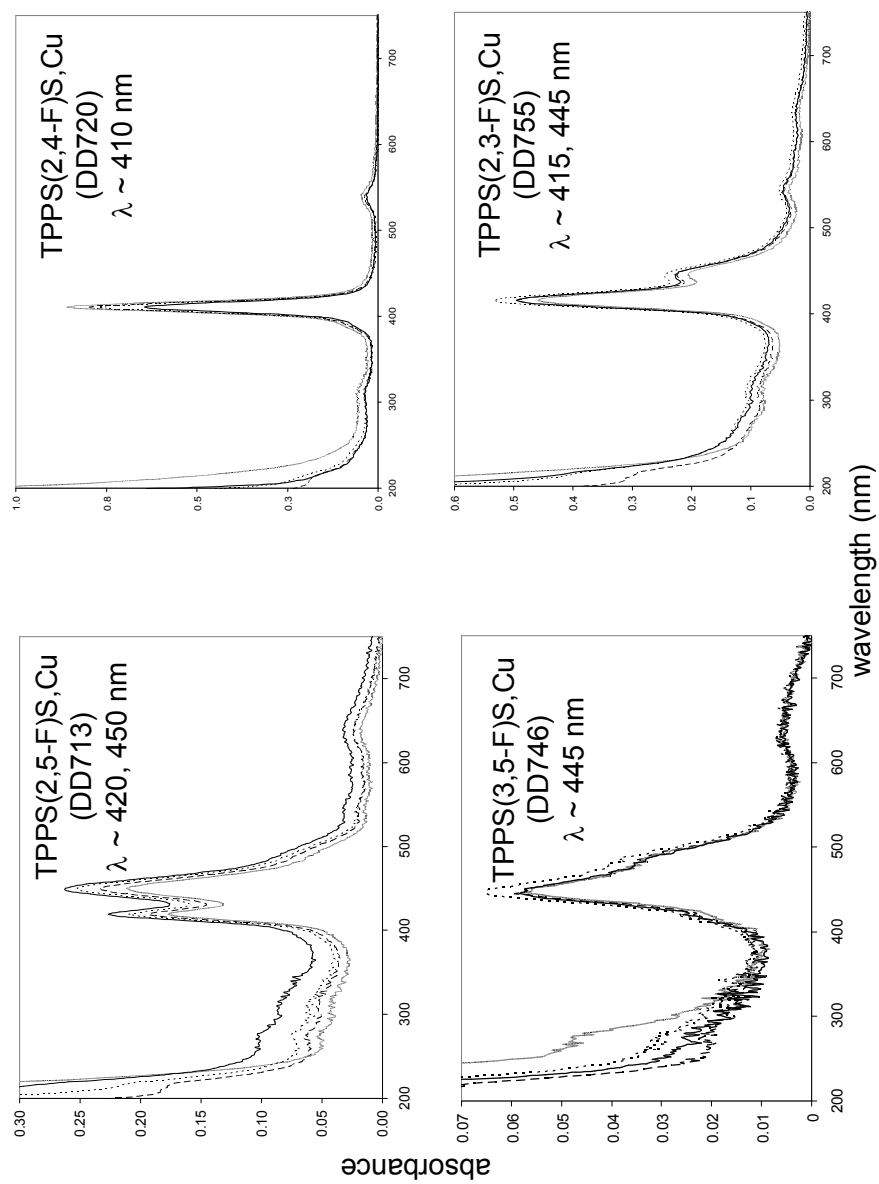


Figure 2.11. UV-vis spectra of the Cu chelates of difluoro derivatives of TPPS4 in various solvents. H<sub>2</sub>O: —; 1 mM EDTA: .....; buffer pH 7.1: -----; buffer pH 9.0: —·—·—

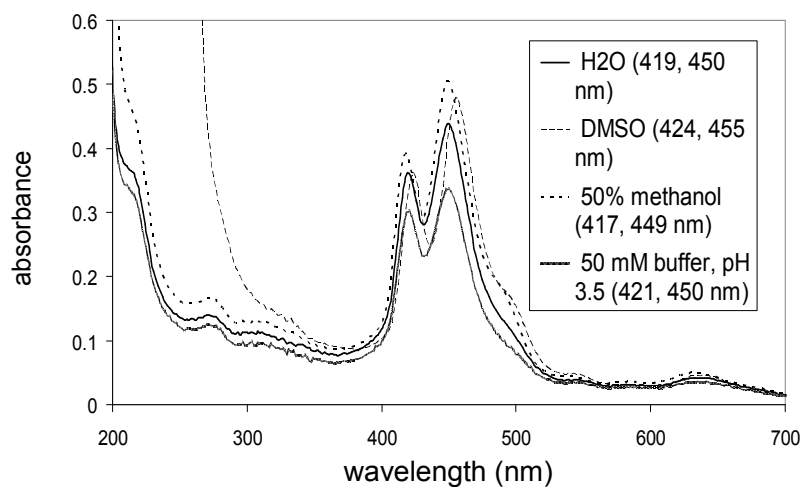


Figure 2.12a. UV-vis Spectra of TPP(2,5-F<sub>2</sub>)S<sub>2</sub>Cu (DD713) in various solvents to check for aggregation.

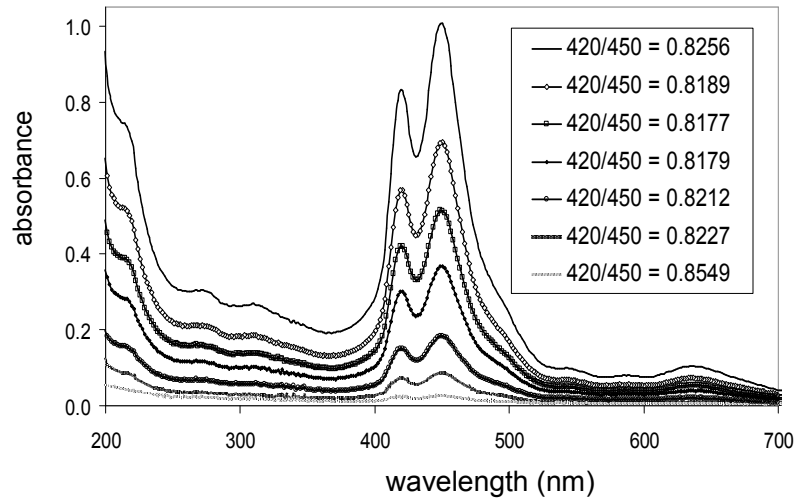


Figure 2.12b. UV-vis Spectra of various dilutions of

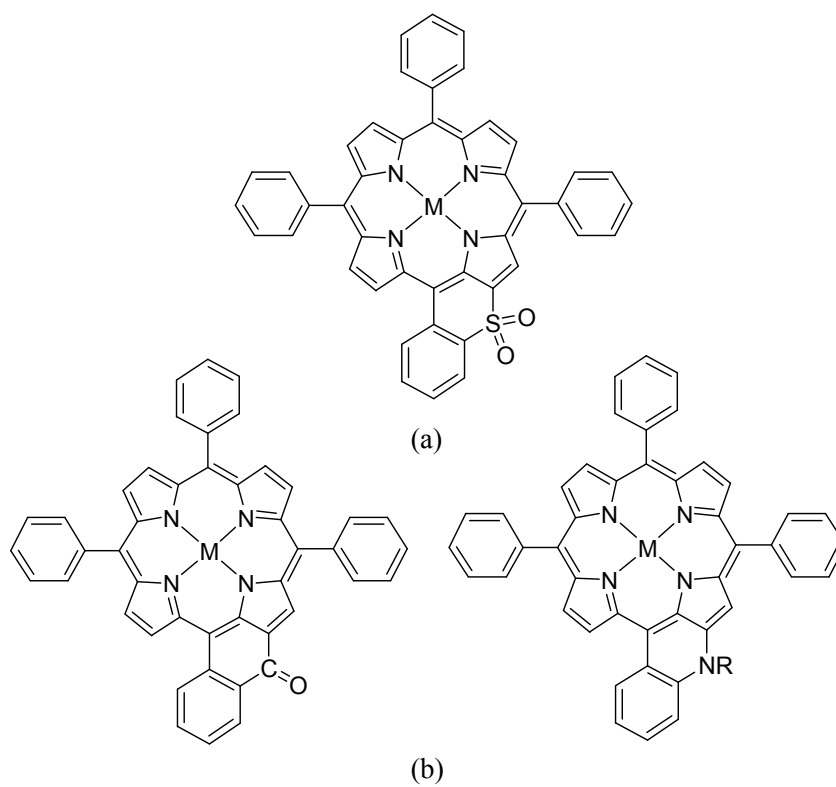


Figure 2.13. Formation of cyclic structures in tetraphenylporphyrins. (a) the proposed cyclic sulfone ring, (b) cyclic ketone and amine rings in tetrapyrroles reported in literature.

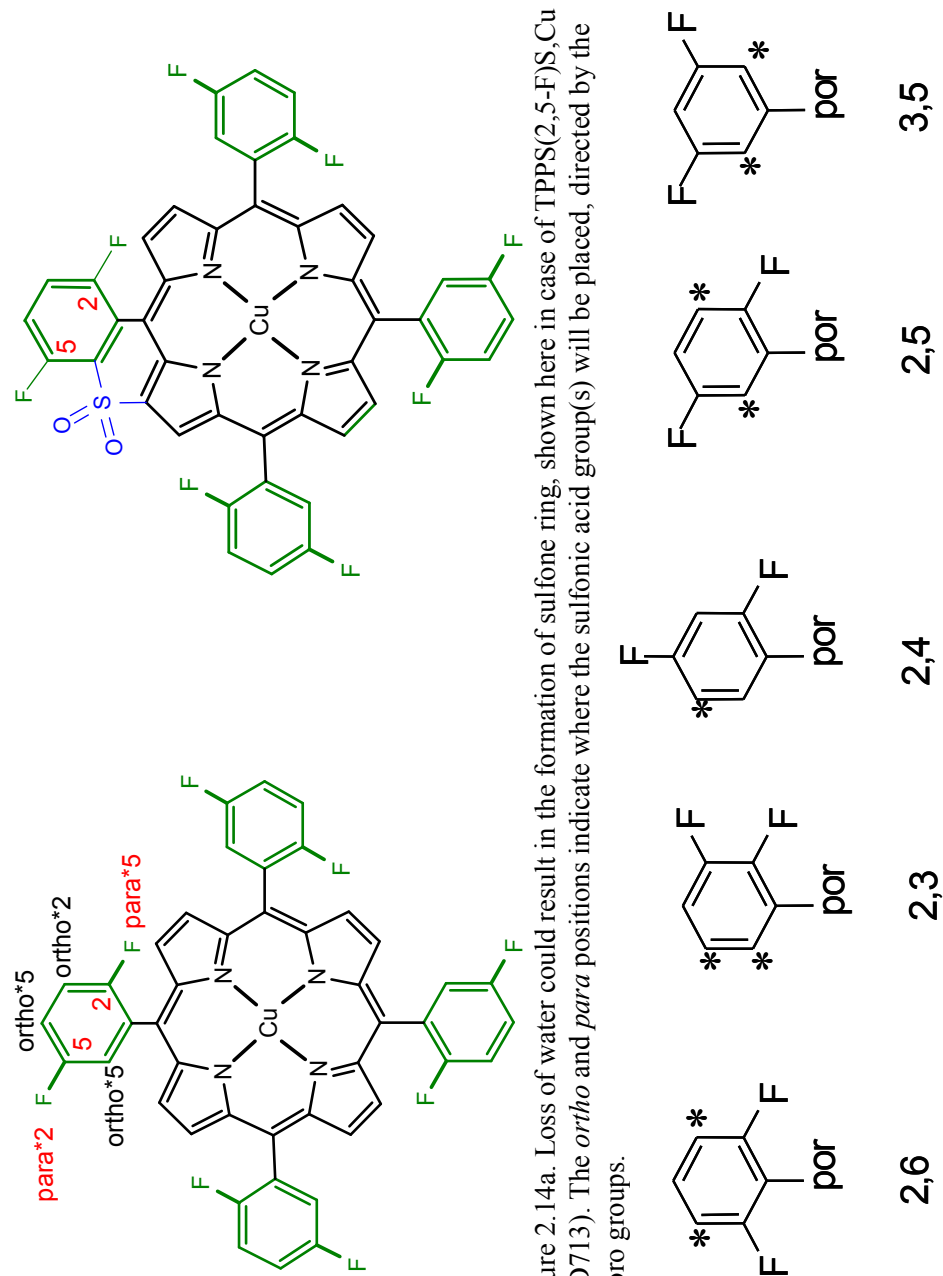


Figure 2.14a. Loss of water could result in the formation of sulfone ring, shown here in case of TPPS(2,5-F)S, Cu (DD713). The *ortho* and *para* positions indicate where the sulfonic acid group(s) will be placed, directed by the fluoro groups.

Table. 2.14b. The asterisks indicate the placement of sulfonic acid groups, as directed by the fluoro groups.

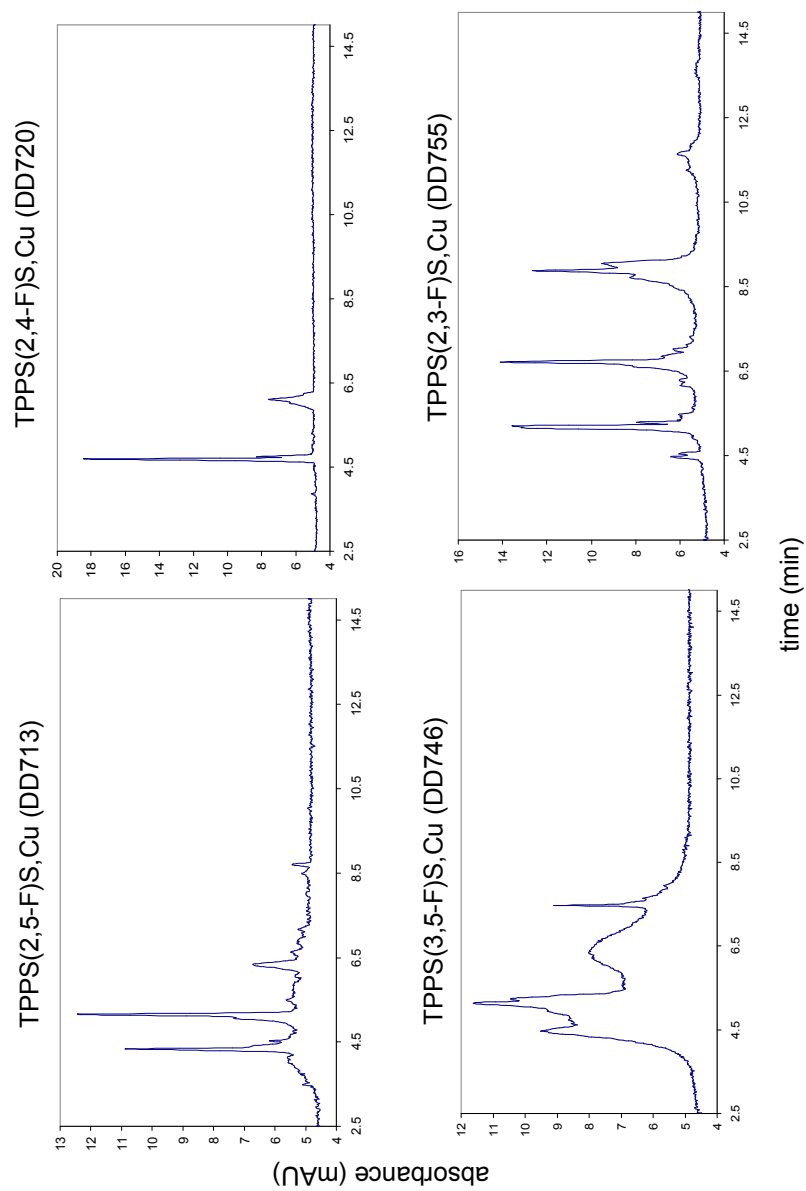


Figure 2.15. Capillary electrophoresis separation of fluoro derivatives of TPPS4. Separation conditions: 10 mM  $\text{KH}_2\text{PO}_4$  buffer + 1 mM  $\beta\text{CD}$ , pH 9.0, 30 kV.

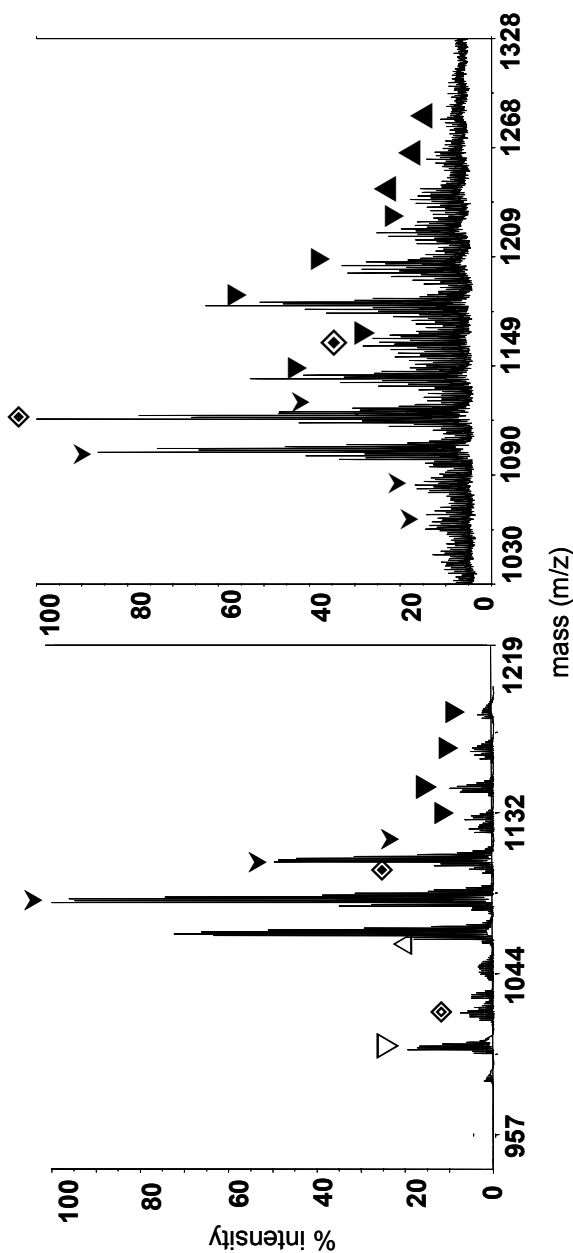


Figure 2.16a. Negative ion MALDI mass spectrum of TPP(3,5-F<sub>2</sub>)S<sub>2</sub>Cu (DD746). Peaks corresponding to mono-(▼, 899), di-(▲, 979), tri-(▼, 1059) and tetrasulfonic acid (▼, 1139) and their sodium adducts are seen. The peak at 1040 (◆) is due to loss of 18 Da from trisulfonic acid. The peak at 1120 (◆) is due to loss of 18 Da from tetrasulfonic acid.

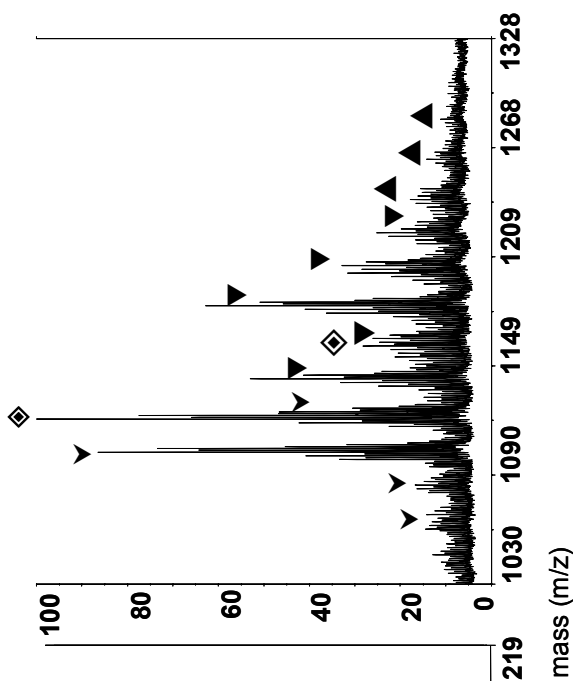


Figure 2.16b. Negative ion MALDI mass spectrum of TPP(2,3-F<sub>2</sub>)S<sub>2</sub>Cu (DD755). Peaks corresponding to tri-(▼, 1059), tetra-(▼, 1139) and penta-sulfonic acid (▲, 1219) and their sodium adducts are seen. The peak at 1120 (◆) is due to loss of 18 Da from tetrasulfonic acid. The peak at 1201 (◆) is due to loss of 18 Da from penta-sulfonic acid.

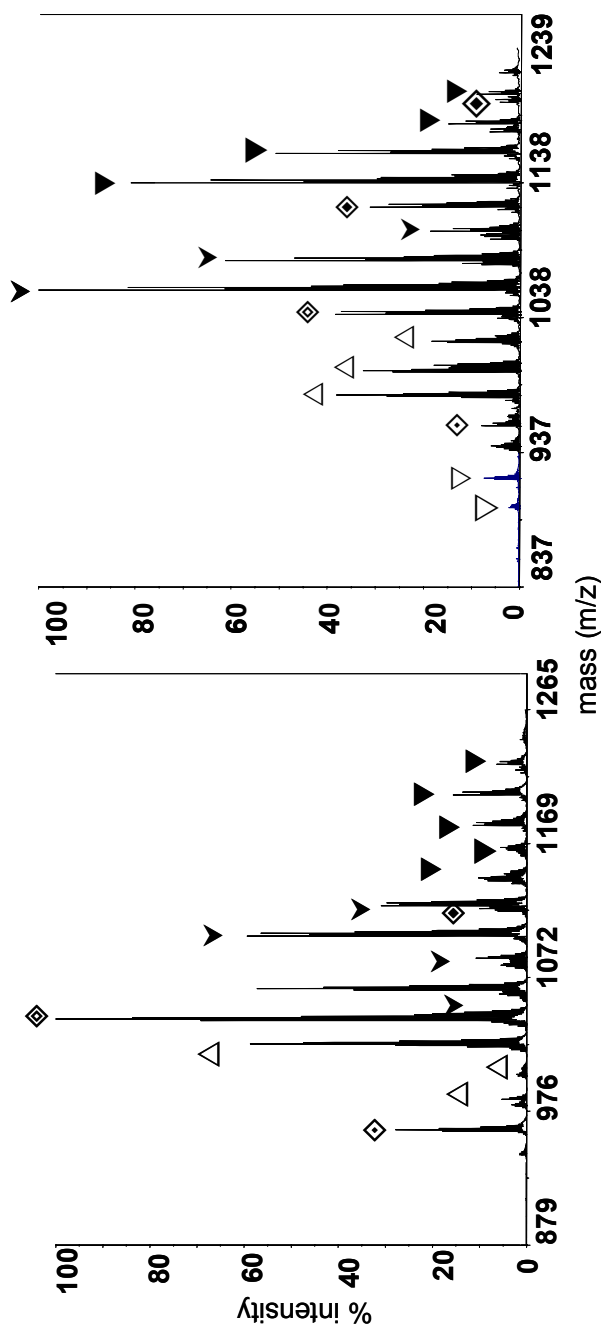


Figure 2.17a. Negative ion MALDI mass spectrum of TPP(2,5-F<sub>2</sub>)S<sub>2</sub>Cu (DD713). Peaks corresponding to di- (△, 979), tri- (▼, 1059) and tetrasulfonic acid (▼, 1139) and their sodium adducts are seen. The peak at 960 (◇) is due to loss of water from disulfonic acid. The peak at 1040 (◇) is due to loss of 18 Da from trisulfonic acid. The peak at 1120 (◇) is due to loss of water from tetrasulfonic acid.

Figure 2.17b. Negative ion MALDI mass spectrum of TPP(2,4-F<sub>2</sub>)S<sub>2</sub>Cu (DD720). Peaks corresponding to mono- (▽, 899), di- (△, 979), tri- (▼, 1059) and tetrasulfonic acid (▼, 1139) and their sodium adducts are seen. The peaks at 960 (◇) is due to loss of water from disulfonic acid. The peak at 1040 (◇) is due to loss of water from trisulfonic acid. The peak at 1120 (◇) is due to loss of f water from tetrasulfonic acid. The peak at 1201 (◇) is due to loss of 18 Da from pentasulfonic acid.

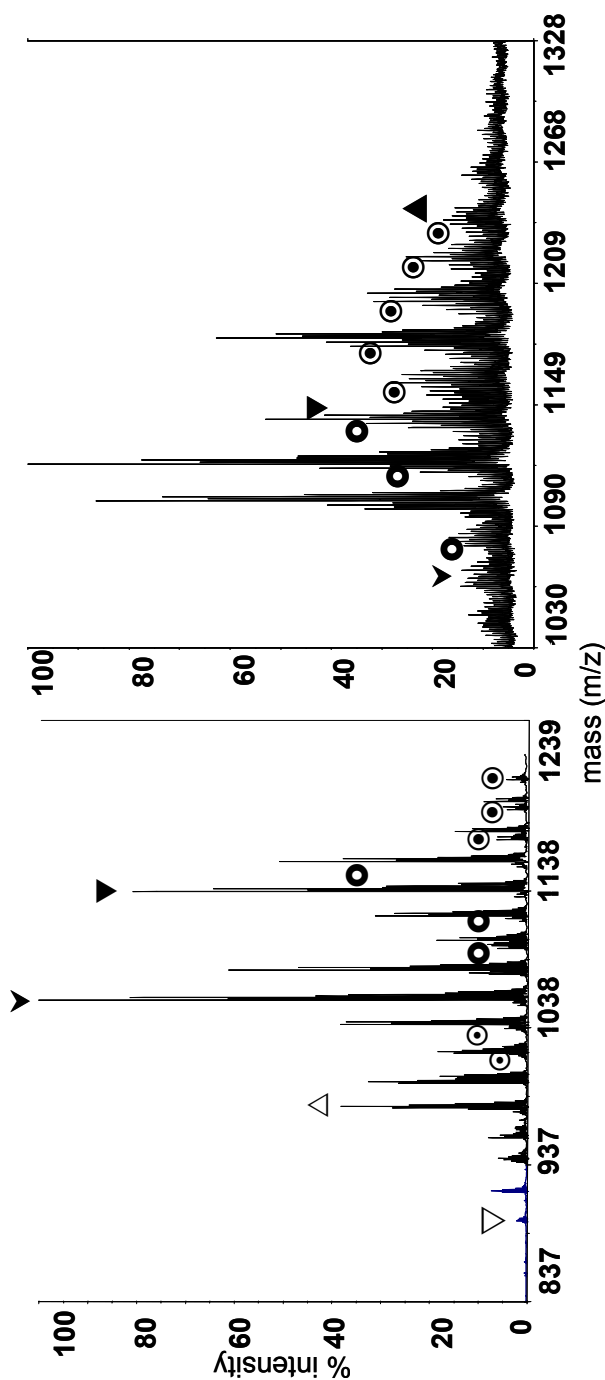


Figure 2.18a. Negative ion MALDI mass spectrum of TPP(2,4-F<sub>2</sub>)S<sub>2</sub>Cu (DD 720). Peaks corresponding to mono-( $\nabla$ , 899), di-( $\Delta$ , 979), tri-( $\blacktriangledown$ , 1059) and tetrasulfonic acid ( $\blacktriangledown$ , 1139) are seen. The peaks at 1017 and 1039 ( $\odot$ ) are due to loss of SO<sub>2</sub> from sodium adducts of trisulfonic acid. The peaks at 1097, 1119 and 1141 ( $\bullet$ ) are due to loss of SO<sub>2</sub> from sodium adducts of tetrasulfonic acid. The peaks at 1177, 1199 and 1221( $\odot$ ) are due to loss of SO<sub>2</sub> from sodium adducts of pentasulfonic acid.

Figure 2.18b. Negative ion MALDI mass spectrum of TPP(2,3-F<sub>2</sub>)S<sub>2</sub>Cu (DD 755). Peaks corresponding to tri-( $\blacktriangledown$ , 1059), tetra-( $\blacktriangledown$ , 1139) and pentasulfonic acid ( $\blacktriangle$ , 1219) are seen. The peaks at 1075, 1097, 1119 and 1141 ( $\bullet$ ) are due to loss of SO<sub>2</sub> from tetrasulfonic acid and its sodium adducts. The peaks at 1155, 1177, 1199 and 1221( $\odot$ ) are due to loss of SO<sub>2</sub> from pentasulfonic acid and its sodium adducts.

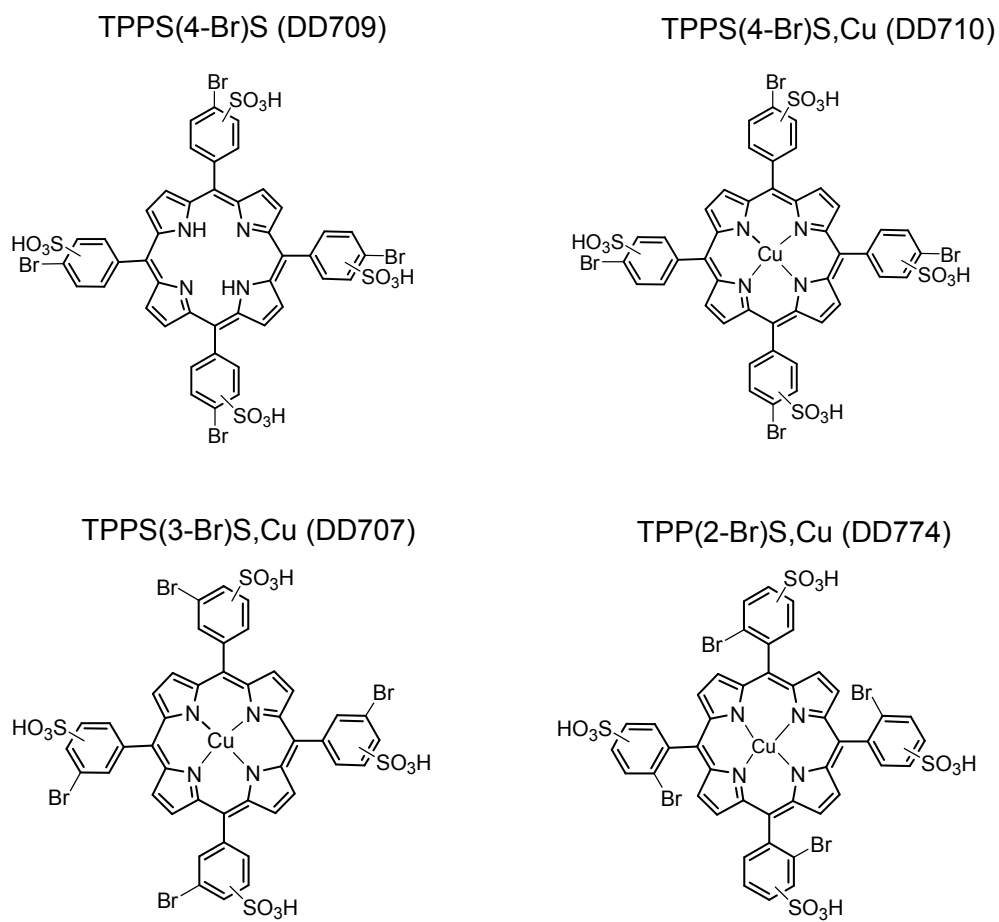


Figure 2.19. Structures of bromo derivatives of TPPS4.

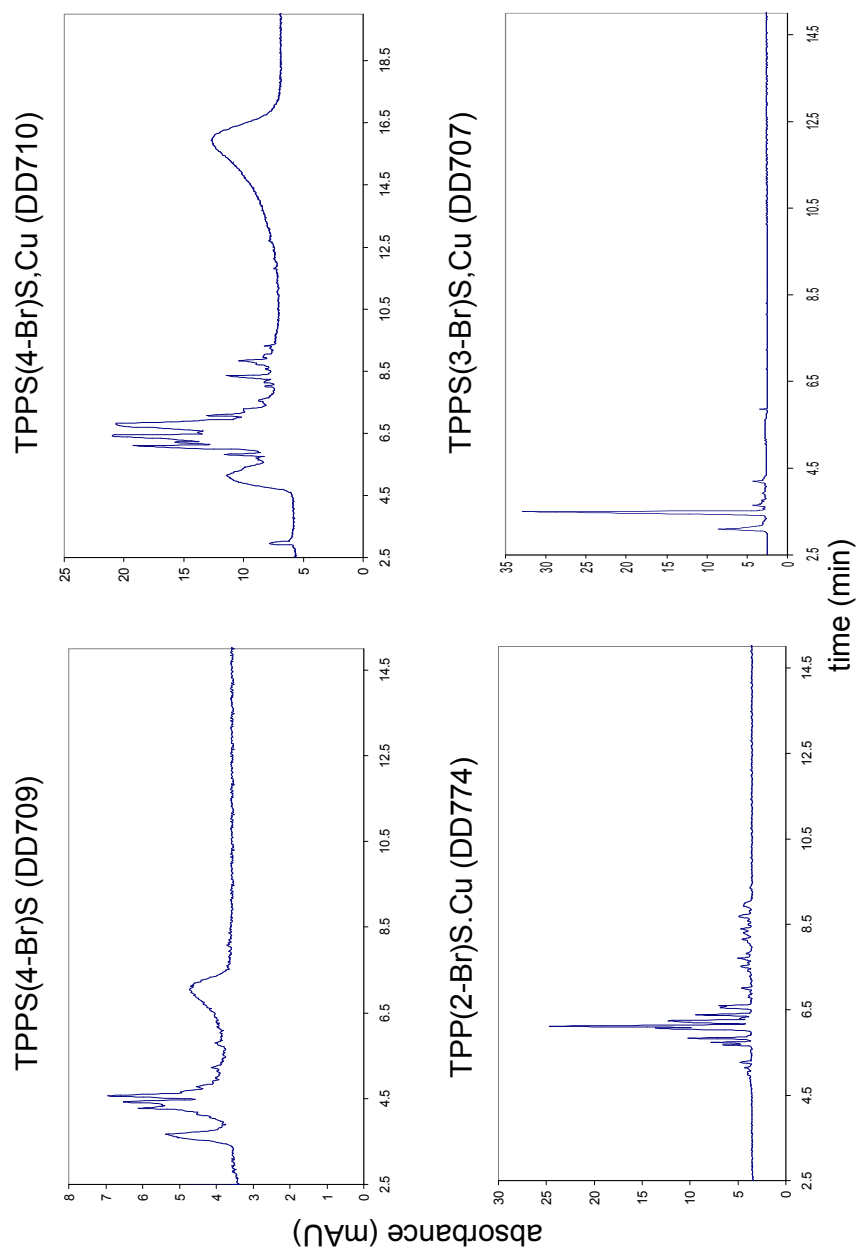


Figure 2.20. Capillary electropherograms of bromo derivatives of TPPS4. Separation conditions: 10 mM  $\text{KH}_2\text{PO}_4$ , pH 9.0 buffer with 1 mM  $\beta\text{CD}$ .

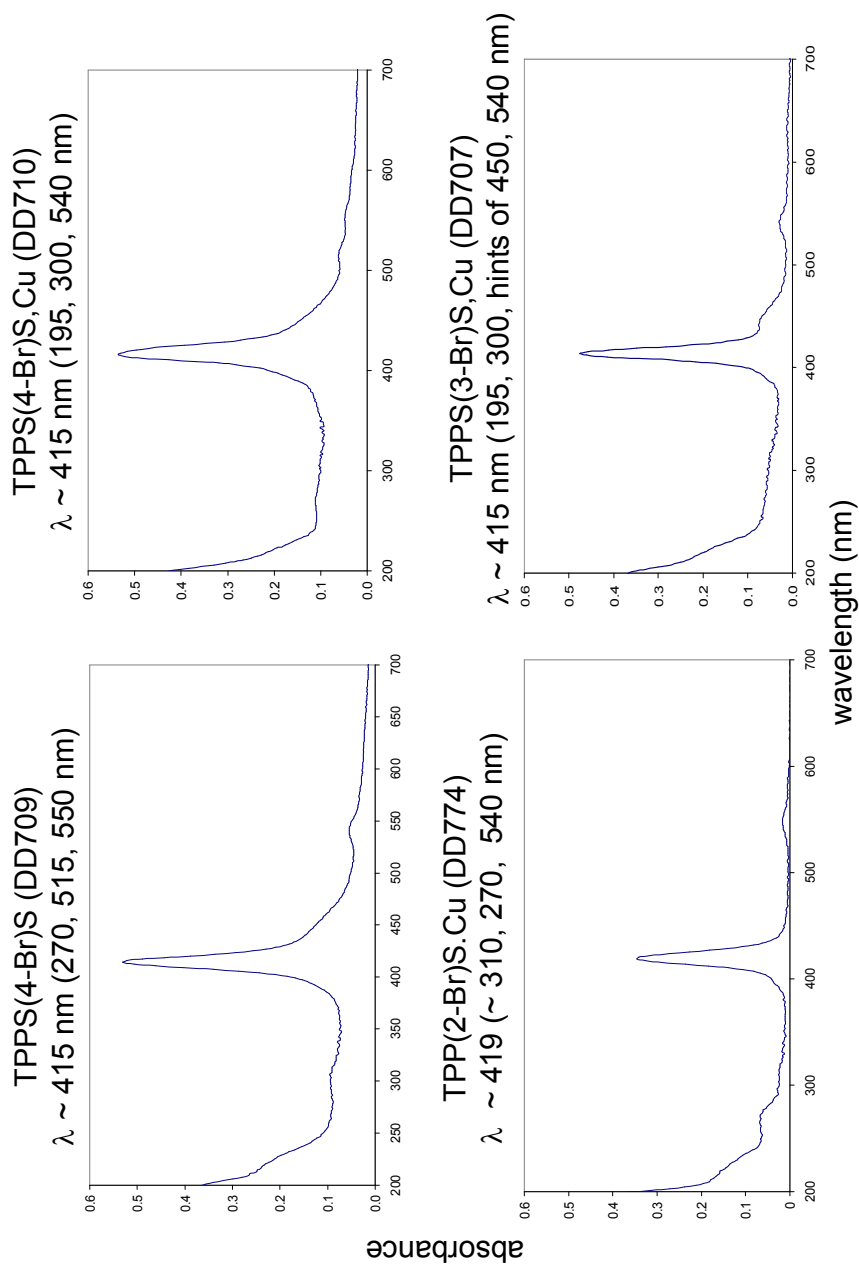


Figure 2.21. UV-vis spectra of bromo derivatives of TPPS4 in water.

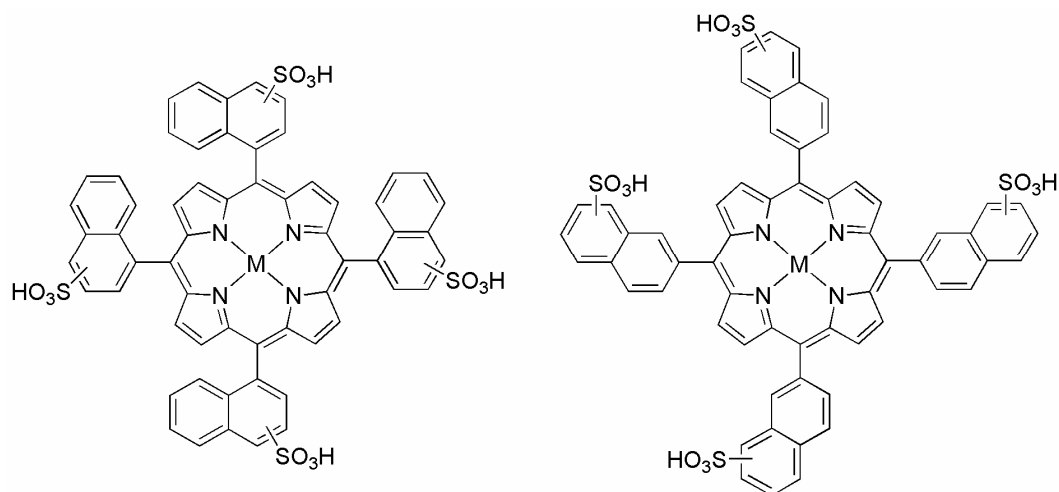


Figure 2.22. Structures of sulfonated 1-naphthyl (T1NapS, left) and 2-naphthyl (T2NapS, right) porphyrins. Tetrasulfonated porphyrins with one sulfonic acid on each side chain are shown. M is Cu, Fe or 2H.

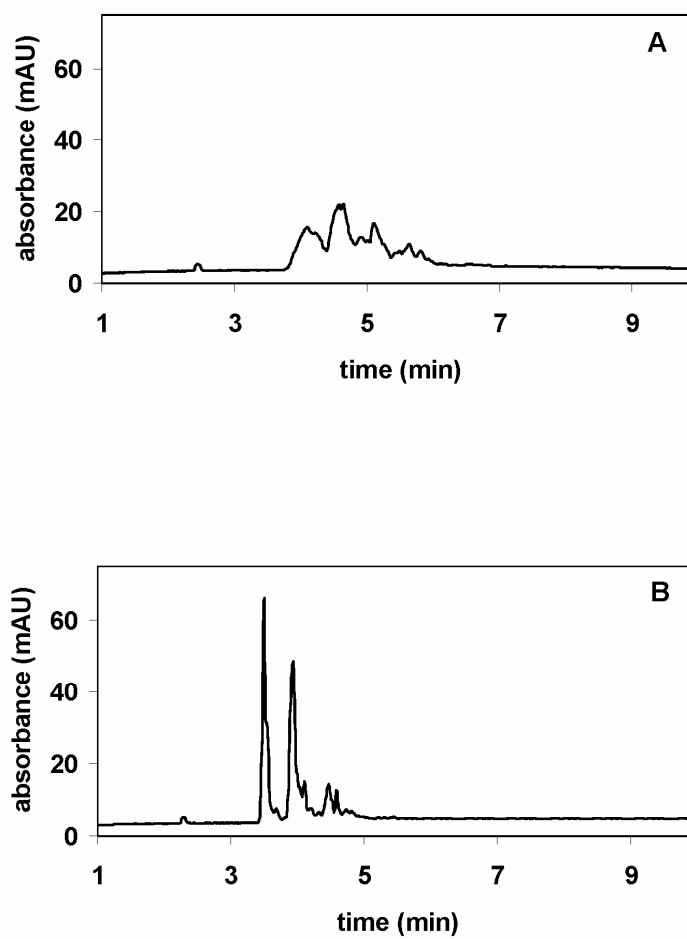


Figure 2.23. CE separation of T2Nap5S,Cu in pH 9.0, 10 mM  $\text{KH}_2\text{PO}_4$  buffer. A: with 1 mM  $\beta$ -cyclodextrin; B: with 1 mM  $\gamma$ -cyclodextrin.

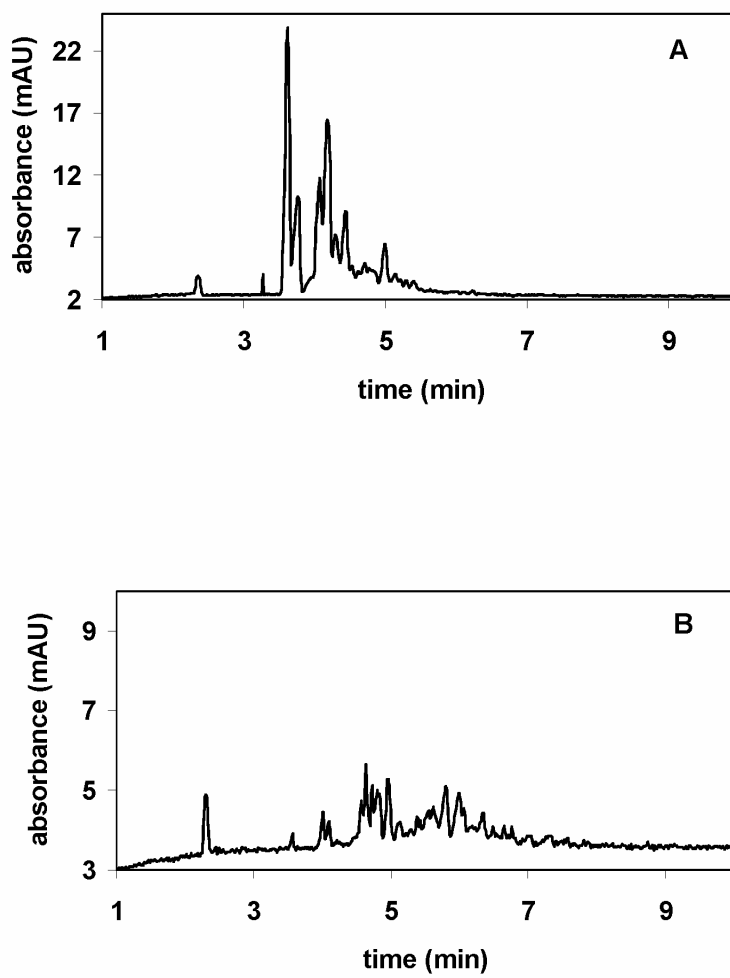


Figure 2.24. CE of T2NapS made by sulfonation for 5 h (A, T2Nap5S) and 20 h (B, T2Nap20S) (pH 9.0, 10 mM  $\text{KH}_2\text{PO}_4$  buffer, 1 mM  $\gamma$ -cyclodextrin).

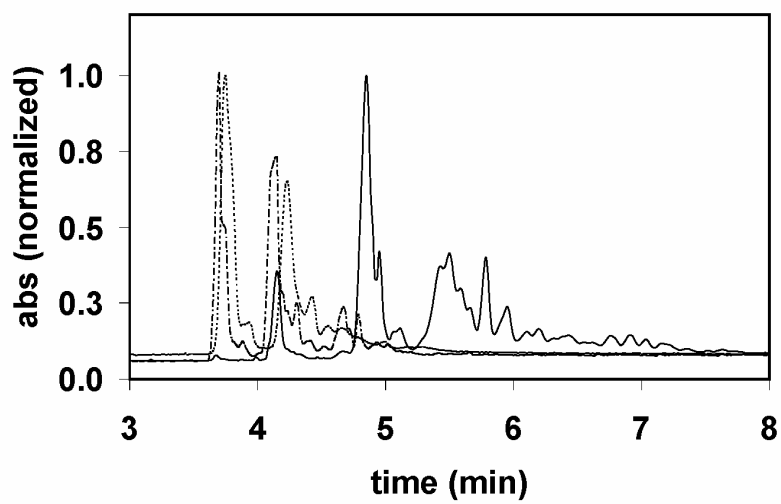


Figure 2.25. CE of T2NapS,Cu (pH 9.0, 10 mM  $\text{KH}_2\text{PO}_4$  buffer, 1 mM  $\gamma$ -cyclodextrin). Sulfonation for 5 h (- . . -), 10 h (- - - -) and 20 h (\_\_\_\_\_).

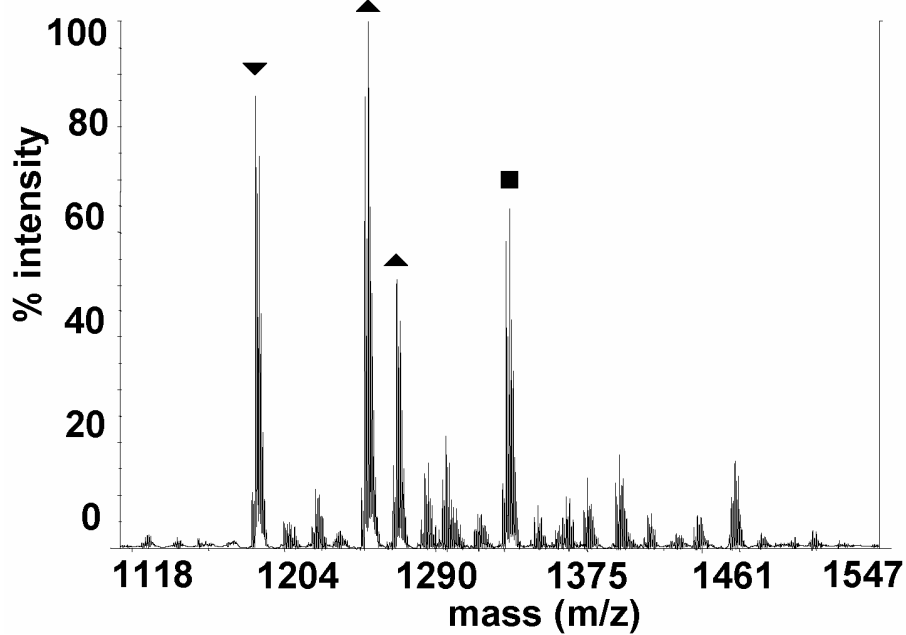


Figure 2.26. Negative ion MALDI mass spectrum of T2Nap5S,Cu. Peaks corresponding to the tetrasulfonic acid (▼, 1195) and pentasulfonic acid (▲, 1275) are seen. The peaks at 1257 and 1337 are attributed to the sulfones (loss of water) from pentasulfonic acid (▲) and hexasulfonic acid (■), respectively.

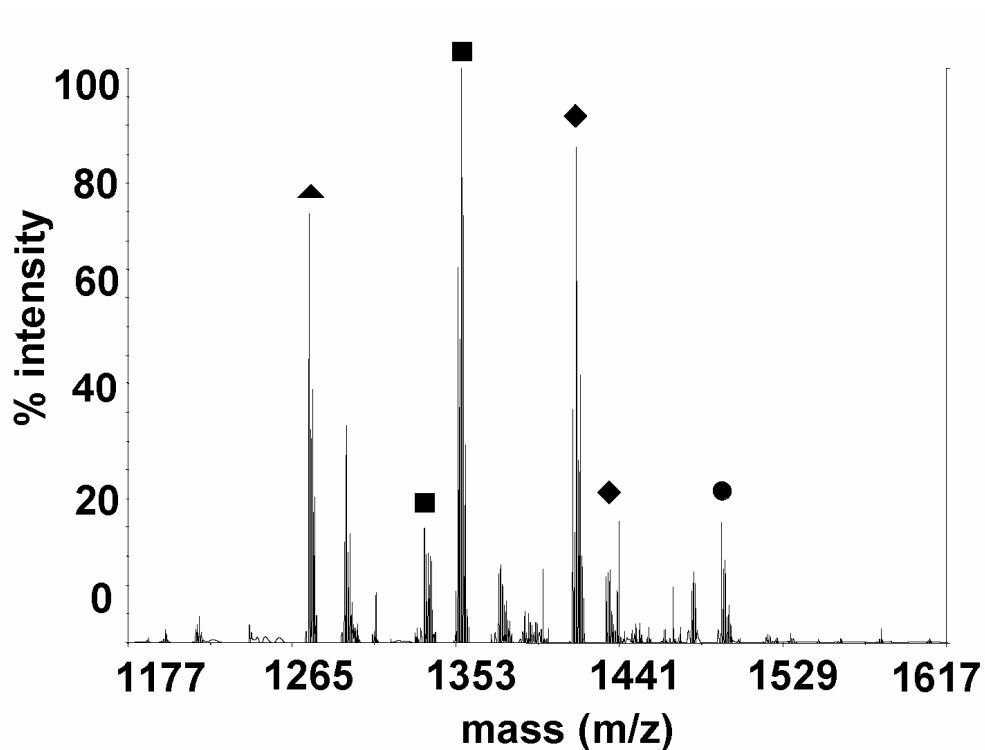


Figure 2.27. Negative ion MALDI mass spectrum of T2Nap20S,Cu showed peaks appropriate for the pentasulfonic acid (▲); the hexa- (■) and heptasulfonic acids (◆) and their  $M - H_2O$  peaks; and the  $M - H_2O$  peak corresponding to the octasulfonic acid (●). Sodium salts of some of the sulfonic acid species are also seen.

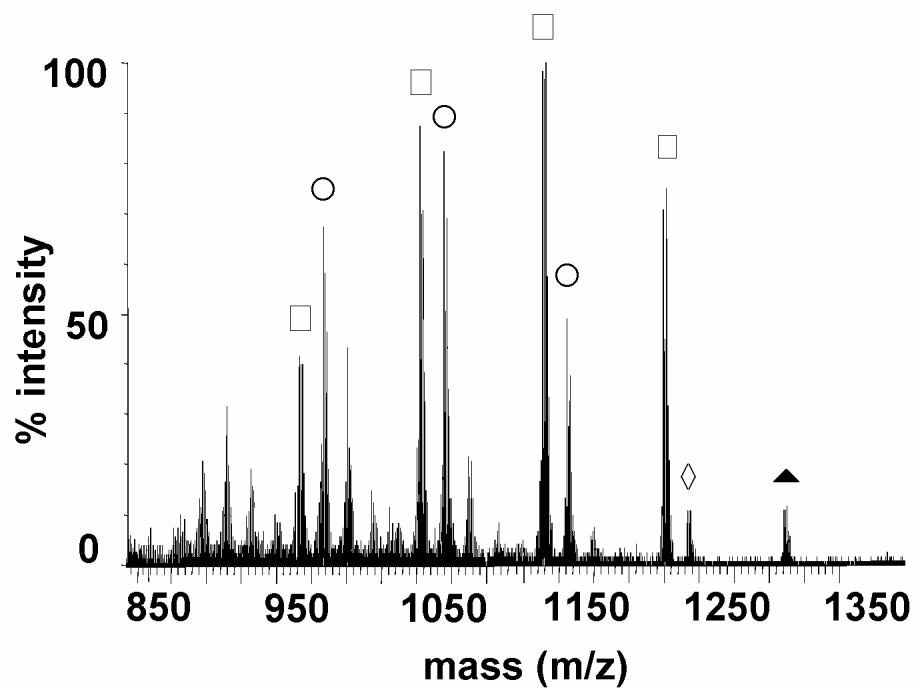


Figure 2.28. Negative ion ESI MS/MS of the pentasulfonic acid peak (▲) at 1274 of T2Nap5S,Cu. The peak at 1210 is attributed to loss of SO<sub>2</sub> (◇). Successive losses of nSO<sub>3</sub> (□) and [SO<sub>2</sub> + (n-1)SO<sub>3</sub>] (○) can be seen (n = 2 - 4). Peaks are also seen for losses of two SO<sub>2</sub> and either one or two SO<sub>3</sub>.

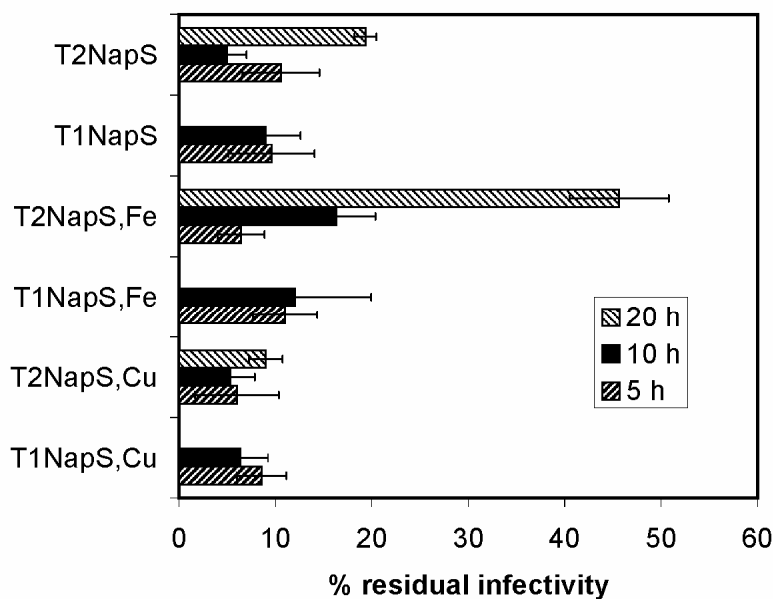


Figure 2.29. Activity of sulfonated naphthyl porphyrins against HIV-1 IIIB. Compounds at a concentration of 50  $\mu\text{g/ml}$  were incubated with HIV-1 IIIB in the dark for 1 h; the compound/virus mixture was diluted 10-fold and used to inoculate MAGI-CCR5 cells. HIV infectivity was measured after three days by removal of the media, fixation and staining with X-gal. The activity against HIV was measured by dividing the number of infected,  $\beta$ -gal expressing cells in wells infected with compound-treated virus by the number in wells infected with untreated virus. Data are plotted as the mean of one or two experiments, each with three or four replications. Error bars represent standard deviations. The naphthyl porphyrins were sulfonated for 5 and 10 hours (T1Nap) and 5, 10 and 20 hours (T2Nap). Data from the laboratory of Dr. Compans.

## References

- Abraham, R. J., Hawkes, G. H., Hudson, M. F., and Smith, K. M. (1975). The nuclear magnetic resonance spectra of porphyrins. Part X. Carbon-13 nuclear magnetic resonance spectra of some *meso*-tetraarylporphyrins and their metal chelates. *J. Chem. Soc. Perkin Trans. 2* 204-211.
- Ackley, K. L., Day, J. A., and Caruso, J. A. (2000). Separation of metalloporphyrins by capillary electrophoresis with UV detection and inductively coupled plasma mass spectrometric detection. *J. Chromatogr. A* **888**, 293-298.
- Adler, A. D., Longo, F. R., Finarelli, J. D., Goldmacher, J., Assour, J., and Korsakoff, L. (1967). A simplified synthesis for *meso*-tetraphenylporphyrins. *J. Org. Chem.* **32**, 476.
- Akins, D. L., Ozcelik, S., Zhu, H. R., and Guo, C. (1996a). Fluorescence decay kinetics and structure of aggregated tetrakis(p-sulfonatophenyl)porphyrin. *J. Phys. Chem.* **100**, 14390-14396.
- Akins, D. L., Zhu, H. R., and Guo, C. (1996b). Aggregation of tetraaryl-substituted porphyrins in homogeneous solution. *J. Phys. Chem.* **100**, 5420-5425.
- Alla, V. and Bonkovsky, H. L. (2005). Iron in nonhemochromatotic liver disorders. *Semin. Liver Dis.* **25**, 461-472.
- Alonso, M. C., Castillo, M., and Barceló, D. (1999). Solid phase extraction procedure of polar benzene- and naphthalenesulfonates in industrial effluents followed by unequivocal determination with ion pair chromatography/electrospray-mass spectrometry. *Anal. Chem.* **71**, 2586-2593.
- Andrighetto, P., Carofiglio, T., Fornasier, R., and Tonellato, U. (2000). Capillary electrophoresis behavior of water-soluble anionic porphyrins in the presence of  $\beta$ -cyclodextrin and its O-methylated derivatives. *Electrophoresis* **21**, 619-626.
- Asanaka, M., Kurimura, T., Toya, H., Ogaki, J., and Kato, Y. (1989). Anti-HIV activity of protoporphyrin. *AIDS* **3**, 403-404.
- Bowser, M. T., Sternberg, E. D., and Chen, D. D. Y. (1996). Development and application of a nonaqueous capillary electrophoresis system for the analysis of porphyrins and their oligomers (PHOTOFRIN). *Anal. Biochem.* **241**, 143-150.
- Buchler, J. W. (1975). Static coordination chemistry of metalloporphyrins. In "Porphyrins and Metalloporphyrins" (K. M. Smith, Ed.), pp. 157-231. Elsevier, New York.

Cabrera, C., Witvrouw, M., Gutierrez, A., Clotet, B., Kuipers, M. E., Swart, P. J., Meijer, D. K., Desmyter, J., De Clercq, E., and Este, J. A. (1999). Resistance of the human immunodeficiency virus to the inhibitory action of negatively charged albumins on virus binding to CD4. *AIDS Res. Hum. Retroviruses* **20**, 1535-1543.

Cerfontain, H., Koeberg-Telder, A., Laali, K., Lambrechts, H. J. A., and de Wit, P. (1982). Aromatic sulfonation 85. Halogen directing and steric effects in the sulfonation of the twelve halogenotoluenes and some related compounds. *Rec. Trav. Chim. Pays-Bas* **101**, 390-392.

Cerfontain, H., Koeberg-Telder, A., van Lindert, H. C. A., and Bakker, B. H. (1997). Aromatic sulfonation 131. Formation of sulfonic acids and sulfonic anhydrides in the sulfur trioxide sulfonation of some dialkylbenzenes and 1,omega-diarylalkanes. *Liebigs Ann. /Recl.* 2227-2233.

Cerfontain, H., Zou, Y. S., and Bakker, B. H. (1994). On the positional reactivity order in the sulfonation of phenyl-substituted and naphthyl-substituted naphthalenes with SO<sub>3</sub>. *Rec. Trav. Chim. Pays-Bas* **113**, 517-523.

Chackerian, B., Long, E. M., Luciw, P. A., and Overbaugh, J. (1997). Human immunodeficiency virus type 1 coreceptors participate in postentry stages in the virus replication cycle and function in simian immunodeficiency virus infection. *J. Virol.* **71**, 3932-3939.

Chen, M. H. and Ding, W. H. (2004). Separation and migration behavior of positional and structural naphthalenesulfonate isomers by cyclodextrin-mediated capillary electrophoresis. *J. Chromatogr. A* **1033**, 167-172.

Chen-Collins, A. R. M., Dixon, D. W., Vzorov, A. N., Marzilli, L. G., and Compans, R. W. (2003). Prevention of poxvirus infection by tetrapyrroles. *BMC Infect. Dis.* **3**, 9.

Chiang, S. C. C. and Li, S. F. Y. (1997). Separation of porphyrins by capillary electrophoresis in fused-silica and ethylene vinyl acetate copolymer capillaries with visible absorbance detection. *Biomed. Chromatogr.* **11**, 366-370.

Christensen, N. H. (1966). Kinetic studies of the hydrolysis of aromatic sulfonic anhydrides. *Acta Chem. Scand.* **20**, 1955-1964.

Conneely, A., McClean, S., Smyth, W. F., and McMullan, G. (2001). Study of the mass spectrometric behaviour of phthalocyanine and azo dyes using electrospray ionisation and matrix-assisted laser desorption/ionisation. *Rapid Commun. Mass Spectrom.* **15**, 2076-2084.

- Cormier, E. G. and Dragic, T. (2002). The crown and stem of the V3 loop play distinct roles in human immunodeficiency virus type 1 envelope glycoprotein interactions with the CCR5 coreceptor. *J. Virol.* **76**, 8953-8957.
- D'Cruz, O. J. and Uckun, F. M. (2004). Clinical development of microbicides for the prevention of HIV infection. *Curr. Pharm. Des.* **10**, 315-336.
- Dairou, J., Vever-Bizet, C., and Brault, D. (2004). Interaction of sulfonated anionic porphyrins with HIV glycoprotein gp120: Photodamages revealed by inhibition of antibody binding to V3 and C5 domains. *Antiviral Res.* **61**, 37-47.
- Dalgleish, A. G., Beverley, P. C., Clapham, P. R., Crawford, D. H., Greaves, M. F., and Weiss, R. A. (1984). The CD4 (T4) antigen is an essential component of the receptor for the AIDS retrovirus. *Nature* **312**, 763-767.
- De Clercq, E. (2002). Strategies in the design of antiviral drugs. *Nat. Rev. Drug Discov.* **1**, 13-25.
- Debnath, A. K., Jiang, S., Strick, N., Lin, K., Haberfield, P., and Neurath, A. R. (1994). Three-dimensional structure-activity analysis of a series of porphyrin derivatives with anti-HIV-1 activity targeted to the V3 loop of the gp120 envelope glycoprotein of the human immunodeficiency virus type 1. *J. Med. Chem.* **37**, 1099-1108.
- Debnath, A. K., Jiang, S. B., Strick, N., Lin, K., Kahl, S. B., and Neurath, A. R. (1999). Anti-HIV-1 activity of carborane derivatives of porphyrins. *Med. Chem. Res.* **9**, 267-275.
- DeCamp, D. L., Babé, L. M., Salto, R., Lucich, J. L., Koo, M.-S., Kahl, S. B., and Craik, C. S. (1992). Specific inhibition of HIV-1 protease by boronated porphyrins. *J. Med. Chem.* **35**, 3426-3428.
- Dettin, M., Ferranti, P., Scarinci, C., Picariello, G., and Di Bello, C. (2003). Is the V3 loop involved in HIV binding to CD4? *Biochemistry* **42**, 9007-9012.
- Dixon, D. W., Gill, A. F., Giribabu, L., Vzorov, A. N., Alam, A. B., and Compans, R. W. (2005). Sulfonated naphthyl porphyrins as agents against HIV. *J. Inorg. Biochem.* **99**, 813-821.
- Dixon, D. W., Gill, A. F., and Sook, B. R. (2004). Characterization of sulfonated phthalocyanines by mass spectrometry and capillary electrophoresis. *J. Porph. Phthalo.* **8**, 1300-1310.
- Dixon, D. W., Kim, M. S., Kumar, V., Obara, G., Marzilli, L. G., and Schinazi, R. F. (1992). Amino- and hydroxytetraphenylporphyrins with activity against the human immunodeficiency virus. *Antiviral Chem. Chemother.* **3**, 279-282.

- Dixon, D. W., Marzilli, L. G., and Schinazi, R. F. (1990). Porphyrins as agents against the human immunodeficiency virus. *Ann. N. Y. Acad. Sci.* **616**, 511-513.
- Dixon, D. W., Pu, G. M., and Wojtowicz, H. (1998). Capillary electrophoretic separation of cationic porphyrins. *J. Chromatogr. A* **802**, 367-380.
- Dolphin, D. (1978). Nomenclature. In "The Porphyrins: Structure and Synthesis, Part A." pp. 1-27. Academic Press Inc., New York.
- Dudic, M., Lhoták, P., Král, V., Lang, K., and Stibor, I. (1999). Synthesis of novel porphyrin-based biscalix[4]arenes. *Tetrahedron Lett.* **40**, 5949-5952.
- El Hachemi, Z., Farrera, J. A., García-Ortega, H., Ramirez-Gutierrez, O., and Ribó, J. M. (2001). Heteroassociation of *meso*-sulfonatophenylporphyrins with  $\beta$ - and  $\gamma$ -cyclodextrin. *J. Porph. Phthalo.* **5**, 465-473.
- Este, J. A., Schols, D., De Vreese, K., Van Laethem, K., Vandamme, A. M., Desmyter, J., and De Clercq, E. (1997). Development of resistance of human immunodeficiency virus type 1 to dextran sulfate associated with the emergence of specific mutations in the envelope gp120 glycoprotein. *Mol. Pharmacol.* **52**, 98-104.
- Falk, J. E. (1964). General Chemistry. In "Porphyrins and metalloporphyrins" Vol. 2, pp. 3-29. Elsevier, Amsterdam.
- Fischer, J., Jandera, P., Cesla, P., and Stanek, V. (2003). Separation of aromatic sulphonic acids by CZE in coated and non-coated capillaries. *J. Sep. Sci.* **26**, 1035-1044.
- Fleischer, E. B., Chapman, R. D., and Krishnamurthy, M. (1979). Synthesis and oxidative demetalation of two new tungsten porphyrins. *Inorg. Chem.* **18**, 2156-2159.
- Fleischer, E. B., Palmer, J. M., Srivastava, T. S., and Chatterjee, A. (1971). Thermodynamic and kinetic properties of an iron-porphyrin system. *J. Am. Chem. Soc.* **93**, 3162-3167.
- Fonda, H. N., Gilbert, J. V., Cormier, R. A., Sprague, J. R., Kamioka, K., and Connolly, J. S. (1993). Spectroscopic, photophysical, and redox properties of some *meso*-substituted free-base porphyrins. *J. Phys. Chem.* **97**, 7024-7033.
- Gallaher, W. R., Ball, J. M., Garry, R. F., Martin-Amedee, A. M., and Montelaro, R. C. (1995). A general model for the surface glycoproteins of HIV and other retroviruses. *AIDS Res. Hum. Retroviruses* **11**, 191-202.
- Garcia-Campana, A. M., Gamiz-Gracia, L., Baeyens, W. R. G., and Barrero, F. A. (2003). Derivatization of biomolecules for chemiluminescent detection in capillary electrophoresis. *J. Chromatogr. B.* **793**, 49-74.

- George, R. G. and Padmanabhan, M. (2003). Studies on some new *meso*-aryl substituted octabromo-porphyrins and their Zn(II) derivatives. *Polyhedron* **22**, 3145-3154.
- Gibbs, E. J., Skowronek, W. R., Jr., Morgan, W. T., Muller-Eberhard, U., and Pasternack, R. F. (1980). Reactions of water-soluble metalloporphyrins with the serum protein, hemopexin. *J. Am. Chem. Soc.* **102**, 3939-3944.
- Gubitz, G. and Schmid, M. G. (1997). Chiral separation principles in capillary electrophoresis. Review. *J. Chromatogr. A* **792**, 179-225.
- Hamai, S. and Koshiyama, T. (1999). Electronic absorption, fluorescence, and circular dichroism spectroscopic studies on the inclusion complexes of tetrakis(4-sulfonatophenyl)porphyrin with cyclodextrins in basic aqueous solutions. *J. Photochem. Photobiol. A* **127**, 135-141.
- Hamai, S., Sasaki, Y., Hori, T., and Takahashi, A. (2006). Interactions of tetrakis(4-sulfonatophenyl)porphyrin with gamma-cyclodextrin and alkyltrimethylammonium bromides in aqueous solutions. *J. Incl. Phen. Mac. Chem.* **54**, 67-76.
- Hamai, S. and Satou, H. (2001). Effects of cyclodextrins on the complexation between Methylene Blue and tetrakis(4-sulfonatophenyl)porphyrin in aqueous solutions. *Spectrochim. Acta A Mol. Biomol. Spectrosc.* **57**, 1745-1750.
- Hambright, P. (2000). Chemistry of water soluble porphyrins. In "The Porphyrin Handbook" (K. M. Kadish, K. M. Smith, and R. Guilard, Eds.), Vol. 3, pp. 129-210. Academic Press, San Diego.
- Hanyz, I. and Wrobel, D. (2002). The influence of pH on charged porphyrins studied by fluorescence and photoacoustic spectroscopy. *Photochem. Photobiol. Sci.* **1**, 126-132.
- Harrison, P. F., Rosenberg, Z., and Bowcut, J. (2003). Topical microbicides for disease prevention: Status and challenges. *Clin. Infect. Dis.* **36**, 1290-1294.
- Herrmann, O., Mehdi, S. H., and Corsini, A. (1978). Heterogeneous metal-insertion: A novel reaction with porphyrins. *Can. J. Chem.* **56**, 1084-1087.
- Ion, R. M. (1999). Spectral analysis of the porphyrins incorporation into human blood. *J. Biomed. Optics* **4**, 319-326.
- Ion, R. M., Planner, A., Wiktorowicz, K., and Frackowiak, D. (1998). The incorporation of various porphyrins into blood cells measured via flow cytometry, absorption and emission spectroscopy. *Acta Biochim. Pol.* **45**, 833-845.
- Jimenez, H. R., Julve, M., and Faus, J. (1991). A solution study of the protonation and deprotonation equilibria of 5,10,15,20-tetra(*p*-sulphonatophenyl)porphyrin. Stability

constants of its magnesium(II), copper(II) and zinc(II) complexes. *J. Chem. Soc. Dalton Trans.* 1945-1949.

Kadish, K. M., Maiya, G. B., Araullo, C., and Guilard, R. (1989). Micellar effects on the aggregation of tetraanionic porphyrins. Spectroscopic characterization of free-base *meso*-tetrakis(4-sulfonatophenyl)porphyrin, (TPPS)H<sub>2</sub>, and (TPPS)M (M = Zn(II), Cu(II), VO<sub>2</sub><sup>+</sup>) in aqueous micellar media. *Inorg. Chem.* **28**, 2725-2731.

Kalny, D., Albrecht-Gary, A. M., and Havel, J. (2001). Highly sensitive method for palladium(II) determination as a porphyrinato complex by capillary zone electrophoresis. *Analytica Chimica Acta* **439**, 101-105.

Kalyanasundaram, K. and Neumann-Spallart, M. (1982). Photophysical and redox properties of water-soluble porphyrins in aqueous media. *J. Phys. Chem.* **86**, 5163-5169.

Kiyohara, C., Saito, K., and Suzuki, N. (1993). Micellar electrokinetic capillary chromatography of haematoporphyrin, protoporphyrin and their copper and zinc complexes. *J. Chromatogr.* **646**, 397-403.

Langley, R. and Hambright, P. (1985). Kinetics of the reduction of manganese(III) porphyrins by hexaammineruthenium(II): A reductive acid solvolysis mechanism. *Inorg. Chem.* **24**, 1267-1269.

Levere, R. D., Gong, Y.-F., Kappas, A., Bucher, D. J., Wormser, G. P., and Abraham, N. G. (1991). Heme inhibits human immunodeficiency virus 1 replication in cell cultures and enhances the antiviral effect of zidovudine. *Proc. Natl. Acad. Sci. USA* **88**, 1756-1759.

Li, Q., Chang, C. K., and Huie, C. W. (2005). Investigation of solvent effects in capillary electrophoresis for the separation of biological porphyrin methyl esters. *Electrophoresis.* **26**, 3349-3359.

Lim, C. K., Razzaque, M. A., Luo, J. L., and Farmer, P. B. (2000). Isolation and characterization of protoporphyrin glycoconjugates from rat Harderian gland by HPLC, capillary electrophoresis and HPLC/electrospray ionization MS. *Biochem. J.* **347**, 757-761.

Lindsey, J. S., Schreiman, I. C., Hsu, H. C., Kearney, P. C., and Marguerettaz, A. M. (1987). Rothmund and Adler-Longo reactions revisited: Synthesis of tetraphenylporphyrins under equilibrium conditions. *J. Org. Chem.* **52**, 827-836.

March, J. (1992). Reactivity. In "Advanced organic Chemistry: reactions, mechanisms and structures" (., Ed.), pp. 683-733. Wiley-Interscience, New York.

- Miller, J. R., Taies, J. A., and Silver, J. (1987). Mossbauer and spectroscopic studies on substituted tetraphenylporphyrinato iron(III) complexes in aqueous-solutions and the formation of the mu-oxo-bridged species. *Inorg. Chim. Acta* **138**, 205-214.
- Mosinger, J., Deumie, M., Lang, K., Kubát, P., and Wagnerová, D. M. (2000). Supramolecular sensitizer: Complexation of *meso*-tetrakis(4-sulfonatophenyl)porphyrin with 2-hydroxypropyl-cyclodextrins. *J. Photochem. Photobiol. A* **130**, 13-20.
- Neurath, A. R., Haberfield, P., Joshi, B., Hewlett, I. K., Strick, N., and Jiang, S. (1991). Rapid prescreening for antiviral agents against HIV-1 based on their inhibitory activity in site-directed immunoassays. I. The V3 loop of gp120 as target. *Antiviral Chem. Chemother.* **2**, 303-312.
- Neurath, A. R., Strick, N., and Debnath, A. K. (1995). Structural requirements for and consequences of an antiviral porphyrin binding to the V3 loop of the human immunodeficiency-virus (HIV-1) envelope glycoprotein gp120. *J. Mol. Recognition* **8**, 345-357.
- Neurath, A. R., Strick, N., Haberfield, P., and Jiang, S. (1992). Rapid prescreening for antiviral agents against HIV-1 based on their inhibitory activity in site-directed immunoassays. II. Porphyrins reacting with the V3 loop of gp120. *Antiviral Chem. Chemother.* **3**, 55-63.
- Neurath, A. R., Strick, N., and Jiang, S. (1994a). Rapid prescreening for antiviral agents against HIV-1 based on their inhibitory activity in site-directed immunoassays. Approaches applicable to epidemic HIV-1 strains. *Antiviral Chem. Chemother.* **4**, 207-214.
- Neurath, A. R., Strick, N., Lin, K., Debnath, A. K., and Jiang, S. (1994b). Tin protoporphyrin-IX used in control of heme metabolism in humans effectively inhibits HIV-1 infection. *Antiviral Chem. Chemother.* **5**, 322-330.
- Ohno, O., Kaizu, Y., and Kobayashi, H. (1993). *J*-aggregate formation of a water-soluble porphyrin in acidic aqueous media. *J. Chem. Phys.* **99**, 4128-4139.
- Pasternack, R. F. (1973). Aggregation properties of water-soluble porphyrins. *Ann. N. Y. Acad. Sci.* **206**, 614-627.
- Pauwels, R., Balzarini, J., Baba, M., Snoeck, R., Schols, D., Herdewijn, P., Desmyter, J., and De Clercq, E. (1988). Rapid and automated tetrazolium-based colorimetric assay for the detection of anti-HIV compounds. *J. Virol. Methods* **20**, 309-321.
- Peng, X., Sternberg, E., and Dolphin, D. (2002). Chiral separation of benzoporphyrin derivative mono- and diacids by laser induced fluorescence-capillary electrophoresis. *Electrophoresis* **23**, 93-101.

- Peng, X., Sternberg, E., and Dolphin, D. (2005). Separation of porphyrin-based photosensitizer isomers by laser-induced fluorescence capillary electrophoresis. *Electrophoresis* **26**, 3861-3868.
- Pico, G. A. and Houssier, C. (1989). Bile salts-bovine serum albumin binding: spectroscopic and thermodynamic studies. *Biochim. Biophys. Acta.* **999**, 128-134.
- Pokric, B., Allinson, N. M., Bergström, E. T., and Goodall, D. M. (1999). Dynamic analysis of capillary electrophoresis data using real-time neural networks. *J. Chromatogr. A* **833**, 231-244.
- Rao, T. A. and Maiya, B. G. (1994). Spectroscopic, redox and emission properties of 2-nitro-substituted free base- and metallo-tetra-aryl porphyrins. *Polyhedron* **13**, 1863-1873.
- Ribo, J. M., Crusats, J., Farrera, J. A., and Valero, M. L. (1994). Aggregation in Water Solutions of Tetrasodium Diprotonated Meso-Tetrakis(4-Sulfonatophenyl)Porphyrin. *J. Chem. Soc. Chem. Comm.* 681-682.
- Ribó, J. M., Farrera, J. A., Valero, M. L., and Virgili, A. (1995). Self-assembly of cyclodextrins with meso-tetrakis(4-sulfonatophenyl)porphyrin in aqueous solution. *Tetrahedron* **51**, 3705-3712.
- Richeter, S., Jeandon, C., Gisselbrecht, J. P., Graff, R., Ruppert, R., and Callot, H. J. (2004). Synthesis of new porphyrins with peripheral conjugated chelates and their use for the preparation of porphyrin dimers linked by metal ions. *Inorg. Chem.* **43**, 251-263.
- Richeter, S., Jeandon, C., Kyritsakas, N., Ruppert, R., and Callot, H. J. (2003). Preparation of six isomeric bis-acylporphyrins with chromophores reaching the near-infrared via intramolecular Friedel-Crafts reaction. *J. Org. Chem.* **68**, 9200-9208.
- Richeter, S., Jeandon, C., Ruppert, R., and Callot, H. J. (2001). Reactivity of oxonaphthoporphyrins. Efficient beta-functionalization of the porphyrin ring on reaction with nitrogen or carbon nucleophiles. *Tetrahedron Lett.* **42**, 2103-2106.
- Robert, J. M. and Spinks, C. D. (1997). Separation of metallated petroporphyrin models using micellar electrokinetic capillary chromatography. *J. Liq. Chromatogr. Relat. Techno.* **20**, 2979-2995.
- Rocha Gonsalves, A. M. D., Johnstone, R. A. W., Pereira, M. M., de SantAna, A. M. P., Serra, A. C., Sobral, A. J. F. N., and Stocks, P. A. (1996). New procedures for the synthesis and analysis of 5,10,15,20- tetrakis(sulphophenyl)porphyrins and derivatives through chlorosulphonation. *Heterocycles* **43**, 829-838.
- Rothmund, P. (1939). Porphyrin Studies. III. The Structure of the Porphine Ring System. *J. Am. Chem. Soc.* **61**, 2912-2915.

- Rubires, R., Crusats, J., El-Hachemi, Z., Jaramillo, T., Lopez, M., Valls, E., Farrera, J. A., and Ribó, J. M. (1999). Self-assembly in water of the sodium salts of *meso*-sulfonatophenyl substituted porphyrins. *New J. Chem.* **23**, 189-198.
- Sattentau, Q. J. and Moore, J. P. (1991). Conformational changes induced in the human immunodeficiency virus envelope glycoprotein by soluble CD4 binding. *J. Exp. Med.* **174**, 407-415.
- Silver, J. and Taies, J. A. (1988). Moessbauer spectroscopic studies of tetrasulfonaphthylporphine iron(II) solutions. *Inorg. Chim. Acta* **151**, 69-75.
- So, T. S. K., Jia, L., and Huie, C. W. (2001). Stacking and separation of coproporphyrin isomers by acetonitrile-salt mixtures in micellar electrokinetic chromatography. *Electrophoresis* **22**, 2159-2166.
- Song, R., Witvrouw, M., Schols, D., Robert, A., Balzarini, J., De Clercq, E., Bernadou, J., and Meunier, B. (1997). Anti-HIV activities of anionic metalloporphyrins and related compounds. *Antiviral Chem. Chemother.* **8**, 85-97.
- Stone, A. (2002). Microbicides: A new approach to preventing HIV and other sexually transmitted infections. *Nat. Rev. Drug Discov.* **1**, 977-985.
- Sutter, T. P. G., Rahimi, R., Hambricht, P., Bommer, J. C., Kumar, M., and Neta, P. (1993). Steric and inductive effect on the basicity of porphyrins and on the site of protonation of porphyrin dianions. *J. Chem. Soc. Faraday Trans.* **89**, 495-502.
- Treibs, A. and Haerberle, N. (1968). Über die synthese und die electronenspektren *ms*-substituierter porphine. *Justus Liebigs Ann. Chem.* 183-207.
- Trujillo, J. R., Goletiani, N. V., Bosch, I., Kendrick, C., Rogers, R. A., Trujillo, E. B., Essex, M., and Brain, J. D. (2000). T-tropic sequence of the V3 loop is critical for HIV-1 infection of CXCR4-positive colonic HT-29 epithelial cells. *J. Acquir. Immune Defic. Syndr.* **25**, 1-10.
- Turpin, J. A. (2002). Considerations and development of topical microbicides to inhibit the sexual transmission of HIV. *Expert Opin. Investig. Drugs* **11**, 1077-1097.
- Venema, F., Nelissen, H. F. M., Berthault, P., Birlirakis, N., Rowan, A. E., Feiters, M. C., and Nolte, R. J. M. (1998). Synthesis, conformation, and binding properties of cyclodextrin homo- and heterodimers connected through their secondary sides. *Chem. Eur. J.* **4**, 2237-2250.
- Vzorov, A. N., Dixon, D. W., Trommel, J. S., Marzilli, L. G., and Compans, R. W. (2002). Inactivation of human immunodeficiency virus type 1 by porphyrins. *Antimicrob. Agents Chemother.* **46**, 3917-3925.

- Vzorov, A. N., Marzilli, L. G., Compans, R. W., and Dixon, D. W. (2003). Prevention of HIV-1 infection by phthalocyanines. *Antiviral Res.* **59**, 99-109.
- Wang, X. P., Pan, J. H., and Shuang, S. M. (2001). Study on the supramolecular system of *meso*-tetrakis(4-sulfonatophenyl) porphyrin and cyclodextrins by spectroscopy. *Spectrochim. Acta A Mol. Biomol. Spectrosc.* **57**, 2755-2762.
- Wang, X. P., Pan, J. H., Shuang, S. M., and Zhang, Y. (2002). Determination of the inclusion constants for the inclusion complexes between *meso*-tetrakis(4-sulfonatophenyl) porphyrin and cyclodextrins by three methods. *Supramol. Chem.* **14**, 419-426.
- Weinberger, R., Sapp, E., and Moring, S. (1990). Capillary electrophoresis of urinary porphyrins with absorbance and fluorescence detection. *J. Chromatogr.* **516**, 271-285.
- Wu, N., Li, B., and Sweedler, J. V. (1994). Recent developments in porphyrin separations using capillary electrophoresis with native fluorescence detection. *J. Liq. Chromatogr.* **17**, 1917-1927.
- Zaider, E. and Bickers, D. R. (1998). Clinical laboratory methods for diagnosis of the porphyrias. *Clin. Dermatol.* **16**, 277-293.
- Zerbinati, O. and Trotta, F. (2003). pH-dependent cyclodextrin capillary electrophoresis resolution of atropisomers. *Electrophoresis* **24**, 2456-2461.
- Zhang, Y., Gong, Z. L., Zhang, H., and Cheng, J. K. (1998). An improved apparatus for on-line chemiluminescence detection with capillary electrophoresis and detection of metal-porphyrins. *Analytical Communications* **35**, 293-296.
- Zhang, Y. H., Chen, D. M., He, T., and Liu, F. C. (2003). Raman and infrared spectral study of *meso*-sulfonatophenyl substituted porphyrins (TPPS<sub>n</sub>, n = 1, 2A, 2O, 3, 4). *Spectrochim. Acta A Mol. Biomol. Spectrosc.* **59**, 87-101.

## Chapter 3

### Irradiation of Cationic Metalloporphyrins Bound to DNA

Radiation is widely used in cancer chemotherapy. It is desirable to reduce damage beyond the tumor cells. One way of doing so is to use brachytherapy seeds, small radioactive seeds which are implanted in the tumors and increasingly used for localized irradiation of tumors (Rivard et al., 2004; Murphy et al., 2004; Williamson et al., 2005). If the tumor could be sensitized to radiation, this would also be helpful. It has been proposed that sensitization might be achieved with photon activation therapy (PAT) (Fairchild et al., 1982b). PAT involves irradiating a high  $Z$  atom near the cellular DNA. The high  $Z$  atom first absorbs a photon, and then releases a number of low energy Auger or Koster-Kronig electrons (Tisljar-Lentulis et al., 1973). This is expected to induce localized or clustered damage in the DNA. Clustered DNA damage may inhibit the cellular repair processes and slow tumor growth.

We have studied a series of metals as PAT candidates. The metals were chosen on the basis that they have appropriate energy levels for irradiation by brachytherapy seeds, which commonly include  $^{103}\text{Pd}$  (21 keV),  $^{125}\text{I}$  (28 keV) and  $^{131}\text{Cs}$  (29.5 - 36.5 keV). **Table 3.1** shows the energy levels of the metals chosen, which include silver, indium, molybdenum, palladium, platinum, ruthenium and zirconium. To allow direct comparison of these metals, the cationic porphyrin, *meso*-tetrakis(4-*N*-methyl-pyridinium) porphyrin (TMPyP4) was chosen as the scaffolding to carry the metal to the DNA. To assess the role of the porphyrin skeleton in determining DNA binding, five indium porphyrins,

alkylated derivatives of tetrapyrrolyl porphyrin with methyl, ethyl, propyl, butyl and benzyl side chains, were investigated. Plasmid cleavage assays were run to evaluate the potential of these molecules to create clustered DNA damage on irradiation. Upon irradiation, the amount of nicked plasmid DNA (OC) increased smoothly as a function of the irradiation time; a small amount of linear (L) form of the DNA was also observed. Section II of this chapter describes the experimental details and results.

## **Section I.**

### **Introduction.**

#### **i. Auger electrons**

##### **a. Background.**

When a heavy metal is irradiated with an x-ray of a suitable energy, a core electron can be ejected (Kassis, 2003; Kassis, 2004). The cascade of external shell electrons towards the core vacancy releases both energy and electrons. The range of Auger electrons in water is from a fraction of a nanometer to several hundreds of micrometers (Kassis, 2004). Auger electrons have high LET (the average amount of energy lost per unit of distance traveled) due to their slow speed, i.e.,  $\sim 26 \text{ keV}/\mu\text{m}$  at low energies of 35 - 55 eV (Cole, 1969). The dimensions of the mammalian DNA and proteins responsible for the biological functions are all within the range of these high-LET Auger electrons, i.e.,  $8 - 26 \text{ keV}/\mu\text{m}$ , low-energy ( $\leq 1.6 \text{ keV}$ ), short range ( $\leq 130 \text{ nm}$ ) electrons (Kassis, 2004).

**b. Auger electrons in radiobiology.**

Fairchild et al., in the early 1980's, proposed Photon Activation Therapy (PAT) (Fairchild et al., 1982a). Their goal was to increase the radiation dose for malignant tumors by incorporating stable IdUrD into DNA and inducing Auger electron emission via external irradiation. They demonstrated an enhancement of radiation dose to using iododeoxyuridine (IdUrD) and bromodeoxyuridine (BrdUrd), and comparing the effects of irradiating above the iodine K edge and below the iodine K edge (Laster et al., 1993).

**c. The damage caused by radionuclides.**

The biological effects could be due in part to the high positive charge of the resulting atom leading to the neutralization and deposition of highly localized energy around the decay site. The damage could be the result of radiation-induced ionizations and excitations, nuclear recoil, chemical transmutations and local charge effects (Frankenberg-Schwager, 1990). Double-stranded DNA breakage (dsb) can be one of the usual consequences of the production of Auger electrons from radioactive metals (Hafliger et al., 2005). The dsb yield is 50- to 100-fold lower than that of the single strand breaks in DNA (ssb) yield for low-LET radiation (Stanton et al., 1993).

Kassis has pointed out that the deleterious effects of low-energy electron emitters in mammalian cells is not solely due to direct ionization of DNA, but caused mainly (~90%) by indirect mechanism(s) (Kassis, 2004). Hydroxyl radicals play a significant role (Chatgililoglu & O'Neill, 2001). Even in the presence of high concentrations of scavengers, it is difficult to estimate the DNA damage due to the direct effect of Auger electrons (Yokoya et al., 2002). Along with the hydroxyl radical, sugar radicals, formed

by ionization of DNA are thought to cause strand breakage (Debije et al., 2001). The nucleobases are also effected by the overall damage leading to damage of DNA (Swarts et al., 1992; Swarts et al., 1996). Along with the oxidation of the DNA bases, and ssb and dsb of the phosphate backbone, DNA damage can also occur by cross-linking with proteins.

## **ii. Metals used in PAT.**

Maeda et al. studied the dsb via photoabsorption at K-shell of phosphorus and L<sub>III</sub>-shell of platinum (Maeda et al., 2004). They irradiated free and platinum-bound pBR322 plasmid DNA using synchrotron radiation, monochromatic X-rays, with energies above and below the phosphorus K- and platinum L<sub>III</sub>-shell. It was reported that the inner-shell photoabsorption of phosphorus and platinum significantly increased the induction of dsb but not the ssb induction. Since the quantum yield for the dsb induction of platinum was significantly larger than that for the phosphorus, Maeda et al. proposed that magnitude of the Auger cascade does affect the dsb.

## **Section II.**

The goal of this work was to survey metals that might be considered as possible PAT candidates in conjunction with brachytherapy seeds. Given the available energies, there are a number of metals that might be considered. Herein are reported the studies of Ag<sup>II</sup>, In<sup>II</sup>, Mo<sup>V</sup>, Pd<sup>II</sup>, Pt<sup>II</sup>, Ru<sup>II</sup> and Zr<sup>IV</sup>. DNA damage was assessed by a nicking plasmid assay. Clustered damage in the DNA was indicated by double stranded cleavage of the plasmid, resulting in a linearized form. If the radiation damage leads to a ssb in the

phosphate backbone, an open circular form of the plasmid results. If the two breaks in the phosphate backbone occur within about a turn of the DNA helix, the plasmid linearizes.

It is important that the high Z nuclei be positioned close to the DNA. We have chosen the cationic porphyrin TMPyP4 as the metal carrier. A porphyrin scaffold is a good choice for studying the effect of various metals in the porphyrin core, because the binding of the metalloporphyrin to the DNA is primarily determined by the four cationic charges on the periphery of the metal. Many of the details of these interactions have been elucidated, particularly of TMPyP4 derivatives (Marzilli, 1990; Pasternack & Gibbs, 1996). A second advantage of using a cationic porphyrin as a scaffold is that it can localize in cancer cells; in particular, studies with  $^{111}\text{InTMPyP4}$  have shown that this compound is taken up somewhat selectively in tumors (Foster et al., 1985; Maric et al., 1988). Cationic porphyrins have been shown to bind to chromosomal DNA (Izbicka et al., 1999). Porphyrin localize subcellularly not only in the chromosomal DNA, but in many structures, such as the cell membrane, nucleus, mitochondria and lysosomes (Woodburn et al., 1991; Georgiou et al., 1994; Tobin & Greene, 1999; Kessel & Poretz, 2000; Kessel et al., 2003; Ricchelli et al., 2005).

## **ii. Experiments.**

### **a. Materials and method.**

The plasmid (pUC19) DNA was purchased from Bayou Biolabs (Harahan, LA) and was used without further purification. Plasmid (pUC19) DNA was also synthesized in the lab with Ms. Beth Wilson's assistance. Transformation of *Escherichia coli*

competent cells (Stratagene, XL-1 blue) with pUC19 plasmid DNA (Sigma) and growth of bacterial cultures in Luria-Bertani broth were performed using standard laboratory protocols (Sambrook et al., 1989). The plasmid DNA was purified with a Qiagen Plasmid Mega Kit. Ethidium bromide (EtBr) and the gel electrophoresis buffers, TAE (Tris-Acetate-EDTA) and TBE (Tris-Borate-EDTA), Tris base, glacial acetic acid, glycerol, monobasic and dibasic sodium phosphate, and EDTA disodium salt were purchased from Fischer Scientific (Fair Lawn, NJ). Metalloporphyrins used included the Ag, In, Mo, Pd, Pt, Ru and Zr chelates of TMPyP4. The alkyl derivatives of InTPyP4 were purchased from Mid-Century Chemicals (Posen, IL) and the rest of the metalloderivatives were purchased from Frontier Scientific Inc. (Logan, UT). Purity was established by CE (< 5% of another porphyrin).

Thermal melting ( $T_m$ ) studies of the 10 mer duplex 5'- GCGAATTCGC-3' (Midland Certified Reagent Company, Inc., Midland, Texas) in the presence of alkyl derivatives of InTPyP4 were conducted on a CARY 3E spectrophotometer (Varian, Palo Alto, CA) attached to a temperature controller. Experiments were performed in a 20 mM phosphate buffer (pH 7.0) containing 100 mM NaCl. The working concentration was 18  $\mu$ M, determined using the extinction coefficient  $1.872 \times 10^5 \text{ M}^{-1} \text{ cm}^{-1}$  (Fasman, 1975).

CE separations were performed with a 50 mM phosphate buffer (pH 3.0). Separations were conducted at normal polarity and the injection size was 6 s. A 11 kV voltage was used for separation. The detailed CE setup is discussed in section IV of Chapter 1. To check the stability of porphyrin solutions, UV-vis spectra were taken in

water and in 50 mM phosphate buffer at pH 3.2 and 8.0. The spectra were recorded on Shimadzu UV-1601 spectrophotometer (Columbia, MD).

The irradiation of samples was performed by Dr. Tomasz Wasowicz in the laboratory of Dr. William H. Nelson (Department of Physics and Astronomy at Georgia State University). The irradiation buffer used was 10 mM phosphate at pH 7.0 with 2 mM glycerol. The samples were irradiated using a Philips PW 2182/00 X-ray tube connected to a Philips MCG 40 power supply with 50 kV voltage and 20 mA current settings resulting in a 0.67 Gy/s dose rate as measured at the centerpoint of the sample. The Dose-rate was calibrated using two independent methods: alanine EPR dosimeters and a Victoreen 550-6A ionization chamber at 250 V with Keithley 487 picoammeter/voltage source (Bradshaw et al., 1962; Nette et al., 1993). The samples were placed for irradiation at room temperature in a Janis SVT-300 cryostat. The x-ray beam was 80 mm in length passing through one 0.3 mm Be window and two Al windows, each 0.3 mm thick. Irradiation was performed with X-rays from a tungsten-target tube operating from a constant-potential supply. The plasmids were irradiated in Eppendorf tubes at room temperature. Reactions were terminated by chilling on ice, where they remained until they were loaded on an agarose gel.

The stock plasmid (pUC19) DNA was 1.00  $\mu\text{g}/\mu\text{l}$ . The irradiated plasmid samples were 20  $\mu\text{M}$  bp unless indicated otherwise. Reactions were conducted in a 10 mM phosphate buffer at pH 7.0 with 2 mM glycerol. The scavenging capacity of 2 mM glycerol is about  $3.8 \times 10^6 \text{ s}^{-1}$  (Klimczak et al., 1993). The irradiation dose was 40 Gy/min (0.667 Gy/s). The control and the irradiated samples were loaded on a 1.5%

agarose gel with 0.5  $\mu\text{g/ml}$  EtBr. Electrophoresis was carried out for 1.5 h in 1 X TAE buffer (40 mM Tris base, 20 mM acetic acid, 1 mM EDTA, pH 8.0; the loading dye contained 0.25% bromophenol blue-15% Ficoll) or TBE buffer (89 mM Tris-borate, 2 mM EDTA, pH 8.0; the loading dye contained 3X TBE buffer, 60% glycerol, 0.6% SDS, 0.06% bromophenol blue).

Gel images were quantified with a Biospectrum AC Imaging System (UVP, Upland, CA). The background was calculated as the average background above and below each DNA band. The amount of SC form of plasmid DNA was corrected by a factor of 1.4 for the less-efficient incorporation of EtBr (Milligan et al., 1993). The relative amounts of the three DNA forms (OC, L and SC) were calculated for each irradiation dose. The average number of nicks (cleavage) per plasmid was calculated using the Poisson distribution (Hertzberg & Dervan, 1982).

The concentration of the porphyrin solutions was determined via UV-vis spectroscopy. The extinction coefficients ( $\epsilon$ ) used for determining the concentrations were:  $2.33 \times 10^5 \text{ M}^{-1}\text{cm}^{-1}$  in water for Ag(II)TMPyP4 at 430 nm (Harriman et al., 1983),  $7.40 \times 10^4 \text{ M}^{-1}\text{cm}^{-1}$  in water for Mo(V)TMPyP4 at 469 nm (Masahiko et al., 1985),  $1.71 \times 10^5 \text{ M}^{-1}\text{cm}^{-1}$  in water for Pd(II)TMPyP4 at 414 nm (Harriman et al., 1983),  $1.72 \times 10^5 \text{ M}^{-1}\text{cm}^{-1}$  in water for Pt(II)TMPyP4 at 402 nm (Pasternack et al., 1990),  $1.47 \times 10^5 \text{ M}^{-1}\text{cm}^{-1}$  in water for RuTMPyP4 at 420 nm (Hartmann et al., 1997),  $3.90 \times 10^5 \text{ M}^{-1}\text{cm}^{-1}$  in nitric acid (pH 2.0) for InTMPyP4 (and assumed for InTBzPyP4) at 424 nm (Hambright et al., 1985), and assumed as  $2.0 \times 10^5 \text{ M}^{-1}\text{cm}^{-1}$  in water for ZrTMPyP4 at 419 nm. The spectra

were taken in the specified solvents and in water. The concentration in water was determined from the known extinction coefficients in the respective solvents.

## **b. Results and discussion.**

### **1. Hydrophobicity.**

XlogP values of the methyl, ethyl, propyl, butyl, and benzyl derivatives of pyridine were calculated using PCModel 9 (Serena Software, Bloomington, IN). The XlogP values were in direct proportion to migration times of CE peaks of these homologous derivatives (**Table 3.2**).

### **2. Thermal melting studies.**

The working concentration of the duplex was 18  $\mu\text{M}$ , with a drug:duplex ratio of 0.1.  $T_m$  melting profiles were obtained by measuring the absorbance at 260 nm as a function of temperature (5 - 95  $^{\circ}\text{C}$ ) at a ramp rate of 0.5  $^{\circ}\text{C}/\text{min}$ . The duplex had a  $T_m$  of 46.9  $^{\circ}\text{C}$ . The  $T_m$  of the methyl, ethyl, propyl, butyl and benzyl derivatives of InTPyP4 was very similar, i.e.,  $59.0 \pm 1$   $^{\circ}\text{C}$  (**Figure 3.1**).

### **3. Capillary electrophoresis separation of porphyrins.**

The most effective method of characterization of cationic porphyrins is by CE (Dixon et al., 1998). The organic impurities can be due to the presence of other porphyrins (often not fully alkylated). The separations were performed at low pH, 3.0 with a 50 mM sodium phosphate running buffer. Each compound was pure as shown by a single peak (data not shown). The CE peaks for the Ag, Mo, Pd, Ru and Zr chelates of

TMPyP4 appeared at 9.5 min (421 nm), 10.9 min (403 nm), 12.3 min (467 nm), 11.2 min (416 nm), 12.0 min (415 nm), and 11.6 min (419 nm), respectively (data not shown).

**Figure 3.2** shows the separation of five alkyl derivatives of InTRPyP4, methyl, ethyl, propyl and butyl and benzyl derivatives. The separation was due to the difference in molecular weight of the alkyl side chains. The peaks for methyl, ethyl, propyl, benzyl and benzyl derivatives appeared at 12.4, 13.3, 14.2, 14.9 and 15.0 min, respectively.

#### **4. UV-vis spectra of cationic porphyrins.**

For most metalloderivatives of TMPyP4 there was no difference in spectra in the three solvents, water and in low (3.2) and high pH (8.1) buffers. **Figure 3.3** shows the spectra of Mo, and Zr chelates of TMPyP4 in the three solvents. MoTMPyP4 had a  $\lambda_{\max}$  of 458 nm as reported by Masahiko et al. (Masahiko et al., 1985). However, the spectrum was blue-shifted at high pH and red-shifted at low pH. This could be due to various ligation patterns of Mo in different solvents.

#### **5. Control experiments.**

Experiments were conducted to evaluate the effect of the following parameters on the quantification of plasmid DNA cleavage via gel electrophoretic assay: gel electrophoresis buffer, concentration of glycerol ( $\cdot$ OH radical scavenger) in the irradiation buffer, irradiation time, ratio of the plasmid to porphyrin for irradiation study, agarose gel composition, use of SDS to prevent fluorescence quenching of EtBr by porphyrin, determination of abasic sites on the plasmid DNA prior to irradiation and the freeze-thaw effects on the plasmid DNA.

### **5.1. Electrophoresis buffer.**

Various gel electrophoresis buffers have been used for the plasmid DNA damage quantification, irrespective of the type of photosensitizer and the irradiation source. Some of the common buffers used are TAE (Barry et al., 2002; Hergueta-Bravo et al., 2002; Yang et al., 2004; Jin & Cowan, 2005; Sissi et al., 2005), TBE (Benimetskaya et al., 1998; Benimetskaya et al., 1998; Leloup et al., 2005b) and Tris-borate (Anzai et al., 2006). Both TAE and TBE were used for the DNA damage quantification. No significant difference in the DNA damage assay was observed between the two buffer systems. The study was then carried out with TAE buffer.

### **5.2. Addition of scavengers.**

DNA damage results from both direct (effect of the x-rays themselves) and indirect (resulting from  $\cdot\text{OH}$  radicals produced by the radiolysis of water surrounding the DNA) effects (Blok & Loman, 1973). A variety of  $\cdot\text{OH}$  radical scavengers has been in radiation studies of plasmid DNA. The scavenging capacities of these scavengers at various concentrations have been reported (Klimczak et al., 1993). The most common  $\text{OH}$  radical scavengers are DMSO (Povirk et al., 1977; Wolf et al., 1993; Yamakawa et al., 2001; Laine et al., 2004; Lobachevsky et al., 2004; Maeda et al., 2004) and glycerol (Klimczak et al., 1993; Blaisdell et al., 2001; Laine et al., 2004; Leloup et al., 2005a). Other scavengers include methanol (Klimczak et al., 1993; Laine et al., 2004), Tris (Klimczak et al., 1993; Gulston et al., 2002), sodium formate (Milligan et al., 2000), sodium azide (Jia et al., 2006) and sodium thiosulfate (Banfi et al., 2003). In this study, the effect of 2 and 200 mM glycerol and 200 mM Tris buffer on DNA damage were

evaluated (Section II). The latter two conditions were chosen to mimic the interior of the cell (Leloup et al., 2005c). The cleavage patterns with the two scavengers were very similar to that observed without scavengers. However, ten times more irradiation time was needed with 200 mM glycerol or with 200 mM Tris buffer than with 2 mM glycerol as scavenger in the irradiation buffer, to give the same extent of cleavage. To minimize irradiation time, thus it was decided to perform the study with 2 mM glycerol.

### **5.3. Irradiation time.**

DNA damage by ssb increases linearly with radiation dose (Freifelder & Trumbo, 1969; Bopp & Hagen, 1970; Siddiqi & Bothe, 1987; Krisch et al., 1991; Klimczak et al., 1993). In this study a mixture of plasmid and buffer alone (no porphyrin) was irradiated up to 1000 s (**Figure 3.4**). After ~ 300 s significant fragmentation of plasmid was observed. Therefore, to avoid significant double stranded cleavage from the irradiation alone, the maximum irradiation time for the rest of the study was 100 - 150 s.

### **5.4. Gel concentration.**

Depending on the size of the DNA, the agarose gel concentration was adjusted for the best separation of the three forms of the plasmid DNA, OC, L and SC. In our hands, a significant effect of the concentration of the agarose was observed. Higher concentrations of agarose (1.5% and 2%) gave a better separation of the bands than lower concentrations (1%). The study was performed at a 1.5% agarose concentration.

### **5.5. Porphyrin:plasmid ratio.**

A control experiment was conducted to determine the appropriate porphyrin:plasmid ratio (R) to be used for the study. In the first part of the experiment,

using 10  $\mu\text{M}$  plasmid, working with lower concentrations of ZrTMPyP4 (0.1, 0.5, 1.0, 3.0 and 5.0  $\mu\text{M}$ ), with 4 s irradiation, significant shifting of the bands was observed (**Figure 3.5**). However, at concentrations higher than 1  $\mu\text{M}$  of ZrTMPyP4, band dimming was also observed. At 5  $\mu\text{M}$  concentration of ZrTMPyP4 bands were significantly dimmed and shifted.

In the second part of the experiment, the effect of much higher concentrations of both ZrTMPyP4 and MoTMPyP4 were studied (data not shown). The mixtures contained 10  $\mu\text{M}$  plasmid and varying concentration of the porphyrin (ZrTMPyP4 or MoTMPyP4; 1, 5, 10, 50, 1.0, and 100  $\mu\text{M}$ ). For both ZrTMPyP4 and MoTMPyP4, with 4 s irradiation, band shifting as well as band dimming was observed in the gel assay. At 1  $\mu\text{M}$  concentration of the both porphyrins, about 50% SC and OC forms were observed. In case of ZrTMPyP4, no DNA bands were seen at 50 and 100  $\mu\text{M}$  concentration of the porphyrin. Hence it was concluded that the most appropriate R value was 0.05, i.e., 1  $\mu\text{M}$  porphyrin and 20  $\mu\text{M}$  plasmid.

### **5.6. Band “dimming.”**

As pointed out above, the DNA bands in the presence of higher concentrations of metalloporphyrin were sometimes dim (**Figure 3.5**). This might be due to the tight binding of the metalloporphyrin, and hence the inability of the EtBr to completely displace the metalloporphyrin in the gel. Alternatively, in the case of diamagnetic porphyrins, it might partly be due to the fluorescence quenching of the porphyrin by the EtBr as has been shown previously (Pasternack et al., 1991). The absorption and emission of EtBr overlaps the absorption region of regular porphyrins (390 - 500 nm).

The  $\lambda_{\max}$  for absorption of EtBr is 480 nm and that for emission is  $\sim 620$  nm (Patel & Canuel, 1976). SDS (up to 2%) was added to the loading dye of the gel assays to try to remove the porphyrin from the DNA and sequester it so that it would not quench the EtBr. However, it was observed that the presence of SDS did not enhance EtBr fluorescence. On the contrary, in some cases the bands were dimmer in the presence of SDS; reasons for which are not known to us at this point. We therefore quantitated the effect of the dimming of the bands, and performed the appropriate corrections (data taken by Ms. Dijana Piljak and given in her reports).

### **5.7. Abasic sites in the DNA.**

Control experiments were conducted to determine presence of abasic sites (apurinic or apyrimidinic, AP-sites) on the plasmid to be irradiated. Formation of abasic sites on the DNA is the most common form of DNA lesions in mammalian cells (Lhomme et al., 1999). The abasic sites are formed when the *N*-glycosidic bond that exists between a nucleic acid base and the deoxyribose sugar moiety is cleaved, creating a “baseless” site (Sugiyama et al., 1994). The abasic sites on the plasmid can cause significant background cleavage in nonirradiated DNA (Steullet et al., 1999). The presence of abasic sites on the plasmid was checked by the addition of variable amounts of amine (3,3'-diamino-*N*-methyldipropylamine), which had been shown previously by our group to be a very effective cleaver of abasic sites (Steullet et al., 1999; McKnight et al., 2002).

As part of this study to determine the presence of abasic sites, in the first part of this experiment, 20  $\mu$ M plasmid was incubated at 37°C for 30 min with 50, 150, 250, 350

and 400  $\mu\text{M}$  amine. The SC form decreased and the OC form increased by 15% in the presence of 50  $\mu\text{M}$  amine. As the concentration of the amine increased, the OC and SC forms remained the same within experimental error. In a second experiment, 20  $\mu\text{M}$  plasmid was incubated at 37  $^{\circ}\text{C}$  with 300  $\mu\text{M}$  amine for variable incubation times (0 - 120 min). The SC form decreased and OC form increased by 14% when incubated for 10 min. Increasing the incubation time did not seem to increase the OC form or decrease the SC form. These two experiments indicated that there were no significant abasic sites on the plasmid (pUC19) DNA that was used for this study.

#### **5.8. Freeze-thaw cycles.**

In some experiments, particularly in time course experiments, reaction mixtures were frozen for a time before the gel electrophoresis was performed. An experiment was conducted to determine if the process of freezing and thawing of the reaction mixtures prior to irradiation induced any DNA damage. A sample was prepared with 20  $\mu\text{M}$  bp plasmid and 1  $\mu\text{M}$  InTBzPyP4 in the irradiation buffer. The reaction mixture was stored at -80  $^{\circ}\text{C}$ . Aliquots were taken from this reaction mixture every hour for five hours, after thawing the frozen reaction mixture. The aliquots were then stored at 4  $^{\circ}\text{C}$ . It was observed that the extent of OC form did not change significantly even when the reaction mixture was thawed after 5 h of incubation at -80  $^{\circ}\text{C}$ . The change in OC form was from 20 to 24% from 0 to 5 h after incubation at -80  $^{\circ}\text{C}$ .

After conducting the control experiments and optimizing the experimental parameters, it was decided that the working plasmid concentration would be 20  $\mu\text{M}$  bp and that of porphyrin would be 1  $\mu\text{M}$ . The porphyrin solutions were made in 100  $\mu\text{M}$

EDTA to prevent the interference of any free metal in the porphyrin solution. The final irradiation mixture contained 20  $\mu\text{M}$  bp plasmid (pUC19) DNA, 1  $\mu\text{M}$  porphyrin in 10 mM phosphate (pH 7.0) with 2 mM glycerol. Multiple irradiation times were chosen, from 5 - 150 s.

## **6. Control experiments with InTBzPyP4.**

As outlined in the introduction, studies with  $^{111}\text{InTMPyP4}$  have shown that this compound is taken up somewhat selectively in tumors (Foster et al., 1985; Maric et al., 1988). An indium cationic porphyrin has also been shown to bind to chromosomal DNA in whole cells (Izbicka et al., 1999). Initially, therefore, indium chelates seemed excellent candidates for PAT. Studies in Dr. Brenda Laster's laboratory (unpublished) showed that the benzyl derivative was taken up into the trichloroacetic acid insoluble fraction (DNA and high molecular weight proteins) of cells the most effectively of any of the derivatives studied (including also Me, Et, Pr, and Bu). Therefore a number of studies were performed on InTBzPyP4, with a particular focus of understanding how the benzyl group might affect the DNA binding, so that this understanding could be applied in the future to other benzyl metalloporphyrin derivatives.

### **6.1. Cleavage of plasmid DNA with increased contact time with porphyrin followed by irradiation.**

An experiment was conducted using the reaction mixture of 20  $\mu\text{M}$  bp plasmid, 1  $\mu\text{M}$  InTBzPyP4 in the irradiation buffer (10 mM phosphate, pH 7.0 with 2 mM glycerol). The reaction mixture was irradiated soon after preparation for variable irradiation times, 0 - 150 s. In the first part of this experiment, an old batch of plasmid DNA, which was

already 33% OC, was used. Upon contact InTBzPyP4, prior to irradiation, the OC content increased to 66% ssb.

In the second part of this experiment a relatively newer batch of plasmid was used with only 19% OC form originally. With this batch of plasmid the OC form did not increase in the absence of irradiation. However, upon irradiation up to 100 s, the OC increased from 19% to 72% upon irradiation for 100 s. Thus, it was apparent that InTBzPyP4 was somehow able to cleave the phosphate backbone in plasmid that had already sustained some type of damage.

In the second experiment in this series, a reaction mixture (20  $\mu$ M bp plasmid, 1  $\mu$ M porphyrin in the irradiation buffer) was irradiated (up to 100 s) after 24 h incubation at 4 °C. It was observed that the OC form changed from 19% to 72% when irradiated up to 100 s. However, the same effect was seen with reaction mixtures which were prepared just before irradiation. Thus, storage of a plasmid (pUC19) DNA in the presence of porphyrin at 4 °C for a shorter time (e.g., 24 h) did not result in plasmid damage. In the absence of irradiation, the porphyrin alone did not seem to increase ssb or dsb, at least after a 24 h period.

In the third experiment in this series, the reaction mixture (20  $\mu$ M bp plasmid, 1  $\mu$ M porphyrin in the irradiation buffer) was irradiated (up to 100 s) after two weeks of incubation at -20 °C. It was observed that prior to irradiation, the OC form had changed from 19% to 41%. Therefore, contact with the porphyrin for extended periods of time, even in a frozen solution, results in significant ssb. Upon irradiation after two weeks of incubation, the plasmid had 70% OC when irradiated for 100 s.

**6.2. Cleavage of plasmid DNA due to presence of abasic sites on the plasmid due to prolonged contact time with InTBzPyP4 (30 days); checked by addition of variable amounts of amine (3,3'-diamino-N-methyldipropylamine); no irradiation.**

The reaction mixture (20  $\mu\text{M}$  bp plasmid, 1  $\mu\text{M}$  porphyrin in the irradiation buffer) was incubated for 30 days at  $-20\text{ }^{\circ}\text{C}$ . After the incubation period, the presence of abasic sites on plasmid DNA was checked by the addition of 0 - 5000  $\mu\text{M}$  3,3'-diamino-N-methyldipropylamine. The reaction mixture containing the triamine was then incubated for 30 min at  $37\text{ }^{\circ}\text{C}$ ; all samples were prepared and stored on ice. An increased fraction of OC in the presence of the triamine indicated that abasic sites had been created on the DNA by the porphyrin, even in frozen solution (**Figure 3.6**). It was observed that the OC/SC of the plasmid before incubation with the porphyrin for 30 days was 24/76 with no linear form. Incubation alone, with the porphyrin, changed the OC and SC to 53% and 46% with  $\sim 1\%$  linear form. Subsequent addition of the amine further increased the OC and SC to 77% and 19% with 4% linear for 50  $\mu\text{M}$  amine. With 5000  $\mu\text{M}$  the OC and SC were 83% and 8% with  $\sim 10\%$  linear form.

**6.3. Cleavage of plasmid DNA due to incubation time (0 - 120 min;  $37\text{ }^{\circ}\text{C}$ ; no irradiation).**

Additional experiments were performed to evaluate DNA damage induced by InTBzPyP4 prior to irradiation. A series of reaction mixtures (20  $\mu\text{M}$  bp plasmid, 1  $\mu\text{M}$  porphyrin in the irradiation buffer) were incubated for 0 - 120 min at  $37\text{ }^{\circ}\text{C}$ ; all samples were prepared and stored on ice. It was concluded that incubation of plasmid DNA with 1  $\mu\text{M}$  InTBzPyP4 up to 120 min did not show significant increase in cleavage. This

indicated that relatively long incubation times of the DNA with the porphyrin was needed for the induction of significant ssb.

Overall, it was concluded that InTBzPyP4 could induce DNA damage, at least partly due to the formation of abasic sites, upon prolonged storage in frozen solution. The mechanism of the process is not known to us. However, because the effect does not seem to be significant on the usual laboratory time scale of a few hours, this study was not pursued. It should be noted that the irradiated mixture of plasmid (pUC19) DNA should be analyzed shortly after irradiation, and should not be stored, even frozen, for lengthy periods of time.

### 7. Irradiation of plasmid DNA with metalloderivatives of TPyP4.

As an example of the experiments performed, that for Ru(CO)TMPyP4 will be discussed (**Figure 3.7**). The plasmid alone was irradiated up to 250 sec. A reaction mixture with 20  $\mu$ M plasmid and 1  $\mu$ M Ru(CO)TMPyP4 in irradiation buffer was irradiated up to 150 s. **Figure 3.7** shows that the presence of porphyrin enhanced DNA damage. Data were fit to the Poisson distribution, using the Freifelder-Trumbo equations (Freifelder & Trumbo, 1969):

$$f_{SC} = \text{supercoiled form} = \exp [-(n_{ss} + n_{ds})]$$

$$f_L = \text{linear form} = n_{ds} \exp (-n_{ds})$$

$$f_{SC} + f_{OC} + f_L = 1$$

where  $n_{ss}$  = average number of single stranded cuts per unit time and  $n_{ds}$  = average number of double stranded cuts per unit time. Rates were obtained by multiplying  $n_{ss}$  and  $n_{ds}$  by the irradiation time. The data for the  $f_{SC}$  and  $f_L$  were fit simultaneously using

Mathematica;  $n_{ss}$  was  $1.82 \times 10^{-2}$  and  $n_{ds}$  was  $1.47 \times 10^{-4}$ . Thus, ssb were 124 times more likely to be formed than dsb for Ru(CO)TMPyP4. For the sample without porphyrin,  $n_{ss}$  was  $1.02 \times 10^{-2}$  and  $n_{ds}$  was  $3.20 \times 10^{-4}$ ; thus, ssb were 32 times more likely to be formed than dsb. It was clear that the addition of the Ru(CO)TMPyP4 did not increase the extent of dsb. However, the extent of ssb is increased by about 80%, indicating that the ruthenium porphyrin served as an effective radiosensitizing agent.

Experiments with the other metalloporphyrins were run analogously. **Table 3.3** and **Figure 3.8** summarize the results of DNA cleavage in the presence of the metalloderivatives of TMPyP4. Significant dsb was not observed with any of the metals. However, substantial ssb was observed. As discussed above, platinum compounds are being investigated by other groups as potential PAT candidates. Our work shows that Ru, and particularly Zr, are far more effective radiosensitizers than Pt. Thus, these are worth pursuing as possible PAT clinical agents.

### **Conclusions.**

A combination of few metalloderivatives of TMPyP4 (Pd, Ru, and Zr) and radiation was more effective than either by itself in changing the plasmid from predominantly SC to mainly open circular. Zr caused the highest extent of ssb. A combination of rest of the metalloderivatives of TMPyP4 studied (Ag, InMe, InBz and Pt) and radiation, was not effective in changing the plasmid from predominantly SC to mainly open circular. The Freifelder-Trumbo equations are an appropriate model for the data. The extent to which the Auger effect contributes to the cell killing is not yet known.

Significant prompt double stranded damage was not observed. It was observed that incubation with InBzPyP4 lead up to 10% linear form (dsb) cleaving with the amine at the induced abasic sites due to prolonged incubation (no irradiation involved).

Table 3.1. The inner shell energies (keV) of the metals chosen for irradiation. All have L or K edge energies suitable for irradiation by clinically used brachytherapy seeds.

<b>Transition metals</b>	<b>Edge energies K shell (keV)</b>
Pt ( $L_1$ )	13.89
Zr	18.00
Mo	20.00
Ru	22.12
Pd	24.35
Ag	25.51
In	27.94

from data at <http://www.csrii.iit.edu/periodictable.html>

Table 3.2. Relationship between XlogP and capillary electrophoresis migration times.

<b>R</b>	<b>XlogP</b>	<b>CE migration time (min)</b>
Me	14.99	12.4
Et	17.27	13.3
Pr	19.07	14.2
Bu	20.87	15.1
Bz	20.82	15.3

Table 3.3. Summary of the results of plasmid (pUC19) DNA cleavage when irradiated in the presence of the metalloderivatives of TMPyP4.

	$n_{ss}$	$n_{ds}$	ratio
<b>no metal</b>	1.02E-02	3.20E-04	32
<b>Pt</b>	1.18E-02	2.57E-04	46
<b>Ru</b>	1.82E-02	1.47E-04	124
<b>InMe</b>	7.96E-03	2.05E-04	39
<b>InBz</b>	8.63E-03	2.60E-04	33
<b>Ag</b>	1.10E-02	3.14E-04	35
<b>Pd</b>	1.56E-02	2.88E-04	54
<b>Zr</b>	5.16E-02	1.91E-04	270

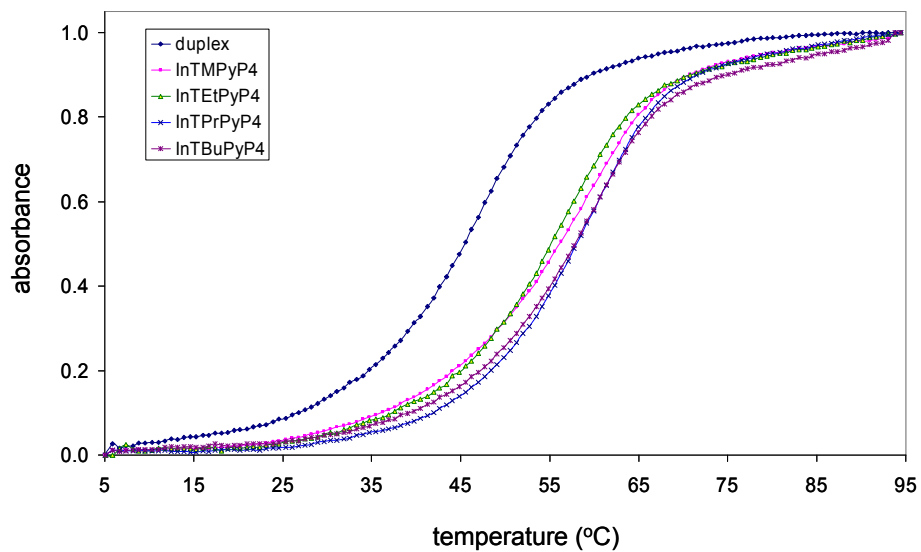


Figure 3.1. Thermal melting profiles of 10 mer duplex DNA (5'-GCGAATTCGC-3') alone (46.9 °C) and after complexation with the alkyl derivatives of InTRPyP4 ( $59.0 \pm 1$  °C).

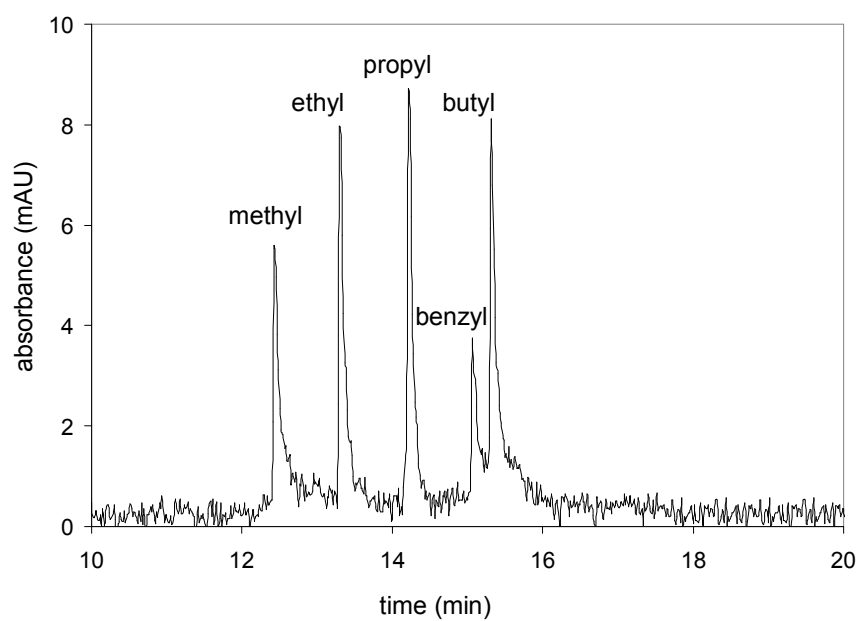


Figure 3.2. Capillary electrophoresis separation of the indium derivatives of InTRPyP4. Separation conditions are discussed in the experimental.

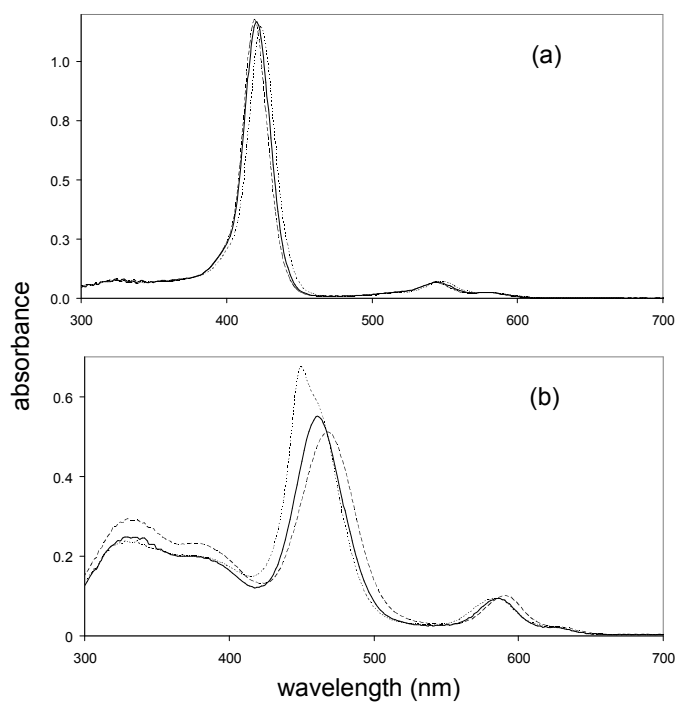


Figure. 3.3. UV-vis spectra of (a) Zr and (b) Mo derivatives of TMPyP4. The porphyrin solutions are in water (\_\_\_\_) and in pH 3.2 (\_\_\_\_) and 8.1 (-----) buffers.

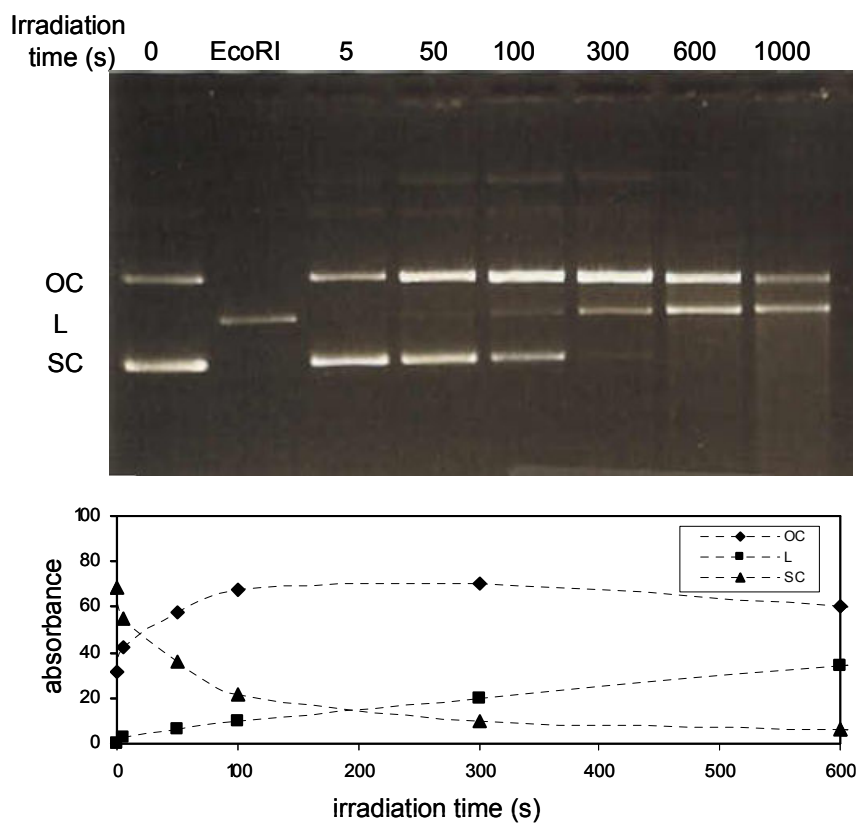


Figure 3.4. Enhancement of pUC19 cleavage was observed due to longer irradiation times. Experimental conditions: 20  $\mu$ M pUC19 in 10 mM phosphate buffer (pH 7.0) + 2 mM glycerol; Rh target tube, 50 kV, 20 mA, 40 Gy/min.

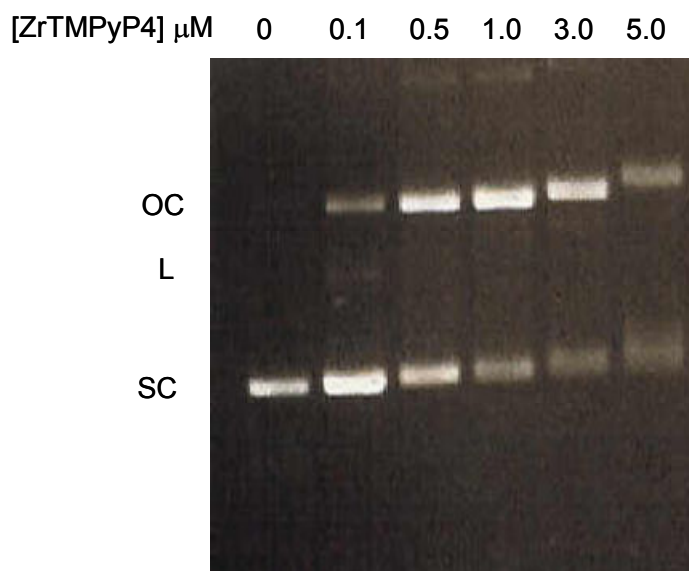


Figure 3.5. Increasing porphyrin concentration enhanced pUC19 Cleavage. “Dimming” of the bands was also observed. Experimental conditions: 10  $\mu\text{M}$  pUC19 in 10 mM phosphate buffer (pH 7.0) + 2 mM glycerol; 4 s irradiation; Rh target tube, 50 kV, 20 mA, 40 Gy/min.

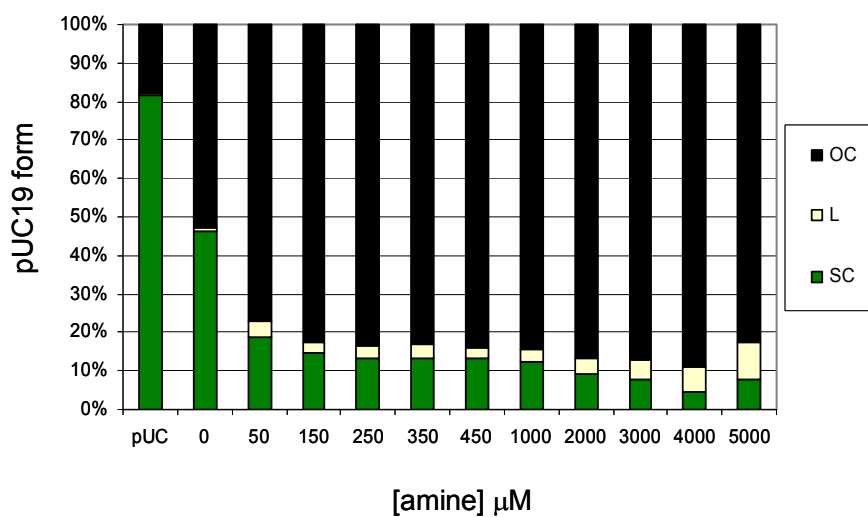


Figure 3.6. An increased fraction of OC was observed by the addition of 3,3'-diamino-*N*-methyldipropylamine to a mixture of plasmid (pUC19) DNA and InTBzPyP4 that was incubated for 30 days. This indicated the formation of abasic sites on the DNA due to the prolonged incubation with the porphyrin, even in a frozen solution (-20 °C). Experimental conditions: 10 μM pUC19 and 1 μM InTBzPyP4 in 10 mM phosphate buffer (pH 7.0) + 2 mM glycerol.

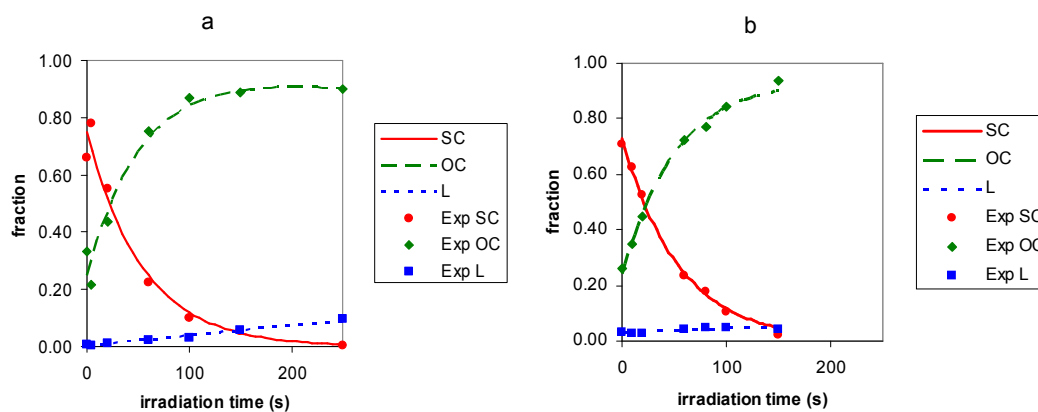


Figure 3.7. Extents of SC, OC and L forms of pUC19 as a function of irradiation time, no porphyrin added. Reactions were run in 10 mM phosphate buffer at pH 7.0 with 2 mM glycerol. Lines are global fits of the data to the Freifelder-Trumbo equations using Mathematica. (a) no porphyrin, (b) 1  $\mu\text{M}$  Ru(CO)TMPyP4.

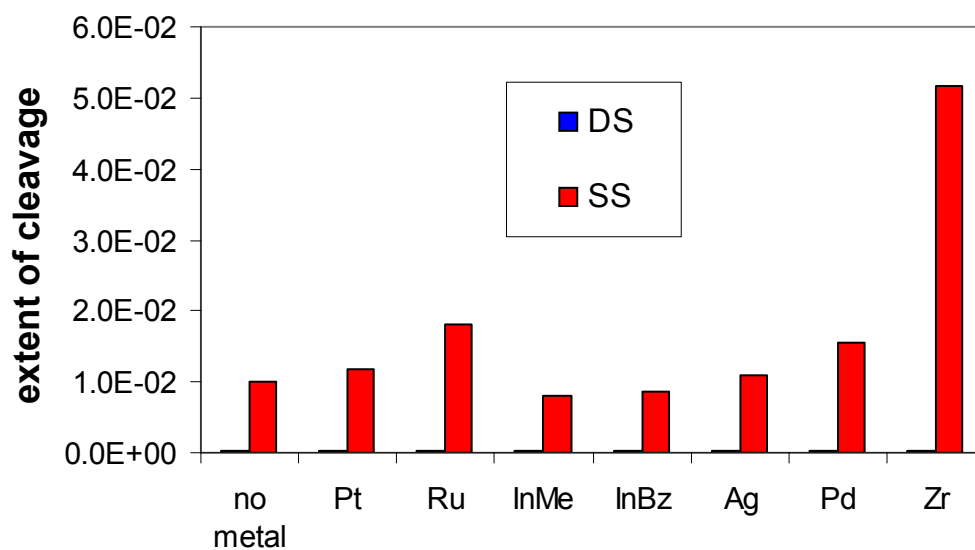


Figure 3.8. The extent of single strand cutting (ssb) and double strand cutting (dsb) and the nss/nds ratio as a function of the metal chelated in the porphyrin. Unless otherwise noted, all porphyrins are TMPyP4. Experimental conditions and data analysis are described in the text.

## References

- Abraham, R. J., Hawkes, G. H., Hudson, M. F., and Smith, K. M. (1975). The nuclear magnetic resonance spectra of porphyrins. Part X. Carbon-13 nuclear magnetic resonance spectra of some *meso*-tetraarylporphyrins and their metal chelates. *J. Chem. Soc. Perkin Trans. 2* 204-211.
- Ackley, K. L., Day, J. A., and Caruso, J. A. (2000). Separation of metalloporphyrins by capillary electrophoresis with UV detection and inductively coupled plasma mass spectrometric detection. *J. Chromatogr. A* **888**, 293-298.
- Adler, A. D., Longo, F. R., Finarelli, J. D., Goldmacher, J., Assour, J., and Korsakoff, L. (1967). A simplified synthesis for *meso*-tetraphenylporphyrins. *J. Org. Chem.* **32**, 476.
- Akins, D. L., Ozcelik, S., Zhu, H. R., and Guo, C. (1996a). Fluorescence decay kinetics and structure of aggregated tetrakis(p-sulfonatophenyl)porphyrin. *J. Phys. Chem.* **100**, 14390-14396.
- Akins, D. L., Zhu, H. R., and Guo, C. (1996b). Aggregation of tetraaryl-substituted porphyrins in homogeneous solution. *J. Phys. Chem.* **100**, 5420-5425.
- Alla, V. and Bonkovsky, H. L. (2005). Iron in nonhemochromatotic liver disorders. *Semin. Liver Dis.* **25**, 461-472.
- Allen, C. M., Sharman, W. M., and van Lier, J. E. (2001). Current status of phthalocyanines in the photodynamic therapy of cancer. *J. Porph. Phthalo.* **5**, 161-169.
- Alonso, M. C., Castillo, M., and Barceló, D. (1999). Solid phase extraction procedure of polar benzene- and naphthalenesulfonates in industrial effluents followed by unequivocal determination with ion pair chromatography/electrospray-mass spectrometry. *Anal. Chem.* **71**, 2586-2593.
- Amaral, C. L. C. and Politi, M. J. (1997). Effect of urea on the dimerization equilibrium of nickel tetrasulfonated phthalocyanine in bulk and in the hydrophilic compartment of AOT reversed micelles. *Langmuir* **13**, 4219-4222.
- Ambroz, M., Beeby, A., MacRobert, A. J., Simpson, M. S., Svensen, R. K., and Phillips, D. (1991). Preparative, analytical and fluorescence spectroscopic studies of sulphonated aluminium phthalocyanine photosensitizers. *J. Photochem. Photobiol. B* **9**, 87-95.

- Andrighetto, P., Carofiglio, T., Fornasier, R., and Tonellato, U. (2000). Capillary electrophoresis behavior of water-soluble anionic porphyrins in the presence of  $\beta$ -cyclodextrin and its O-methylated derivatives. *Electrophoresis* **21**, 619-626.
- Anzai, K., Ueno, M., Yoshida, A., Furuse, M., Aung, W., Nakanishi, I., Moritake, T., Takeshita, K., and Ikota, N. (2006). Comparison of stable nitroxide, 3-substituted 2,2,5,5-tetramethylpyrrolidine-N-oxyls, with respect to protection from radiation, prevention of DNA damage, and distribution in mice. *Free Radic. Biol. Med.* **40**, 1170-1178.
- Arnold, K., Balaban, T. S., Blom, M. N., Ehrler, O. T., Gilb, S., Hampe, O., van Lier, J. E., Weber, J. M., and Kappes, M. M. (2003). Electron autodetachment from isolated nickel and copper phthalocyanine-tetrasulfonate tetraanions: Isomer specific rates. *J. Phys. Chem. A* **107**, 794-803.
- Asanaka, M., Kurimura, T., Toya, H., Ogaki, J., and Kato, Y. (1989). Anti-HIV activity of protoporphyrin. *AIDS* **3**, 403-404.
- Banfi, S., Cassani, E., Caruso, E., and Cazzaro, M. (2003). Oxidative cleavage of plasmid bluescript by water-soluble Mn-porphyrins and artificial oxidants or molecular oxygen. *Bioorg. Med. Chem.* **11**, 3595-3605.
- Barbosa, C. A. S., Constantino, V. R. L., and Tavares, M. F. M. (1997). Use of capillary electrophoresis in the characterization of sulfonated metallophthalocyanines: A comparative evaluation of purification procedures following synthesis by the condensation method. *J. Capillary Electrophor.* **4**, 157-166.
- Barry, C. G., Turney, E. C., Day, C. S., Saluta, G., Kucera, G. L., and Bierbach, U. (2002). Thermally inert metal amines as light-inducible DNA-targeted agents. Synthesis, photochemistry, and photobiology of a prototypical rhodium(III)-intercalator conjugate. *Inorg. Chem.* **41**, 7159-7169.
- Beeby, A., Bishop, S. M., Khoo, B. J., MacRobert, A. J., and Phillips, D. (1992). Chemical and spectroscopic characterization of disulphonated aluminum phthalocyanine. In "Photodynamic Therapy and Biomedical Lasers: Proceedings of the International Conference on Photodynamic Therapy and Medical Laser Applications" (P. Spinelli, M. Dal Fante, and R. Marchesini, Eds.), pp. 845-850. Elsevier Science, Amsterdam.
- Beeby, A., FitzGerald, S., and Stanley, C. F. (2001). Protonation of tetrasulfonated zinc phthalocyanine in aqueous acetonitrile solution. *Photochem. Photobiol.* **74**, 566-569.
- Ben-Hur, E., Barshtein, G., Chen, S., and Yedgar, S. (1997). Photodynamic treatment of red blood cell concentrates for virus inactivation enhances red blood cell aggregation: Protection with antioxidants. *Photochem. Photobiol.* **66**, 509-512.

Benimetskaya, L., Takle, G. B., Vilenchik, M., Lebedeva, I., Miller, P., and Stein, C. A. (1998). Cationic porphyrins: novel delivery vehicles for antisense oligodeoxynucleotides. *Nucleic Acids Res.* **26**, 5310-5317.

Blaisdell, J. O., Harrison, L., and Wallace, S. S. (2001). Base excision repair processing of radiation-induced clustered DNA lesions. *Radiat. Prot. Dosimetry* **97**, 25-31.

Blok, J. and Loman, H. (1973). The effects of gamma-radiation in DNA. *Curr. Top. Radiat. Res. Q.* **9**, 165-245.

Bopp, A. and Hagen, U. (1970). End group determination in gamma-irradiated DNA. *Biochim. Biophys. Acta.* **209**, 320-326.

Bowser, M. T., Sternberg, E. D., and Chen, D. D. Y. (1996). Development and application of a nonaqueous capillary electrophoresis system for the analysis of porphyrins and their oligomers (PHOTOFRIN). *Anal. Biochem.* **241**, 143-150.

Bradshaw, W. W., Cadena, D. G., Jr., Crawford, G. W., and Spetzler, H. A. (1962). The use of alanine as a solid dosimeter. *Radiat. Res.* **17:11-21**, 11-21.

Brasseur, N., Ali, H., Langlois, R., and van Lier, J. E. (1988). Biological activities of phthalocyanines-IX. Photosensitization of V-79 chinese hamster cells and EMT-6 mouse mammary tumor by selectively sulfonated zinc phthalocyanines. *Photochem. Photobiol.* **47**, 705-711.

Brasseur, N., Ali, H., Langlois, R., Wagner, J. R., Rousseau, J., and van Lier, J. E. (1987a). Biological activities of phthalocyanines--V. Photodynamic therapy of EMT-6 mammary tumors in mice with sulfonated phthalocyanines. *Photochem. Photobiol.* **45**, 581-586.

Brasseur, N., Ali, H., Langlois, R., Wagner, J. R., Rousseau, J., and van Lier, J. E. (1987b). Biological activities of phthalocyanines--V. Photodynamic therapy of EMT-6 mammary tumors in mice with sulfonated phthalocyanines. *Photochem. Photobiol.* **45**, 581-586.

Brasseur, N., Ali, H., Langlois, R., Wagner, J. R., Rousseau, J., and van Lier, J. E. (1987c). Biological activities of phthalocyanines--V. Photodynamic therapy of EMT-6 mammary tumors in mice with sulfonated phthalocyanines. *Photochem. Photobiol.* **45**, 581-586.

Brasseur, N., Ali, H., Langlois, R., Wagner, J. R., Rousseau, J., and van Lier, J. E. (1987d). Biological activities of phthalocyanines--V. Photodynamic therapy of EMT-6 mammary tumors in mice with sulfonated phthalocyanines. *Photochem. Photobiol.* **45**, 581-586.

- Bressan, M., Celli, N., d'Alessandro, N., Liberatore, L., Morvillo, A., and Tonucci, L. (2000). Ruthenium sulfophthalocyanine catalyst for the oxidation of chlorinated olefins with hydrogen peroxide. *J. Organometal. Chem.* **594**, 416-420.
- Buchler, J. W. (1975). Static coordination chemistry of metalloporphyrins. In "Porphyrins and Metalloporphyrins" (K. M. Smith, Ed.), pp. 157-231. Elsevier, New York.
- Cabrera, C., Witvrouw, M., Gutierrez, A., Clotet, B., Kuipers, M. E., Swart, P. J., Meijer, D. K., Desmyter, J., De Clercq, E., and Este, J. A. (1999). Resistance of the human immunodeficiency virus to the inhibitory action of negatively charged albumins on virus binding to CD4. *AIDS Res. Hum. Retroviruses* **20**, 1535-1543.
- Cerfontain, H., Koeberg-Telder, A., Laali, K., Lambrechts, H. J. A., and de Wit, P. (1982). Aromatic sulfonation 85. Halogen directing and steric effects in the sulfonation of the twelve halogenotoluenes and some related compounds. *Rec. Trav. Chim. Pays-Bas* **101**, 390-392.
- Cerfontain, H., Koeberg-Telder, A., van Lindert, H. C. A., and Bakker, B. H. (1997). Aromatic sulfonation 131. Formation of sulfonic acids and sulfonic anhydrides in the sulfur trioxide sulfonation of some dialkylbenzenes and 1,omega-diarylalkanes. *Liebigs Ann. /Recl.* 2227-2233.
- Cerfontain, H., Zou, Y. S., and Bakker, B. H. (1994a). On the positional reactivity order in the sulfonation of phenyl-substituted and naphthyl-substituted naphthalenes with SO<sub>3</sub>. *Rec. Trav. Chim. Pays-Bas* **113**, 517-523.
- Cerfontain, H., Zou, Y. S., and Bakker, B. H. (1994b). The positional reactivity order in the sulfur-trioxide sulfonation of benzene and naphthalene derivatives containing an electron-withdrawing substituent. *Rec. Trav. Chim. Pays-Bas* **113**, 403-410.
- Chackerian, B., Long, E. M., Luciw, P. A., and Overbaugh, J. (1997). Human immunodeficiency virus type 1 coreceptors participate in postentry stages in the virus replication cycle and function in simian immunodeficiency virus infection. *J. Virol.* **71**, 3932-3939.
- Chatgililoglu, C. and O'Neill, P. (2001). Free radicals associated with DNA damage. *Exp. Gerontol.* **36**, 1459-1471.
- Chen, M. H. and Ding, W. H. (2004). Separation and migration behavior of positional and structural naphthalenesulfonate isomers by cyclodextrin-mediated capillary electrophoresis. *J. Chromatogr. A* **1033**, 167-172.
- Chen-Collins, A. R. M., Dixon, D. W., Vzorov, A. N., Marzilli, L. G., and Compans, R. W. (2003). Prevention of poxvirus infection by tetrapyrroles. *BMC Infect. Dis.* **3**, 9.

- Chiang, S. C. C. and Li, S. F. Y. (1997). Separation of porphyrins by capillary electrophoresis in fused-silica and ethylene vinyl acetate copolymer capillaries with visible absorbance detection. *Biomed. Chromatogr.* **11**, 366-370.
- Christensen, N. H. (1966). Kinetic studies of the hydrolysis of aromatic sulfonic anhydrides. *Acta Chem. Scand.* **20**, 1955-1964.
- Cole, A. (1969). Absorption of 20-eV to 50,000-eV electron beams in air and plastic. *Radiat. Res.* **38**, 7-33.
- Conneely, A., McClean, S., Smyth, W. F., and McMullan, G. (2001). Study of the mass spectrometric behaviour of phthalocyanine and azo dyes using electrospray ionisation and matrix-assisted laser desorption/ionisation. *Rapid Commun. Mass Spectrom.* **15**, 2076-2084.
- Conneely, A., Smyth, W. F., and McMullan, G. (2002). Study of the white-rot fungal degradation of selected phthalocyanine dyes by capillary electrophoresis and liquid chromatography. *Anal. Chim. Acta* **451**, 259-270.
- Cormier, E. G. and Dragic, T. (2002). The crown and stem of the V3 loop play distinct roles in human immunodeficiency virus type 1 envelope glycoprotein interactions with the CCR5 coreceptor. *J. Virol.* **76**, 8953-8957.
- Corsini, A. and Herrmann, O. (1986). Aggregation of *meso*-tetra(*p*-sulphonatophenyl)porphine and its Cu(II) and Zn(II) complexes in aqueous solution. *Talanta* **33**, 335-339.
- D'Cruz, O. J. and Uckun, F. M. (2004). Clinical development of microbicides for the prevention of HIV infection. *Curr. Pharm. Des.* **10**, 315-336.
- Dairou, J., Vever-Bizet, C., and Brault, D. (2004). Interaction of sulfonated anionic porphyrins with HIV glycoprotein gp120: Photodamages revealed by inhibition of antibody binding to V3 and C5 domains. *Antiviral Res.* **61**, 37-47.
- Dalgleish, A. G., Beverley, P. C., Clapham, P. R., Crawford, D. H., Greaves, M. F., and Weiss, R. A. (1984). The CD4 (T4) antigen is an essential component of the receptor for the AIDS retrovirus. *Nature* **312**, 763-767.
- De Clercq, E. (2002). Strategies in the design of antiviral drugs. *Nat. Rev. Drug Discov.* **1**, 13-25.
- Debije, M. G., Razskazovskiy, Y., and Bernhard, W. A. (2001). The yield of strand breaks resulting from direct-type effects in crystalline DNA X-irradiated at 4 K and room temperature. *J. Am. Chem. Soc.* **123**, 2917-2918.

- Debnath, A. K., Jiang, S., Strick, N., Lin, K., Haberfield, P., and Neurath, A. R. (1994). Three-dimensional structure-activity analysis of a series of porphyrin derivatives with anti-HIV-1 activity targeted to the V3 loop of the gp120 envelope glycoprotein of the human immunodeficiency virus type 1. *J. Med. Chem.* **37**, 1099-1108.
- Debnath, A. K., Jiang, S. B., Strick, N., Lin, K., Kahl, S. B., and Neurath, A. R. (1999). Anti-HIV-1 activity of carborane derivatives of porphyrins. *Med. Chem. Res.* **9**, 267-275.
- DeCamp, D. L., Babé, L. M., Salto, R., Lucich, J. L., Koo, M.-S., Kahl, S. B., and Craik, C. S. (1992). Specific inhibition of HIV-1 protease by boronated porphyrins. *J. Med. Chem.* **35**, 3426-3428.
- Dettin, M., Ferranti, P., Scarinci, C., Picariello, G., and Di Bello, C. (2003). Is the V3 loop involved in HIV binding to CD4? *Biochemistry* **42**, 9007-9012.
- Dixon, D. W., Gill, A. F., Giribabu, L., Vzorov, A. N., Alam, A. B., and Compans, R. W. (2005). Sulfonated naphthyl porphyrins as agents against HIV. *J. Inorg. Biochem.* **99**, 813-821.
- Dixon, D. W., Gill, A. F., and Sook, B. R. (2004). Characterization of sulfonated phthalocyanines by mass spectrometry and capillary electrophoresis. *J. Porph. Phthalo.* **8**, 1300-1310.
- Dixon, D. W., Kim, M. S., Kumar, V., Obara, G., Marzilli, L. G., and Schinazi, R. F. (1992). Amino- and hydroxytetraphenylporphyrins with activity against the human immunodeficiency virus. *Antiviral Chem. Chemother.* **3**, 279-282.
- Dixon, D. W., Marzilli, L. G., and Schinazi, R. F. (1990). Porphyrins as agents against the human immunodeficiency virus. *Ann. N. Y. Acad. Sci.* **616**, 511-513.
- Dixon, D. W., Pu, G. M., and Wojtowicz, H. (1998). Capillary electrophoretic separation of cationic porphyrins. *J. Chromatogr. A* **802**, 367-380.
- Dolphin, D. (1978). Nomenclature. In "The Porphyrins: Structure and Synthesis, Part A." pp. 1-27. Academic Press Inc., New York.
- Dudic, M., Lhoták, P., Král, V., Lang, K., and Stibor, I. (1999). Synthesis of novel porphyrin-based bis(calix[4]arenes). *Tetrahedron Lett.* **40**, 5949-5952.
- El Hachemi, Z., Farrera, J. A., García-Ortega, H., Ramirez-Gutierrez, O., and Ribó, J. M. (2001). Heteroassociation of *meso*-sulfonatophenylporphyrins with  $\beta$ - and  $\gamma$ -cyclodextrin. *J. Porph. Phthalo.* **5**, 465-473.
- Este, J. A., Schols, D., De Vreese, K., Van Laethem, K., Vandamme, A. M., Desmyter, J., and De Clercq, E. (1997). Development of resistance of human immunodeficiency

virus type 1 to dextran sulfate associated with the emergence of specific mutations in the envelope gp120 glycoprotein. *Mol. Pharmacol.* **52**, 98-104.

Fairchild, R. G., Brill, A. B., and Ettinger, K. V. (1982a). Radiation enhancement with iodinated deoxyuridine. *Invest Radiol.* **17**, 407-416.

Fairchild, R. G., Brill, A. B., and Ettinger, K. V. (1982b). Radiation enhancement with iodinated deoxyuridine. *Invest Radiol.* **17**, 407-416.

Falk, J. E. (1964). General Chemistry. In "Porphyrins and metalloporphyrins" Vol. 2, pp. 3-29. Elsevier, Amsterdam.

Fasman, G. D. (1975). "Handbook of Biochemistry and Molecular Biology: Nucleic Acids." CRC Press, Boca Raton.

Fingar, V. H., Wieman, J. T., Karavolos, P. S., Weber Doak, K., Ouellet, R., and van Lier, J. E. (1993). The effects of photodynamic therapy using differently substituted zinc phthalocyanines on vessel constriction, vessel leakage and tumor response. *Photochem. Photobiol.* **58**, 251-258.

Fischer, J., Jandera, P., Cesla, P., and Stanek, V. (2003). Separation of aromatic sulphonic acids by CZE in coated and non-coated capillaries. *J. Sep. Sci.* **26**, 1035-1044.

Fleischer, E. B., Chapman, R. D., and Krishnamurthy, M. (1979). Synthesis and oxidative demetalation of two new tungsten porphyrins. *Inorg. Chem.* **18**, 2156-2159.

Fleischer, E. B., Palmer, J. M., Srivastava, T. S., and Chatterjee, A. (1971). Thermodynamic and kinetic properties of an iron-porphyrin system. *J. Am. Chem. Soc.* **93**, 3162-3167.

Fonda, H. N., Gilbert, J. V., Cormier, R. A., Sprague, J. R., Kamioka, K., and Connolly, J. S. (1993). Spectroscopic, photophysical, and redox properties of some *meso*-substituted free-base porphyrins. *J. Phys. Chem.* **97**, 7024-7033.

Foster, N., Woo, D. V., Kaltovich, F., Emrich, J., and Ljungquist, C. (1985). Delineation of transplanted malignant melanoma with indium-111-labeled porphyrin. *J. Nucl. Med.* **26**, 756-760.

Frankenberg-Schwager, M. (1990). Induction, repair and biological relevance of radiation-induced DNA lesions in eukaryotic cells. *Radiat. Environ. Biophys.* **29**, 273-292.

Freifelder, D. and Trumbo, B. (1969). Matching of single-strand breaks to form double-strand breaks in DNA. *Biopolymers* **7**, 681.

- Gallaher, W. R., Ball, J. M., Garry, R. F., Martin-Amedee, A. M., and Montelaro, R. C. (1995). A general model for the surface glycoproteins of HIV and other retroviruses. *AIDS Res. Hum. Retroviruses* **11**, 191-202.
- Garcia-Campana, A. M., Gamiz-Gracia, L., Baeyens, W. R. G., and Barrero, F. A. (2003). Derivatization of biomolecules for chemiluminescent detection in capillary electrophoresis. *J Chromatogr. B* **793**, 49-74.
- George, R. G. and Padmanabhan, M. (2003). Studies on some new *meso*-aryl substituted octabromo-porphyrins and their Zn(II) derivatives. *Polyhedron* **22**, 3145-3154.
- Georgiou, G. N., Ahmet, M. T., Houlton, A., Silver, J., and Cherry, R. J. (1994). Measurement of the rate of uptake and subcellular localization of porphyrins in cells using fluorescence digital imaging microscopy. *Photochem. Photobiol.* **59**, 419-422.
- Gibbs, E. J., Skowronek, W. R., Jr., Morgan, W. T., Muller-Eberhard, U., and Pasternack, R. F. (1980). Reactions of water-soluble metalloporphyrins with the serum protein, hemopexin. *J. Am. Chem. Soc.* **102**, 3939-3944.
- Gubitz, G. and Schmid, M. G. (1997). Chiral separation principles in capillary electrophoresis. Review. *J. Chromatogr. A* **792**, 179-225.
- Gulston, M., Fulford, J., Jenner, T., de Lara, C., and O'Neill, P. (2002). Clustered DNA damage induced by radiation in human fibroblasts (HF19), hamster (V79-4) cells and plasmid DNA is revealed as Fpg and Nth sensitive sites. *Nucleic Acids Res.* **30**, 3464-3472.
- Hafliger, P., Agorastos, N., Spingler, B., Georgiev, O., Viola, G., and Alberto, R. (2005). Induction of DNA-double-strand breaks by auger electrons from <sup>99m</sup>Tc complexes with DNA-binding ligands. *Chembiochem.* **6**, 414-421.
- Halkiotis, K., Yova, D., and Pantelias, G. (1999). In vitro evaluation of the genotoxic and clastogenic potential of photodynamic therapy. *Mutagenesis* **14**, 193-198.
- Hamai, S. and Koshiyama, T. (1999). Electronic absorption, fluorescence, and circular dichroism spectroscopic studies on the inclusion complexes of tetrakis(4-sulfonatophenyl)porphyrin with cyclodextrins in basic aqueous solutions. *J. Photochem. Photobiol. A* **127**, 135-141.
- Hamai, S., Sasaki, Y., Hori, T., and Takahashi, A. (2006). Interactions of tetrakis(4-sulfonatophenyl)porphyrin with gamma-cyclodextrin and alkyltrimethylammonium bromides in aqueous solutions. *J. Incl. Phen. Mac. Chem.* **54**, 67-76.

- Hamai, S. and Satou, H. (2001). Effects of cyclodextrins on the complexation between Methylene Blue and tetrakis(4-sulfonatophenyl)porphyrin in aqueous solutions. *Spectrochim. Acta A Mol. Biomol. Spectrosc.* **57**, 1745-1750.
- Hambright, P. (2000). Chemistry of water soluble porphyrins. In "The Porphyrin Handbook" (K. M. Kadish, K. M. Smith, and R. Guilard, Eds.), Vol. 3, pp. 129-210. Academic Press, San Diego.
- Hambright, P., Adeyemo, A., Shamim, A., and Lemelle, S. (1985). [[4,4',4'',4'''-Porphyrin-5,10,15,20-tetrayltetrakis(1-methylpyridiniumato(2-))-indium(III) pentaperchlorate. *Inorg. Synth.* **23**, 55-59.
- Hanyz, I. and Wrobel, D. (2002). The influence of pH on charged porphyrins studied by fluorescence and photoacoustic spectroscopy. *Photochem. Photobiol. Sci.* **1**, 126-132.
- Harriman, A., Richoux, M. C., and Neta, P. (1983). Redox chemistry of metalloporphyrins in aqueous solution. *J. Phys. Chem.* **87**, 4957-4965.
- Harrison, P. F., Rosenberg, Z., and Bowcut, J. (2003). Topical microbicides for disease prevention: Status and challenges. *Clin. Infect. Dis.* **36**, 1290-1294.
- Hartmann, M., Robert, A., Duarte, V., Keppler, B. K., and Meunier, B. (1997). Synthesis of water-soluble ruthenium porphyrins as DNA cleavers and potential cytotoxic agents. *J. Biol. Inorg. Chem.* **2**, 427-432.
- Hergueta-Bravo, A., Jimenez-Hernandez, M. E., Montero, F., Oliveros, E., and Orellana, G. (2002). Singlet oxygen-mediated DNA photocleavage with Ru(II) polypyridyl complexes. *J. Phys. Chem. B* **106**, 4010-4017.
- Herrmann, O., Mehdi, S. H., and Corsini, A. (1978). Heterogeneous metal-insertion: A novel reaction with porphyrins. *Can. J. Chem.* **56**, 1084-1087.
- Hertzberg, R. P. and Dervan, P. B. (1982). Cleavage of double helical DNA by (methidiumpropyl-EDTA)iron(II). *J. Am. Chem. Soc.* **104**, 313-315.
- Hoffmann, P., Labat, G., Robert, A., and Meunier, B. (1990). Highly selective bromination of tetramesitylporphyrin: An easy access to robust metalloporphyrins, M-Br<sub>8</sub>TMP and M-Br<sub>8</sub>TMPS. Examples of application in catalytic oxygenation and oxidation reactions. *Tetrahedron Lett.* **31**, 1991-1994.
- Howe, L. and Zhang, J. Z. (1997). Ultrafast studies of excited-state dynamics of phthalocyanine and zinc phthalocyanine tetrasulfonate in solution. *J. Phys. Chem. A* **101**, 3207-3213.

- Howe, L. and Zhang, J. Z. (1998). The effect of biological substrates on the ultrafast excited-state dynamics of zinc phthalocyanine tetrasulfonate in solution. *Photochem. Photobiol.* **67**, 90-96.
- Ion, R. M. (1999). Spectral analysis of the porphyrins incorporation into human blood. *J. Biomed. Optics* **4**, 319-326.
- Ion, R. M., Planner, A., Wiktorowicz, K., and Frackowiak, D. (1998). The incorporation of various porphyrins into blood cells measured via flow cytometry, absorption and emission spectroscopy. *Acta Biochim. Pol.* **45**, 833-845.
- Izbicka, E., Wheelhouse, R. T., Raymond, E., Davidson, K. K., Lawrence, R. A., Sun, D., Windle, B. E., Hurley, L. H., and Von Hoff, D. D. (1999). Effects of cationic porphyrins as G-quadruplex interactive agents in human tumor cells. *Cancer Res.* **59**, 639-644.
- Jia, T., Jiang, Z. X., Wang, K., and Li, Z. Y. (2006). Binding and photocleavage of cationic porphyrin-phenylpiperazine hybrids to DNA. *Biophys. Chem.* **119**, 295-302.
- Jimenez, H. R., Julve, M., and Faus, J. (1991). A solution study of the protonation and deprotonation equilibria of 5,10,15,20-tetra(*p*-sulphonatophenyl)porphyrin. Stability constants of its magnesium(II), copper(II) and zinc(II) complexes. *J. Chem. Soc. Dalton Trans.* 1945-1949.
- Jin, Y. and Cowan, J. A. (2005). DNA cleavage by copper-ATCUN complexes. Factors influencing cleavage mechanism and linearization of dsDNA. *J. Am. Chem. Soc.* **127**, 8408-8415.
- Kadish, K. M., Maiya, G. B., Araullo, C., and Guilard, R. (1989). Micellar effects on the aggregation of tetraanionic porphyrins. Spectroscopic characterization of free-base *meso*-tetrakis(4-sulfonatophenyl)porphyrin, (TPPS)H<sub>2</sub>, and (TPPS)M (M = Zn(II), Cu(II), VO<sub>2</sub><sup>+</sup>) in aqueous micellar media. *Inorg. Chem.* **28**, 2725-2731.
- Kalny, D., Albrecht-Gary, A. M., and Havel, J. (2001). Highly sensitive method for palladium(II) determination as a porphyrinato complex by capillary zone electrophoresis. *Analytica Chimica Acta* **439**, 101-105.
- Kalyanasundaram, K. and Neumann-Spallart, M. (1982). Photophysical and redox properties of water-soluble porphyrins in aqueous media. *J. Phys. Chem.* **86**, 5163-5169.
- Kassis, A. I. (2003). Cancer therapy with Auger electrons: Are we almost there? *J. Nucl. Med.* **44**, 1479-1481.
- Kassis, A. I. (2004). The amazing world of Auger electrons. *Int. J. Radiat. Biol.* **80**, 789-803.

- Kessel, D., Luguya, R., and Vicente, M. G. (2003). Localization and photodynamic efficacy of two cationic porphyrins varying in charge distributions. *Photochem. Photobiol.* **78**, 431-435.
- Kessel, D. and Poretz, R. D. (2000). Sites of photodamage induced by photodynamic therapy with a chlorin e6 triacetoxymethyl ester (CAME). *Photochem. Photobiol.* **71**, 94-96.
- Kiyohara, C., Saito, K., and Suzuki, N. (1993). Micellar electrokinetic capillary chromatography of haematoporphyrin, protoporphyrin and their copper and zinc complexes. *J. Chromatogr.* **646**, 397-403.
- Klimczak, U., Ludwig, D. C., Mark, F., Rettberg, P., and Schulte-Frohlinde, D. (1993). Irradiation of plasmid and phage DNA in water-alcohol mixtures. Strand breaks and lethal damage as a function of scavenger concentration. *Int. J. Radiat. Biol.* **64**, 497-510.
- Krisch, R. E., Flick, M. B., and Trumbore, C. N. (1991). Radiation chemical mechanisms of single- and double-strand break formation in irradiated SV40 DNA. *Radiat. Res.* **126**, 251-259.
- Kudrevich, S. V., Brasseur, N., La Madeleine, C., Gilbert, S., and van Lier, J. E. (1997). Syntheses and photodynamic activities of novel trisulfonated zinc phthalocyanine derivatives. *J. Med. Chem.* **40**, 3897-3904.
- Kuznetsova, N. A., Gretsova, N. S., Derkacheva, V. M., Kaliya, O. L., and Luk'yanets, E. A. (2003). Sulfonated phthalocyanines: Aggregation and singlet oxygen quantum yield in aqueous solutions. *J. Porph. Phthal.* **7**, 147-154.
- Laine, M., Richard, F., Tarnaud, E., Bied-Charreton, C., and Verchere-Beaur, C. (2004). Synthesis of novel types of copper-bipyridyl porphyrins and characterization of their interactions and reactivity with DNA. *J Biol. Inorg. Chem.* **9**, 550-562.
- Langley, R. and Hambright, P. (1985). Kinetics of the reduction of manganese(III) porphyrins by hexaammineruthenium(II): A reductive acid solvolysis mechanism. *Inorg. Chem.* **24**, 1267-1269.
- Laster, B. H., Thomlinson, W. C., and Fairchild, R. G. (1993). Photon activation of iododeoxyuridine: biological efficacy of Auger electrons. *Radiat. Res.* **133**, 219-224.
- Leloup, C., Garty, G., Assaf, G., Cristovao, A., Breskin, A., Chechik, R., Shchemelinin, S., Paz-Elizur, T., Livneh, Z., Schulte, R. W., Bashkurov, V., Milligan, J. R., and Grosswendt, B. (2005c). Evaluation of lesion clustering in irradiated plasmid DNA. *Int. J. Radiat. Biol.* **81**, 41-54.

- Leloup, C., Garty, G., Assaf, G., Cristovao, A., Breskin, A., Chechik, R., Shchemelinin, S., Paz-Elizur, T., Livneh, Z., Schulte, R. W., Bashkirov, V., Milligan, J. R., and Grosswendt, B. (2005a). Evaluation of lesion clustering in irradiated plasmid DNA. *Int. J. Radiat. Biol.* **81**, 41-54.
- Leloup, C., Garty, G., Assaf, G., Cristovao, A., Breskin, A., Chechik, R., Shchemelinin, S., Paz-Elizur, T., Livneh, Z., Schulte, R. W., Bashkirov, V., Milligan, J. R., and Grosswendt, B. (2005b). Evaluation of lesion clustering in irradiated plasmid DNA. *Int. J. Radiat. Biol.* **81**, 41-54.
- Levere, R. D., Gong, Y.-F., Kappas, A., Bucher, D. J., Wormser, G. P., and Abraham, N. G. (1991). Heme inhibits human immunodeficiency virus 1 replication in cell cultures and enhances the antiviral effect of zidovudine. *Proc. Natl. Acad. Sci. USA* **88**, 1756-1759.
- Leznoff, C. C. and Lever, A. B. P. (1989). "Phthalocyanines: Properties and Applications - Vol I." New York, NY.
- Leznoff, C. C. and Lever, A. B. P. (1993). "Phthalocyanines: Properties and Applications - Vol III." VCH, New York.
- Lhomme, J., Constant, J. F., and Demeunynck, M. (1999). Abasic DNA structure, reactivity, and recognition. *Biopolymers* **52**, 65-83.
- Li, Q., Chang, C. K., and Huie, C. W. (2005). Investigation of solvent effects in capillary electrophoresis for the separation of biological porphyrin methyl esters. *Electrophoresis*. **26**, 3349-3359.
- Lim, C. K., Razzaque, M. A., Luo, J. L., and Farmer, P. B. (2000). Isolation and characterization of protoporphyrin glycoconjugates from rat Harderian gland by HPLC, capillary electrophoresis and HPLC/electrospray ionization MS. *Biochem. J.* **347**, 757-761.
- Lindsey, J. S., Schreiman, I. C., Hsu, H. C., Kearney, P. C., and Marguerettaz, A. M. (1987). Rothmund and Adler-Longo reactions revisited: Synthesis of tetraphenylporphyrins under equilibrium conditions. *J. Org. Chem.* **52**, 827-836.
- Lobachevsky, P. N., Karagiannis, T. C., and Martin, R. F. (2004). Plasmid DNA breakage by decay of DNA-associated Auger electron emitters: Approaches to analysis of experimental data. *Radiat. Res.* **162**, 84-95.
- Maeda, M., Kobayashi, K., and Hieda, K. (2004). Efficiencies of induction of DNA double strand breaks in solution by photoabsorption at phosphorus and platinum. *Int. J. Radiat. Biol.* **80**, 841-847.

- March, J. (1992). Reactivity. In "Advanced organic Chemistry: reactions, mechanisms and structures" (., Ed.), pp. 683-733. Wiley-Interscience, New York.
- Margaron, P., Grégoire, M. J., Šcasnár, V., Ali, H., and van Lier, J. E. (1996). Structure-photodynamic activity relationships of a series of 4-substituted zinc phthalocyanines. *Photochem. Photobiol.* **63**, 217-223.
- Maric, N., Chan, S. M., Hoffer, P. B., and Duray, P. (1988). Radiolabeled porphyrin vs gallium-67 citrate for the detection of human melanoma in athymic mice. *Int. J. Rad. Appl. Instrum. B* **15**, 543-551.
- Martin, P. C., Gouterman, M., Pepich, B. V., Renzoni, G. E., and Schindele, D. C. (1991). Effects of ligands, solvent, and variable sulfonation of dimer formation on aluminum and zinc phthalocyaninesulfonates. *Inorg. Chem.* **30**, 3305-3309.
- Marzilli, L. G. (1990). Medical aspects of DNA porphyrin interactions. *New J. Chem.* **140**, 4090-4200.
- Masahiko, I., Shigenobu F., Yoshio I., Yoshiki H., and Motoharu T (1985). Reactions of hydrogen peroxide with metal complexes. 8. Equilibria and kinetics of the reactions of water-soluble molybdenum(V) porphyrins with hydrogen peroxide in aqueous solutions. *Inorg. Chem.* **24**, 2468-2478.
- McKnight, R. E., Santana-Jorgenson, W., Alam, A. B., and Dixon, D. W. Binding of metalloporphyrins to bovine and human serum albumin. *Journal of Biological Inorganic Chemistry* . 2002.  
Ref Type: In Press
- Miller, J. R., Taies, J. A., and Silver, J. (1987). Mossbauer and spectroscopic studies on substituted tetraphenylporphyrinato iron(III) complexes in aqueous-solutions and the formation of the mu-oxo-bridged species. *Inorg. Chim. Acta* **138**, 205-214.
- Milligan, J. R., Aguilera, J. A., Nguyen, T. T. D., Paglinawan, R. A., and Ward, J. F. (2000). DNA strand-break yields after post-irradiation incubation with base excision repair endonucleases implicate hydroxyl radical pairs in double-strand break formation. *Int. J. Radiat. Biol.* **76**, 1475-1483.
- Milligan, J. R., Aguilera, J. A., and Ward, J. F. (1993). Variation of single-strand break yield with scavenger concentration for plasmid DNA irradiated in aqueous solution. *Radiat. Res.* **133**, 151-157.
- Mosinger, J., Deumie, M., Lang, K., Kubát, P., and Wagnerová, D. M. (2000). Supramolecular sensitizer: Complexation of *meso*-tetrakis(4-sulfonatophenyl)porphyrin with 2-hydroxypropyl-cyclodextrins. *J. Photochem. Photobiol. A* **130**, 13-20.

Murphy, M. K., Piper, R. K., Greenwood, L. R., Mitch, M. G., Lamperti, P. J., Seltzer, S. M., Bales, M. J., and Phillips, M. H. (2004). Evaluation of the new cesium-131 seed for use in low-energy x-ray brachytherapy. *Med. Phys.* **31**, 1529-1538.

Nette, H. P., Onori, S., Fattibene, P., Regulla, D., and Wieser, A. (1993). Coordinated research efforts for establishing an international radiotherapy dose intercomparison service based on the alanine ESR system. *Applied Radiation and Isotopes* **44**, 7-11.

Neurath, A. R., Haberfield, P., Joshi, B., Hewlett, I. K., Strick, N., and Jiang, S. (1991). Rapid prescreening for antiviral agents against HIV-1 based on their inhibitory activity in site-directed immunoassays. I. The V3 loop of gp120 as target. *Antiviral Chem. Chemother.* **2**, 303-312.

Neurath, A. R., Strick, N., and Debnath, A. K. (1995). Structural requirements for and consequences of an antiviral porphyrin binding to the V3 loop of the human immunodeficiency-virus (HIV-1) envelope glycoprotein gp120. *J. Mol. Recognition* **8**, 345-357.

Neurath, A. R., Strick, N., Haberfield, P., and Jiang, S. (1992). Rapid prescreening for antiviral agents against HIV-1 based on their inhibitory activity in site-directed immunoassays. II. Porphyrins reacting with the V3 loop of gp120. *Antiviral Chem. Chemother.* **3**, 55-63.

Neurath, A. R., Strick, N., and Jiang, S. (1994a). Rapid prescreening for antiviral agents against HIV-1 based on their inhibitory activity in site-directed immunoassays. Approaches applicable to epidemic HIV-1 strains. *Antiviral Chem. Chemother.* **4**, 207-214.

Neurath, A. R., Strick, N., Lin, K., Debnath, A. K., and Jiang, S. (1994b). Tin protoporphyrin-IX used in control of heme metabolism in humans effectively inhibits HIV-1 infection. *Antiviral Chem. Chemother.* **5**, 322-330.

Ohno, O., Kaizu, Y., and Kobayashi, H. (1993). J-aggregate formation of a water-soluble porphyrin in acidic aqueous media. *J. Chem. Phys.* **99**, 4128-4139.

Oppenheimer, L. E. (1981). Ion-pair chromatography of sulfonated copper phthalocyanine. *J. Chrom. Sci.* **19**, 266-269.

Pasternack, R. F. (1973). Aggregation properties of water-soluble porphyrins. *Ann. N. Y. Acad. Sci.* **206**, 614-627.

Pasternack, R. F., Brigandi, R. A., Abrams, M. J., Williams, A. P., and Gibbs, E. J. (1990). Interactions of porphyrins and metalloporphyrins with single-stranded poly(dA). *Inorg. Chem.* **29**, 4483-4486.

Pasternack, R. F., Caccam, M., Keogh, B., Stephenson, T. A., Williams, A. P., and Gibbs, E. J. (1991). Long-range fluorescence quenching of ethidium ion by cationic porphyrins in the presence of DNA. *J. Am. Chem. Soc.* **113**, 6835-6840.

Pasternack, R. F. and Gibbs, E. J. (1996). Porphyrin and metalloporphyrin interactions with nucleic acids. *Metal Ions Biol. Syst.* **33**, 367-397.

Patel, D. J. and Canuel, L. L. (1976). Ethidium bromide-(dC-dG-dC-dG)<sub>2</sub> complex in solution: intercalation and sequence specificity of drug binding at the tetranucleotide duplex level. *Proc. Natl. Acad. Sci. U. S. A.* **73**, 3343-3347.

Pauwels, R., Balzarini, J., Baba, M., Snoeck, R., Schols, D., Herdewijn, P., Desmyter, J., and De Clercq, E. (1988). Rapid and automated tetrazolium-based colorimetric assay for the detection of anti-HIV compounds. *J. Virol. Methods* **20**, 309-321.

Peng, X., Sternberg, E., and Dolphin, D. (2002). Chiral separation of benzoporphyrin derivative mono- and diacids by laser induced fluorescence-capillary electrophoresis. *Electrophoresis* **23**, 93-101.

Peng, X., Sternberg, E., and Dolphin, D. (2005). Separation of porphyrin-based photosensitizer isomers by laser-induced fluorescence capillary electrophoresis. *Electrophoresis* **26**, 3861-3868.

Phillips, D. (1997). Chemical mechanisms in photodynamic therapy with phthalocyanines. *Prog. React. Kinet.* **22**, 175-300.

Pico, G. A. and Houssier, C. (1989). Bile salts-bovine serum albumin binding: spectroscopic and thermodynamic studies. *Biochim. Biophys. Acta.* **999**, 128-134.

Pokric, B., Allinson, N. M., Bergström, E. T., and Goodall, D. M. (1999). Dynamic analysis of capillary electrophoresis data using real-time neural networks. *J. Chromatogr. A* **833**, 231-244.

Povirk, L. F., Wubter, W., Kohnlein, W., and Hutchinson, F. (1977). DNA double-strand breaks and alkali-labile bonds produced by bleomycin. *Nucleic Acids Res.* **4**, 3573-3580.

Priola, S. A., Raines, A., and Caughey, W. S. (2000). Porphyrin and phthalocyanine antiscrapie compounds. *Science* **287**, 1503-1506.

Rajendiran, N. and Santhanalakshmi, J. (2002). Interaction of sulfur dioxide with zinc(II) tetrasulfophthalocyanine in aqueous medium: steady state fluorescence quenching studies. *Polyhedron* **21**, 951-957.

Rao, T. A. and Maiya, B. G. (1994). Spectroscopic, redox and emission properties of 2-nitro-substituted free base- and metallo-tetra-aryl porphyrins. *Polyhedron* **13**, 1863-1873.

- Reynolds, W. L. and Kolstad, J. J. (1976). Aggregation of 4,4',4'',4'''-tetrasulfophthalocyanine in electrolyte solutions. *J. Inorg. Nucl. Chem.* **38**, 1835-1838.
- Ribo, J. M., Crusats, J., Farrera, J. A., and Valero, M. L. (1994). Aggregation in Water Solutions of Tetrasodium Diprotonated Meso-Tetrakis(4-Sulfonatophenyl)Porphyrin. *J. Chem. Soc. Chem. Comm.* 681-682.
- Ribó, J. M., Farrera, J. A., Valero, M. L., and Virgili, A. (1995). Self-assembly of cyclodextrins with *meso*-tetrakis(4-sulfonatophenyl)porphyrin in aqueous solution. *Tetrahedron* **51**, 3705-3712.
- Ricchelli, F., Franchi, L., Miotto, G., Borsetto, L., Gobbo, S., Nikolov, P., Bommer, J. C., and Reddi, E. (2005). *Meso*-substituted tetra-cationic porphyrins photosensitize the death of human fibrosarcoma cells via lysosomal targeting. *Int. J. Biochem. Cell Biol.* **37**, 306-319.
- Richeter, S., Jeandon, C., Gisselbrecht, J. P., Graff, R., Ruppert, R., and Callot, H. J. (2004). Synthesis of new porphyrins with peripheral conjugated chelates and their use for the preparation of porphyrin dimers linked by metal ions. *Inorg. Chem.* **43**, 251-263.
- Richeter, S., Jeandon, C., Kyritsakas, N., Ruppert, R., and Callot, H. J. (2003). Preparation of six isomeric bis-acylporphyrins with chromophores reaching the near-infrared via intramolecular Friedel-Crafts reaction. *J. Org. Chem.* **68**, 9200-9208.
- Richeter, S., Jeandon, C., Ruppert, R., and Callot, H. J. (2001). Reactivity of oxonaphthoporphyrins. Efficient beta-functionalization of the porphyrin ring on reaction with nitrogen or carbon nucleophiles. *Tetrahedron Lett.* **42**, 2103-2106.
- Rivard, M. J., Coursey, B. M., DeWerd, L. A., Hanson, W. F., Huq, M. S., Ibbott, G. S., Mitch, M. G., Nath, R., and Williamson, J. F. (2004). Update of AAPM Task Group No. 43 Report: A revised AAPM protocol for brachytherapy dose calculations. *Med. Phys.* **31**, 633-674.
- Robert, J. M. and Spinks, C. D. (1997). Separation of metallated petroporphyrin models using micellar electrokinetic capillary chromatography. *J. Liq. Chromatogr. Relat. Techno.* **20**, 2979-2995.
- Rocha Gonsalves, A. M. D., Johnstone, R. A. W., Pereira, M. M., de SantAna, A. M. P., Serra, A. C., Sobral, A. J. F. N., and Stocks, P. A. (1996). New procedures for the synthesis and analysis of 5,10,15,20- tetrakis(sulphophenyl)porphyrins and derivatives through chlorosulphonation. *Heterocycles* **43**, 829-838.
- Rocha Gonsalves, A. M. D., Varejao, J. M. T. B., and Pereira, M. M. (1991). Some new aspects related to the synthesis of *meso*-substituted porphyrins. *J. Heterocycl. Chem.* **28**, 635-640.

- Rothemund, P. (1939). Porphyrin Studies. III. The Structure of the Porphine Ring System. *J. Am. Chem. Soc.* **61**, 2912-2915.
- Rubires, R., Crusats, J., El-Hachemi, Z., Jaramillo, T., Lopez, M., Valls, E., Farrera, J. A., and Ribó, J. M. (1999). Self-assembly in water of the sodium salts of *meso*-sulfonatophenyl substituted porphyrins. *New J. Chem.* **23**, 189-198.
- Sambrook, J., Fritsch, E. F., and Maniatis, T. (1989). "Molecular Cloning A Laboratory Manual." Cold Spring Harbor Press, New York.
- Sanchez, M., Fache, E., Bonnet, D., and Meunier, B. (2001). Synthesis of organo-soluble metallophthalocyanines bearing electron-withdrawing substituents. *J. Porph. Phthalo.* **5**, 867-872.
- Sanderson, W. A. (2000). Di- & octa-sulpho-phthalocyanine & naphthalocyanine dye derivatives for use in tissue demarcation, imaging & diagnosis of tumour cells & diseased lymph nodes. *UK Patent Application GB 2,343,187A*.
- Sattentau, Q. J. and Moore, J. P. (1991). Conformational changes induced in the human immunodeficiency virus envelope glycoprotein by soluble CD4 binding. *J. Exp. Med.* **174**, 407-415.
- Schofield, J. and Asaf, M. (1997). Analysis of sulphonated phthalocyanine dyes by capillary electrophoresis. *J. Chromatogr. A* **770**, 345-348.
- Siddiqi, M. A. and Bothe, E. (1987). Single- and double-strand break formation in DNA irradiated in aqueous solution: dependence on dose and OH radical scavenger concentration. *Radiat. Res.* **112**, 449-463.
- Silver, J. and Taies, J. A. (1988). Moessbauer spectroscopic studies of tetrasulfonaphthylporphine iron(II) solutions. *Inorg. Chim. Acta* **151**, 69-75.
- Sissi, C., Mancin, F., Gatos, M., Palumbo, M., Tecilla, P., and Tonellato, U. (2005). Efficient plasmid DNA cleavage by a mononuclear copper(II) complex. *Inorg. Chem.* **44**, 2310-2317.
- So, T. S. K., Jia, L., and Huie, C. W. (2001). Stacking and separation of coproporphyrin isomers by acetonitrile-salt mixtures in micellar electrokinetic chromatography. *Electrophoresis* **22**, 2159-2166.
- Sobolev, A. S., Jans, D. A., and Rosenkranz, A. A. (2000). Targeted intracellular delivery of photosensitizers. *Prog. Biophys. Mol. Biol.* **73**, 51-90.

- Song, R., Witvrouw, M., Schols, D., Robert, A., Balzarini, J., De Clercq, E., Bernadou, J., and Meunier, B. (1997). Anti-HIV activities of anionic metalloporphyrins and related compounds. *Antiviral Chem. Chemother.* **8**, 85-97.
- Spikes, J. D., van Lier, J. E., and Bommer, J. C. (1995). A comparison of the photoproperties of zinc phthalocyanine and zinc naphthalocyanine tetrasulfonates - model sensitizers for the photodynamic therapy of tumors. *J. Photochem. Photobiol. A* **91**, 193-198.
- Stanton, J., Taucher-Scholz, G., Schneider, M., Heilmann, J., and Kraft, G. (1993). Protection of DNA from high LET radiation by two OH radical scavengers, tris (hydroxymethyl) aminomethane and 2-mercaptoethanol. *Radiat. Environ. Biophys.* **32**, 21-32.
- Steullet, V., Edwards-Bennett, S., and Dixon, D. W. (1999). Cleavage of abasic sites in DNA with intercalator-amines. *Bioorg. Med. Chem.* **7**, 1-10.
- Stone, A. (2002). Microbicides: A new approach to preventing HIV and other sexually transmitted infections. *Nat. Rev. Drug Discov.* **1**, 977-985.
- Stranadko, E. F., Meshkov, V. M., Koraboyev, U. M., and Riabov, M. V. (1999). Clinical photodynamic therapy using Russian photosensitizers Photoheme and Photosense: six-year experience. *Proc. SPIE* **4059**, 25-31.
- Sugiyama, H., Fujiwara, T., Ura, A., Tashiro, T., Yamamoto, K., Kawanishi, S., and Saito, I. (1994). Chemistry of thermal degradation of abasic sites in DNA. Mechanistic investigation on thermal DNA strand cleavage of alkylated DNA. *Chem. Res. Toxicol.* **7**, 673-683.
- Sutter, T. P. G., Rahimi, R., Hambricht, P., Bommer, J. C., Kumar, M., and Neta, P. (1993). Steric and inductive effect on the basicity of porphyrins and on the site of protonation of porphyrin dianions. *J. Chem. Soc. Faraday Trans.* **89**, 495-502.
- Swarts, S. G., Becker, D., Sevilla, M., and Wheeler, K. T. (1996). Radiation-induced DNA damage as a function of hydration. II. Base damage from electron-loss centers. *Radiat. Res.* **145**, 304-314.
- Swarts, S. G., Sevilla, M. D., Becker, D., Tokar, C. J., and Wheeler, K. T. (1992). Radiation-induced DNA damage as a function of hydration. I. Release of unaltered bases. *Radiat. Res.* **129**, 333-344.
- Tabata, K., Fukushima, K., Oda, K., and Okura, I. (2000). Selective aggregation of zinc phthalocyanines in the skin. *J. Porph. Phthalo.* **4**, 278-284.

- Tapley, K. N. (1995). Capillary electrophoretic analysis of the reactions of bifunctional reactive dyes under various conditions including a study of the analysis of the traditionally difficult to analyze phthalocyanine dyes. *J. Chromatogr. A* **706**, 555-562.
- Tedesco, A. C., Rotta, J. C. G., and Lunardi, C. N. (2003). Synthesis, photophysical and photochemical aspects of phthalocyanines for photodynamic therapy. *Curr. Org. Chem.* **7**, 187-196.
- Tisljar-Lentulis, G., Feinendegen, L. E., and Bond, V. P. (1973). [Biological radiation effects of inclusion of moderately heavy nuclei into the tissue and use of soft roentgen rays]. *Strahlentherapie*. **145**, 656-662.
- Tobin, W. R. and Greene, R. S. (1999). Meso-substituted cationic porphyrins interact with dsDNA and exhibit different localization patterns in radiation-induced fibrosarcoma cells. *Anticancer Res.* **19**, 2953-2958.
- Treibs, A. and Haerberle, N. (1968). Uber die synthese und die electronenspektren *ms*-substituierter porphine. *Justus Liebigs Ann. Chem.* 183-207.
- Trujillo, J. R., Goletiani, N. V., Bosch, I., Kendrick, C., Rogers, R. A., Trujillo, E. B., Essex, M., and Brain, J. D. (2000). T-tropic sequence of the V3 loop is critical for HIV-1 infection of CXCR4-positive colonic HT-29 epithelial cells. *J. Acquir. Immune Defic. Syndr.* **25**, 1-10.
- Turpin, J. A. (2002). Considerations and development of topical microbicides to inhibit the sexual transmission of HIV. *Expert Opin. Investig. Drugs* **11**, 1077-1097.
- Venema, F., Nelissen, H. F. M., Berthault, P., Birlirakis, N., Rowan, A. E., Feiters, M. C., and Nolte, R. J. M. (1998). Synthesis, conformation, and binding properties of cyclodextrin homo- and heterodimers connected through their secondary sides. *Chem. Eur. J.* **4**, 2237-2250.
- Vzorov, A. N., Dixon, D. W., Trommel, J. S., Marzilli, L. G., and Compans, R. W. (2002). Inactivation of human immunodeficiency virus type 1 by porphyrins. *Antimicrob. Agents Chemother.* **46**, 3917-3925.
- Vzorov, A. N., Marzilli, L. G., Compans, R. W., and Dixon, D. W. (2003). Prevention of HIV-1 infection by phthalocyanines. *Antiviral Res.* **59**, 99-109.
- Wainwright, M. (1996). Non-porphyrin photosensitizers in biomedicine. *Chem. Soc. Rev.* **25**, 351-359.
- Wainwright, M. (2002). The emerging chemistry of blood product disinfection. *Chem. Soc. Rev.* **31**, 128-136.

- Wang, X. P., Pan, J. H., and Shuang, S. M. (2001b). Study on the supramolecular system of *meso*-tetrakis(4-sulfonatophenyl) porphyrin and cyclodextrins by spectroscopy. *Spectrochim. Acta A Mol. Biomol. Spectrosc.* **57**, 2755-2762.
- Wang, X. P., Pan, J. H., and Shuang, S. M. (2001c). Study on the supramolecular system of *meso*-tetrakis(4-sulfonatophenyl) porphyrin and cyclodextrins by spectroscopy. *Spectrochim. Acta A Mol. Biomol. Spectrosc.* **57**, 2755-2762.
- Wang, X. P., Pan, J. H., and Shuang, S. M. (2001a). Study on the supramolecular system of *meso*-tetrakis(4-sulfonatophenyl) porphyrin and cyclodextrins by spectroscopy. *Spectrochim. Acta A Mol. Biomol. Spectrosc.* **57**, 2755-2762.
- Wang, X. P., Pan, J. H., Shuang, S. M., and Zhang, Y. (2002). Determination of the inclusion constants for the inclusion complexes between *meso*-tetrakis(4-sulfonatophenyl) porphyrin and cyclodextrins by three methods. *Supramol. Chem.* **14**, 419-426.
- Weber, J. H. and Busch, D. H. (1965). Complexes derived from strong field ligands. XIX. Magnetic properties of transition metal derivatives of 4,4',4'',4'''-tetrasulfophthalocyanine. *Inorg. Chem.* **4**, 469-471.
- Weinberger, R., Sapp, E., and Moring, S. (1990). Capillary electrophoresis of urinary porphyrins with absorbance and fluorescence detection. *J. Chromatogr.* **516**, 271-285.
- Williamson, J. F., Butler, W., DeWerd, L. A., Huq, M. S., Ibbott, G. S., Mitch, M. G., Nath, R., Rivard, M. J., and Todor, D. (2005). Recommendations of the American Association of Physicists in Medicine regarding the impact of implementing the 2004 task group 43 report on dose specification for  $^{103}\text{Pd}$  and  $^{125}\text{I}$  interstitial brachytherapy. *Med. Phys.* **32**, 1424-1439.
- Winkelman, J., Slater, G., and Grossman, J. (1967). The concentration in tumor and other tissues of parenterally administered tritium and  $^{14}\text{C}$ -labeled tetraphenylporphinesulfonate. *Cancer Res.* **27**, 2060-2064.
- Wolf, P., Jones, G. D. D., Candeias, L. P., and O'Neill, P. (1993). Induction of strand breaks in polyribonucleotides and DNA by the sulphate radical anion: Role of electron loss centres as precursors of strand breakage. *Int. J. Radiat. Biol.* **64**, 7-18.
- Woodburn, K. W., Vardaxis, N. J., Hill, J. S., Kaye, A. H., and Phillips, D. R. (1991). Subcellular localization of porphyrins using confocal laser scanning microscopy. *Photochem. Photobiol.* **54**, 725-732.
- Wu, N., Li, B., and Sweedler, J. V. (1994). Recent developments in porphyrin separations using capillary electrophoresis with native fluorescence detection. *J. Liq. Chromatogr.* **17**, 1917-1927.

- Yamakawa, N., Ishikawa, Y., and Uno, T. (2001). Solution properties and photonuclease activity of cationic bis-porphyrins linked with a series of aliphatic diamines. *Chem. Pharm. Bull. (Tokyo)* **49**, 1531-1540.
- Yang, P., Ren, R., Guo, M. L., Song, A. X., Meng, X. L., Yuan, C. X., Zhou, Q. H., Chen, H. L., Xiong, Z. H., and Gao, X. L. (2004). Double-strand hydrolysis of DNA by a magnesium(II) complex with diethylenetriamine. *J. Biol. Inorg. Chem.* **9**, 495-506.
- Yokoya, A., Cunniffe, S. M. T., and O'Neill, P. (2002). Effect of hydration on the induction of strand breaks and base lesions in plasmid DNA films by gamma-radiation. *J. Am. Chem. Soc.* **124**, 8859-8866.
- Zaider, E. and Bickers, D. R. (1998). Clinical laboratory methods for diagnosis of the porphyrias. *Clin. Dermatol.* **16**, 277-293.
- Zelina, J. P., Njue, C. K., Rusling, J. F., Kamau, G. N., Masila, M., and Kibugu, J. (1999). Influence of surfactant-based microheterogeneous fluids on aggregation of copper phthalocyanine tetrasulfonate. *J. Porph. Phthalo.* **3**, 188-195.
- Zelina, J. P. and Rusling, J. F. (1995). Molecular orientation in self-assembled films of copper phthalocyanine tetrasulfonate and a cationic surfactant. *Microporous Materials* **5**, 203-210.
- Zerbinati, O. and Trotta, F. (2003). pH-dependent cyclodextrin capillary electrophoresis resolution of atropisomers. *Electrophoresis* **24**, 2456-2461.
- Zhang, Y., Gong, Z. L., Zhang, H., and Cheng, J. K. (1998). An improved apparatus for on-line chemiluminescence detection with capillary electrophoresis and detection of metal-porphyrins. *Analytical Communications* **35**, 293-296.
- Zhang, Y. H., Chen, D. M., He, T., and Liu, F. C. (2003b). Raman and infrared spectral study of *meso*-sulfonatophenyl substituted porphyrins (TPPS<sub>n</sub>, n = 1, 2A, 2O, 3, 4). *Spectrochim. Acta A Mol. Biomol. Spectrosc.* **59**, 87-101.
- Zhang, Y. H., Chen, D. M., He, T., and Liu, F. C. (2003c). Raman and infrared spectral study of *meso*-sulfonatophenyl substituted porphyrins (TPPS<sub>n</sub>, n = 1, 2A, 2O, 3, 4). *Spectrochim. Acta A Mol. Biomol. Spectrosc.* **59**, 87-101.
- Zhang, Y. H., Chen, D. M., He, T., and Liu, F. C. (2003a). Raman and infrared spectral study of *meso*-sulfonatophenyl substituted porphyrins (TPPS<sub>n</sub>, n = 1, 2A, 2O, 3, 4). *Spectrochim. Acta A Mol. Biomol. Spectrosc.* **59**, 87-101.